



MODECO – Modelling study on the role of energy communities in the energy transition

Jiménez Martínez, M., Igualada L., Valdés Martín, R., Farriol Salas, A., Heredia Julbe, P., Noris, F., García Muñoz, F., Corchero, C.

2023

This publication is a study ordered by the Joint Research Centre (JRC), the European Commission's science and knowledge service. It aims to provide evidence-based scientific support to the European policymaking process. The contents of this publication do not necessarily reflect the position or opinion of the European Commission. Neither the European Commission nor any person acting on behalf of the Commission is responsible for the use that might be made of this publication. For information on the methodology and quality underlying the data used in this publication for which the source is neither Eurostat nor other Commission services, users should contact the referenced source. The designations employed and the presentation of material on the maps do not imply the expression of any opinion whatsoever on the part of the European Union concerning the legal status of any country, territory, city or area or of its authorities, or concerning the delimitation of its frontiers or boundaries.

EU Science Hub

<https://joint-research-centre.ec.europa.eu>

JRC132896

PDF ISBN 978-92-68-03084-4 doi:[10.2760/118421](https://doi.org/10.2760/118421) KJ-03-23-143-EN-N

Luxembourg: Publications Office of the European Union, 2023

© European Union, 2023



The reuse policy of the European Commission documents is implemented by the Commission Decision 2011/833/EU of 12 December 2011 on the reuse of Commission documents (OJ L 330, 14.12.2011, p. 39). Unless otherwise noted, the reuse of this document is authorised under the Creative Commons Attribution 4.0 International (CC BY 4.0) licence (<https://creativecommons.org/licenses/by/4.0/>). This means that reuse is allowed provided appropriate credit is given and any changes are indicated.

For any use or reproduction of photos or other material that is not owned by the European Union/European Atomic Energy Community, permission must be sought directly from the copyright holders.

How to cite this report: Jiménez Martínez, M., Igualada L., Valdés Martín, R., et al., *MODECO – Modelling study on the role of energy communities in the energy transition*, Publications Office of the European Union, Luxembourg, 2023, doi:[10.2760/118421](https://doi.org/10.2760/118421), JRC132896

Ares(2023)2767878

MODECO

Modelling study on the role of energy communities in the energy transition

Service Contract no. 942132-IPR-2021

April 2023

Authors: Jiménez Martínez, M., Igualada L., Valdés Martín, R., Farriol Salas, A., Heredia Julbe, P., Noris, F., García Muñoz, F., Corchero, C.

Contents

| | |
|--|----|
| Abstract | 1 |
| Acknowledgements | 2 |
| Executive summary | 3 |
| 1 Introduction | 8 |
| 1.1 Objectives | 10 |
| 1.2 Report scope | 11 |
| 2 Case studies definition | 12 |
| 2.1 Selected target regions | 12 |
| 2.1.1 Climatic differences | 13 |
| 2.1.2 Regionalized cost of capital | 15 |
| 2.2 Definition of Energy community archetypes | 16 |
| 2.2.1 Number and type of members | 18 |
| 2.2.2 Energy carriers | 19 |
| 2.2.3 Available investment options | 20 |
| 2.3 Economic scenarios | 22 |
| 2.3.1 Energy prices calculation | 23 |
| 2.3.2 Use-of-Network charges | 23 |
| 2.3.2.1 Time-of-Use tariff | 25 |
| 2.3.2.2 Peak power tariff | 26 |
| 2.3.2.3 Bandwidth tariff | 26 |
| 2.3.3 Taxes | 27 |
| 3 Modelling of Energy communities | 29 |
| 3.1 Energy demand simulation | 29 |
| 3.1.1 Non-residential and residential users | 29 |
| 3.1.1.1 Electrical baseload demand | 29 |
| 3.1.1.2 Adjustment for space cooling demand in Spain | 31 |
| 3.1.1.3 Heat demand | 32 |
| 3.1.2 Industrial users | 35 |
| 3.1.2.1 Ambient temperature dependent users | 35 |
| 3.1.2.2 Ambient temperature independent users | 37 |
| 3.2.1 Heat pumps' flexibility potential | 40 |
| 3.3 Electric vehicles | 41 |
| 3.3.1 Private charging stations (non-smart charges) | 41 |
| 3.3.2 Community-led charging points (V2G) | 43 |
| 3.3.3 Community's CO ₂ emissions | 46 |
| 4 Models description | 47 |
| 4.1 Power system model | 47 |

| | | |
|-------|--|-----|
| 4.1.1 | Model adaptation to the reference ESES | 50 |
| 4.2 | Investment model..... | 51 |
| 4.2.1 | Representative day's selection..... | 51 |
| 4.2.2 | Objective function..... | 52 |
| 4.2.3 | Key model constraints..... | 53 |
| 4.2.4 | Energy balance equations..... | 55 |
| 4.2.5 | Energy assets modelling..... | 56 |
| 4.3 | Operational model..... | 58 |
| 4.3.1 | Objective function..... | 58 |
| 4.3.2 | Balance equations..... | 58 |
| 4.3.3 | Energy assets modelling..... | 59 |
| 4.3.4 | Calculation of CO ₂ emissions..... | 62 |
| 5 | Energy communities' description..... | 63 |
| 5.1 | Business park..... | 63 |
| 5.1.1 | Business park: Heat demand..... | 64 |
| 5.1.2 | Business park: Electrical demand..... | 65 |
| 5.2 | Industrial polygon | 67 |
| 5.2.1 | Industrial polygon: Heat demand..... | 68 |
| 5.2.2 | Industrial polygon: Electrical demand | 70 |
| 5.3 | Rural town | 70 |
| 5.3.1 | Rural town: Heat demand..... | 71 |
| 5.3.2 | Rural town: Electrical demand | 72 |
| 5.4 | Urban district..... | 74 |
| 5.4.1 | Urban district: Heat demand | 75 |
| 5.4.2 | Urban district: Electrical demand | 77 |
| 5.5 | Virtual community | 79 |
| 5.5.1 | Virtual community: Heat demand | 80 |
| 5.5.2 | Virtual community: Electrical demand | 81 |
| 6 | Energy price scenarios | 84 |
| 6.1 | Power system indicators | 84 |
| 6.2 | Marginal prices | 85 |
| 6.3 | Energy tariffs | 88 |
| 7 | Investment model results | 91 |
| 7.1 | Tariff structures: TOU, Peak power, Bandwidth..... | 91 |
| 7.1.1 | Business park..... | 91 |
| 7.1.2 | Industrial polygon | 96 |
| 7.1.3 | Rural town | 100 |
| 7.1.4 | Urban district..... | 103 |
| 7.1.5 | Virtual community | 107 |

| | |
|--|-----|
| 7.2 Sensitivity tests..... | 111 |
| 7.2.1 Sensitivity to different price rates..... | 112 |
| 7.2.2 Sensitivity to different discount rates..... | 114 |
| 8 Operational model results..... | 117 |
| 8.1 Local generation mix..... | 117 |
| 8.1.1 Emitted and avoided CO ₂ emissions..... | 122 |
| 8.2 Economic benefits..... | 126 |
| 8.2.1 Avoided energy costs..... | 127 |
| 8.3 Energy costs..... | 133 |
| 8.3.1 Disaggregated energy payments..... | 133 |
| 9 Conclusions..... | 138 |
| References..... | 141 |
| Definitions..... | 149 |
| List of boxes..... | 152 |
| List of figures..... | 153 |
| List of tables..... | 157 |
| Annexes..... | 160 |
| Annex 1. Mathematical Formulation for MODECO's Investment Model..... | 160 |
| Annex 2. Mathematical Formulation for MODECO's Operational Model..... | 180 |
| Annex 3. Technical parameters for energy assets in the investment and operational models | 196 |
| Annex 4. Gap values obtained for the scenarios executed in the EC investment model | 208 |
| Annex 5. Gap values obtained for the scenarios executed in the EC operational model | 210 |

Abstract

This report assesses the influence on the operational and investment decisions of five representative Energy Community typologies (in Germany and Spain) of a variety of external factors, namely energy taxes, levies and tariff schemes. In particular, four schemes were tested: No Charges, Time-of-Use (TOU), Subscription Bandwidth and Peak power. The study indicates that none of the evaluated tariff structures poses significant barriers to Energy communities' future expansion. As long as investment and operational costs are competitive against electricity prices, communities will have incentives to form and invest in the energy assets that better fit their demand and geographical conditions. The TOU tariff, however, could lead to overinvestments in batteries under certain pricing conditions. The introduction of power-based charges, e.g. Bandwidth and Peak power, avoids this pitfall even in future scenarios with high price differentials. The Bandwidth tariff also offers an opportunity to adapt Use-of-Network charges to a future system with high prosumers participation as it ensures higher grid cost recovery. Another interesting alternative is the Portuguese regulation in which partial charges are always applied to self-consumption. Considering the impacts of self-generation while still recognizing its benefits is relevant as the study shows that self-consumption is the largest economic benefit in the short-term, but energy arbitrage and electricity sales will become relevant incomes for future Energy communities.

Acknowledgements

The authors would like to thank JRC staff Stamatios Chondrogiannis, Georg Thomassen and Rade Cadenovic for their valuable feedback and support through this work. The report also benefitted from insights and feedback from our colleague Josh Eichmann.

Authors

Catalonia Institute for Energy Research (IREC): Jiménez Martínez, Mariana; Igualada, Lucía; Valdés Martín, Roger; Farriol Salas, Albert; Heredia Julbe, Pol; García Muñoz, Fernando; Corchero, Cristina.

R2M Solution Spain: Noris, Federico

Executive summary

Policy context

As part of the European Commission's ambitious Greenhouse Gas (GHG) emissions reduction targets, the Clean Energy for all European Package introduced the concept of Renewable Energy Communities and Citizen Energy Communities. Several Energy communities across Europe have been created and support the energy transition efforts towards greater utilization of renewable energy sources, decarbonisation of the energy system and energy democratisation (e.g., energy poverty, energy justice) with significant social elements associated with them. Since there is a great variety of already existing energy community projects, it is becoming increasingly important to analyse different use cases and understand which best practices to follow for new implementations and policies. The differences between the legislative framework, the user engagement practices, and the potential revenue streams represent a valuable resource for defining the needed boundary conditions for the implementation of energy community projects at a national and European level.

Considering the novelty and complexities of these participating structures, it is important to assess the impact of a variety of factors on the energy communities' operational and investment decisions that will influence their further deployment and penetration. This varies depending on, for instance, the community typology, the geographic location (e.g. weather and legislative framework) and trends for several factors including the technology's performance and costs, and available energy prices. One major element is the legislative and regulatory framework, including energy taxes, tariffs and levies that are placed upon the energy generated and used. Within the above context, the JRC contracted R2M and IREC to assess the impact of policy and regulatory instruments (e.g. network tariffs and energy taxes) on the expected operational and investment decisions made by different Energy community types. MODECO stands out for being one of the initiatives contributing to the development of technical tools that support better understanding the implications of Energy communities in the energy future of Europe.

Work scope

The scope of this work is to analyse how investment and operational decisions within Energy communities are affected by different tariff structures through the evaluation of four scenarios. These tariff scenarios are formed by considering a dynamic price obtained from a Unit Commitment and Economic Dispatch (UCED) reflecting a future energy transition scenario and different Use-of-Network charges (i.e., No Charges, Time-Of-Use [TOU], Bandwidth subscription, Peak power based) during a 16-year period (2025-2040). Taxes are also applied except in the No Charges case, which is only used for comparative purposes. Additionally, we explore the sensitivity to the TOU tariff structure by using an annual flat rate instead of the dynamic prices, and a Power Purchase Agreement (PPA) for industrial users; as well as different discount rates.

In particular, we consider five Energy community archetypes (i.e. Business park, Industrial polygon, Rural Town, Urban District, Virtual community) in two European regions (i.e., Germany and Spain). The number and type of members considered for each archetype is defined based on existing European Energy communities and the archetype intrinsic characteristics. Electricity, natural gas and heat are present in all archetypes, while we only consider biomass for the Rural town and green hydrogen for industrial users. The potential **investments considered are combined heat and power, hydrogen electrolyser, hydrogen storage tank, solar photovoltaics (ground-mounted and on rooftop), wind turbines, batteries and vehicle-to-grid charging points**. The use of Heat pumps and non-smart electric vehicle chargers are also considered for the community energy modelling but not as part of the investment decisions. Depending on the archetypes' characteristics some energy assets are disregarded as a viable investment option (e.g. wind turbines on land-restricted areas). Based on existing data regarding national conditions for renewable asset financing in European countries, we considered different Weighted Average Cost of Capital values for Germany and Spain.

We assumed that each community acts as a single economic entity with one interconnection point with the external energy markets. For the Virtual community, the Portuguese regulation for virtual self-consumption happening at the same or different voltage levels, the only of its kind so far in Europe, is used as an inspiration to define the applicable rules to this archetype. Under these rules, partial Use-of-Network charges are applied to self-consumption by the Virtual community, the only in which members are not within geographical proximity. In the rest of archetypes, self-consuming implies avoiding taxes and Use-of-Network payments. The considered dynamic energy prices scenarios are based on the results obtained from the wholesale market module. We consider selling prices to be always equal to the regional marginal price while electricity purchased costs depend on the applicable tariff structure scenario.

To assess how Energy communities would invest and operate under such conditions, we executed **three optimization models, namely the UCED, the investment and the operational models**. The investment and operational models are specifically designed for MODECO and suited to Energy community applications, while the UCED model corresponds to an existing model adapted using an external Energy System Evolution Scenario (ESES) as reference. The Distributed Energy scenario from ENTSO-ES' Ten Year Network Development Plan 2022, which considers a high future usage of wind and solar technologies and the dismantling of all nuclear and carbon-based power plants, is used for this purpose. Possible impacts of the effect on energy prices of the war in Ukraine and other geopolitical unstable areas are not considered and are outside the scope of the present work, although adaptations from the selected ESES were done to incorporate higher gas prices.

To model the behaviours and assumptions of the different archetypes across the range of scenarios considered, the following steps are implemented:

1. Simulate the **energy demand and resources** for both residential and non-residential (tertiary and industrial) users. This includes electricity baseload, heat demand as well as heat pump and electric vehicles usage (via private and public charging stations).
2. Define economic **scenarios** and select the model's **economic and technical parameters** based on existing literature.
3. **Adapt ESES** to the selected UCED model.
4. Develop and **execute investment and operation models** using the outputs from items #1 and #2 as inputs. For the investment model, this included an algorithm for selecting a set of representative days from each evaluated year.

The proposed investment model contains a series of constraints to avoid excessive surplus generation and energy arbitrage activities, prioritizing self-consumption. We proposed this set of constraints considering that, according to current European Directives, Energy communities' primary objective is not to generate financial profits but to create economic, social and environmental benefits. However, the following question remains: **what is the balance between prioritizing economic benefits rather than financial profits in the Energy community's context?** We consider this feature a key characteristic differentiating Energy communities from other types of energy investors that needs to be clearly delimited in future models, for example by incorporating different business models in the community archetypes. This becomes a **relevant issue as current directives also encourage a level playing field for communities and larger participants**, mandating members to allow the participation of Energy communities in all market activities, which makes delimiting this balance harder.

Key conclusions

Our results show that under most pricing conditions the **three evaluated tariffs** (TOU, Bandwidth, Peak Power) **result in similar investment decisions for the Energy communities**. Specially, investments in generation assets are not significantly affected by the Use-of-Network charges applied, meaning that at the end of the 16-year period the communities have a similar technological mix regardless of the tariff, although the year at which they installed the assets slightly varies from case to case. In particular, investments in renewable energies (solar, wind) are mostly driven by the trade-off between investment and operational costs and electricity market, and the community's demand behaviour and spatial restrictions. Similarly, at the considered costs, CHP installations tend to be done early, regardless of the tariff, to replace boilers and supply the community's heat demand.

When the price curves have hours with extreme low and high prices, Energy communities under a TOU tariff invest in significantly larger storage capacity that remains unutilized most of the time and is only profited in this particular hours. This indicates that **storage investments are more sensitive to price variations under a TOU tariff** with pure energy-based charges. We did not observe a similar response when considering the Peak power or Bandwidth models, which indicates that power-based components avoid overinvestments even when wide price spreads are present. We corroborated the high sensitivity of battery investments to electricity price differences by using a flat rate instead of the dynamic market price. Under this scenario, battery installations were reduced drastically while for other types of technologies a similar power was installed. No sensitivity tests were conducted on the Peak power or Bandwidth models, but we recommend it for future analysis.

The TOU and Peak power tariffs resulted in higher economic benefits for Energy communities although which tariff offers the highest gains is influenced by regional costs: in Germany the highest benefits are associated

to the TOU and in Spain to the Peak power scheme. In both regions, **the Bandwidth model offered the least benefits**. Furthermore, for the Bandwidth model, Energy communities were not able to reduce as much costs as in other tariffs given that we assumed the contracted power to be a fixed value for the 16-year period, not subject to optimization. We consider that including the contracted bandwidth as a variable in future investment optimization models will be advisable to get a better picture of this tariff's potential effects on future communities.

The Subscription Bandwidth model also considers penalizations for power injections and withdrawals beyond certain limits. In most of the evaluated scenarios, the communities' energy assets' operations avoided incurring in excess penalizations as the proposed investment model follows a cost minimization approach. However, in the cases in which extremely high peak prices are registered, the communities bear the penalizations costs as the potential revenues are significantly higher. This situation happens just a few hours per year, but the exceeding power is significantly larger than the contracted bandwidth. To prevent this outcome, we suggest testing the **utilization of scalable penalizations with different prices depending on the percentage of power exceeded above the contracted bandwidth and not a fixed cost**.

The proposed Bandwidth model is the only that poses a cost over energy injections, including the monthly fee per contracted bandwidth and the associated penalizations to excess energy injections. This becomes relevant in scenarios in which energy communities significantly reduce their electricity grid consumption but are active generators and use the grid to provide surplus electricity to the market pool. Our results, for instance, show that **in the archetypes with lower demand (Business Park, Rural Town, Urban district), small or no charges at all would be paid by communities under the TOU o Peak power tariff**. Generally, generation is not subjected to Use-of-Network charges as these are imposed to consumption points. **In the future grid**, however, when energy prosumers – including Energy communities – become more numerous, **associating part of the costs to generation as done in the Bandwidth model is an interesting alternative to ensure the recovery of grid costs**.

Another interesting feature is the application of the **Portuguese regulation** on self-consumed energy in the Virtual community. In this archetype, members are not located in close proximity but share energy assets such as batteries and local generation technologies. In this case, the self-generated energy has Use-of-Network charges associated with its consumption but with a discount over the full cost paid by users consuming from the market pool. The applicable discount depends on the voltage level in which both load and generation are located as well as the energy flow direction. By using these rules, **Energy communities always pay for network usage**, even when self-generating. Our results indicate that **their usage makes battery investments less attractive** than when no charges are associated with self-generation. We, however, recommend performing a sensitivity test using the same scenario but no charges associated with self-consumption, as well as evaluating different user types to better understand these rules' implications on Energy communities.

Overall, our study indicates that none of the evaluated tariff structures poses significant barriers to the expansion of Energy communities. As long as investment and operational costs are competitive against electricity prices, communities have an incentive to form and invest in self-generation assets. Storage installations will be also encouraged to promote energy injections and withdrawals in convenient times for the power system operation. Purely energy-based tariffs (TOU), however, could lead to overinvestments in storage units that would be only used for a few hours annually. The introduction of power-based charges, e.g. in the Bandwidth and Peak power models, seems to avoid this pitfall even in future power scenarios in which wide price differences are present. In particular, the Bandwidth tariff presents an opportunity to adapt Use-of-Network charges to a future system with high prosumers participation as it ensures higher grid cost recovery. This becomes especially relevant as our study shows that not only self-consumption, but energy arbitrage and electricity sales will become relevant activities. Another interesting alternative in this regard is the Portuguese regulation in which partial charges are applied to self-consumption taking place at the same or different voltage levels.

Main findings

The investment model's decisions are based on a set of representative days for the entire 16-year evaluation period. The **representative days selected have a strong influence** on the final investment decisions made by the communities, particularly in the TOU tariff model. In general, **total investments tend to be larger in the German than Spanish communities** due to more favourable economic conditions (higher marginal prices, lower investment costs) as well as larger energy, and in particular heat demand. A significant

economic parameter is the **selected WACC**, which showed **significant differences between South and Central-West regions** and is based on a European-level study of financing conditions for renewable energies (wind, solar) and different member countries. This not only highlights the importance of using country-specific data to better represent the economic context affecting Energy communities, but also the importance of counting with such information at the European member level.

The **Business park** archetype invests in gas-fuelled CHP, rooftop solar photovoltaics, V2G charging stations and batteries. The community in Spain invests in larger sums than the same archetype in Germany. The Bandwidth and the No Charges scenarios result in the largest investments, while the TOU and the Peak-power scenarios have the lowest investments. Interestingly, installed batteries in Spain are much greater than in Germany largely due to the low electricity purchase price and the high selling price registered in Spain during certain hours from the selected representative days. In the Peak power scenario, batteries are mostly charged with excess on-site production with limited charging from the grid due to the extra costs associated with rising peak demand. This characteristic reduces the number of V2G-capable chargers and the storage capacity installed. In the TOU scenario – with different representative days and, thus, price curves – grid battery charging is less favourable due to the price curves' characteristics, limiting the opportunities for energy arbitrage and leading to lower storage capacity. The TOU scenario in this archetype is associated with the lowest CHP, storage and the highest V2G-capable charging points.

For the **Industrial polygon**, there are the smallest regional differences in heat and electricity demand and therefore in investments across locations. These communities mostly invest in PV solar rooftop, wind turbines, V2G-capable chargers, batteries and gas-fuelled CHP. The installed CHP is constant across the different tariff scenarios and so are the PV solar rooftop and wind turbines that corresponds to the maximum installable and allows for energy arbitrage by leveraging the installed storage capacity. The only exception is the Spanish polygon under a Peak power tariff in which less storage and CHP capacity is installed. Under the Bandwidth model, the Spanish community does incur some penalizations for excess energy withdrawal and injections, but these are small. For the Peak Power tariff case, ground-mounted solar is installed in Spain in addition to the wind capacity put on land in all other scenarios, although its capacity is small in comparison to the wind farms.

The **Rural town** communities invest in wind, PV solar (land and rooftop), gas-fuelled CHP, batteries and V2G-capable chargers. In Germany there are significant variations across tariffs, with the TOU scenario having the largest investments mostly for CHP and storage, while in Spain the profiles vary less and result in lower investments. In the Peak power tariff, batteries are used to store excess local energy at times in which demand and prices are low to discharge at higher-priced hours or when demand peaks occur. The CHP is aligned with the thermal demand in all scenarios, except for the TOU scenario. In Spain, the lowest CHP capacity is installed under the TOU tariff, while in Germany the opposite is observed. The largest wind capacity is observed for the TOU scenario in Spain. In this region, no solar is installed despite its better radiation levels as the wind profile better matches the community's demand curve and the high-priced periods. Similar to what happens in other archetypes, these differences can be attributed to the selected representative days' price curves.

In the **Urban district** archetype, investments occur in gas-fuelled CHP, storage and PV solar rooftop as ground renewable generation is not allowed. V2G-capable chargers are also installed but in a small number (five) that remains constant across scenarios. In Germany, investments are significantly greater than in Spain to cover the larger heat and electricity demand. For the No Charges scenario, the investments in Germany are the lowest while in Spain are the greatest. Such variations result from differences in the price curves from the selected representative days. The main differences across tariffs are associated with decisions regarding CHP and storage, as the amount of solar rooftop installed remains fairly constant across scenarios using the same representative days. For the TOU scenario, storage in Germany is much greater than in Spain, due to the existence of wide price spreads, leading to increased CHP extra capacity.

The **Virtual community** invests in storage, PV solar (land and rooftop), wind turbines, and V2G-capable chargers with greater investments in Germany than in Spain, especially for the Peak power scenario. This archetype presents the most V2G chargers, also used as storage, due to the larger influence area considered, which results in a higher number of electric vehicles circulation. For the Power peak in Germany, the main difference is associated with the installed storage (used mainly to lower summer demand peaks as wind load factor is lower during this summer) and solar on the ground. As happens in the Rural town, wind is preferred over solar in the Spanish community as the wind generation profile offers a better match with high-priced hours.

With the considered economic assumptions, **biomass-fuelled CHP and green hydrogen-related assets (electrolyzer, storage tank) do not result in profitable investments**. Solar and wind installations depend on energy prices, technological costs and land space restrictions. Due to its higher marginal prices, renewable energy investments take place earlier in the German than the Spanish region. Under future system scenarios with high shares of renewables, local generation might not always result in carbon offsets when natural gas-fuelled CHP technologies are installed and compared to importing energy from the electricity grid.

We observed that using a **Peak power** tariff encourages investments in renewable sources that match demand curves (for instance, solar photovoltaics in the German Rural town) even when batteries are installed. This tariff also encourages self-consumption and disincentives grid electricity purchasing for battery charging to be resold at later times. The **TOU tariff** is the most sensible to price curve selection, resulting in significantly larger energy storage investment when wide price spreads are present (German Rural town and Urban district).

Regardless of the region or archetype, the **No Charges** scenario results in the largest economic value for most scenarios, while the **Bandwidth model** tends to result in the lowest. Despite these opposite trends, both tariffs result in similar investment decisions. In the Bandwidth scenario, Energy communities operate their assets looking to avoid penalizations as much as possible, except when there is a significant amount of surplus energy during high-cost periods or opportunities to perform energy arbitrage in contexts in which wide price spreads are present. We observed this in the German Rural town and Urban district, and the Spanish Industrial polygon but to a minimum extent.

We studied **the impact of different energy prices**, namely dynamic (baseline), flat and PPA under a TOU structure for four archetypes (all except Business park) as a sensitivity analysis. For Flat rate prices, storage investments are reduced as low as zero for the Industrial polygon and Virtual community storage assets to the selected price curve, highlighting the high risk level and price exposure of these assets, which might not be assumed by real Energy communities despite the potential high revenues calculated by the investment model. For the PPA fixed price, investments are reduced for the Industrial polygon, the only case in which it is considered, but not as significantly as with the Flat rate. This as the PPA price results in lower purchase prices for 2040 than the Flat rate, providing a larger margin with the high selling prices registered at the end of the period. An additional sensitivity analysis of **different discount rates** is done for the German base cases, considering larger WACC. A higher discount rate slightly reduces the investments in energy assets as revenues are reduced considering the present value of future cash flows.

Regardless of the tariff or archetype, **self-consumption represents the largest economic benefit in 2025 and 2030** for all scenarios modelled, although electricity sales take place in all cases. The latter meaning that with the assumed energy prices, surplus energy sales result in an economically attractive activity up to different levels. **In 2040** when peak prices rise considerably but off-peak are actually cheaper, **electricity sales become a more significant revenue source** for all communities. At the end of the evaluation period, energy arbitrage activities also tend to become more relevant, which is why batteries show a higher usage at the later years.

Related and future JRC work

The present study adds a technical perspective to previous reports commissioned by JRC regarding Energy communities in Europe. It also benefits from previous research conducted by the institute regarding the modelling of the European power system and whose outcomes are used in MODECO to model future electricity prices. Although the findings in this work contribute to better understanding the impact of different tariff structures on future Energy communities' investment and operational decisions, it also opens new questions to be answered by future research, which will require rethinking some features of the proposed operational and investment models.

Quick guide

In this document, we discuss the key assumptions used to simulate the Energy community archetypes, build the community investment and operational models and design the tariff scenarios. A extended description of the obtained results upon which we based our conclusions is also presented. We also include a brief description of the models while the complete mathematical formulation can be found in Annexes so other modellers can build on them for further analysis.

1 Introduction

As part of its climate change mitigation strategy, the European Union (EU) has pledged to raise its 2030 Greenhouse Gas (GHG) emissions reduction target to at least 55% compared to 1990 levels. To achieve this goal, the European Commission has set specific targets for the energy sector as it is responsible for more than 75% of the EU's GHG emissions. Among the most important are the binding target of reaching at least 32% of renewable energy in the EU's gross final energy consumption by 2030, which might be increased up to 40% to help in achieving the overall GHG emissions reduction goal (European Commission, n.d.-c).

Europe's climate goals are expected to unlock important investments in renewable energy assets at different levels. To ensure European citizens are an active part of this transition, the climate and energy framework contemplates specific figures to promote their participation in the energy markets, for instance, individual and collective self-consumption, or Energy communities. The "Energy community" figure was first introduced in European legislation through the Clean Energy for all Europeans Package, where the concepts of "Citizen energy communities" and "Renewable energy communities" were defined (European Commission, n.d.-a). These figures show a series of commonalities, as can be seen from the definitions shown in the table below, but also key differences such as the geographical and technological constraints applicable to Renewable energy communities.

Table 1. Definition of Renewable and Citizen energy community in the European legislation

| Article 2(16) Recast Renewable Energy Directive "Renewable energy community" | Article 2(11) Recast Electricity Market Directive "Citizen energy community" |
|---|---|
| A legal entity: (a) which, in accordance with the applicable national law, is based on open and voluntary participation, is autonomous, and is effectively controlled by shareholders or members that are located in the proximity of the renewable energy projects that are owned and developed by that legal entity; (b) the shareholders or members of which are natural persons, Small and medium enterprises or local authorities, including municipalities; (c) the primary purpose of which is to provide environmental, economic or social community benefits for its shareholders or members or for the local areas where it operates, rather than financial profits. The directive further states that Renewable energy communities shall be entitled to produce, consume, store and sell renewable energy, including through renewables power purchase agreements. | A legal entity that: (a) is based on voluntary and open participation and is effectively controlled by members or shareholders that are natural persons, local authorities, including municipalities, or small enterprises; (b) has for its primary purpose to provide environmental, economic or social community benefits to its members or shareholders or to the local areas where it operates rather than to generate financial profits; and (c) may engage in generation, including from renewable sources, distribution, supply, consumption, aggregation, energy storage, energy efficiency services or charging services for electric vehicles or provide other energy services to its members or shareholders. |

Source: Obtained from (Frieden et al., 2020).

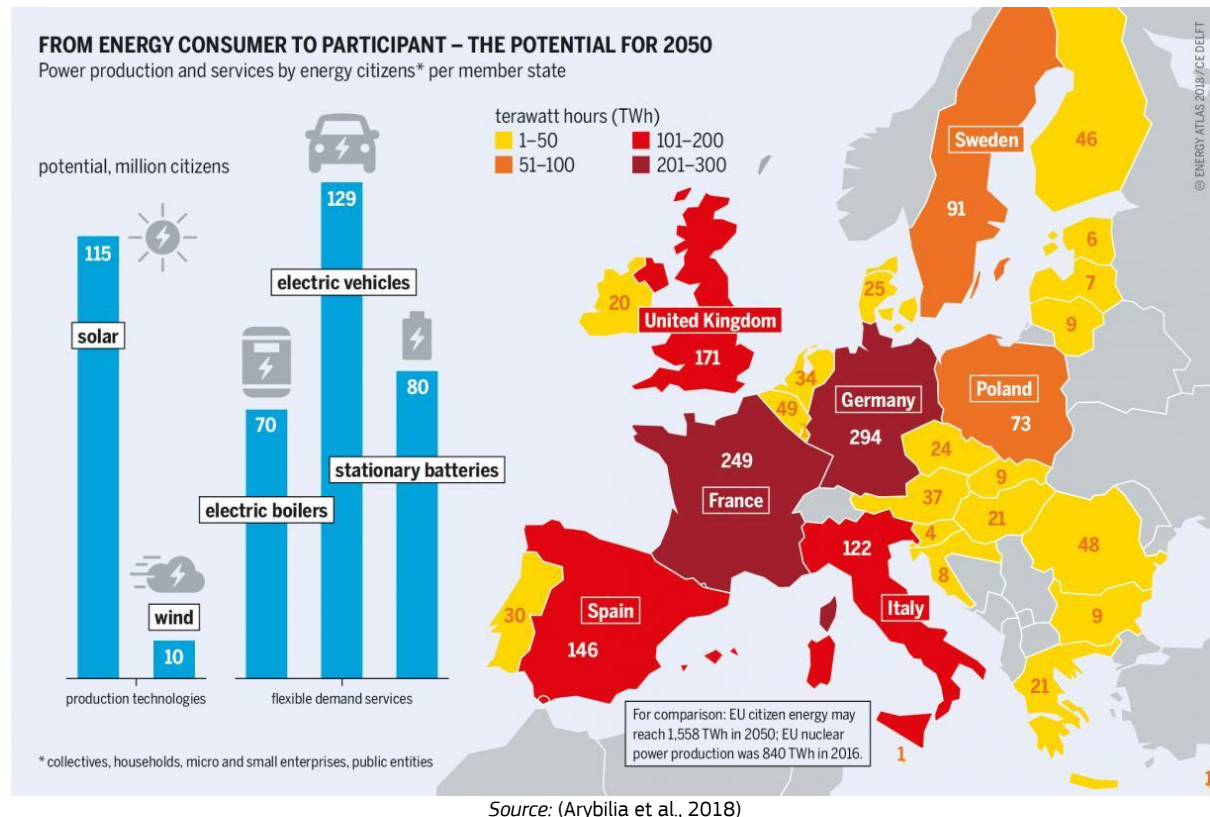
Furthermore, the Directive on common rules for the internal electricity market (EU 2019/944) laid out a series of rules to enable consumers' participation – individually or through Citizen energy community – in all energy markets, either by generating, consuming, sharing or selling electricity, or associated services such as flexibility products. The revised Renewable energy directive (2018/2001/EU) built on these precedents by mandating EU countries to enable the participation of renewable self-consumers and Renewable energy communities in all available support schemes for larger participants (European Commission, n.d.-a).

Among others, the policy framework for the emergence of community-based energy business models at EU level is set, offering new opportunities for citizens and SMEs on how to satisfy their energy needs. In fact, by 2019, the Joint Research Centre (JRC) had already identified 3,500 renewable energy cooperatives – a type of Energy communities – in 9 European member states, most of which were located in Germany and Denmark,

two countries with strong traditions of community ownership and social enterprises. The most common activity performed by these communities is energy generation, although electricity supply, energy efficiency, distribution, electro mobility, consumption and sharing, flexibility and storage, and financial services are also provided. Among a sample of European Energy communities studied by JRC, solar is found to be the most widespread energy source (38%), followed by wind (19%), biomass (17%), biogas (15%), and hydro (4%). Examples of Energy communities included Photovoltaic (PV) solar energy systems installed in school buildings or farm rooftops; small biomass installations, heat pumps, solar thermal and district heating networks for communities in colder climates; or community-owned wind farms (Caramizaru and Uihlein, 2019).

More recently, European policies favouring citizen-driven energy projects have already prompted an important number of pilots to test innovative business models and investment schemes for Energy communities in different contexts and member states. Some examples are the LIGHTNESS Project that promotes the formation of Citizen energy communities in seven pilot sites spread among five countries (Project Lightness, n.d.); the DECIDE initiative that works towards the implementation of seven Energy communities' pilots providing different energy services in seven European member states (DECIDE Project, 2020); and the COME RES Project that focuses on advancing Renewable energy communities by supporting the installation of pilots with community PV, on-shore wind, storage and integrated energy solutions in nine European countries (COME RES Project, 2020). In the future, a further growth in Energy communities' initiatives can be expected given that the potential for citizens' energy participation is very large with projections suggesting that prosumer citizens could produce twice as much power as nuclear power stations produce now, accounting for 1558 TWh (\approx 77.90B€), see below.

Figure 1. Power production and services by energy citizens per member state expected in 2050



Under this context, Energy Communities present a tremendous opportunity to simultaneously accomplish several important objectives including: i) increasing renewable energy penetration, ii) energy savings, iii) self-consumption of locally generated energy, iv) citizen empowerment and participation, v) tackle energy poverty, vi) ensuring energy security, vii) local economy benefits, viii) job creation, ix) environmental awareness, and x) education of future generations; these co-benefits ultimately support decarbonisation of different sectors of the economy needed to achieve the ambitious EU targets mentioned above. There are several kinds of Energy communities including residential, industrial, tertiary, island (both geographical and energy islands) with

specific needs and challenges. Importantly, users can contribute to a usable implementation of solutions for local energy trading.

Considering the novelty and complexities of these participating structures, it is important to assess the impact of a variety of factors on the operational and investment decisions of the energy communities that will therefore influence their further deployment and penetration. This varies depending on, for instance, the typology of the energy community, the geographic location (e.g., weather and legislative framework) and trends for several factors including technology performance, costs penetration and energy prices. One major element is the legislative and regulatory framework, including energy taxes, tariffs and levies on the energy generated and used.

However, a lack of tools analysing the viability of Energy community-led investments under different economic conditions is identified, particularly under the perspective of policy makers that want to assess the potential impact that energy regulatory decisions might have on these new market participants. The MODElling study on the role of Energy COmmunities in the energy transition (MODECO) aims to help closing this gap by developing a set of simulation and optimization tools to analyse long-term investment decisions at the community level within an energy transition context and under different economic scenarios. In particular, the project looks to shed some light on the effect that different energy pricing, tariff and taxes structures would have on the investment decisions made by Energy communities under different local and regional contexts.

1.1 Objectives

MODECO's objective is to analyse how investment and operational decisions within Energy communities are affected by the usage of different energy pricing, Use-of-Network tariff and tax designs during a 16-year period (2025-2040). The considered options for each case are the following:

- **Pricing structures:** Dynamic pricing (based on wholesale market), Power-Purchase-Agreement (PPA) and Flat rate.
- **Use-of-Network charges:** Time-of-Use (TOU), Bandwidth subscription model; and Peak power-based. In all cases in which Use-of-Network charges are applied, taxes on electricity are also added based on the current fiscal structure used in each analysed location.
- **No Charges:** As a comparison point, a scenario without any charges or taxes is also tested in the investment model.

The described economic conditions are evaluated over five Energy community archetypes designed considering typical configurations across European projects (Task 1). Furthermore, the impact of different Weighted Average Cost of Capital (WACC) on the Energy communities' investment decisions are tested through a sensitivity analysis. The Energy community design includes delimiting the type and number of members in each archetype, the expected hourly electricity and heat demand registered in each year of the studied period, and the energy carriers and technologies supplying this demand in the analysis starting year (2025).

For each archetype, a set of potential energy investments are selected considering the available space and resources on a case by case basis. The five selected archetypes are analysed in two countries representing two different European regions (South-West and Central-West). As the communities interact and are embedded within the regional electricity markets, a reference Energy System Evolution Scenario (ESES) are selected for modelling the wholesale electricity market. The potential growth and participation of Energy communities as a whole is also considered in the wholesale market participants.

Afterwards, three optimization models are used to test how the Energy community archetypes would behave under the different economic circumstances analysed. The first consists of a Unit Commitment and Economic Dispatch (UCED) model representing the wholesale electricity market in each target location. The hourly prices obtained from this model are then used as an input to the scenarios using the Dynamic pricing structure as a base case, and also to calculate the Flat rates used in a sensitivity analysis. The PPA price is calculated with the annual long-term average unit cost of energy from the generation units included in the modelled wholesale markets. The second model consists of a long-term community investment decision tool that allows selecting the type of technologies most suitable to each Energy community archetype, as well as the optimal installation year. The third is an operational model allowing to see in hourly detail how the installed energy technologies will function in three target years: 2025, 2030 and 2040.

1.2 Report scope

Modelling is a robust tool to forecast and assess the impact of different policies on the potential penetration of Energy Communities across a range of typologies, configurations and scenarios. This report presents the results of extensive modelling and assessment aimed at shedding light on the implications of different legislative and policy frameworks on the deployment of Energy Community as a structure to foster energy transition while enabling active participation of users. For this purpose, a Unit Commitment and Economic Dispatch (UCED) model as well as an investment/expansion model are created and used to model the different scenarios considering Heating & Cooling, Transport and Gas sectors. White-box models populated with real data from previous projects and information from established sources were used, such as ENTSO-E (2021a) Ten-Year Network Development Plan (TYNDP). were used. For operational decisions, three target years were considered, while for investment/expansion a 16-year timespan was used. The models considered the interrelations between the wholesale system/market and the "individualistic" operational, and investment decisions of the Energy Communities archetypes. Different types of electricity contracts, network tariff, energy contracts/pricing per energy carrier were modelled to execute targeted sensitivity analysis.

The methodology and results from this process are presented in this document. The main assumptions considered for the community archetypes design and the construction of the economic scenarios are presented in **Chapter 2**, while **Chapter 3** contains the specific methodology for the simulation of the communities' electrical and thermal demand. **Chapter 4** describes the main features of three optimization models developed, the inputs used, the constraints and outputs expected including the assumptions for the different assets considered. The diagram above summarizes the correlation among the different models and the main inputs and outputs. **Chapter 5** describes in detail the five Energy Community archetypes, namely Urban district, the Rural town, the Business Park, the Virtual Community and the industrial polygon. The descriptions include the types, numbers and features of the buildings as well as the energy assets included. The heat and electricity demand are presented for as the base case without local energy investments. **Chapter 6** illustrates the Energy Prices scenarios, penetration of renewable energy sources, associated CO₂ emissions, marginal prices and energy tariffs for both countries and time horizons. The results obtained from the execution of the investment model are discussed in **Chapter 7**, while **Chapter 8** presents the results from the Operational model. Finally, the project' main outcomes and conclusions are summarized in **Chapter 9**.

2 Case studies definition

The case studies analysed within the MODECO initiative use the Energy System Evolution Scenario (ESES) as their reference, ESES is largely based on the **Distributed energy scenario** from the well-known TYNDP developed by ENTSO-E (2021a). The TYNDP 2020 edition is selected as it is the most complete recent version available. In addition to the Distributed Energy Scenario, two additional story lines – National trends and Global ambition – are included in the TYNDP 2020 (ENTSO-E, 2021a). However, the Distributed energy scenario is preferred for this project as it specifically considers the active participation of prosumers and distributed resources in the future energy systems, which makes it more relevant for the analysis carried out in MODECO project, which focuses on projects driven by Energy community. The storyline given by ENTSO-E describing the selected scenario is presented below.

Distributed energy, a full energy scenario as well compliant with the 1.5°C target of the Paris Agreement, presents a decentralised approach to the energy transition. On this ground, prosumers actively participate in a society driven by small scale decentralised solutions and circular approaches. Distributed energy reaches carbon neutrality by 2050 (ENTSO-E, 2021a).

Some relevant differences between the Distributed Energy and the National Trends scenario –based on current Member States National Energy and Climate Plans as well as on EU climate targets – are expected to impact on the energy prices obtained by MODECO's wholesale market model and, therefore, in the investment and operational decisions taken by the modelled communities. One of the most critical is the high CO₂ price considered in the Distributed energy scenario for 2030 (53 €/ton), which almost doubles that considered for the National trends scenario (28 €/ton)¹ (ENTSO-E, 2021a). The higher carbon price impacts on the technological mix considered for the target regions in 2030 and 2040, which have a higher share of low or non-emitting sources such as renewable energies. The specific future mix considered for each target region is explained in the next section.

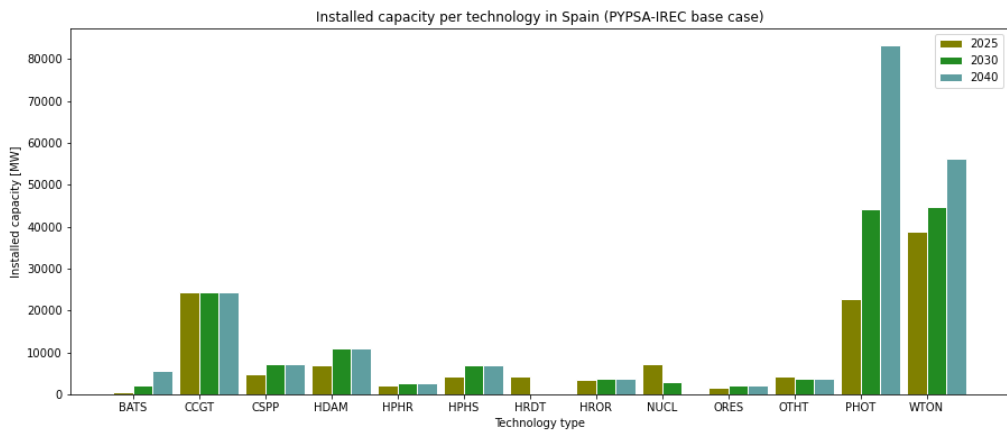
2.1 Selected target regions

The Energy community archetypes developed within MODECO project are evaluated in the South-West and Central-West European regions, with two representative countries being analysed, namely Spain and Germany. As explained before, Germany is a country with a long-term tradition of community-owned projects, being the European member state with more Energy community initiatives in place. Spain, on the other hand, is a more recent player in the development of citizen-led energy projects, but has some prominent examples, such as the energy cooperative Som Energia, included in the Energy community projects evaluated in JRC's 2019 report (Caramizaru and Uihlein, 2019).

From the modelling perspectives, the two selected countries offer an interesting contrast as their regional weather conditions reflect on distinct consumption patterns, which are expected to translate into different investment choices even when the same Energy community archetypes and tariffs are considered. Furthermore, the assumptions made by ENTSO-E in its TYNDP 2020 reflect differently on the future energy mix for both countries. As can be seen in Figure 2 and Figure 3, both the German and Spanish systems will rely heavily on solar Photovoltaic (PV) and wind energy by 2030 and 2040. Nonetheless, the Spanish energy mix englobes substantial fossil-fuelled power in the form of Combined Cycle Gas Turbines (CCGT) even by 2040 whereas the German system will have a lower share of traditional technologies in comparison to the total power installed as it will phase out not only nuclear but most of its fossil fuels-driven technologies with the exception of CCGT.

¹ By the end of 2021, the average price for future carbon credits in the European Union Emission Trading System – known as European Union Allowances (EUA) – was 52 euros per tonne (Qin et al., 2021). Analysts estimate that carbon credits will reach average prices of 85.22 euros per tonne in 2022 and 94.23 euros per tonne in 2023 (Twidale, 2022), which are significantly higher than the carbon price defined in the Distributed energy scenario, despite considering more aggressive prices than in the base case.

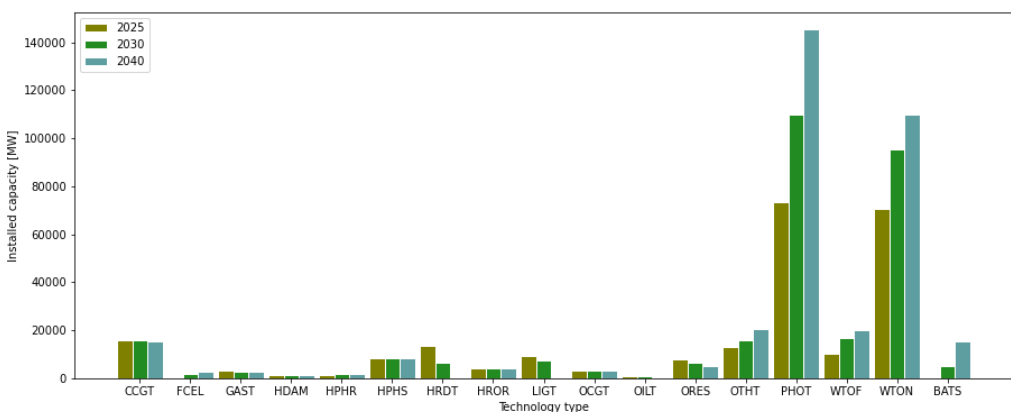
Figure 2. Installed power by technology in Germany in 2025, 2030 and 2040 for selected reference scenario



CCGT: Combined Cycle Gas Turbines; FCEL: Fuel Cell; GAST: Gas Turbines; HDAM: Hydro-reservoirs; HPHR: Open-loop hydro pumped storage; HPHS: Closed-loop hydro pumped storage; HRDT: Hard coal-fuelled generators; HROR: Hydro Run-of-River; LIGT: Lignite-fuelled generators, OCGT: Open Cycle Gas Turbines; OILT: Oil-fuelled generators; ORES: Other Renewables; OTHT: Other non-renewables (combined heat and power); PHOT: solar photovoltaics; WTON: wind onshore; BATS: batteries.

Source: Own elaboration with data from (ENTSO-E, 2021b).

Figure 3. Installed power by technology in Spain in 2025, 2030 and 2040 for selected reference scenario



BATS: batteries; CCGT: Combined Cycle Gas Turbines; CSPP: Concentrated Solar Power; HDAM: Hydro-reservoirs; HPHR: Open-loop hydro pumped storage; HPHS: Closed-loop hydro pumped storage; HRDT: Hard coal-fuelled generators; HROR: Hydro Run-of-River; LIGT: Lignite-fuelled generators, NUC: Nuclear; ORES: Other Renewables; OTHT: Other non-renewables (combined heat and power); PHOT: solar photovoltaics; WTON: wind onshore.

Source: Own elaboration with data from (ENTSO-E, 2021b).

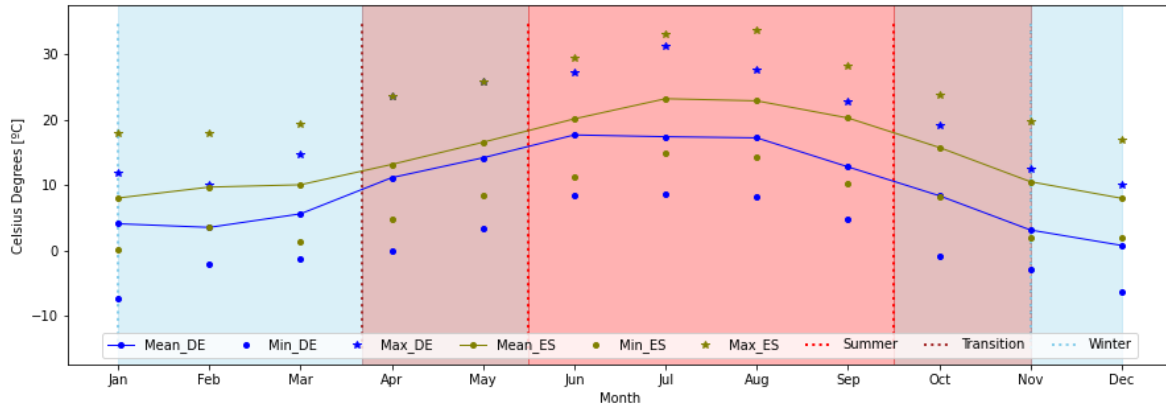
2.1.1 Climatic differences

Hourly geographically aggregated weather data published by the Open Power System Data (Open Power System Data, 2020) is preferred for the local temperature at the Energy community case studies representing both target regions. This dataset is mostly used for national-level simulations to represent the population-weighted mean weather within a given country, but it is used in this case to represent a random location within the target regions. The provided values are aggregated by Renewables.ninja using the NASA MERRA-2 reanalysis as explained by the dataset authors (Open Power System Data, 2020). Hourly temperature values from the year 2007 are used for the base year calculations explained in this report.

As can be seen in the figure below, the reported mean monthly air temperatures for Spain (Mean_ES) are higher than those registered in Germany (Mean_DE) throughout the year; which indicates that the weather in Spain is significantly warmer than in the German case. The regions' temperatures get closer during the first transition season in April and May, when the German values rise considerably, even reaching maximum temperatures (Max_DE) similar to Spain (Max_ES), while the mean values grow apart during the second

transition season as the minimum values registered in Germany (Min_DE) during Autumn get considerably lower after the summer whereas in Spain the temperature drop takes place in winter.

Figure 4. Monthly mean, maximum and minimum air temperature values registered in each target region



Mean_DE: Mean hourly temperature registered per month in Germany; Min_DE: Minimum hourly temperature registered per month in Germany; Max_DE: Maximum hourly temperature registered per month in Germany; Mean_ES: Mean hourly temperature registered per month in Spain; Min_ES: Minimum hourly temperature registered per month in Spain; Max_ES: Maximum hourly temperature registered per month in Spain.

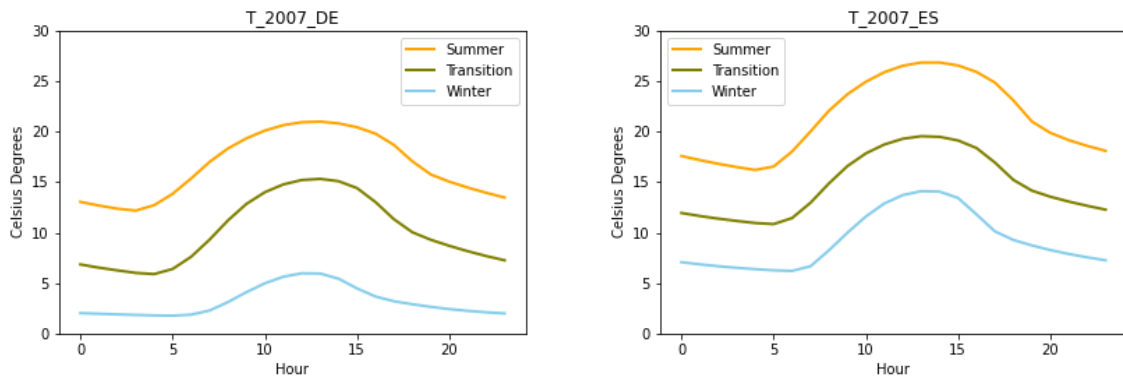
Source: Own elaboration with 2007 data from (Open Power System Data, 2020).

Looking at the mean hourly temperature registered each season (Figure 5), it is notable that mean hourly temperatures in the German case rarely exceed 22°C, even in the summer, whereas in Spain, 22°C are registered most hours of the day in the summer season, reaching values above 25°C around midday. On the contrary, winter mean temperatures in Germany are below 5°C for all hours in winter, while in Spain, all hours registered temperatures above this same value. The observed differences will impact the Cooling Degree Days (CDD) considered for each case and, thus, the electricity demand for space cooling purposes. Similarly, the colder temperatures registered in the German winter season will influence the heat demand calculated for the Energy community archetypes located in this region, which is significantly higher than in Spain that experiences more temperate winters. The summer, winter and transition seasons shown in Figure 5 are defined in accordance with the selected methodology for electricity load modelling as will be explained in Chapter 3.

The differences in the solar irradiation and wind speed resources presented in each region are also observable through the load factor curves for each technology that are used in MODECO to model solar PV and wind speed generation. These curves are part of the European Resource Adequacy Assessment (ERA) 2021 Climatic Database (ENTSO-E, 2022) and are used in the selected ESES reference model to simulate solar and wind generation in each European country. As seen in Figure 6, solar resources are considerably higher in Spain than in Germany, particularly during the winter season when it is cold but with clear skies in the southern country.

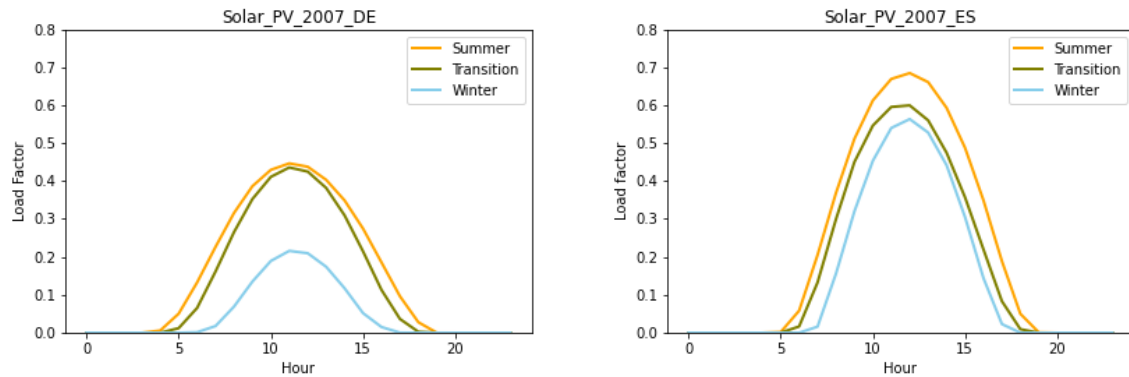
Onshore wind (Figure 7), on the other hand, shows different trends depending on the season. In winter, wind speeds are considerably higher in Germany than Spain as indicated by the load factor curves. However, in the summer and transition periods, wind resources are more favourable in Spain, especially in the evening hours when values increase considerably, which is not the case of the German region, where the load factor curve has less pronounced peaks across all seasons. It must be noted that offshore wind is not considered an available technology within MODECO's Energy community case studies, meaning it is not included in the options available at the communities' investment portfolios. Nonetheless, offshore wind is relevant in Germany's future energy mix as observed in Figure 2 and will impact on its wholesale market prices, which will serve as an economic signal for the defined energy communities in this location.

Figure 5. Mean air temperature per hour registered each season in the analysed regions



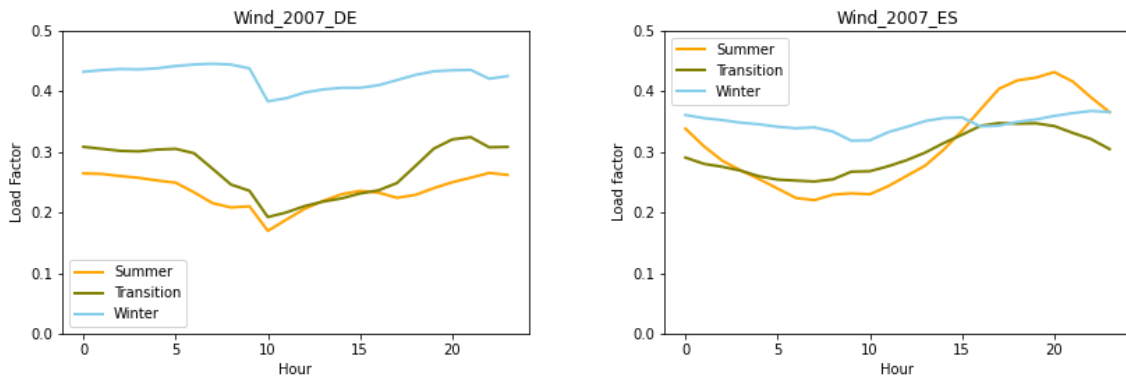
Source: Own elaboration with 2007 data from (Open Power System Data, 2020).

Figure 6. Mean solar load factor per hour registered each season in the analysed regions



Source: Own elaboration with data from (EERA, 2022). Data corresponds to TYNPD market nodes DE07 and ES06.

Figure 7. Mean wind load factor per hour registered each season in the analysed regions



Source: Own elaboration with data from (ENTSO-E, 2022). Data corresponds to TYNPD market nodes DE07 and ES06.

2.1.2 Regionalized cost of capital

In addition to the climatic and energy system difference, different Weighted Average Cost of Capital (WACC) are assumed for the target regions based on the findings of a recent study on renewable energy financing conditions in Europe (Roth et al., 2021). This document draws conclusions from a series of surveys and in-depth interviews with renewable energy project developers, bankers, financial experts and other key stakeholders in the renewable energy financing sector. In general terms, the report found that there are significant differences in the WACC reported in European member states, although an overall reduction in

reported WACC has been observed at the EU level in comparison with previous years (Roth et al., 2021). This does not consider the recent significant increase in material costs resulting from the increase of energy prices and geopolitical instability from certain regions suppliers of important raw materials.

Regarding the two target countries, the report found that Germany is one of the European markets with lowest reported WACC while Spain has an average WACC within Europe. However, Spain is one of the countries with a higher spread between minimum and maximum WACC values, whereas Germany has the narrowest gap. The report associates this trend to the wider range of investors present in the Spanish market, which are characterised by different return expectations (Roth et al., 2021).

From the technologies of interest to MODECO, only PV solar and onshore wind are included in this analysis (wind offshore is not considered in any of the investment options for the Energy community case studies). However, the findings can be extrapolated to other technologies as the WACC varies little from the technological perspective and is mostly dependent on location. This is explained by the study' findings that show that **country risk is the main driver of WACC**, although experience with renewables is also significant (experiences of a country with deployment of renewables tend to reduce cost of capital) (Roth et al., 2021).

In MODECO, the minimum WACC values reported for wind onshore for Spain and Germany in the AURES 2021 study (Roth et al., 2021), which can be seen in the following table, are used as the default discount rate for the investment model. The presented values are the same reported for PV solar in Spain, and that no data for solar is available for Germany. However, the same values are assumed for all technologies as data from countries reporting values for both, PV solar and onshore wind, show strong similarities between both technologies. This might be explained by the reliance on balance sheet financing and the investment portfolio diversification approach taken by some market players, which benefit from applying a more general WACC to different technologies (Roth et al., 2021). To test the effect of using a different discount rate, a sensitivity analysis is run on the German archetypes considering the maximum WACC value instead of the base case.

Table 2. Minimum and maximum WACC values considered for each target region

| Country | Minimum WACC | Maximum WACC |
|---------|--------------|--------------|
| Germany | 1.3% | 2.5% |
| Spain | 3.0% | 9.0% |

Source: Own elaboration with data from (Roth et al., 2021).

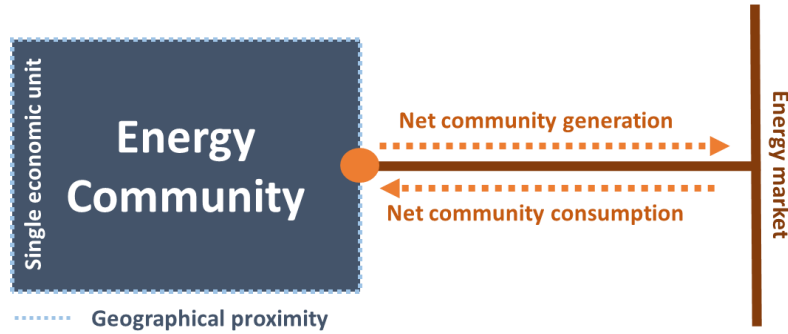
2.2 Definition of Energy community archetypes

As mentioned before, five Energy community archetypes are designed as part of the MODECO initiative, looking to replicate typical contexts found in European communities: **Urban district, Rural town, Business park, Industrial polygon and Virtual community**. All of the proposed Energy community archetypes can be considered Citizen energy communities within the European legislation framework, as gas-fuelled is considered a potential investment.

For those archetypes where geographical proximity is a constraint, it is assumed that all members inside the community are neighbours and interconnected through a shared electrical network (public or private), theoretically considering only one interconnection point with the external energy market (Figure 8). In this way, only the net electricity injected and consumed through this point is considered in the calculations of the obtained revenues for excess energy sold, the energy purchasing expenses and the avoided costs by community thanks to self-consumption.

Although in reality peer-to-peer trading or differentiated internal energy prices could take place among energy community members, these possibilities are not assessed in this work as it is assumed that under perfect market conditions the overall welfare gained by the community remains the same regardless of how this is distributed among members, thus, it is considered that the community acts as a single economic entity. A similar assumption is made for gas, considering that the community buys all gas from a bulk provider to be later distributed among its members at a fixed price. This is relevant in those cases where heat-and-power investments are considered.

Figure 8. Community-energy market interaction considered for all archetypes except the Virtual community

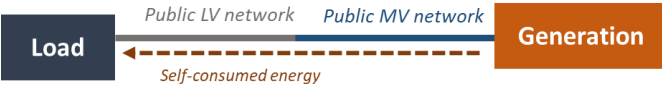
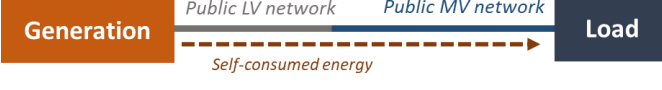


Source: Own elaboration.

In the scenarios in which Use-of-Network tariffs are considered, the Portuguese regulation for self-consumption (*Regulamento do Autoconsumo nº. 8/2021*, RAC 8/2021) is used as inspiration to define the rules applicable within the MODECO analysis (ERSE, 2021). Under the Portuguese regulation, Use-of-Network tariffs applicable to self-consumption through the public network result from the Use-of-Network tariffs applicable to consumption deducted from the tariffs applied to the voltage levels upstream of the generation interconnection voltage. In the occurrence of reverse flows upstream to the generation interconnection level, these are not computed in the Use-of-Network tariffs. Finally, in cases where the generation is interconnected at a voltage level downstream of the load voltage level connection, the tariffs applicable to the self-consumed energy correspond to those applicable to the case where both are at the same voltage, with no reverse flows between voltage levels. The applicable rules from RAC 8/2021 are summarised in Table 3.

In the Urban district, Rural town and Business park archetypes, Case 1 applies as **all non-industrial loads are assumed to be in the low voltage network** and within the same neighbourhood. For the Industrial polygon, Case 2 (Table 3) is used as **industrial users are assumed to be connected at the medium voltage level**. In all these cases, generation assets can only be connected at the same voltage level as the loads due to the assumed geographical vicinity constraints. The **Virtual community** is the only case in which the geographical limits are relaxed as it is assumed that **members and generator assets inside this archetype are not necessarily neighbours**. In this archetype, it is assumed that full Use-of-Network tariffs are applicable to all energy produced and consumed by the community.

Table 3. Summary of the rules applied to self-consumption under the Portuguese normative

| Scheme | Use-of-Network charges applicable to self-consumption |
|--|--|
| Case 1. Load and generation at the same level – LV  | Load network access charges– network usage (MV) – network usage (HV) |
| Case 2. Load and generation at the same level – MV  | Load network access charges –network usage (HV) |
| Case 3. Load and generation at different voltage levels – <i>upstream</i> generation  | Load network access charges –network usage (HV) |
| Case 4. Load and generation at different voltage levels – <i>downstream</i> generation  | Load network access charges– network usage (MV) – network usage (HV) |

*LV = Low Voltage, MV = Medium Voltage, HV = High Voltage

Source: Own elaboration based on RAC 8/2021 (ERSE, 2021).

2.2.1 Number and type of members

The number and type of members considered inside each archetype is defined based on existing European Energy community initiatives and the archetype's intrinsic characteristics; for instance, it is assumed that households in the Urban district archetype are all located in Multi-family buildings. Four general dwelling types are considered within the archetypes design: Multi-family buildings, Single-family buildings, Non-residential buildings, Mixed buildings and Industrial buildings. Non-residential buildings englobe commercial and public dwellings, and Mixed buildings refer to mostly residential dwellings in which the first floor is dedicated to commercial activities. The exact number of households and businesses per building is indicated as part of the Energy community case studies definition and will be described in Chapter 4.

It must be noted that the number and type of buildings considered for each Energy community archetype is the same regardless of the region considered. Nonetheless, different energy consumption patterns are observed for the same Energy community archetype due to regional differences driven by climatic conditions. In particular, energy demand for space heating and cooling is highly dependent on the outdoor temperature registered, which highlights the importance of the temperature data selection in the final results obtained from the case studies simulation. The applicable building types per Energy community archetype are summarized in Table 4.

Table 4. Number and type of building in each archetype for year 2025

| Archetype | Type of buildings* | | | | |
|---------------------------|--------------------|-----|-----|----|----|
| | MFB | SFB | NRB | MB | IB |
| Business park | ✓ | | ✓ | ✓ | |
| Industrial polygon | | | ✓ | | ✓ |
| Rural town | ✓ | ✓ | ✓ | ✓ | |
| Urban district | ✓ | | ✓ | ✓ | |
| Virtual community | ✓ | | ✓ | ✓ | |

*MFB = Multi-family building, SFB = Single-family building, NRB = Non-residential building, MB = Mixed building, IB = Industrial building.
Source: Own elaboration.

2.2.2 Energy carriers

Different energy carriers are considered for each Energy community archetype. **Electricity, natural gas** and **heat** are present in all communities. However, **biomass** is only considered for the Rural town archetype, and **green hydrogen** is assumed to be available only for industrial users. The electricity price assumed by the energy communities are defined based on the economic scenarios described in Section 2.3. Prices for natural gas, biomass and green hydrogen are defined using different sources.

For natural gas, two different prices are considered: **a retail price for the Energy communities**, and a **wholesale price for the gas-driven generators** considered in the wholesale energy market module. The natural gas price for the Energy communities is assumed to **vary on a daily basis** following the behaviour of the price index reported for the Iberian market (MIBGAS-ES index) in 2019 (Mercado Ibérico del Gas, 2020). The daily price vector is adjusted per user using the bi-annual values reported for residential and non-residential consumers in Germany and Spain in Eurostat database (Eurostat, 2022). Finally, the yearly variation in the natural gas price is defined based on the annual gas prices considered in the reference ESES and representing the wholesale price. The retail price vectors are available at the associated database.

The biomass prices are assumed to be mostly stable throughout the year, so only yearly updates are assumed. These are defined based on the projections made by the Heat Roadmap Europe (HRE4, n.d.) initiative for 2030 and 2050 (Duić et al., 2017). Pricing regional differences are considered, assuming that biomass prices in Spain are similar to those reported for Greece as no specific information is provided for this country. The projected values for MODECO cases are summarised in the following table.

Table 5 Biomass prices considered for Germany and Spain in the target years [EUR/MWh]

| Biomass type | Country | 2025 | 2030 | 2040 |
|------------------|----------------|-------|-------|-------|
| Woodchips | Germany | 29.65 | 30.90 | 33.71 |
| | Spain | 26.20 | 27.31 | 29.79 |
| Pellets | Germany | 36.35 | 34.23 | 38.49 |
| | Spain | 36.37 | 38.74 | 38.26 |

Source: Own elaboration with data from (Duić et al., 2017).

Future green hydrogen prices are dependent on the future costs of electricity and electrolyzers, as well as the efficiency levels and the operating lifetime reached by the latter. The cost component with the largest impact on green hydrogen's production cost is the cost of renewable electricity used to power the electrolyser unit, while the second is the electrolyser's investment cost. The International Renewable Energy Agency (IRENA,

2020) projects that **by 2040 green hydrogen could cost² between 25.08 €/MWh³ and 75.26 €/MWh⁴** assuming electricity prices of 21.4 €/MWh and 69.6 €/MWh, respectively. Similarly, the International Energy Agency (IEA, 2020) estimates that by 2050, green hydrogen could cost⁵ between 27.17 €/MWh and 68.96 €/MWh, under electricity prices of 20 €/MWh and 60 €/MWh.

An analysis performed by the International Council on Clean Transportation (ICCT) for the cost of renewable hydrogen towards 2050 estimates future hydrogen production costs by using a discounted cash flow model and three common technologies: Alkaline, Proton Exchange Membrane (PEM) and solid oxide electrolyser. The electrolyser system is assumed to be connected to the grid and consume energy from a renewable energy producer under a PPA agreement. The production cost is calculated per country considering different renewable electricity prices based on projected Levelized Costs of Electricity (LCOE) for wind power generation in 2030 and 2050 (Zhou and Searle, 2022). The resulting hydrogen prices for 2025, 2030 and 2040 are shown in Table 6 for Germany and Spain.

Table 6 Green hydrogen prices for Germany and Spain in the target years [EUR/MWh]

| Country | Original prices | | |
|----------------|-----------------|-------|-------|
| | 2025 | 2030 | 2040 |
| Germany | 29.65 | 30.90 | 33.71 |
| Spain | 26.20 | 27.31 | 29.79 |

Source: Own elaboration with data from (Zhou and Searle, 2022).

The original prices obtained by the ICCT study (Zhou and Searle, 2022) are close to those projected by IRENA (25.08 €/MWh) and IEA (27.17 €/MWh) under optimistic electricity pricing conditions (20-22 €/MWh). From the cost assumptions used in MODECO (see Annex database) the LCOE for wind power in 2025 is 25.53 €/MWh and 31.33 €/MWh for high and low capacity turbines in Germany; while for Spain is 24.94 €/MWh and 30.93 €/MWh, respectively. The LCOE from low-capacity turbines are within the optimistic price scenarios from IEA (2020) and IRENA (2020), which result in similar hydrogen prices to those projected by the ICCT. In 2030 and 2040 the costs from this technology decreases for both technologies, which would result in a downwards trend for hydrogen prices instead of the rising trend proposed by ICCT. Moreover, within MODECO assumptions, solar energy is expected to become a key technology for both regions (Figure 2 and Figure 3), which would indicate that a mix of solar and wind energy costs must be taken into account into the calculation of future hydrogen prices instead of just wind as in the ICCT methodology. Still, the prices shown in Table 6 are considered to be a fair assumption, although in future analysis more robust approaches would be recommended.

2.2.3 Available investment options

The potential investment options shown in Table 7 differ per Energy community archetype based on available resources and available land space. Only investments in renewable energy assets and Combined Heat and Power (CHP) are considered. For some of the technological categories, some sub-categories are defined. The Capital (CAPEX) and Operational (OPEX) expenses associated to wind, solar photovoltaic (PV) and batteries are taken from the cost projections for low-carbon and storage technologies made by the European Joint Research Centre (JRC) (Tsiropoulos et al., 2018b) and the costs for thermal technologies are based on projections made by the HRE4 (n.d.) project. Non-smart chargers and individual heat pumps are considered individual investments made according to expected adoption trends and not decided by the community as a

² The costs are approximately values taken from “Figure ES2. Cost of green hydrogen production as a function of electrolyser deployment, using an average (USD 65/MWh) and a low (USD 20/MWh) electricity price, constant over the period 2020-2050”, available at (IRENA, 2020). As in the original source these are given in USD/kg H₂, values are converted using a Low Heating Value of 51.2 kWh/kg H₂ and a currency value of 1 USD = 1.07 EUR.

³ Electrolyser initial cost of 696 €/kW, discount rate of 8% and a stack lifetime of 80,000 hours (IRENA, 2020).

⁴ Electrolyser initial cost of 1000 €/kW, discount rate of 8% and a stack lifetime of 80,000 hours (IRENA, 2020).

⁵ Hydrogen produced from low-carbon electricity sources reported by (International Energy Agency, 2020) is considered as green hydrogen. To convert to desired units, the same Low Heating Value and currency value from previous calculations are used.

joint investment. The rest of technologies are part of the investment portfolio from which the Energy community can invest based on their expected return under the different economic scenarios evaluated.

Table 7 Technologies considered in each Energy community archetype as potential investment options

| Type | Technology | Characteristics | Archetype | | | | |
|-------------------------|---------------------------------|--|-----------|----------|-------|------------|---------|
| | | | Urban | Business | Rural | Industrial | Virtual |
| Power | Wind Energy | Medium specific capacity (kW/m2), medium hub height (100m) | | | ✓ | | ✓ |
| | | High specific capacity (kW/m2), low hub height (50m) | | | ✓ | ✓ | ✓ |
| | Solar Photovoltaics (PV) | Land PV (utility scale) | | | ✓ | ✓ | ✓ |
| | | Rooftop PV flat surface | ✓ | ✓ | ✓ | ✓ | ✓ |
| | Li-ion batteries | Stationary storage system (energy-designed, C-rate 0.25) | ✓ | ✓ | ✓ | ✓ | ✓ |
| | | Stationary storage system (power-designed, C-rate 2) | ✓ | ✓ | ✓ | ✓ | ✓ |
| | Electrolyzer | PEM | | | | ✓ | |
| Heat & Power | Small CHP | Unidirectional EV charger | ✓ | ✓ | ✓ | ✓ | ✓ |
| | | Bidirectional EV charger | ✓ | ✓ | ✓ | ✓ | ✓ |
| Heat | Heat pumps* | CHP - Biomass (woodchips) | | | ✓ | | |
| | | CHP - Gas engine | ✓ | ✓ | ✓ | ✓ | |
| | | Air-to-air heat pumps | ✓ | ✓ | ✓ | ✓ | ✓ |
| | Boilers* | Air-to-water heat pumps | ✓ | ✓ | ✓ | ✓ | ✓ |
| | | Ground sourced heat pumps | ✓ | ✓ | ✓ | ✓ | ✓ |
| Others | Hydrogen storage | Hydrogen storage | | | | ✓ | |

*Private investments decided exogenously based on assumptions and not as an outcome of the investment model.

Source: Own elaboration.

The proposed costs for solar PV, on-shore wind and Li-ion batteries are compared against those assumed by the references ESES in Table 8. In the data originally reported by JRC for onshore wind and PV solar (Tsiropoulos et al., 2018b), operation and maintenance costs are assumed as a fixed fraction of the CAPEX over the entire lifetime of the technology, and the fraction is based on literature review and expert validation. The report does not specify whether this fraction includes both fixed and variable operation and maintenance costs, but it is assumed it does. The ESES documentation (ENTSO-E, 2020), on the other hand, indicates that

the provided values correspond to “Fixed VOM” or fixed variable operation and maintenance costs, but no further explanation of the concepts included is provided.

Table 8 Comparison of CAPEX and OPEX values proposed by MODECO against ESES’ assumptions for available technologies

| Technology | Source | 2030 | | 2040 | |
|---|--------|------------------|-----------------|------------------|-----------------|
| | | CAPEX [€/kWe] | OPEX [€/kWe] | CAPEX [€/kWe] | OPEX [€/kWe] |
| On-shore wind – Medium specific capacity | JRC | 1,190 | 35.7 | 1,140 | 34.20 |
| | ESES | 1,066 | 21 | 915 | 21 |
| On-shore wind – High specific capacity | JRC | 960 | 28.8 | 920 | 27.6 |
| | ESES | 1,066 | 21 | 915 | 21 |
| Solar PV – Land | JRC | 450 | 7.7 | 370 | 6.29 |
| | ESES | 439 | 9 | 319 | 8 |
| Solar PV – Rooftop | JRC | 500 | 12.5 | 410 | 10.25 |
| | ESES | 439 | 9 | 319 | 8 |
| Li-ion batteries – energy designed | JRC* | 892 | 17.8 | 656 | 13.1 |
| | ESES | 500 | 11 | 379 | 10 |
| Li-ion batteries – power designed | JRC* | 191 | 3.8 | 141 | 2.8 |
| | ESES | 500 | 11 | 379 | 10 |

*Original data was given in €/kWh, but these are converted to €/kWe using the C-rate values. OPEX are assumed to be 2% of the CAPEX as reported by Tsiropoulos et al. (2018a) as no data was provided in Tsiropoulos et al. (2018b).

Source: Own elaboration with data from Tsiropoulos et al. (2018a), Tsiropoulos et al. (2018b) and ENTSO-E (2020).

For on-shore wind, the initial investment costs considered by JRC are slightly higher than those considered in the reference ESES, except for the values projected by 2030 for the high specific capacity model. CAPEX costs are always higher when considering the JRC values for on-shore wind technologies. In the case of solar PV, the investment costs projected by JRC are higher for all cases than the assumptions taken in the reference ESES. Solar OPEX costs assumed by JRC are lower than in the ESES when considering PV installations on land (utility scale), but higher when considering installations over rooftops. Nonetheless, it must be noted that the ESES does not differentiate between systems’ arrangements, and when considering the average OPEX costs for both land and rooftop installations, the obtained values are closer to that reported by the ESES.

As happens with solar PV technologies, the reference ESES does not differentiate between battery types. Thus, the values are higher or lower depending on the specific technology considered as the JRC source offer differentiated values depending on the battery type. For energy-designed storage systems, the CAPEX values projected by JRC are much higher than in the ESES, but for power-designed systems the opposite is true. For OPEX values a similar trend is observed when considering the actual values, but in percentage terms, the operation and maintenance costs considered by the ESES represent close to 2% of the CAPEX as proposed for the JRC values.

The higher disaggregation in the JRC database is preferred for the MODECO analysis as it offers more possibilities for the communities’ investment portfolios, which might result in interesting insights than using the general categories defined in the reference ESES, which were thought for a larger scale (Europe-wide). Moreover, it is considered that the values proposed by JRC do not divert greatly from the ESES assumptions, particularly considering solar and wind energy technologies. Still, the differences between both sources must be taken into account when analysing the results.

The specific cost considered for each year and technology can be consulted in the associated database.

2.3 Economic scenarios

MODECO evaluates how different economic conditions affect the investment and operational decisions of Energy communities under different local and regional contexts that influence the associated costs to electricity consumption. The evaluated energy prices scenarios are based on the results obtained from the wholesale market module developed as part of the project and whose design will be discussed in the final report. Nonetheless, the conceptualization behind each energy pricing scenario and the methodology to calculate them are specified in this report at least in general terms. On the other hand, the approach to set the costs applicable to the network tariff and taxes scenarios considered is explained in this section in addition to its conceptual definition.

To evaluate the impact of different tariff structures on Energy communities' investment decisions, three tariff scenarios (TOU, Peak Power, Bandwidth) are defined considering three different structures for Use-of-Network charges:

- **Energy-based charges (TOU):** Network costs are recovered through the application of a charge based on consumption volume. The applicable charge is different depending on the time of the day as it follows a **Time of Use (TOU)** structure.
- **Peak-power based model (Peak Power):** Use-of-Network costs are charged to users based on their peak power consumption. The charge is applied on a monthly basis
- **Bandwidth model (Bandwidth);** Users pay a fixed fee for a symmetrical kW-band. The subscription allows users to freely used the contracted bandwidth; this fee is set as a monthly cost paid for kW-band contracted. Energy consumed or injected beyond this limit are subjected to a penalization cost that depends on the excess volume and duration.

In all of these cases, **dynamic prices** changing by the hour according to market conditions are considered, and taxes are applied following the applicable rules in each region. To serve as a comparison point, a case without any charges and taxes is also tested (**No Charges**) using dynamic prices. A sensitivity test (**TOU_Flat**) is run for the TOU tariff structure considering the use of an annual flat rate instead of the dynamic prices. For the industrial polygon archetype, a variation of this case is additionally tested, considering that the community has a bilateral contract with a fixed price established for the 16-year period analysed (**TOU_PPA**). The process and assumptions used to calculate each of the tariff components (active energy price, Use-of-Network charges and taxes) are explained in the following sections.

2.3.1 Energy prices calculation

- The **dynamic price** represents the case in which the community buys energy directly from the wholesale market, and thus, the energy price obtained from MODECO's wholesale market modules for Germany and Spain is directly used as input for this case. Thus, the dynamic prices used in scenarios TOU, Bandwidth and Peak Power, as well as the No Charges correspond to the resulting price vector from the UCED model. The **flat rate** can be interpreted as a fixed price contract between an electricity supplier and the community. The flat rate price used in the TOU_Flat scenario is calculated for each year and country as the weighted average from the marginal prices obtained.
- Finally, the **PPA scenario represents a long-term contract**, where the community acquires electricity from a power generator at a fixed price, which is calculated based on a long-term average cost. This scenario is only applied to the Industrial polygon archetype, which is the community type where this type of contracts is expected to be more common. The fixed energy cost applied during the 16-year period is defined considering the fixed and variable operational costs from renewable and efficient gas-based generators⁶ in the wholesale market, including the annualized capital expenditure. The cost data is taken from the database available at the documentation from the TYNDP scenarios published in 2020 (Entso-E, 2021), except for the investment costs for solar, wind and Combined Heat and Power (CHP) that are obtained from (Tsiropoulos et al., 2018b). As a result of this process, active energy costs of 52.44 EUR/MWh and 38.35 EUR/MWh are obtained for Germany and Spain, respectively. As this scenario represents a long-term contract with a generator, the same active energy cost is applied throughout the 16-year period.
- The resulting energy tariffs for each case are presented and discussed in Chapter 6.

2.3.2 Use-of-Network charges

As previously explained, three types of tariffs based on existing and theoretical schemes are tested in MODECO's Energy community archetypes. The first corresponds to the **TOU** scheme, where different prices are set for different periods that can be determined in advance for a determined period (static Time-of-Use) or determined in real time based on actual system conditions (dynamic Time-of-Use) (IRENA, 2019). MODECO's TOU tariff is considered static and has two different pricing periods – peak and off-peak – which

⁶ The specific generation technologies considered for this calculation are solar photovoltaics, concentrated solar power, onshore wind, offshore wind, combined-cycle gas turbines, and combined heat and power. The generic unit that englobes all renewable generators in the selected ESES reference scenario is also included.

are defined for each region based on the regional wholesale module parameters (demand and available generation). The off-peak hours correspond to the time slot with the less system constraints, whereas the peak period is set during the higher congestion hours. The hours' classification is assumed to be known by users in advance and will be updated every five years based on the regional system evolution.

The second tariff scenario consists on a **Peak Power** scheme, where users pay a fixed price based on the maximum power demanded each month (€/kW-peak) as suggested in (Koski et al., 2019). Finally, the **Bandwidth** subscription scenario is based on the bandwidth tariff model proposed by ENEXIS, a Dutch Distributor System Operator in (EDSO, 2020). Under this mode, customers subscribe to a symmetrical kW-band and pay a fixed monthly fee for using the contracted power for both energy injections and withdrawal from the grid. Consumption or feed-in outside the contracted limit is possible, but an exceedance fee must be paid considering the amount of power exceeded and the duration. Thus, the exceedance is set as €/kWh above the contracted power limit. In this sense, not only the energy consumption must be known for the Peak Power Based and Subscription Based scenarios, but also the registered power at each time step.

The Use-of-Network charges considered in each scenario are based on the costs associated with the distribution and transmission networks reported for Germany and Spain. For **transmission costs**, the Unit Transmission Tariffs calculated by ENTSO-E in 2019 are used as a base cost. The defined values are **22.52 €/MWh** for **Germany**, and **9.33 €/MWh** for **Spain** (Entso-E, 2020). It is assumed that all users pay for transmission costs, directly or through their DSO, which passes the cost to its customers via distribution network fees.

Distribution tariffs, on the other side, apply differently to those connected to the distribution grid in Low Voltage (< 1kV), Medium Voltage (1 kV–36 kV) and High Voltage (> 36 kV) level according to the ranges used in (Eurelectric Union of the Electricity Industry, 2013) and based on the values proposed by the European standardisation bodies CEN/CENELEC. The total cost to recover via distribution tariffs is based on the data reported in the Study on tariff design for distribution systems commissioned by the European Commission Directorate General for Energy in 2015 (Ref-e et al., 2015). A more updated version containing similar data could not be found. According to the European Agency for the Cooperation of Energy Regulators (ACER), Spain updated its tariff methodology for the 2020–2025 period and Germany has amended its own constantly, with last changes being introduced in 2019 and 2020 (ACER, 2021). Thus, the numbers used for this analysis are not completely up to date, but present a fair understanding of the cost associated with distribution activities in both countries.

Within MODECO, consumers pay for the costs corresponding to the voltage levels used to supply them electricity. This means that users at the low voltage level (e.g. those in the Business park, Urban district, Rural town and Virtual community) pay for the costs associated to the low voltage, medium voltage and high voltage networks, but users connected at the medium voltage level (Industrial polygon) only pay for the costs associated with the medium and high voltage networks. Thus, it is necessary to disaggregate the total costs to recover per voltage level. This is done by dividing the total allowed revenues – without transmission costs, taxes and levies – between the circuit length corresponding to each level and reported in (Ref-e et al., 2015).

Afterwards, the Unit Distribution Tariff applicable to consumers connected at each level, is calculated by dividing the disaggregated cost to recover between the total electricity flowing into that circuit, this includes the energy delivered into each level plus the energy delivered in upstream circuits. This means that high voltage costs are divided into energy delivered at low, medium and high voltage, but low voltage costs are only allocated among users connected to the low voltage network. As disaggregated electricity delivered data is not available for Germany, the same energy shares per connection point as in Spain is assumed, calculating the corresponding volume per voltage level using the number of connection points and the total electricity delivered reported for the German case. The final distribution costs to recover and the resulting Unit Distribution Tariff per country and voltage level are summarized below.

Table 9 Regional data used to calculate the applicable Unit Distribution Tariff per voltage level

| Country | Voltage level | Connection Points | Circuit length [km] | Electricity delivered [MWh/year] | Cost to recover [€/year] | Unit Distribution Tariff [€/MWh] |
|---------|---------------|-------------------|---------------------|----------------------------------|--------------------------|----------------------------------|
| Germany | HV | 3,923 | 31,380 | 98,380,118 | 586,251,250 | 1.25 |

| Country | Voltage level | Connection Points | Circuit length [km] | Electricity delivered [MWh/year] | Cost to recover [€/year] | Unit Distribution Tariff [€/MWh] |
|--------------|---------------|-------------------|---------------------|----------------------------------|--------------------------|----------------------------------|
| | MV | 72,336 | 280,345 | 141,587,507 | 5,237,495,429 | 21.83 |
| | LV | 39,714,305 | 383,202 | 229,632,375 | 7,159,102,975 | 31.18 |
| | Total | 49,934,777 | 694,927 | 469,600,000 | 12,982,849,654 | - |
| Spain | HV | 2,572 | 96,084 | 49,127,000 | 276,343,969 | 1.18 |
| | MV | 105,591 | 509,866 | 70,703,000 | 1,466,408,498 | 12.24 |
| | LV | 28,592,609 | 1,156,785 | 114,669,000 | 3,326,990,532 | 29.01 |
| | Total | 28,700,772 | 1,762,735 | 234,499,000 | 5,069,743,000 | - |

Source: Own elaboration with data from (Ref-e et al., 2015).

Within MODECO, a community in **Germany** that is connected at the low voltage level would pay Use-of-Network tariffs equivalent to the sum of the Unit Distribution Tariff (low, medium and high voltage) plus the Unit Transmission Tariff. This is equivalent to paying 76.77 €/MWh or **7.68 €cents/kWh**, which is close to the 7.71 €cents/kWh reported to be paid by German households in 2020 (BDEW, 2020). For **Spain**, the network tariffs for low voltage users would be 42.43 €/MWh or **4.24 €cents/kWh**; this value, however, is not directly comparable to existing prices as Spain recovers its network costs through a combination of energy and power-based charges (ACER, 2021).

The values obtained through this process and shown in Table 9 are used to define the applicable charges in each of the network tariff scenarios evaluated in this study. The specific methodology followed in each case is explained in the following sections.

2.3.2.1 Time-of-Use tariff

As explained, TOU tariffs are energy-based charges that have different values depending on the time of the day. The peak and off-peak periods are defined for 2025, 2030, 2035 and 2040, considering five-year updates. For each year, the following steps are applied, differentiating between target regions:

1. Per each hour of the day, the difference between demand and available renewable generation is calculated, identified as “residual demand”.
2. The mean residual demand per hour registered during each season (i.e. winter, transition, summer) is calculated.
3. For each season, the 8 hours of the day with the largest mean values are classified as “peak” and the rest as “off-peak”.
4. The demand registered during peak and off-peak hours is added for the entire year to identify the total demand share associated with each period.
5. The total costs to recover per voltage level (Table 9) are divided into “peak costs” and “off-peak costs” depending on the demand share corresponding to each period and calculated in the step before. The same is done to the electricity delivered per voltage level.
6. Finally, the costs are allocated considering the principle used in (Li et al., 2022) to define Time-of-Use tariffs for an integrated community energy system, which states that the costs of satisfying base demand (“off-peak” in this case) should be allocated to both periods while the costs of satisfying peak demand should be allocated to peak hours only. For instance, a consumer connected to the low voltage network would pay the following distribution tariffs for unit of consumption (€/MWh) during peak and off-peak hours:

Eq. 1 Use-of-Network charges applicable to users in medium voltage networks during off-peak hours

$$Tariff_{off-peak} = \frac{Dist. Costs_{LV,off-peak}}{Electricity Delivered_{LV}} + \frac{Dist. Costs_{MV,off-peak}}{Electricity Delivered_{MV}} + \frac{Dist. Costs_{HV,off-peak}}{Electricity Delivered_{HV}}$$

Eq. 2 Use-of-Network charges applicable to users in medium voltage networks during peak hours

$$Tariff_{peak} = \frac{Dist. Costs_{LV,off-peak}}{Electricity Delivered_{LV}} + \frac{Dist. Costs_{MV,off-peak}}{Electricity Delivered_{MV}} + \frac{Dist. Costs_{HV,off-peak}}{Electricity Delivered_{HV}} \\ + \frac{Dist. Costs_{LV,peak}}{Electricity Delivered_{LV,peak}} + \frac{Dist. Costs_{MV,peak}}{Electricity Delivered_{MV,peak}} + \frac{Dist. Costs_{HV,peak}}{Electricity Delivered_{HV,peak}}$$

The value of the charges applied during peak and off-peak hours are the same through the year, but the hours classified as peak and off-peak vary according to the season. The resulting values from this process will be discussed in the final report, in alignment with the inputs considered for the wholesale market module. Nonetheless, the steps to calculate the applicable costs per period ensure that these are differentiated and that Use-of-Network tariffs in peak hours are more expensive than in off-peak time slots.

2.3.2.2 Peak power tariff

Under this scenario, network costs are recovered through a **capacity-based charge** (€/kWe) that is applied over the maximum power registered by each user during the billing period (assumed as one month). Thus, for this case, it is necessary to transform the estimated Unit Transmission Tariff and Unit Distribution Tariff charges into capacity-based values. In this case, it is defined that the price per kWe is the same for users connected in low voltage than in medium or high voltage. Per each voltage level, the applicable charge per kWe is calculated using the assigned costs to recover, the number of connection points and the typical contractual powers defined by (Ref-e et al., 2015) for the following customer groups: households (6 kW), users in medium voltage (220 kW) and large industrial users (400 kW). The first are assigned to the low voltage category, the second to the medium voltage level and the last to the high voltage level. The obtained costs per kWe are defined below.

Table 10 Applicable capacity-based charges per country and voltage level.

| Country | Voltage level* | Connection Points | Typical contracted power considered [kW] | Capacity-based charge [€/kW-month] |
|---------|----------------|-------------------|--|------------------------------------|
| Germany | HV | 3,923 | 6 kW | 3.11 |
| | MV | 72,336 | 220 kW | 30.53 |
| | LV | 39,714,305 | 4000 kW | 33.04 |
| Spain | HV | 2,572 | 6 kW | 2.24 |
| | MV | 105,591 | 220 kW | 7.50 |
| | LV | 28,592,609 | 4000 kW | 9.11 |

*LV = Low Voltage, MV = Medium Voltage, HV = High Voltage

Source: Own elaboration with data from (Ref-e et al., 2015)

2.3.2.3 Bandwidth tariff

The bandwidth tariff scheme consists of a fixed price per month that customers pay and allows them to inject and extract energy from the public network. When this limit is surpassed, a penalization fee (€/kWh) is applied considering the amount and duration of the power exceeded. As it is assumed that users try to avoid penalization fees, the applicable charges per kWe contracted must be enough to recover the applicable network costs. Thus, the charged values are defined considering the cost to recover on a monthly basis and

the number of connection points at each voltage level, whereas the penalization fees are defined as equal to the sum of the applicable Unit Transmission Tariff and Unit Distribution Tariff. The proposed values per region and voltage level are defined in the table below:

Table 11 Applicable contracted bandwidth cost and penalization fees per country and voltage level.

| Country | Voltage level | Connection Points | Contracted bandwidth cost [€/kWe month] | Penalization fees [€/kWh] |
|---------|---------------|-------------------|---|---------------------------|
| Germany | HV | 3,923 | 12.45 | 0.024 |
| | MV | 72,336 | 18.49 | 0.046 |
| | LV | 39,714,305 | 18.50 | 0.077 |
| Spain | HV | 2,572 | 8.95 | 0.011 |
| | MV | 105,591 | 10.11 | 0.023 |
| | LV | 28,592,609 | 10.12 | 0.052 |

*LV = Low Voltage, MV = Medium Voltage, HV = High Voltage

Source: Own elaboration with data from (Ref-e et al., 2015)

2.3.3 Taxes

Energy taxes are considered excise taxes as these are paid by the seller but passed to the buyers as part of the final cost. Excise taxes come in two forms, *ad valorem* and *per unit*, which will be evaluated as part of MODECO economic scenarios. *Ad valorem* taxes are levied as a percentage of the good's value, whereas *in the per unit* option these are paid per unit of a good sold (Lyndon et al., 2020). Two general energy taxes types are considered in this analysis following the classification proposed by the Organization for Economic Cooperation and Development (OECD, 2020)(Organisation for the Economic Cooperation and Development (OECD), 2020):

- **Fuel excise tax:** All excise taxes that are levied on fuels and that are not carbon taxes.
- **Electricity excise tax:** All excise taxes that are levied on electricity.

In the case of fuel excise taxes, different values are defined per energy carrier according to the current taxes imposed on each fuel in Germany and Spain. The values considered to define the theoretical taxes are based on the OECD's estimations that are set in *per unit* basis (€/GJ) and are in turn calculated considering the applicable normative in each country and the energy content of the taxed products, to have a comparable value for all energy sources (OECD, 2020).

In Spain, the main applicable taxes on energy usage are the **Tax on Hydrocarbons** (*per unit*) that applies to liquid and gaseous fuels, including bio fuels, as well as to coal tar, crude oil, waste oils and coal and coke-related gases; the **Special Tax on Coal** (*per unit*), which applies to coal and coke products except for peat; and the **Special Tax on Electricity**, an *ad valorem* tax applied to electricity consumption by end users. Industrial cogeneration is also subjected to the latter tax (OECD, 2019b), but it is not the case for MODECO's industrial communities. For Germany, only two taxes are considered, the **Energy Tax** (*per unit*) applicable to specific uses of liquid, gaseous and solid fuels and biofuels and the **Electricity Tax** (*per unit*), which is charged to certain electricity consumption usages (OECD, 2019a).

For all evaluated scenarios, except the No Charges case, the current situation in each country is considered. This means that for Spain, *per unit* taxes are applied to fuels while electricity is taxed via an *ad valorem* charge. In Germany, both, fuels and electricity are taxed using *per unit* charges. The applicable charges to each energy carrier are defined based on the OECD tax report for 2019, where effective energy tax rates in €/GJ are calculated for member countries – including Germany and Spain – using data on actual taxation schemes and total energy consumptions per energy carrier (OECD, 2020). The applicable values used in this

report for natural gas and electricity are listed in the table below. It must be noted that, as happened with the natural gas prices, taxes on this fuel are differentiated per final usage.

Table 12 *Per unit* taxes applicable to energy carriers of interest according to OECD data.

| Energy carrier | Usage | Germany | Spain |
|--------------------|-------------------------------------|-----------|------------|
| Electricity | Residential, commercial, industrial | 2.85 €/GJ | 1.44 €/GJ* |
| Natural gas | Residential, commercial | 1.53 €/GJ | 0.65 €/GJ |
| Natural gas | Industrial | 0.60 €/GJ | 0.30 €/GJ |

* Not used in the final scenario; substituted for an *ad valorem* tax of 5.11%

Source: Own elaboration with data from OECD (2020).

To incorporate the *ad valorem* tax in the Spanish case, the *per unit* value tax shown in Table 12 is substituted by a charge of 5.11% calculated on the total energy costs paid by the user, which corresponds to the actual tax currently in place in Spain. This is applied over the cost of energy consumed plus the power-based costs in the scenarios in which these are considered (bandwidth and peak power-based). By using the proposed *ad valorem* tax, the annual amount of money recovered via taxes stays similar as in the *per unit* case (calculated considering the total amount of energy consumed and the mean electricity price charged to residential and non-residential consumers (Eurostat, 2022)). This was expected as the OECD's values used for the *per unit* taxes are based on the actual revenues collected by existing energy taxes in Germany and Spain (OECD, 2020).

3 Modelling of Energy communities

This chapter focuses on the definition and modelling of the case studies representing the defined Energy community archetypes for the two target regions (Germany and Spain). The methodology to model the communities' electricity and heat demand, accounting for the weather differences between the selected target regions is explained in the following section. Additionally, further details are provided for the modelling of Electric Vehicles (EV) and Heat Pumps (HP), and the consideration of these assets' demand response potential. The results obtained from this process are used as inputs in the operational and investment models developed as part of MODECO and are presented and discussed in Chapter 5, following the description of the optimization models in Chapter 4.

3.1 Energy demand simulation

In MODECO project, the **electricity base load** refers to the electricity demand from users related to heating or EV usage, as the latter are modelled separately and added to the baseload demand to get the community's **final electricity consumption**. The purpose of having disaggregated demand for electrical heating and EV is to account for their potential usage for demand response services, which are considered in the operational and investment models. Due to the mathematical formulation used to represent demand response and smart EV charging, the models require visibility over the electrical consumption associated to these assets to perform this task. As described in the next sections, different methodologies are applied according to the type of user considered (residential, non-residential, and industrial). The reasons for this are the different energy-weather relations and the lack of in-depth information for industrial consumers. Similarly, **heat demand** refers to all the thermal energy consumed by the users for space and water heating services, independently of the heat source. Later, it is assumed that a part of this heat demand is served by electrical heat pumps while the rest is obtained by gas-driven equipment. As happened with the electricity baseload modelling, different methodologies are applied to non-residential and residential buildings, and to industrial users, as information on the latter is scarce.

3.1.1 Non-residential and residential users

Energy demand from residential and non-residential buildings has been widely studied in the literature. Thus, a number of open data and detailed models are available to simulate electricity and heat demand from these users. In particular, detailed models representing different typologies of residential and non-residential consumers in Germany are found useful to MODECO purposes. Nonetheless, as these models are built for colder climates, adjustments are needed to incorporate the effect of space cooling, which is relevant in the case of warmer regions such as Spain. The implementation of the German models in the corresponding Energy community archetypes, including the proposed adjustments for the Spanish case, are explained below.

3.1.1.1 Electrical baseload demand

The load shape for non-residential and residential (Multi-family and Single-family) buildings are based on the electrical standard load profiles developed by the German Association of Energy and Water Industries⁷ (BDEW, 2017) that represent different customer groups (Table 13) for which similar consumption behaviours can be assumed. As the electrical standard load profiles were built based on consumption data from German customers, it is assumed that electricity usage for heating and cooling is not considered, as heat demand is practically fully covered by fossil fuels (Entranze Project, 2008) and cooling demand is minimal as shown by the European Building Stock Observatory's data on energy consumption of space cooling by member state (European Commission, n.d.-b).

⁷ In German: Bundesverband der Energie-und Wasserwirtschaft.

Table 13 Type of customer represented in the electrical standard load profiles developed by BDEW

| Profile | Customer group description | Examples |
|-----------|---|---|
| H0 | Private households. | Private households. |
| G0 | General purpose industrial profile, defined as a weighted mean of all commercial customers. | Assigned if none of the profiles G1 to G6 apply. |
| G1 | Industrial profile for businesses which operate on weekdays from 8 to 18 o'clock. | Offices, workshops, kindergartens, public administration facilities, doctor's office |
| G2 | Industrial profile for businesses which operate mostly during the evening. | Street lights, gas stations, evening restaurants and recreational facilities (if their peak consumption is not during the weekend). |
| G3 | Industrial profile for continuous, relatively uniform demand, including a noticeable, continuous peak demand. | Purification plants, drinking water pumps, communal facilities in residential complexes, cold storage warehouses. |
| G4 | Industrial profile for continuous, relatively uniform demand, including a noticeable, continuous peak demand. | Shops, hairdressers. |
| G5 | Industrial profile for bakeries with baking in house which typically start operating at 3 o'clock during weekdays and at midnight on Saturdays. | Bakeries with in-house baking facilities. |
| G6 | Industrial profile for businesses with a strong consumption focus during weekends. | Youth clubs, cinemas, restaurants, petrol stations |
| L0 | General purpose agricultural profile, defined as a weighted mean of all agricultural customers. | Assigned if the energy provider does not differentiate between agricultural customers according to the profiles L1 and L2. |
| L1 | Agricultural profile for dairy farms and side-line stockbreeding businesses. | Dairy farms, side-line stockbreeding farms |
| L2 | Agricultural profile for businesses with a mixture of household and farming. | Assigned if neither L1 nor time-of-the-day-independent industrial profiles apply. |

Source: Translated English version from the table reported by Bock (2019).

Each of the electrical standard load profiles listed above contains 9 representative daily curves for three day types – weekday, Saturday, Sunday – and 3 seasons: “Winter”, “Summer” and “Transition”. As power (kW) data is provided using 15-minute time steps, hourly electricity consumption is calculated before building a yearly vector. The representative daily curves are adjusted considering that the base year starts on Monday and each season covers the following periods as done in the BDEW’s H0 example (BDEW, 2017):

- 1st January to 20th March – “Winter”
- 21st March to 14th May – “Transition”
- 15th May to 14th September – “Summer”
- 15th September to 31st October – “Transition”
- 1st November to 31st December – “Winter”

National holidays are not taken into account in this process.

Once the yearly vector is formed, the data is normalized and multiplied by the corresponding annual electricity consumption in kilowatt-hour. For Multi-family and Single-family buildings, the annual demand (Table 14) is based on the households' mean electricity demand reported for Spain and Germany, and differentiated between multifamily and Single-family units. The mean annual consumption per household in both countries was obtained from the Spanish Transmission System Operator (Red Eléctrica de España, n.d.), and from the German Federal Statistical Office (German Federal Statistical Office, 2020), respectively. To differentiate between households in Single-family and Multi-family buildings, it is assumed that the latter have an annual consumption 7% lower than the national average while Multi-family units had a consumption 16% larger, assuming a similar relation to that reported in the SECH-SPAHOUSEC project, a national-level analysis performed in Spain in 2011 (Proyecto SECH-SPAHOUSEC, 2011). In the case of Spain, the estimated demand for space cooling is subtracted from the base load value as this will be allocated later. Considering the data reported by SECH-SPAHOUSEC, this demand is considered as 5% of the annual electricity demand.

Table 14 Annual electricity demand from Single-family and Multi-family units without considering space cooling

| Country | National average | Single-family units | Multi-family units |
|----------------|------------------|---------------------|--------------------|
| Germany | 3,113 kWh/year | 3,611 kWh/year | 2,895 kWh/year |
| Spain | 3,108 kWh/year | 3,606 kWh/year | 2,890 kWh/year |

Source: Own elaboration with data from Red Eléctrica de España (n.d.); German Federal Statistical Office (2020) and Proyecto SECH-SPAHOUSEC (2011).

For Single-family *buildings* the yearly demand is equal to the set value for Single-family *units*, whereas demand for Mixed buildings and Multi-family buildings is obtained by multiplying the value for Multi-family units by the number of households assigned to each building.

For non-residential buildings, a different approach is needed as energy demand varies greatly depending on the economic sector considered. As no comprehensive data was found for Spain or Germany, the results from a study conducted in Hellenic non-residential dwellings (Droutsa et al., 2020) was used as a reference to define yearly electricity demands for the Non-residential buildings considered in each archetype. This reference provides a database with Energy Use Intensity (EUI) values – provided in kWh/m² – for different building types, differentiating among energy usage for heating, cooling, domestic water heating and lighting. For the construction of the electricity base load, the EUI values for lighting are used as a reference. No regional differentiation is considered. The EUI values for the different building types can be consulted in the attached database.

3.1.1.2 Adjustment for space cooling demand in Spain

As the used load shapes are based on consumption data from German customers, electricity usage for space cooling is not clearly incorporated, which results in a lower summer consumption than expected for the Spanish case studies. Thus, a correction method is used to incorporate this consumption in the modelled communities' electricity baseload demand. First, CDD are calculated for the base year, following Eq. 3 from Eurostat methodology (Eurostat, 2021) and a $T_{Baseline}$ of 22°C as considered by the European Environment Agency (Crespi et al., 2020), and being suitable for Spain as reported by (Pablo-Romero et al., 2021).

Eq. 3 Calculation of Cooling Degree Days

$$\text{If } T_D \geq T_{Baseline} \text{ Then } [\text{CDD} = T_D - T_{Baseline}], \text{ Else } [\text{CDD} = 0]$$

The daily mean air temperature (T_D) is calculated for each day using the corresponding 24 hourly values reported in the input weather data for each region. The daily CDD results obtained from .

Eq. 3 are then added to obtain the total CDD registered in the base year (CDD_{Spain}). This value is used to estimate El_{Spain} , the specific electricity demand in kWh per square meter of fully cooled floor area in the non-residential buildings considered in the Spanish case studies, using a linear equation proposed in (Aebischer et al., 2007) for locations in temperate and Mediterranean cities (Eq. 4).

Eq. 4 Specific electricity demand for fully cooled floor areas in kWh/m²

$$El_{Spain} = 12.7 + 0.013 * \text{CDD}_{Spain}$$

As not all the area in non-residential buildings is fully cooled, the obtained El_{Spain} value is adjusted for each building using the reported EUI values for space cooling in the Hellenic buildings database (Droutsas et al., 2020). This is done by assuming that the building type with the highest EUI for space cooling has a 70% share of its area fully cooled (SC_{share}) – which is the maximum value reported in (Aebischer et al., 2007) for Non-residential dwellings – and the rest are adjusted accordingly. In this way, the yearly electricity demand for space cooling in Non-residential buildings ($El_{space_cooling}$) is estimated using the resulting values, the floor area (Area in m^2) and the number of floors per dwelling (N_{Floors}), as shown in Eq. 5.

Eq. 5 Electricity demand for space cooling in Spanish buildings

$$El_{Spain_cooling} = El_{Spain} * SC_{share} * N_{floors} * Area$$

The space cooling demand per dwelling is allocated through the users' yearly vector by assigning a share of the annual demand to each day, proportional to the daily CDD registered by applying Eq. 3. For households, the same process is applied but the annual electricity demand for space cooling is estimated based on the data reported in the SECH-SPAHOUSEC (2011) and set as 5% of the total household electricity demand as explained before. For Single-family units the electricity usage for space cooling is estimated as 190 kWh/year and for Multi-family units, 152 kWh/year.

3.1.1.3 Heat demand

The heat demand of the non-residential and residential users is modelled by adapting the 2006 guidelines (BGW, 2006) and the gas standard load profiles methodology defined by the German Federation of the Gas and Water Industry (BGW) and the German Association of Local Utilities (VKU) in 2016 (BDEW, 2016). The 2016 methodology uses Eq. 6 to calculate the daily heat demand for a given customer, using the consumer's expected daily consumption⁸ (KW), the corresponding h-Wert or h-value – $h(\theta)$ – and a weekday factor (F) to adjust daily consumption according to the day of the week. The weekday factors provided in the methodological guidelines are differentiated by building category and can be consulted in MODECO's database.

Eq. 6 Daily heat demand for a given customer

$$Q_{day}(\theta) = KW * h(\theta) * F$$

The customer value, KW, is calculated using the user's specific consumption between two meter readings, usually corresponding to monthly or bi-monthly consumption, and the h-values registered during this same period. As there is no monthly or bimonthly information available regarding typical buildings heat consumption, the KW value is set to one. Later the vector is normalized and adjusted to the heat annual demand for each consumer, which can be more easily accessed.

To obtain the h-value, Eq. 7 is applied considering the original sigmoid function and the linear function added to the original methodology in 2016 to improve demand distribution during the year. The coefficients A, B, C, D, m_H y b_H are given for the different building types listed in Table 15. To align these values with the electrical standard load profiles used for the definition of the electrical baseload demand, each building considered in the Energy community case studies must be assigned a building category and a standard load profile. The applicable coefficients to each building type can be consulted in the associated database. The original methodology provides different coefficients for buildings located in windy and no windy locations. For MODECO, it is assumed that all Energy community case studies are located in windy locations (meaning average wind speeds above 4 m/s) and only those values are presented in Annexes.

Eq. 7 Calculation of the h-Wert or h-value using a mix from the sigmoid and linear functions

$$h(\theta) = \left[\frac{A}{1 + (\frac{B}{\theta - \theta_0})^c} \right] + \left[\max \left\{ \begin{array}{l} m_H * \theta + b_H \\ m_W * \theta + b_W \end{array} \right\} \right] + D$$

⁸ The customer value (KW) must be specified individually for each consumer (metering point) based on actual metered consumption and related temperature data. The methodology specifies that KW values must be calculated for an average daily temperature of 8°C when the h-value is equal to 1 (BDEW, 2016).

Table 15 Building types considered in the gas standard load profiles methodology

| Category | Building type description |
|------------|---|
| EFH | Single-family building. |
| MFH | Multi-family building. |
| GMK | Buildings in the metal and automotive sector. |
| GHA | Retail and wholesale. |
| GKO | Local authorities, credit institutions and insurance companies. |
| GBD | Other operational services. |
| GGA | Restaurants. |
| GBH | Accommodations. |
| GWA | Laundries, dry cleaning. |
| GGB | Horticulture. |
| GBA | Bakery. |
| GPD | Paper and printing. |
| GMF | Household-like business enterprises. |
| GHD | Total load profile for Non-residential buildings. |

Source: Translated English version from the table in (BDEW , 2016).

To account for the thermal inertia in the sigmoid function part of the h-value equation, the geometric series approach (Eq. 8) is used, while the mean daily temperatures (T_D , T_{D-1} , T_{D-2} , T_{D-3}) are obtained using the 24 hour values for each corresponding day as done to calculate the daily CDD. The reference temperature (θ_0) is defined as 40°C as in the original methodology.

Eq. 8 Temperature geometric series

$$\theta = \frac{T_D + 0.5 * T_{D-1} + 0.25 * T_{D-2} + 0.125 * T_{D-3}}{1 + 0.5 + 0.25 + 0.125}$$

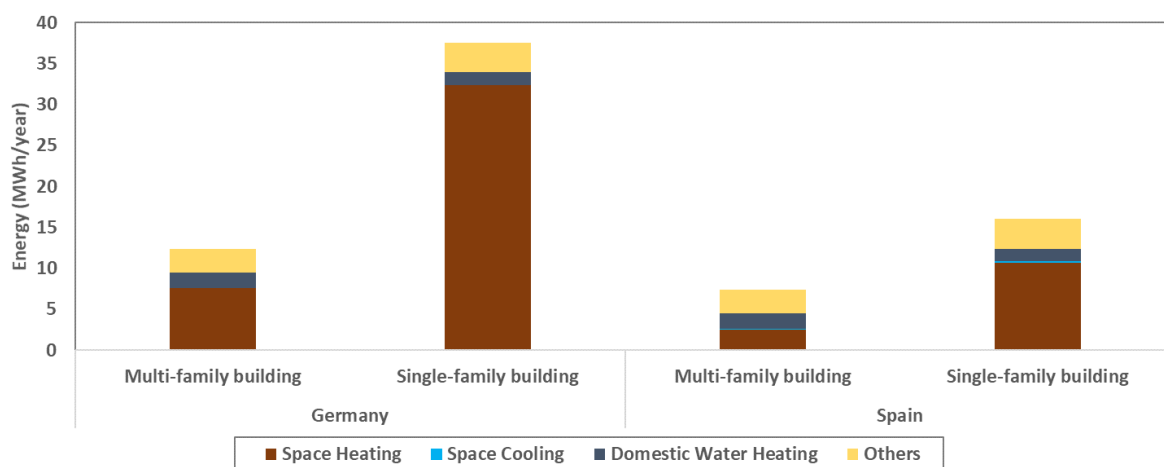
The intraday consumption is modelled by using the hourly factors (SF) defined for each building category in the gas standard load profiles methodology and provided in the 2006 documentation from BGW (BGW, 2006). In this previous version, there were 11 classes considered for residential buildings representing the percentage of old (built prior to 1978) and new buildings (built after 1978) present in the area whose heat demand is being modelled. As the 2016 methodology applied in MODECO does not contemplate these categories, the hourly factors for class 11 – corresponding to the German average – were considered for all residential members. The hourly factors are also differentiated by the temperature range in which the daily mean temperature is located. The exact values applicable to each building category and temperature range can be consulted in MODECO's database.

Finally, the resulting vector is normalized and adjusted to the building's annual heat demand in kWh_{th}/year. For Spanish households, the annual heat demand is set assuming the same shares per usage – Space Heating

(SH), Domestic Water Heating (DWH), Space Cooling (SC), and Others – as reported by the Spanish government in 2011 for households in Single-family and Multi-family buildings (IDAE, 2014). **For German residential buildings, it is assumed that space heating demand is 3.04 larger than in Spain** given the space heating unit consumption per dwelling reported for both countries in the Entranze Project database (Entranze Project, 2008), and that heat demand for domestic water heating is similar to Spanish households. The final values resulting from this process are shown in Figure 9, and can be consulted in the Annex data.

The obtained values for Germany were compared against the shares of space and domestic water heating in total residential consumption reported by the Entranze Project (Entranze Project, 2008). To do so, the weighted national average was calculated considering the number of Single-family and Multi-family buildings reported in the same source. This calculation showed that the suggested total heat demands are representative for the German national average, although demand for space heating seems to be slightly overestimated.

Figure 9. Annual energy consumption in MWh/year per household (Single-family and Multi-Family buildings) and region disaggregated by end usage



Source: Own elaboration with data from Entranze Project (2008) and Proyecto SECH-SPAHOUSEC (2011).

For Non-residential buildings, the EUI values for space and domestic water heating reported in the Hellenic building database was used as a reference to define the annual heat demand values for each case. As Greece (GR) has lower Heating Degree Days (HDD) than Spain or Germany, the values are adjusted with a similar approach to that used by (Aebischer et al., 2007) to account for heat demand under different HDD conditions using Eq. 9. As can be seen, the specific heat demand per Hellenic building type ($EUI_{Heat, GR}$) – equal to the sum of the specific energy demand for space heating ($EUI_{SH, GR}$) and domestic water heating ($EUI_{DWH, GR}$) – is adjusted considering the share of the building's heat demand that varies proportionally to the number of HDD ($\alpha_{Building}$) and the HDD in Greece and the target region. This share is roughly estimated by dividing EUI_{SH} by the specific energy demand for DHW, as water heating is less dependent on climatic conditions as stated in (Aebischer et al., 2007).

Eq. 9 Calculation of specific heat demand for space heating in kWh/m²

$$EUI_{Heat, Location} = EUI_{Heat, GR} * \alpha_{Building} * \left(\frac{HDD_{Location}}{HDD_{GR} - 1} \right)$$

The HDD for each location – including Greece – are calculated using Eq. 10 from the Eurostat methodology (Eurostat, 2021) with a $T_{Baseline}$ of 15.5°C as indicated by the European Environmental Agency (Crespi et al., 2020), and the weather data from the Open Power System Data (Open Power System Data, 2020) used in other calculations and presented in Section 2.1.1.

Eq. 10 Calculation of Heating Degree Days

$$\text{If } T_D \leq T_{Baseline} \text{ Then } [\text{HDD} = (T_{Baseline} - T_D)] \text{ Else } [\text{HDD} = 0]$$

3.1.2 Industrial users

Heat consumption in industrial processes differs from customer to customer as there are a wide range of individual needs for process, water and space heating. Consequently, industrial heat load profiles are more diverse than for residential and Non-residential buildings, having users with nearly constant demand throughout the year to load profiles with significant seasonality (Jesper et al., 2021). Moreover, unlike residential and non-residential dwellings, recent data indicates that there is no generalized relation between heat and electricity usage in industrial consumers as this relation depends on the type of process itself. For industries with a high proportion of ambient temperature independent (process) heat demand, there seems to be a correlation between both energy carriers. However, for consumers whose heat demand is highly dependent on ambient temperature, little or no correlation between both carriers exist (Jesper et al., 2022).

Consumers whose heat demand depends on ambient temperature are most frequent even in the secondary sector, for instance, manufacturing and assembly of goods such as wood furniture manufacturers. Industries in which space heating is a relevant heat sink are usually within this category. On the contrary, some economic divisions like basic metals or the food industry are not influenced significantly by ambient temperature due to the nature of their processes. For instance, the first **requires high temperatures (> 500 °C)** that are practically not affected by ambient temperature changes, while food industries rely on hot water for most of its processes (e.g. cooking, cleaning, steaming, sterilization, and hot water) that, as explained previously, are temperature independent (Jesper et al., 2021).

Considering the above, separate methodologies are used for modelling the energy demand of industrial users depending on their process type. For users with ambient temperature dependent processes, a methodology to calculate heat demand based on ambient temperature is proposed to maintain a regional differentiation between communities in Spain and Germany. This means that the profiles generated for this type of users are specific to each target region. Hourly electricity demand is taken from real users' data as little or no relation between both is assumed for this type of customers.

On the other hand, users with heat demand not affected by ambient temperature are modelled based on an existing database, called JERICHO-E, that provides estimated hourly energy consumption data for seven energy intensive industries in Germany (Priesmann et al., 2021). Both, process heat and electricity demand are taken from this database to ensure a relation is maintained between both carriers as field data seems to corroborate (Jesper et al., 2022). Demand for space heating and cooling is modelled separately considering these are temperature-related and they can be served by electrical heat pumps. The consideration of these users in the Industrial Polygon, the only archetype in which they are included, is relevant for MODECO as this type of industries – chemical and refineries, steel manufacturers, other industries with high heating requirements – are expected to be the main consumers of green hydrogen (IRENA, 2022).

More details about the methodologies proposed for both types of industrial customers is provided in the next sections.

3.1.2.1 Ambient temperature dependent users

The total annual electricity demand for the industrial users within this category is defined based on an open data set of 50 small and mid-size enterprises with industrial operations in Germany. This dataset contains 15-minute power data for an entire year, so hourly energy values are calculated before being introduced in the model (Brauer, 2020). Loads are classified into 5-days and 7-days consumption schedules so they can be matched with the time series from suitable heat clusters as schedule is one of the determinants for heat demand in this category as will be explained in this section. Additionally, loads with annual consumption over 5 GWh are extracted from the sample and classified as high energy users to be used as reference values for the ambient temperature independent users.

The daily heat demand for the industrial users is estimated through a linear regression model adaptable to different customer groups and daily temperature values (Eq. 11). The model is based on a sample of 566 large-scale natural gas consumers and is differentiated by weekday and weekend consumption, and usage cluster. The original sample consisted of 797 consumers, but 231 were excluded because of missing data or not presenting a linear relation between natural gas consumption and heat demand as the model parameters were defined on gas meter readings. According to the authors, the found cluster correlations are almost as accurate as individual correlation (Jesper et al., 2021).

Eq. 11 Linear regression model to estimate industrial users' heat demand

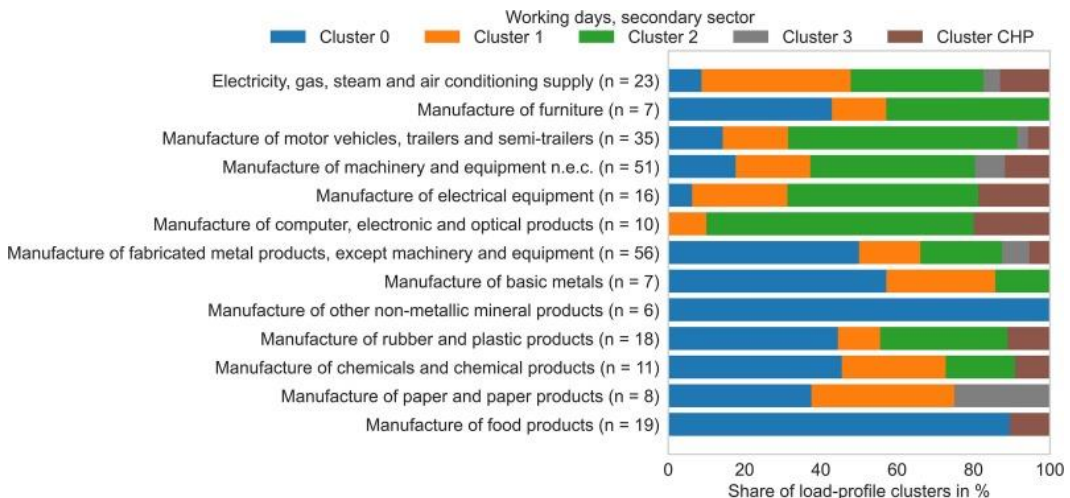
$$Q_d = h_{lin}(T_{amb}) = \begin{cases} \max(0, m_h * T_{amb} + b_h) & \text{if } T_{amb} < T_{hl} \\ \max(0, m_w * T_{amb} + b_w) & \text{if } T_{amb} \geq T_{hl} \end{cases}$$

To simulate a user's heat demand, the weekday and weekend cluster applicable to each customer must be indicated. To assign a cluster to the industrial users inside the Energy community archetypes, the distribution per economic division found by the model authors is considered. In working days (Figure 10), the authors of the study found out that Cluster 0 and Cluster 1 are most likely to better represent a customer if industrial production is the dominant activity. On the other hand, Cluster 2 and Cluster 3 are most likely for consumers where assembly, logistics, general administration, research and development, sales or service are the main activities in the site. Weekend distribution shows similar trends and the data is available in the attached database (Jesper et al., 2021).

The cluster assignment can be explained in most cases by the users' heat sink and their respective time schedules. The authors found that dependency of heat demand on mean daily ambient temperature increases from weekday cluster 0 to cluster 3 and weekend cluster 0 to cluster 4, thus, existing a weaker relation between temperature and heat demand in industrial customers with heavily industrialized processes (Jesper et al., 2021). As this model is selected to represent temperature dependent users, only weekday clusters 2 and 3, and weekend clusters 2, 3, 4 are used to create industrial profiles in MODECO.

Additionally, it was found that users in weekend cluster 3 have a reduced heat load, which indicates a 5-day production schedule. In contrast, the rest of the clusters – all weekday clusters and weekend clusters 2 and 4 – show similar demand levels, which makes them suitable for customers producing seven days a week. Weekend cluster 2 and cluster 4 can also be used for industrial customers with 5-day production days, if space heating is the main heat use and room temperature is not reduced on the weekends (Jesper et al., 2021). As mentioned, this characteristic is taken into account when matching the heat load with an electricity time series (i.e. heat loads built with weekend cluster three parameters are only matched with five-week schedule electrical loads).

Figure 10. Distribution of companies per working day cluster in each economic sector



Source: Obtained from Jesper et al. (2021).

Daily water and space heating requirements for these users are calculated using the same methodology as for residential and Non-residential buildings. In this case, the GMK profile – buildings in the automotive and metal sector – is always used as it is assumed to be representative of industrial users. The resulting values are subtracted from the previously obtained daily demand to separate process heat from these other applications. The hourly behaviour for space and domestic water heating is obtained using the weekday and hourly factors applicable to this building type, except that for seven-day schedules all days are treated as weekdays.

Hourly loads for process heat are constructed using information from the U.S. National Renewable Energy Laboratory (NREL) regarding process heat load shapes (McMillan, 2019). Specific loads are selected, maintaining consistency between the process represented and the sector to which the simulated industrial user belongs and that is linked to the clusters used to model heat demand. To do so, each load shape from

the NREL database is assigned an economic sector from the Nomenclature of Economic Activities (NACE) system used in the clustering model (Jesper et al., 2021), suitable to its indicated North American Industrial Classification System (NAICS) code. Moreover, as the NREL database differentiates between industries by number of employees, only those with less than 250 employees are considered as the modelled users are assumed to be small and mid-size enterprises in consistency with the used source for the electrical load.

In the case of the Spanish industrial users, a load correction associated with space cooling will be done following the same process explained for residential and Non-residential buildings.

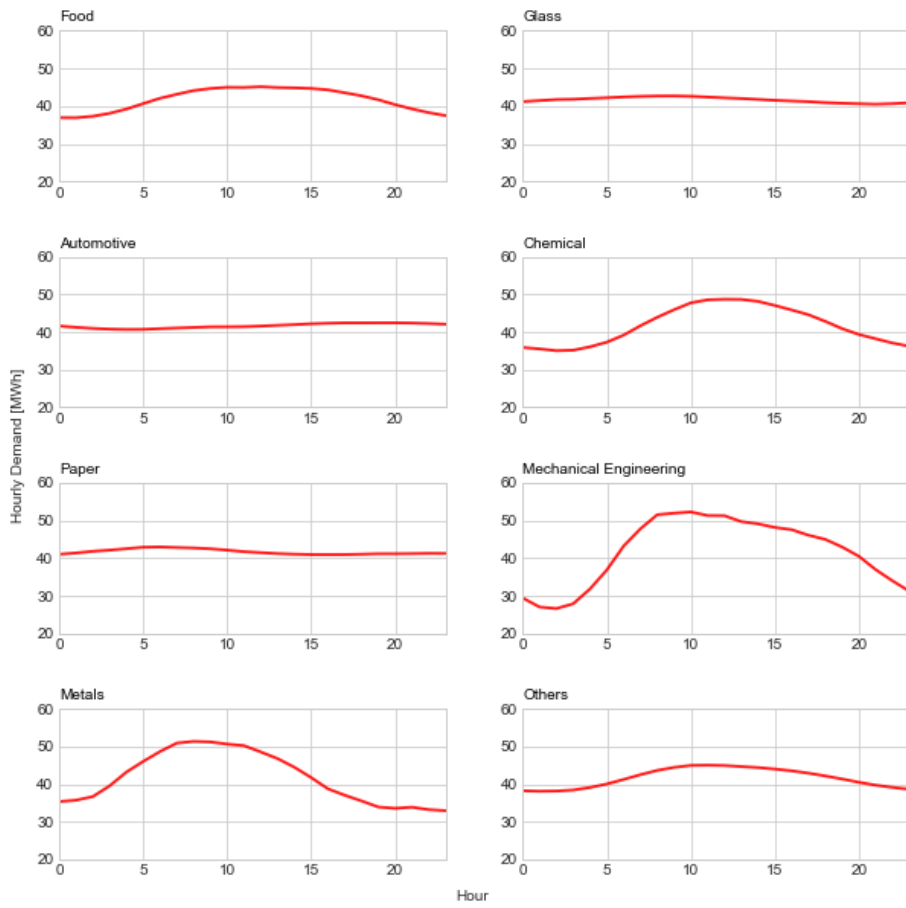
3.1.2.2 *Ambient temperature independent users*

The electrical demand for the industrial users, considered only in the industrial polygon and business park archetypes is designed based on the JERICHO-E database that contains comprehensive data on energy consumption patterns for heat, cold, mechanical energy, information and communication, and light in high special and temporal resolution. The model was originally developed for Germany and can be disaggregated by sector – residential, industrial, commerce and mobility – using a combination of bottom-up and top-down approaches and multiple open data sources such as weather time series and standard load profiles (Priesmann et al., 2021).

To model the industrial electricity load, the authors of JERICHO-E use 8 Industrial Standard Load Profiles (ISLP) representing the following sectors: food; glass, ceramic, and stones; automotive, chemical, paper, mechanical engineering; iron and steel; and other industries (Priesmann et al., 2021). The load shapes for chemical, paper, and iron and steel are used in MODECO to simulate the electricity and heat consumption of four large industrial users within these categories. The normalized heat and electricity hourly demand is presented in the Figure 11 for the 3 analysed seasons (winter, summer, transition) although the original load profiles contain individual data for the 8760 hours in a year and are inputted as such in the models.

The database permits disaggregating the electricity and heat load shapes by end use. Although its share in the final energy consumption is low, as it is practically fully related to the process requirements, space heating and cooling demand is not included in the total energy consumption curve to maintain methodological consistency. Instead, it is modelled as for ambient temperature dependent users, which means that there will be slight differences between Spanish and German users in this category. The annual energy demand used to adjust the normalized curve for these users is defined based on the annual consumption from the industrial users classified as high energy consumers as explained above. Heat process demand is assumed to follow the same shape, and have a total annual demand equal to 48% of the registered annual electricity demand as reported in a study (Jesper et al., 2022) evaluating the relation between both energy carriers in industrial consumers.

Figure 11. Hourly curves showing total energy demand (heat and electricity) for selected industrial standard load profiles from the JERICHO-E database [data adjusted to 1000 MWh/day]



Source: Own elaboration with data from (Priesmann et al., 2021).

3.2 Heat pumps

Since the starting year (2025), it is assumed that a share of the communities' total heat demand is already served by electric heat pumps. Differentiated values are assumed for Germany and Spain and based on the share of space heating unit consumption per dwelling (kWh/dwelling) supplied by electricity reported in the Entranz database for residential buildings in European member states (Entranz Project, 2008). As no differentiated data was found for Non-residential buildings, the same distribution is assumed for this group. Therefore, in the Spanish case studies it is assumed that 18% of the heat demand from residential and Non-residential buildings is supplied by electric heat pumps by 2025, while in Germany this share is just 4% as most heat demand is met by fossil fuels combustion. Every year, it is assumed that the amount of heat served by heat pumps grows by 2.6% in comparison with the previous year, in line with the electrification rates assumed by the ESES for 2030 and 2040.

To calculate the electricity demand associated with the heat load served by electrical heat pumps, a methodology similar to that used by (Heitkoetter et al., 2021) and (Ruhnau et al., 2019) is applied. As the heat pumps' Coefficient of Performance (COP) varies with ambient temperature, hourly COP values for Air Sourced Heat Pumps (ASHP), Ground Sourced Heat Pumps (GSHP), and Water Sourced Heat Pumps (WSHP) are calculated based on the quadratic regression of manufacturer data used by (Heitkoetter et al., 2021) and described in Eq. 12.

Eq. 12 Calculation of hourly COP values for different heat pump types

$$COP_t^{HP} = \begin{cases} 6.08 - 0.09 * \Delta T + 0.0005 * \Delta T^2, & ASHP \\ 10.29 - 0.21 * \Delta T + 0.0012 * \Delta T^2, & GSHP \\ 9.97 - 0.20 * \Delta T + 0.0012 * \Delta T^2, & WSHP \end{cases}$$

The values for ΔT ($T_{sink} - T_{source}$) comprise all possible combinations of source and sink temperatures applicable to each heat pump type. The applicable sink and source temperature for each heat pump technology are listed in the table below.

Table 16 Sink and source temperature applicable to considered heat pump technologies

| Type | T _{source} | T _{sink} |
|-------------|---------------------|--|
| ASHP | Air | Radiator heating, floor heating, water heating |
| GSHP | Ground | Radiator heating, floor heating, water heating |
| WSHP | Water | Radiator heating, floor heating, water heating |

*ASHP = Air Sink Heat Pump; WSHP = Water Sink Heat Pump; GSHP = Ground Sink Heat Pump;

Source: Own elaboration with data from Heitkoetter et al., (2021).

For air and ground source temperature, hourly data from Open Power System Data (2020) are used, while for water source a constant ground water temperature of 10 °C is assumed as in (Heitkoetter et al., 2021). For the calculation of sink temperatures, the approach of Ruhnau et al. (2019) is applied, considering 50°C as the heat sink temperature for water heating – value based on German field measurements and considered the same for Spain – and Eq. 13 to calculate hourly values in the case of radiator and floor heating.

Eq. 13 Hourly sink temperatures used for radiation and heating applications

$$T_h^{sink} = \begin{cases} 40\text{ }^{\circ}\text{C} - 1.0 * T_h^{amb}, \text{radiator heating} \\ 30\text{ }^{\circ}\text{C} - 0.5 * T_h^{amb}, \text{floor heating} \end{cases}$$

Subsequently, the obtained COP time series are used to calculate a weighted average for the different technologies considering different market shares for Germany and Spain. For the German case, the shares proposed by (Heitkoetter et al., 2021) are considered: 55% ASHP, 39% GSHP, and 6% WSHP. In the case of Spain, a larger usage of ASHP is considered – 90% ASHP, 8% GSHP, 2% WSHP – as market sources show it is by far the dominant heat pump technology in the country (Observ'ER, 2021).

Finally, hourly weighted average COP are used to calculate the electrical load (El_{HP}) from heat pumps' usage by applying Eq. 14 considering that x_{HP} is the share of the community's heat load (Q_h) that is supplied via electrical heat pumps.

Eq. 14 Electrical demand associated to heat pumps operations Electrical demand associated to heat pumps operations

$$El_{HP} = \frac{Q_h * x_{HP}}{COP_h}$$

The investment and operation and maintenance costs associated with the different types of heat pumps are obtained from the HER4 cost database (HRE4, n.d.). The values for 2030 and 2040 are shown in the following table. CAPEX is assumed constant during the 16-year period, while the CAPEX values considered for each year can be consulted in the associated database. For comparison, the cost of the natural gas boilers is also presented in Table 17. This information is also used in the Total Cost of Ownership analysis and the investment model as an input for decision-making regarding the potential installation of Combined Heat and Power (CHP) units.

As investment costs are given in € per heat pump and boiler unit, the given values are transformed to € per heat unit (kWh-year), assuming that this equipment is sized to cover the households' entire space and domestic water heating demand. Thus assuming that one unit is able to generate the annual heat demand for single-family and multi-family buildings, respectively, which permits to estimate the cost per heat unit generated by each thermal technology. As no specific data is provided for commercial buildings, it is assumed that the investment cost is equal to 33% of the estimated cost for residential users (considering the mean value between single and multifamily homes), maintaining the relationship presented in the work of Heitkoetter et al. (2021) for domestic and commercial applications.

Table 17 CAPEX, OPEX and useful life considered for heat pumps and boilers used in residential users

| Technology | Type | User | 2030 | 2040 |
|------------|------|------|------|------|
|------------|------|------|------|------|

| | | type | CAPEX [€/unit] | OPEX [% CAPEX] | Life [years] | CAPEX [€/unit] | OPEX [% CAPEX] | Life [years] |
|-------------------|------------------------|-------------|---------------------------|-------------------------------|-------------------------|---------------------------|---------------------------|-------------------------|
| Heat pumps | ASHP | All | 1660 | 9.8% | 10 | 1570 | 9.8% | 10 |
| | WSHP | SFH | 7830 | 2.1% | 15 | 7000 | 2.1% | 15 |
| | | MFH | 116990 | 0.7% | 20 | 105020 | 0.7% | 20 |
| | GSHP | SFH | 12900 | 1.3% | 20 | 11050 | 1.3% | 20 |
| | | MFH | 206350 | 0.4% | 20 | 186080 | 0.4% | 20 |
| Boiler | Natural gas | SFH | 2760 | 6.6% | 20 | 2490 | 6.6% | 20 |
| | | MFH | 21560 | 2.8% | 25 | 19440 | 2.8% | 25 |

*ASHP = Air Sink Heat Pump; WSHP = Water Sink Heat Pump; GSHP = Ground Sink Heat Pump; SFH = Single-family home; MFH = Multi-family home.

Source: Own elaboration with data from HRE4 (n.d.).

3.2.1 Heat pumps' flexibility potential

As previously mentioned, the electrical demand associated with heat pump operation is considered in the optimization models as an electrical consumption profile. Given that heat pumps can shift their operation without greatly affecting users' comfort by taking advantage of the building thermal inertia, the participation of these items in Demand Side Response (DSR) programs is considered, assuming there is a portion of the heat pumps electrical demand that can be increased or decreased as required. To implement it in MODECO models, some considerations have been taken from Heitkoetter et al. (2021) as explained.

In DSR, heat pumps' flexible operation must consider some established limits that are associated with the equipment technical restrictions as well as socio-economic factors that account for users' comfort. Regarding technical restrictions, it is considered that the load decrease share for these assets is 0%, whereas the load increase share is 75%. Additionally, the use of a flexible share parameter representing socio-technical load shifting potential restrictions, e.g., the social acceptance or the regulation framework can hamper the implementation of load shifting, is included as done by Heitkoetter et al. (2021). This is considered to be 40% in all cases as defined for Germany by the authors.

At every time step, the potential amount of up and down flexible energy has to be within the maximum load increase and the maximum load decrease. Both bounds are calculated by multiplying the calculated heat pumps' electrical demand at each hour by the load increase and load decrease share values. Additionally, it is multiplied by the flexible share parameter mentioned above to obtain the available amount of flexible energy at each time step. Moreover, the time frame of management, which is **the maximum duration that loads can be postponed or postponed**, is also incorporated as a constraint for the model. This value is set at **3 hours** for all heat pump types (residential, commercial) as proposed by Heitkoetter et al. (2021).

Finally, three different costs associated to heat pumps participation in DSR are assumed in: 1) a specific investment cost for information and communication technology (ITC) components; 2) annual fixed costs caused by maintenance works and the electricity consumption of the ITC components; and 3) variable costs reflecting compensations for losses in production and comfort (Heitkoetter et al., 2021). These costs differ for domestic and commercial heat pumps as shown in the following table; but no differences are assumed between target regions. It is also assumed that these costs – as well as the load shifting parameters – remained the same during the studied period.

Table 18 Installation and operation costs of equipment for heat pump's participation in DSR programs

| Heat pump category | Investment cost [€/MW] | Fixed cost [€/MW/year] | Variable cost for DSR [€/MWh] |
|---------------------------|-----------------------------------|-----------------------------------|--|
| Residential | 62,000 | 12,000 | 10 |
| Commercial | 20,000 | 600 | 10 |

Source: Own elaboration with data from Heitkoetter et al. (2021).

3.3 Electric vehicles

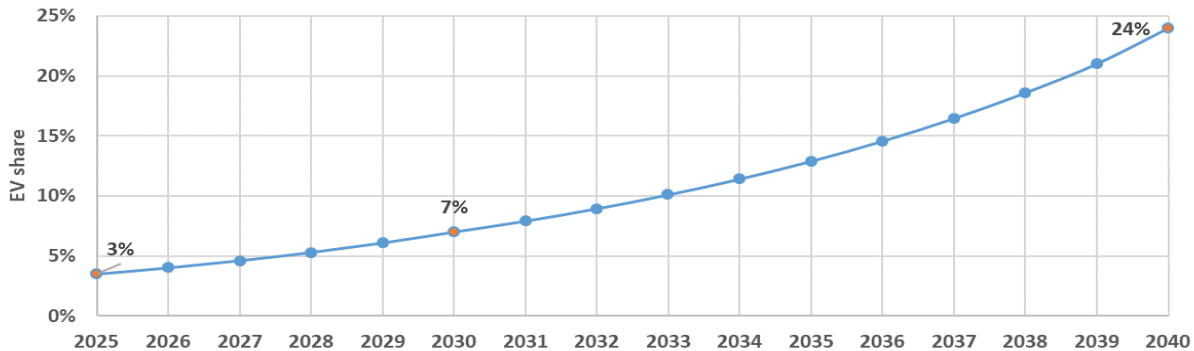
Electricity demand associated to electric vehicles is modelled differently for **private charging points** (households and work stations) and **Community-led stations** as the second type allows for smart charging and participates in demand response programs, via Vehicle-to-Grid (V2G), so its modelling must permit optimizing the vehicles' charging and discharging at these points. Electrical usage from private charging points, on the other hand, is perceived by the model as part of the Community's electricity demand. The methodology and assumptions considered in each case are explained in the following sections, while the specific data inputted in each case can be consulted in the associated database.

3.3.1 Private charging stations (non-smart charges)

The number of non-smart domestic and commercial charging points available in each archetype by 2025, 2030 and 2040 is defined exogenously considering the following assumptions,

- For the starting year (2025), it is assumed that there are 56 passenger cars per 100 inhabitants in each archetype, as reported at the European level in (ACEA, 2022b), or 1.29 passenger cars per household assuming a population density of 2.3 persons per household based on the average European household size (Eurostat, 2022);
- The number of EV belonging to commercial fleets owned by community members is defined on a case-to-case basis.
- The total cars fleet (including both domestic and commercial vehicles) inside the communities is assumed to increment by 1.2% each year, as reported by (ACEA, 2022b) for the EU.
- The percentage of EV within the total vehicles fleet is based on the electrification rates set by the ESES reference model for the transportation sector in 2030 (7%) and 2040 (24%). For 2025 a similar backwards trend is assumed for 2025 as observed in Figure 12. It must be noted that currently less than 1% of the total vehicles fleet are electric in both Germany (0.8%) and Spain (0.3%) (Robinson and Erickson, 2016).
- From the total number of EVs owned by community members (residential and non-residential), it is assumed that all commercial EVs have their own private charging station, but only 50% of residential EV owners have a private charging point at home in the Business park, Urban district and Virtual community archetypes. In the Rural town case, this number is assumed higher (60%) as single-family houses are more likely to have access to home charging facilities as reported by (Hensley and Knupfer, 2018).
- All the charging points owned by community members are assumed to be non-smart.
- Additionally, it is assumed that some public non-smart chargers are already installed inside each archetype based on the number of electrical chargers currently available in Europe.

Figure 12. EV share in total passenger cars fleet per year



Source: Own elaboration based on electrification rates assumed for the transportation sector in the ESES

The final number of non-smart charging points considered in each archetype are summarized in the following table per usage category and year.

Table 19 Number of non-smart charging stations considered in each archetype by year and owner category.

| Archetype | Category | Number of installed charging points | | |
|---------------------------|----------|-------------------------------------|------|------|
| | | 2025 | 2030 | 2040 |
| Business park | Domestic | 4 | 7 | 28 |
| | Business | 22 | 22 | 22 |
| | Public | 2 | 4 | 6 |
| Industrial polygon | Domestic | - | - | - |
| | Business | 25 | 25 | 25 |
| | Public | 2 | 4 | 6 |
| Rural town | Domestic | 4 | 9 | 34 |
| | Business | 4 | 4 | 4 |
| | Public | 1 | 2 | 4 |
| Urban district | Domestic | 10 | 21 | 79 |
| | Business | 14 | 14 | 14 |
| | Public | 2 | 4 | 6 |
| Virtual community | Domestic | 27 | 54 | 207 |
| | Business | 50 | 50 | 50 |
| | Public | 8 | 16 | 32 |

Source: Own elaboration with data from Eurostat (2020) and the selected ESES.

The electrical load associated with the usage of the private charging points is **modelled using the Electric Vehicle Charging Infrastructure Simulator (ELVIS)**, an open source software developed at the Distributed Artificial Intelligence DAI-Laboratory from TU Berlin university (DAI-Laboratory, 2020). For each private non-smart charging point category, the assumptions summarized in Table 20 are used as inputs to the model. Similarly, the relative charging frequency of start charging time per hour of the day reported by (Corchero García, 2015) for European domestic and business users is used to indicate the model the most likely initial charging hour per day. It is assumed that one charging per day is the most common frequency for all users as reported by (Quiros-Tortos et al., 2018).

Table 20 Assumptions considered for charging stations for domestic and business use

| Data | Domestic | Business use |
|-----------------------------|----------|--------------|
| Station power rating | 3.7 kW | 11.0.kW |
| Average initial SOC | 58.6% | 62.7% |
| Average parking time | 5 hours | 5 hours |

Source: Own elaboration with data from Corchero García (2015).

In addition to these parameters, the model requires basic information from the vehicles that charge energy at each point. In MODECO, 5 EV generic types (Table 21) are considered based on the characteristics of existing EV models and provided by the Emobpy open source model (Gaete-Morales et al., 2021). For simplification purposes, one EV type is assigned to one charging point even in work stations. In 2025, the EV types with lower battery capacity (35.8 kWh) are used as default models, while in future periods, cars with larger capacities are favoured, representing technological improvements. In all cases, a 95% charging efficiency is assumed.

Table 21 Assumptions for standard EV models considered

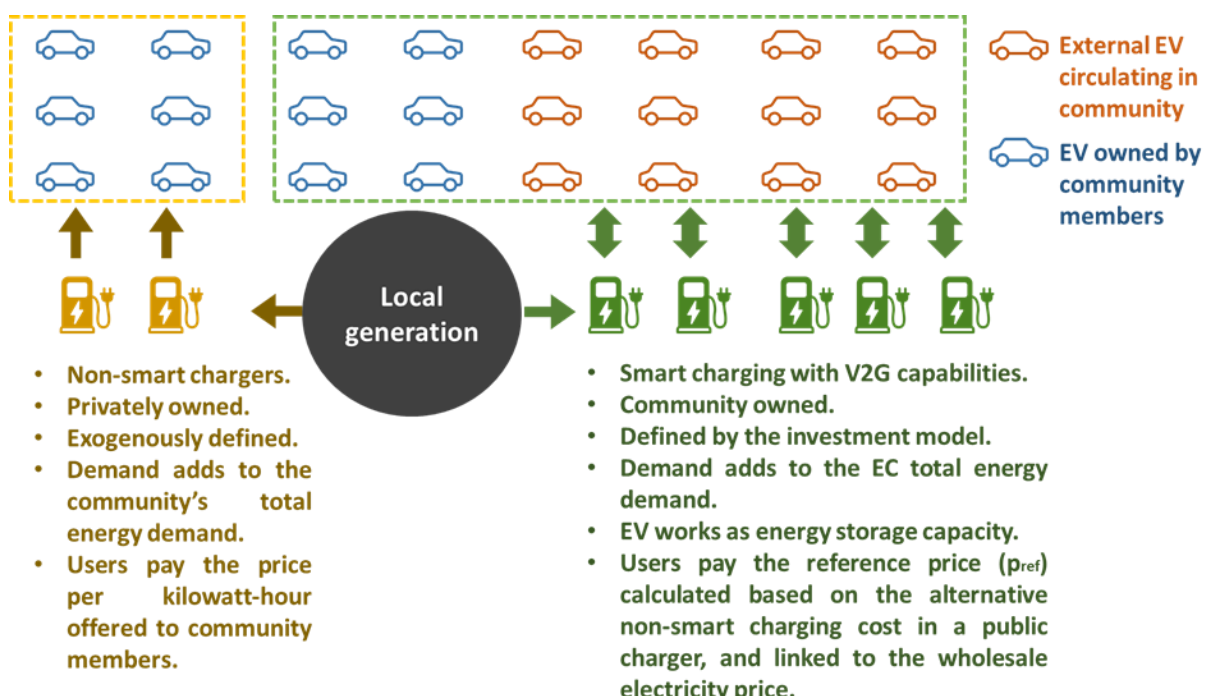
| EV generic model | Power | Capacity |
|------------------|--------|----------|
| EV_Model_1 | 100 kW | 35.8 kWh |
| EV_Model_2 | 386 kW | 60 kWh |
| EV_Model_3 | 386 kW | 70 kWh |
| EV_Model_4 | 386 kW | 90 kWh |
| EV_Model_5 | 386 kW | 100 kWh |

Source: Own elaboration with data from Gaete-Morales et al. (2021).

3.3.2 Community-led charging points (V2G)

In addition to the non-smart EV chargers operating inside the community and privately owned by homeowners or businesses, smart-charging stations with V2G capabilities are considered an available technology at the Energy communities' potential investments portfolio. These community-led EV charging points are expected to provide electricity to EV owners from the community without access to private charging points, as well as to external EVs that are circulating in the community's area and are in need of recharging their batteries. A summary of the EV charging assumptions is provided in Figure 13.

Figure 13. Economic assumptions considered for smart and non-smart EV charging stations



Source: Own elaboration.

All smart charging stations are considered to have a capacity of 11 kWe and be located in public points (parking, streets) accessible to all vehicles circulating inside the community area. The investment cost for the starting year is set at 4,500 euros per installed charger based on data from the European Federation for Transport and Environment (EFTE, 2020). This source considers the investment costs to remain similar up to 2030 as it estimates that only fast chargers will experience a cost decline in the next 16 years. However, the 2022 European EV Charging Infrastructure Masterplan estimates that by 2030, EV chargers between 4 and 22 kWe capacity will have an initial cost of 125 €/kWe (ACEA, 2022a), which translates into an investment of 1375 euros per charging point in MODECO scenario. This drop in price is considered to take place in the current analysis. However, from 2030 to 2040, prices are assumed to remain the same as originally assumed in (EFTE, 2020). Operation and maintenance costs are assumed to be 10% of CAPEX based on data from (Nationale Plattform Elektromobilität, 2015) and lifetime is considered 10 years as reported in (Hecht et al., 2020).

The number of external EV assumed to be circulating daily inside each archetype is related to the number and size of Non-residential buildings⁹ considered in each case, as these vehicles are assumed to be owned by commuters that live outside the community area but work there. It is assumed that the percentage of workers owning an EV is equal to the value considered for community residential members; in the same fashion, a similar annual growth is assumed. For the Virtual community archetype, the obtained number is tripled as it is assumed that workers from non-residential buildings that are close to the Virtual community members might also use these chargers.

The final number of community and external EV circulating in each archetype is shown in the following table, whereas the number of employees considered per non-residential building is available at the associated database. On weekends, the employees from business with typical Monday-to-Friday schedules (for instance, offices) are assumed to charge elsewhere and are not accounted for in the circulating units. Although it is possible for a fraction of the community members' EVs to shift some of their charging from their private charger to a community-owned station, this is ignored as it is assumed most of them will continue using their own charger as it is most comfortable.

The decision to install or not a smart charging point will depend on the economic benefits obtained by using the EV as storage to optimize the communities' energy management, as well as on the potential revenues obtained from providing charging services to the EVs circulating inside the community. In this sense, it is assumed that, when possible, the community uses locally generated energy to provide this service, but users always pay a charging fee equivalent to what they would have paid in regular public chargers, minus a discount of 5% that is defined based on the willingness to pay value reported by (Ensslen et al., 2018) for this application and obtained through a survey for German and French EV owners. This means that the smart charging cost must be 95% the cost of the alternative regular charging to be attractive to the users.

Table 22 Number of EV circulating in the energy communities per year disaggregated by owner type

| Archetype | Owner | Number of circulating EV per category | | | | | |
|----------------------|-------------------|---------------------------------------|-----|------|----|------|----|
| | | 2025 | | 2030 | | 2040 | |
| | | WD* | WK* | WD | WK | WD | WK |
| Business park | Community members | 29 | 29 | 36 | 36 | 78 | 78 |
| | External | 37 | 10 | 74 | 21 | 287 | 80 |

⁹ Non-residential buildings are classified into micro, small, medium and large. The considered number of employees per category are based on the classification used by the European Commission (Eurostat, 2015). In particular, the following values are assigned: micro (5 employees), small (30 employees), medium (100 employees), large (250 employees).

| Archetype | Owner | Number of circulating EV per category | | | | | |
|---------------------------|-------------------|---------------------------------------|-----|-----|-----|-----|-----|
| Industrial polygon | Community members | 25 | 25 | 25 | 25 | 25 | 25 |
| | External | 73 | 58 | 146 | 117 | 563 | 450 |
| Rural town | Community members | 11 | 11 | 18 | 18 | 60 | 60 |
| | External | 4 | 2 | 8 | 4 | 31 | 14 |
| Urban district | Community members | 34 | 34 | 55 | 55 | 172 | 172 |
| | External | 11 | 2 | 22 | 3 | 84 | 13 |
| Virtual community | Community members | 103 | 103 | 157 | 157 | 464 | 464 |
| | External | 56 | 18 | 112 | 36 | 434 | 137 |

*WD = Working days, WK = Weekend

Source: Own elaboration with data from Eurostat (2020) and the selected ESES.

The alternative charging cost is calculated using Eq. 15 from the methodology proposed in (Ensslen et al., 2018), setting a reference charging price based on the cost of charging at non-smart stations at the applicable wholesale hourly price (p_t). This reference price is the same for all hours of the year and is based on the average cost associated with immediately charging all EVs arriving at the station points (without smart management). The energy required by each EV at each hour (e_{tx}) is defined as shown in Eq. 16 considering the mean SOC at initial and departure times explained before, and the technical characteristics assumed for the EVs' batteries (particularly the battery's capacity, E_b , and charging efficiency, $eff_{charging}$) and the public station chargers. In the original article (Ensslen et al., 2018), the number of chargers is known, but as this is not the case here, the calculation of the reference price is done considering that there is always a charger available for an upcoming EV. This is considered a fair assumption as the reference price is just an approximation to the alternative cost of charging that same EV in a non-smart station, which might be located at any point.

Eq. 15 Reference charging price

$$p_{ref} = \frac{\sum_{t=1}^{8760} \sum_{x=1}^X p_t * e_{t,x}}{\sum_{t=1}^{8760} \sum_{x=1}^X e_{t,x}}$$

Eq. 16 Energy required to charge an EV battery

$$e_{tx} = \frac{(SOC_{departure} - SOC_{initial}) * E_b}{eff_{charging}}$$

In MODECO operational and investment models, it is assumed that all EVs arrive and leave with the same SOC values. Thus, the energy needed to charge the EVs in a non-smart charger is the same for all vehicles. Therefore, once the reference price is set (p_{ref}), it is possible to calculate a service cost (S_{cost}) that can be directly applied to each EV connecting into the Energy community's chargers as stated in Eq. 17. The users' willingness to pay is accounted for in these costs, discounting 5% to the resulting reference price. This is viewed as an incentive for users to participate in smart charging instead of regular charging, which implies more intensive battery use. This service cost is used in the operational and investment models to estimate the economic gains of the Energy community through the provision of EV charging services. The extra costs and benefits associated with the actual smart energy charging and discharging are accounted for in the model as part of the total energy that the community injects and extracts from the grid.

Eq. 17 Service cost applied to EV connecting to V2G charging stations

$$S_{cost} = 0.95 * p_{ref}$$

3.3.3 Community's CO₂ emissions

The Carbon Dioxide (CO₂) emissions associated to the community's energy usage are calculated for the different electricity and heat sources prior to the installation of any energy asset. The emissions associated to the baseload electrical demand and EV usage is calculated based on the CO₂ emissions from the energy mix used in each evaluated region, and obtained from the UCED model execution. In the case of heat, the CO₂ emissions associated to Heat pump operation is calculated on a similar fashion, based on the electrical consumption from these assets obtained with the methodology explained in Section 3.2.

The emissions associated to boiler usage are calculated through the volume of natural gas consumed by these units, which is obtained by multiplying the annual heat energy provided by these assets to cover the community's demand not supplied by heat pumps (MWh), plus efficiency losses, by the conversion factor from volume to energy provided by the European Union of the Natural Gas Industry (Eurogas). This factors indicates that 1 m³ of natural gas is equal to 10.83 kWh (Eurogas, 2011), considering the gas gross calorific value. No conversion from gross to net calorific value is done as it is assumed that the substituted boilers are able to capture latent heat as most modern gas-based technologies do (Eurogas, 2011). The Greenhouse Gas Emissions (GHG) associated to natural gas burned in fuel -based boilers is estimated using the default emissions factors for stationary combustion in the residential sector from the Intergovernmental Panel on Climate Change guidelines (Chernova, 1966), presented in Table 23. To convert the GHG factors from TJ to MWt the heat unit equivalents from Eurogas are considered, assuming gross calorific values due to the reasons explained above (Eurogas, 2011). Methane (CH₄) and Nitrous Oxide (N₂O) are converted to CO₂ equivalent considering typical conversion factors¹⁰.

Table 23 GHG emission factors for natural gas combustion in the residential sector

| GHG | kg GHG/TJ | Kg GHG/MWt |
|------------------|------------|------------|
| CO ₂ | 56100.0000 | 201.9438 |
| CH ₄ | 5.0000 | 0.0179 |
| N ₂ O | 0.1000 | 0.0004 |

Source: Own elaboration with data from Eurogas (2011) and Chernova (1966).

Finally, the avoided CO₂ emissions from boiler substitution by heat pumps is calculated considering the difference between the CO₂ emissions associated to the electricity consumed by heat pump operation and the CO₂ emissions calculated considering that the same heat would be supplied by boilers. The latter is calculated following the same steps used for the boilers actively used by the community.

¹⁰ The emission of 1 kg of nitrous oxide (N₂O) equals 298 kg of CO₂ equivalents, and the emission of 1 kg of methane (CH₄) is equal to 25 kg CO₂ equivalents (Statistics Netherlands, 2023).

4 Models description

As mentioned before, three optimization models are used in MODECO to evaluate the impact of different energy tariffs in the investment and operational decisions of Energy communities. The key outputs and inputs to each model are summarized in Figure 14, while the specific values inputted to each case can be found in the Annex database. As observed in Figure 14, the models are interlinked as the outputs from one model serve as inputs in another. Specifically, the main output from the UCED model are the hourly marginal prices, which are used to build the energy price scenarios tested in the investment model. Similarly, the installed capacity per technology and year decided by the investment model are used as inputs for the operational model, in which the optimal operation of such assets is decided. Finally, the results from the investment and operational models are used to modify the inputs to the UCED model, before re-executing to evaluate changes in the hourly marginal prices obtained.

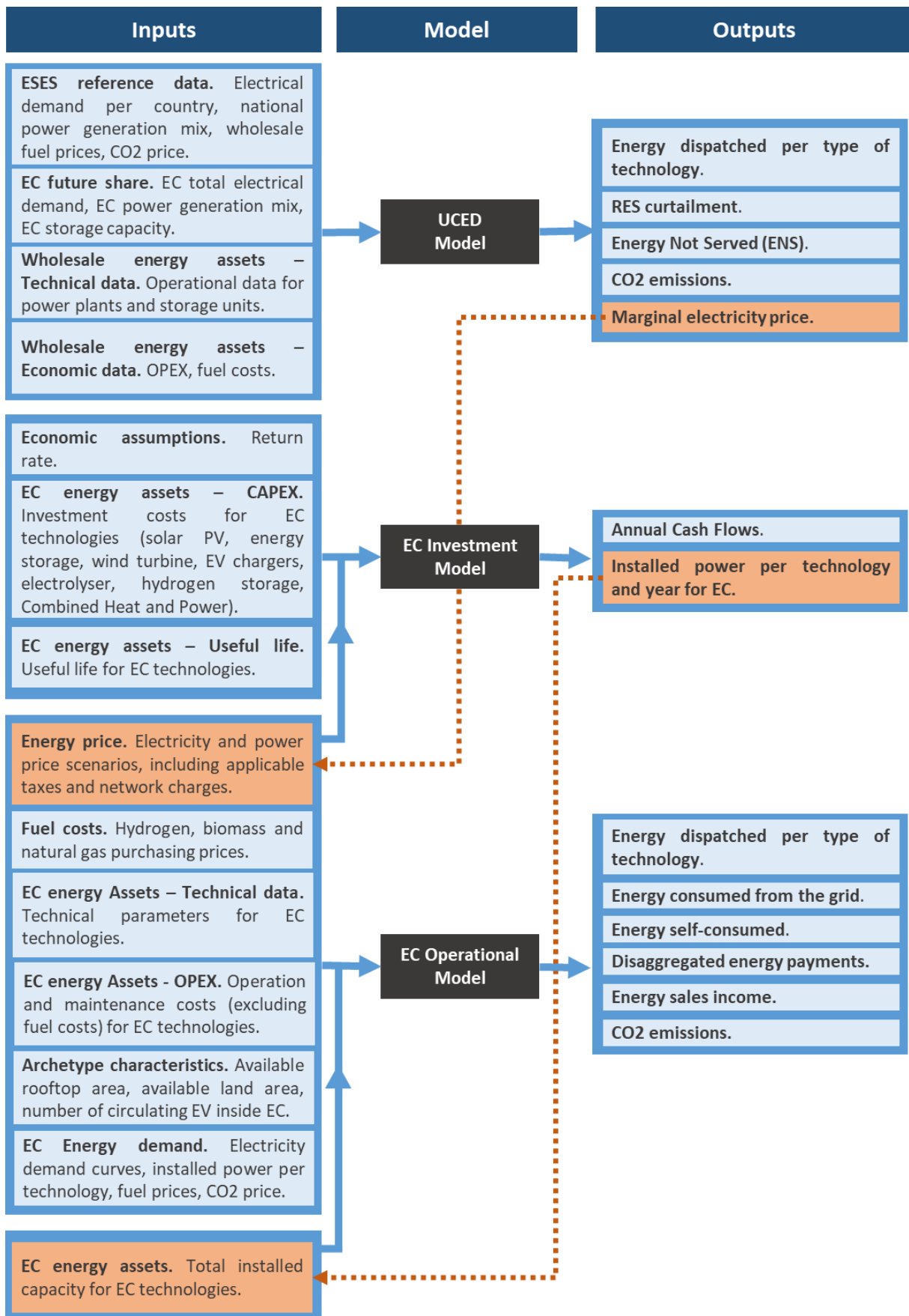
In the following sections, the main features from each model are described. Particular focus is given to the investment and operational models, as these are developed specifically for MODECO. For the UCED model, which was externally developed, only a general description is presented.

4.1 Power system model

The selected UCED model representing the entire European power system is built by the Joint Research Centre (JRC) using the object-based modelling toolbox PyPSA, an open source toolbox based on Python for simulating and optimizing modern power systems that include features such as conventional generators with unit commitment, variable wind and solar generation, storage units, coupling to other energy sectors, and mixed alternating and direct current networks. PyPSA can calculate the linear optimal power flow, which is the least-cost optimization of power plant and storage dispatch within network constraints, using the linear network equations, over several time steps. The project is maintained by the Department of Digital Transformation in Energy Systems at the Technical University of Berlin and further details be consulted in (Brown et al., 2018) .

One key characteristic is that the model covers all Europe, including Germany and Spain, and is based on ENTSO-E (2020) terminology, which permits adapting it to the reference ESES with minor modifications. In particular, it is considered an advantage that power plants are aggregated according to type – based on fuel, class, efficiency, etcetera – avoiding the need to have data for each specific unit in the European power system and being able instead to use general technical parameters per type as done in the analysis by ENTSO-E (2020). Other important aspects are that flows between zones are based on NTC time series, and that demand response is modelled according to the ERAA methodology, where, similar to dispatchable power plants, energy is “generated” by reducing demand.

Figure 14. Schematic diagram of the optimization models used within MODECO project



Source: Own elaboration.

4.1.1 Model adaptation to the reference ESES

As the selected UCED model was already based on ENTSO-E terminology, only a few parameters are changed to consider the evolution of the power system contemplated in the reference ESES used in MODECO. The capacity installed per type of technology in 2025, 2030 and 2040 is defined according to the distributed energy scenario's data available at the documentation from TYNDP's 2020 edition (ENTSO-E, 2021). The considered capacities per technology and year can be seen in Section 2.1.

In addition to the power plants capacity, the Demand Side Response (DSR) capacity per country and the cost associated with using it are also taken from the reference ESES database (ENTSO-E, 2021). Finally, the fuel and CO₂ emissions costs are also based on the values from the TYNDP 2020 scenarios. However, the costs for natural gas and CO₂ emissions are updated based on recent data, as current prices are much higher than those projected in the reference ESES, even though an increasing trend is also considered in the reference scenario. Therefore, the prices registered in 2021 for natural gas (Eurostat, 2022) and carbon permits (Ember, 2022) in the European Union are used as the starting cost in 2025, while a similar relative increase to that reported in the original ESES is assumed for 2030 and 2040. The results from this process are shown in Table 24, while the rest of the fuel costs can be consulted in (ENTSO-E, 2021).

Table 24 Indicators associated with solar PV and Energy communities.

| Year | Natural gas cost [EUR/GJ] | | Carbon emissions cost [EUR/tCO ₂] | |
|-------------|---------------------------|----------|---|----------|
| | Original | Modified | Original | Modified |
| 2025 | 6.46 | 11.96 | 23 | 54 |
| 2030 | 6.91 | 12.79 | 53 | 124 |
| 2040 | 7.31 | 13.54 | 100 | 235 |

*Used for the UCED model executions whose results are used and presented in this document.
Source: own elaboration with data from Eurostat (2022), Ember (2022) and ENTSO-E (2021b).

In order to avoid the occurrence of several hours per year in which demand is not met and the energy price is set as the Value of Lost Load (VOLL), the capacity of gas-based generation (CCGT, OCGT, GAST) originally considered in the reference ESES for all countries is expanded by 60% in 2040 in comparison to 2030. This was proposed after testing the model with the original inputs, which led to a high percentage (over 50% of hours in the year) of scarcity events reported for Germany in 2040. These findings do not necessarily reflect those obtained by ENTSO-E for the distributed energy scenario presented in the TYNDP 2020 report (ENTSO-E, 2021a), as the model and technical parameters used are not the same. Given that MODECO's objective is not to study resource adequacy in the future power system, expanding the available gas capacity is proposed as a simple way to ensure enough generation is available to cover demand at most of the annual hours. As would be further explained in Chapter 7, this modification managed to reduce the number of hours in which load is not met to 16 for Germany's 2040 system. In those cases, the VOLL was set as 3,000 €/MWh as this is the price cap set for day-ahead markets in Europe up to the beginning of 2022.

All the models' macro parameters are inputted directly in the Python code whereas the component data is imported through CSV files and hdf5 tables. Once all inputs are introduced to the model, its resolution is performed in two steps:

1. Seasonal Hydro Optimization to determine the minimum storage levels through a temporal aggregation of the energy volumes based on a predefined resolution.
2. Rolling Horizon Dispatch Optimization. The storage bounds are fed to the model as a lower bound for the reservoir levels.

Once these steps are completed, the yearly optimization of the power system is done and the results analysed. As seen in Figure 14, in addition to the hourly marginal prices, the CO₂ emissions and volume of energy dispatched per type of technology, renewable energies curtailed, and Energy Not Served (ENS) are also obtained for further analysis.

4.2 Investment model

The investment model is implemented in the GAMS/CPLEX solver as a Mixed Integer Linear Programming problem (MILP). The temporal scope of the model is 16 years, and its temporal resolution is hourly. The potential investments included in the model are shown in Table 7. As explained before, not all energy assets are available to all archetypes; for instance, biomass-fuelled CHP is only considered in the Rural town case. In that case, the technologies that are not available are left out of the potential investments portfolio and do not form part of the investment decision process for that archetype. As observed in Table 7 some of the technologies have subcategories with two available options. These are represented using a common modelling approach but specific costs and operational parameters (see Annex database).

4.2.1 Representative day's selection

Due to the complexity of the model, in the optimization process it is not possible to consider 8760 hours as time steps for each year. Thus, a set of representative days per month are selected, reducing the amount of data inputted to the model. This is a common approach used in other similar models, such as the investment problem targeted in (Nahmmacher et al., 2016). The outcome of running the model for a different number of days selected, ranging from 1 to 100 representative days for a single year, was compared. As expected, the more number of days used, the more the results tend to approach the outcome using all representative days. However, the authors found that by using six representative days, the model output diverged in less than a 4% from the solution with the 100 representative days. The conclusion is that the number of days selected has to be determined by analysing the trade-off between computational time and the solution's accuracy.

The specific process used in MODECO is based on the methodology proposed by (Nahmmacher et al., 2016) and it is applied for every month of the years between 2025 to 2040 to each specific case (country, archetype, tariff scenario) considering a number of key variables influencing investment decisions: electricity purchase price (€/kWh), wind load factor, solar load factor, electricity demand (kWe), and thermal demand¹¹ (kWt). The methodology that the authors follows is based on the hierarchical clustering algorithm developed by (Ward, 1963) and can be observed with full detail in (Nahmmacher et al., 2016). On a fast note, the algorithm proceeds as follows:

1. Normalize all the time series considered.
2. Apply the clustering algorithm:
 - (a) For every historical day d a vector V_d is created, which incorporates all values of the variables considered in that day. The dimension of this vector is the number of time slices multiplied by the number of variables considered.
 - (b) Initially, set the clusters $C_d = [V_d]$ as a cluster containing the vector V_d .
 - (c) Compute the centroid \bar{C}_d of each cluster C_d as the mean value of vectors in cluster,
 - (d) Compute the distance between clusters (metric = Euclidean distance), by using the centroid \bar{C}_d as the representative value for the cluster.
 - (e) Join the two clusters where the minimum distance between clusters is obtained.
 - (f) Update the centroid of each cluster.
 - (g) Repeat steps (c) to (f) until only one cluster remains.
 - (h) Choose a number of representative days selected. This means to select the step of the process where the desired number of representative days corresponds to the number of clusters at hand.
 - (i) For each cluster C_d , choose the closer vector V_d to the centroid C_d as the representative day for the cluster,
 - (j) Define a weight ω_d to each cluster C_d , to each cluster C_d , as the number of vectors V_d that it contains.
3. Scale back the time series using the weight ω_d assigned to each day.

¹¹ The thermal demand variable is not considered in the Virtual community archetype as CHP installations are not considered a viable investment option.

Finally, in this study case, two days per month are selected, with a total of 24 days being considered for every year. The investment planning's scope is 16 years, and each day is composed by 24 time-slices, meaning that the optimization algorithm is executed for a total of 9216 time steps. This number of days has been determined after comparing the behaviour of the optimization algorithm with a different number of days. When selecting more than two days per month, the optimization algorithm did not reach a solution within an acceptable gap and time (see Box 1). It is worth mentioning that the computational power and the time available in order to study the model heavily influences this selection, and in other contexts a greater number of days could have been selected.

Box 1. Defining “close enough” optimal solutions under limited testing times

The GAMS/CPLEX solver, in which MODECO’s investment and operational models are built, permits to set criterions to stop the optimization process even when the optimal solution (BP) is not found. For this study, the Optcr parameter is used as a primary option, considering acceptable a solution with Optcr of 0.1%. This entails that the CPLEX solver will stop finding an optimal solution when the objective function value of the current best solution (BF) is within that tolerance level $[(|BP - BF|)/(1.0e - 10 + |BF|) < Optcr]$. This reduces solution time as the solver stops not looking for better solutions.

Although this tolerance level is reached in most of the results presented in this report, the solver was not able to find a solution within this range for some scenarios in a reasonable time (< 24 hours) to finalize this study. In these cases, the process stop criteria was changed to a time limit, registering the theoretical difference between the found and the best possible solution, refer as gap in this document. Given that the gap registered for these cases was significantly large (>10%), an additional constraint was imposed to these scenarios, defining the objective function as positive. This change managed to lower the registered gap to acceptable levels for most cases, but not all as will be discussed in Chapter 7. In these cases, the results are discussed after warning the reader about this issue to be interpreted with caution.

More information about the solver parameters can be consulted in GAMS documentation (McCarl, 2016).

4.2.2 Objective function

The model’s **objective function** (Eq. 18) is designed to minimize the difference between economic benefits and energy costs for the community. The general form of the model’s objective function is shown in the equation below.

Eq. 18 Objective function for the investment model.

$$F = -Ben + (Cost_{buy}^{el,tariff} + Cost_{inv} + Cost_{op} + Cost_{dr} + Cost_{fuel} + Cost_{gen}), \text{tariff } \in \{TOU, PP, BW\}$$

The first term **Ben** accounts for all the benefits obtained in the 16-year period as compensation for the injection of surplus energy from the Energy community to the distribution network and the provision of EV charging services. The rest of the terms are all the costs related to meeting the community’s thermal and electrical demand in that same period, whether it is by generating it locally through the energy assets installed or purchasing it from the grid. The specific definition for each term can be consulted in Table 25.

The cost of purchasing electricity $Cost_{buy}^{el,tariff}$ is modeled differently depending on the tariff scenario; the rest of the terms in the objective function equation are handled equally regardless of the tariff scenario imposed. Scenarios with **Energy-based** charges only (TOU, TOU_Flat, TOU_PPA, No Charges) are modelled considering a price vector specifying the hourly cost of electricity, which is then multiplied by the electricity purchased at each time step. As explained before, the hourly prices values are calculated according to the energy price case (dynamic, flat rate, PPA) plus taxes and Time-of-Use charges in the applicable scenarios. For the **Bandwidth tariff** scenario, a similar approach is used, but an additional charge is imposed to the consumed and injected power above the established limits. In this case, the price vector consists of the marginal prices plus taxes, as the network costs are recovered through fixed monthly costs that the users pay for their contracted bandwidth power. This fixed cost is not included in the optimization as is not subjected to changes within the modelled variables. Finally, in the **Peak power** case, the same price vector as in the Bandwidth tariff is used, but an additional charge is imposed over the maximum power registered by the community on a monthly basis.

To incorporate the effect of time in the value of money, all cash inflows and outflows in future years are brought to a present value by using the discount rate considered in each scenario. This is done by multiplying

all costs and revenues by the term $\frac{1}{(1+R)^{y-1}}$, where R is the discount rate and y is the number of time periods (years) since the starting year. We did not incorporate avoided energy costs as an explicit cash flow in the objective function as this benefit is already implicit in the minimization of the electricity purchased costs $Cost_{buy}^{el,tariff}$. Therefore, if the objective function is positive, meaning there are higher costs than benefits, it does not mean that the proposed investments necessarily result in economic losses for the community as the avoided costs also need to be taken into account as an economic benefit.

Table 25 Definition of the cost terms used in the investment model's objective function

| Cost term | Description |
|--------------------------|---|
| $Cost_{buy}^{el,tariff}$ | It accounts for the total cost of electrical energy purchased in the evaluated timeframe. Three different types of electrical purchase costs are considered, depending on the scenario category: Energy-based (EB) for No Charges, TOU, TOU_Flat and TOU_PPA scenarios, Bandwidth (BW) and Peak Power (PP) for the Bandwidth and Peak power scenarios, respectively. |
| $Cost_{inv}$ | Total investment costs from all the energy assets installed in the 16-year period. It is computed by multiplying the capital expenses associated with each technology type for the capacity installed. As most assets have a useful lifespan beyond 16 years, the equivalent annual investment costs from these years are discounted from the total investment sum. In the case of the technologies that have a useful life lower than the investment period (V2G chargers and Electrolyser), the replacement cost is considered. |
| $Cost_{op}$ | Total fixed operational expenses – defined as an annual fixed sum dedicated to the equipment's operation and maintenance – expected in the 16-year period. It is calculated using an OPEX factor equivalent to a percentage of the asset's investment cost. The used factors for each technology can be consulted in the Annex database. |
| $Cost_{dr}$ | Variable costs associated with the activation of demand response, which depends on the total volume of energy shifted. |
| $Cost_{fuel}$ | Total cost associated with fuel purchasing for the operation of CHP units and boilers. Note that three types of fuels are considered in MODECO – natural gas, hydrogen and biomass – but not all are available for all archetypes (2.2.2). |
| $Cost_{gen}$ | Use-of-Network tariffs applied to all energy produced in the Virtual Community archetype. The rest of archetypes are exempt from this cost given the network charges rules for physically closed generation and demand explained in Chapter 2. |

Source: own elaboration.

4.2.3 Key model constraints

As listed below, a set of general constraints are used in the investment model to serve different purposes:

- *Time decision constraint*. With the objective of reducing computational stress, the annual investments are always decided in the first hour (time step) of each year.
- *Electrical oversizing constraint*. The installed storage power cannot be larger than the local power generation installed by the community.
- *Storage oversizing constraint*. The installed capacity from heat generation assets (boilers and CHP) cannot be higher than 15% above the maximum thermal energy demanded by the community in the 16-year period.
- *Rooftop surface constraint*. The total area occupied by PV solar systems installed in rooftops cannot exceed the total area available at the community's rooftops.
- *Land surface constraint*. The total area occupied by ground-mounted solar PV systems, wind turbines and hydrogen tanks cannot be higher than the total land surface available at the community for this purpose.

- *Thermal oversizing constraint.* The installed capacity from heat generation assets (boilers and CHP) cannot be higher than 15% above the maximum thermal energy demanded by the community in the 16-year period.

The *surface constraints* are implemented to reflect the physical limitations typically encountered in the defined archetypes regarding the surface availability to installed energy assets such as those considered in MODECO. In particular, it is important to consider that ground-mounted PV solar and wind turbines compete for the same area as both need to be in open air spaces. Hydrogen tanks are also expected to be installed in open air surfaces, which is why their area is also taken into consideration for the *land surface constraint*. CHP, electrolyzer and batteries are not contemplated in this limitation as it is assumed that they can be installed in other available spaces, such as already existing facilities like a warehouse. In the case of the *rooftop surface constraint*, only the area from solar PV systems installed in rooftops is considered.

The rest of constraints limit the amount of power generation and storage that can be installed inside the community. These limits, however, are based on arbitrary decisions interpreting the definition of Renewable and Citizen energy communities that indicates that generating financial profits must not be the community's main purpose although they are able to provide economic benefits to their members, shareholders or local areas in which they operate. Within MODECO, it is assumed that installing excess generation capacity with the sole purpose to sell energy in the wholesale market should not be promoted as it would be a financial profit-led activity. Still, it is reasonable that communities could generate excess energy at some hours in which demand is low and stored in batteries to be consumed at later times, when it is needed. A reasonable limit to ensure this is to limit power generation capacity to the community's peak demand as proposed in the *electrical oversizing constraint*.

The storage capacity is also restricted to fit the maximum local generation capacity installed (*storage constraint*), preventing the installation of numerous storage units to act as stand-alone batteries that charge at low-priced periods, increasing the community's demand to re-sell energy later during peak priced hours. Notably, a first version of the model did not include such constraint and with the future reference scenario prices, it led to extremely high storage installations that were financed through energy arbitrage revenues obtained at specific days towards the end of the evaluation period. Nonetheless, it is relevant that communities could still engage in energy arbitrage up to a certain extent, which supported battery usage for increasing self-consumption. This is important considering that grid flexibility is also an important benefit that communities could provide to the system.

Finally, the *thermal oversizing constraint* restricts the heat generation capacity of CHP units to the community's peak thermal demand as wasted heat production is considered misaligned to sustainable and efficient energy usage, which goes against the provision of environmental benefits and towards maximizing financial gains. In this case, however, the power generated could be larger than the community's demand, thus generating surplus electricity to be sold to the grid. As noted, a 15% margin is considered to provide some operational flexibility.

Box 2 Drawing the line between economic benefits and purely financial profit generation

Three of the investment model constraints were proposed based on the principle that Energy communities should not engage in energy activities with the sole purpose to generate financial profits. Nevertheless, representing such nature into an optimization model that could be applied to different archetypes and regions presents new conceptual challenges. In national regulations, communities' investments might be constraint by rules such as those currently applied to collective self-consumption in Spain (Ministerio para la Transición Ecológica, 2019) which limits the number of members that can be part of it to a certain geographical extension (maximum of 2 km between furthest participants) and provides larger financial incentives to energy that is released (generated or discharged) at the same time as demand. However, a generic model like that designed for MODECO cannot rely on such specific rules. Still, it must reflect the difference between community-led energy investments and those guided by maximizing financial profits, especially as the latter are also expected to be risk takers while communities would probably follow a more conservative investment strategy. The proposed set of constraints seems to fit this purpose to a certain extent, but as will be seen in Chapter 7, they might need some further thought to better reflect communities' nature in contexts in which prices promote the installation of purely merchant projects. Nonetheless, the question of whether or not communities should be assumed, or even encourage, to take part in these activities remains, particularly if they represent potential benefits for the whole system, for instance, by providing flexibility services or contributing to shifting demand to hours when more generation is available. This is a relevant point considering that the internal electricity market directive (EU 2019/944) and the revised renewable energy directive (2018/2001/EU) mandate EU countries to allow the participation of Energy communities on all market activities, accessing the same support schemes as larger participants. So, where is the line between an energy investment led by profit and one whose main purpose is to return economic, environmental or social benefits? Reaching a consensus over this aspect might help to improve the design of models such as that proposed by MODECO. Another important aspect is the incorporation of different business models into the Energy community archetypes proposed in this study, for instance, energy cooperatives might have more in common with traditional energy investors than a group of neighbours looking to become self-sufficient and reduce their energy bills.

4.2.4 Energy balance equations

The mathematical formulation for the investment model can be consulted in Annex 1 while a summary of the balance equations applied in the investment model are presented in this section. These are used to maintain an equilibrium between the different energy flows, including energy generated and consumed within the Energy community's boundaries, and that imported and exported from outside. This balance includes not only electrical but also thermal energy flows, and the energy carriers that might be potentially used to generate heat and power (natural gas, hydrogen and biomass).

Electrical power balance. In the electrical power balance, at each hour, the constraint indicated in Eq. 19 must be satisfied. The term for the electrical power generated by assets [$EP_{generated}$] is calculated from all the generation assets that can be potentially installed in each archetype and which were described in Table 7. This includes solar and wind generation, CHP electrical generation, and power discharged from batteries or EV through the V2G charging points. The electrical power consumed by assets [EP_{assets}] is defined by the power charged by storage devices (batteries and EV) and, in the case of the industrial polygon, the electricity consumed by the electrolyzer. The electrical demand [ED] refers to the electricity needed by the community to satisfy its members' demand, which considers the community's electrical load modelled and the shifting possibilities offered by the Demand Side Response (DSR) characteristics considered. Finally, the electrical power bought [EP_{bought}] and electrical power sold [EP_{sold}] refer to the electricity imported and exported from the grid to complement the local generated electricity to satisfy the community and the assets' demand.

Eq. 19 Electrical power balance

$$EP_{generated} + EP_{bought} = ED + EP_{sold} + EP_{assets}$$

Heat balance. The thermal energy balance is satisfied at each hour given the constraint indicated in Eq. 20. The thermal power generated by assets [$TP_{generated}$] term is calculated from the thermal energy generated by CHP units and boilers, while the thermal demand [TD] corresponds to the heat demanded by the community to meet its water and space heating requirements, plus the process heat in the case of the

Industrial polygon. This balance is not considered for the Virtual community archetype as investments in CHP units are not considered a possibility in this case.

Eq. 20 Thermal balance

$$TP_{generated} = TD$$

Fuel balance. The balance for the supply and demand of the fuels used by the community are given by Eq. 21, Eq. 22 and Eq. 23 for natural gas, biomass and hydrogen, respectively. In the natural gas balance, the fuel consumption from CHP and boilers [$CH4_{assets}$] must be equal to the gas bought [$CH4_{bought}$] as it is the only source possible. A similar equation is applied to biomass, a fuel only available in the Rural town archetype. Lastly, the hydrogen balance considers that the hydrogen stored in the hydrogen tank or consumed by the community's boilers and CHP [$H2_{assets}$] must be equal to that bought from outside [$H2_{bought}$] plus the internally produced hydrogen by the electrolyzer [$H2_{produced}$] in those cases in which this equipment is available (Industrial polygon).

Eq. 21 Hydrogen balance

$$CH4_{bought} = CH4_{assets}$$

Eq. 22 Biomass balance

$$BIO_{bought} = BIO_{assets}$$

Eq. 23 Hydrogen balance

$$H2_{bought} + H2_{produced} = H2_{assets}$$

4.2.5 Energy assets modelling

The mathematical formulation of the energy assets considered in MODECO is done based on standard approaches used in the literature and can be consulted in Annex 1. For most energy assets, a similar approach is used in the investment and operational models, except when adaptations are needed to take into consideration that the capacity installed in the investment model is unknown at the start of the optimization or that representative days are used instead of the whole year vector. The values used for all the technical parameters required can be consulted in the Annex database associated with this report.

Wind turbines and **Solar PV**. Both systems are modelled considering the load factor curves applicable to each country. The hourly generation is then obtained by multiplying the hourly load factor by the asset's installed capacity, which is defined as a variable.

Electrical storage assets are represented with a modified approach to the typical equation (Eq. 24) used to model batteries in which the State of Charge (SOC) is represented as a percentage (%) of the total capacity, which results in a nonlinear model as the installed capacity is unknown. To avoid non-linearity, instead of modelling the SOC (%), the approach used in MODECO, models the energy (kWh) inside the battery (e) as shown in Eq. 25.

Eq. 24 Traditional approach used for modelling electrical storage

$$SOC_t \cdot e_t^{inst} = SOC_{t-1} \cdot e_{t-1}^{inst} + CHARGING P_t - DISCHARGING P_t$$

Eq. 25 Proposed approach to avoid nonlinearity when modelling electrical storage

$$e_t = e_{t-1} + CHARGING P_t - DISCHARGING P_t$$

Note that the maximum charging/discharging power of the battery cannot be known in advance, as it depends on the capacity installed as a result of the investment decisions made. Thus, the charging/discharging power given to the Electrical Storage is limited by the product of the C-rate and the current installed capacity and not by a maximum charging/discharging power, which avoids nonlinearity problems. The C-rate gives a relation between the capacity installed and the maximum charging/discharging power available. It must be noted that the battery can only charge or discharge at a given time step, as a restriction is imposed to avoid the simultaneity of these two activities.

As the investment model is applied to a certain number of representative days in the year, the investment strategy and the assets management is not decided over a continuous time period. Thus, a constraint is set to define the initial SOC of the battery in the first time step as equal to 50% on a daily basis. The SOC of the battery at the end of each day is also set to a predefined value (50%) as, without this constraint, the model would try to discharge the battery at the final time steps of each day to sell electrical surpluses to the grid.

Hydrogen tank. For this asset type a similar problem to the electrical storage is found as the pressure level (Pa) of the tank must be modelled while having the tank's volume as a variable, which results in a nonlinear

equation when the typical approach is used. Let q_t , v^{inst} be the pressure level of the tank and the total volume installed, respectively, then the pressure inside the tank is typically modelled as shown in Eq. 26 where K is a constant given by two parameters (mean temperature inside the vessel and the universal gas constant).

Eq. 26 Traditional approach used for modelling hydrogen tank storage

$$q_t = q_{t-1} + K \cdot \frac{H2\ inflow_t - H2\ outflow_t}{v^{inst}}$$

As observed in the equation above, the volume of the tank divides the hydrogen inflow/outflow. Given that all these three are variables, it results in a nonlinear model. To solve this problem, instead of modelling the pressure level (Pa), the quantity of Hydrogen (mol) inside the tank is used, which ensures linearity. Let mol_{H2} be the mols inside the tank, the following equation is proposed:

Eq. 27 Proposed approach to avoid nonlinearity when modelling the hydrogen storage tank

$$mol_{H2,t} = mol_{H2,t-1} + H2\ inflow_t - H2\ outflow_t$$

In order to bound the moles of hydrogen inside the tank by the installed volume v^{inst} , a constraint to limit the maximum hydrogen inflow/outflow is applied using the product from the C-rate and the tank volume. The C-rate gives a relation between the volume installed and the maximum possible inflow/outflow of hydrogen. The initial and final state of the tank's pressure is imposed through a set of constraints for the start and end of each day. The initial state value is applied as non-continuous days are used, while defining a minimum tank's pressure for the final state prevents the tank from fully discharging at the end of each day. Similar to the electrical storage case, the tank cannot simultaneously charge and discharge hydrogen at a given time step.

Electrolyzer is modelled by assuming a linear relation between power consumption and hydrogen generation. The maximum power consumed by the electrolyzer at each time step (hour) is limited by the power installed.

V2G charging stations. As the number of V2G chargers installed is a variable in the investment model, the input curves with the number of vehicles connecting and disconnecting at each time step are built assuming a high number of chargers available. These are then interpreted by the model as the number of vehicles *wanting to connect* and *leave* the station. For the individual EV, the following assumptions are made:

- All the EVs considered are assumed to have the same battery capacity E^b each year. This battery capacity is calculated considering a mean value from the typical sizes in current and future EV models. More information about these assumptions can be consulted in Section 3.3.2.
- All the vehicles are assumed to arrive at the station with the same state of charge SOC^{ini} and leave at the same state of charge SOC^{fin} .
- The EV's SOC has to be in a certain range $[SOC^{min}, SOC^{max}]$.
- All EVs are assumed to stay connected at the charging station for time periods between 3 and 7 hours with a mean charging duration of 5 hours as reported by (Corchero García, 2015).

To reduce computational stress, all the batteries from the vehicles connected to the V2G points are treated as a single unit whose total power and capacity is the sum of all the batteries in the connected EV pool. The charging and discharging power of the battery pool is limited by the product between the number of vehicles connected and the maximum charging/discharging power of each V2G charger. It must be noted that each of the V2G chargers is assumed to have a maximum charging/discharging power P_{V2G}^{max} that limits the power that can be delivered to the vehicle. Constraints to limit the upper and lower bounds of the battery pool's energy levels are applied using the number of vehicles connected at time t , the vehicles that *want to connect* at t and the vehicles that want to leave at time $t-1$, as well as constraints applied to the individual EV regarding their SOC levels and explained above. The specific constraints used and its mathematical formulation can be consulted in this document's Annex.

Combined Heat and Power (CHP). A simplified model considering a linear relation between the heat and power production of the CHP units is selected for the investment model. The linear relation is established through a conversion factor specific to each CHP subtype [CHP_{gas} , $CHP_{biomass}$]. The use of more detailed approaches, such as that applied in the operational model, is discarded as it adds complexity as the installed capacity is a variable in this case. In the proposed linear model, the following constraints are applied:

- The CHPs cannot generate more electrical power than the nominal power installed.
- The CHP's state (on/off) at each time step is controlled via a binary variable.

- CHPs are considered to be always on at the first time step of each day.
- The CHPs can only be switched off and on once per day; respecting minimum up and down times is obliged.
- A linear relation between electrical power generated and fuel consumption is established using a conversion factor specific to each fuel. Note that CHP_{gas} can consume both hydrogen and natural gas, although not at the same time, while $CHP_{biomass}$ can only consume biomass.

Boilers. The same model is applied to the two boiler categories considered in MODECO: regular and industrial. It considers that a linear relation exists between the thermal power produced and the fuel consumed at each time step. As assumed for the CHP equipment, the communities' boilers can be fuelled by hydrogen or natural gas, but not simultaneously. Only one fuel can be used at each time step. Finally, a constraint is applied to limit the maximum thermal power produced by the boilers to the total boiler capacity installed each year.

Demand Response. In MODECO, demand response is provided by heat pumps, which are considered a flexible load within the modelled communities. Within the model, demand response operations are constrained by an upper and lower limit for increasing or decreasing the heat pump's demand. These are defined based on the percentage of customers assumed to be willing to participate in the provision of this service and the technical restrictions associated with heat pumps. If the increase or decrease is higher than the limit, customers' needs will not be satisfied. Additionally, an upper limit for the consecutive hours that the demand response service might be used is imposed. If demand response is used for large periods of time, there is a risk that customers' needs won't be fulfilled causing a future loss of profit. For similar reasons, a maximum number of times that demand side response can be activated per day is set as an operational constraint.

The assumptions made for demand response and the energy assets considered in the investment model can be consulted in Chapter 3.

4.3 Operational model

The goal of this model is to obtain the optimal energy planning of the communities' energy assets at an hourly level in an annual horizon, by minimizing its operational costs. The mathematical model is classified as a Mixed Integer Linear Problem (MILP) as integer and binary variables are needed to describe the energy asset's operational modes. As such, the objective function and all the constraints needed are linear. Contrary to the investment model, the operational model is executed individually for each target year and scenario considered in this analysis. This permits to use the 8760 time steps in a year without the need to select representative days. The operational model outputs the optimal usage of the technology for every combination of year, archetype, and energy tariff scenario studied in this project, indicating the corresponding energy production, energy usage, heat produced, biomass consumed, gas consumed, hydrogen produced, hydrogen consumed, emissions and marginal prices for technology. The key inputs and outputs used for the operational model are presented in Figure 14.

4.3.1 Objective function

The **objective function** used in the operational model consists of the minimization of the difference between the economic benefits and costs associated with the community's energy management in the evaluated year (Eq. 28). Aside from a shorter time horizon, the main difference when compared to the objective function used for the investment model is that the investment costs ($Cost_{inv}$) are not included in the function as this is no longer a variable to be optimized. Moreover, as CHP is modelled with more detail in this case (see Section 4.2.5), the equipment's start-up cost is computed as a specific term ($Cost_{CHP}$). The rest of the components are the same as in the investment model, which also includes the differentiation between the purchase electricity costs depending on the tariff structure evaluated.

Eq. 28 Objective function for the operational model

$$F = -Ben + (Cost_{buy}^{el,tariff} + Cost_{op} + Cost_{dr} + Cost_{fuel} + Cost_{gen} + Cost_{CHP}), \text{tariff } \in \{EB, PP, BW\}$$

4.3.2 Balance equations

The balance equations used for the operational model are similar to those described for the investment model in Section 4.3.2. The specific equations applicable to this model can be consulted in Annex 3.

4.3.3 Energy assets modelling

All the energy assets that can be potentially installed in the Energy communities are modelled and included in the operational model (see Table 7). Nonetheless, these are only activated if their availability in the evaluate year has been decided by the investment model. Note that some of the energy assets are only considered a potential investment for some specific archetypes, for instance, the biomass-fuelled CHP is only available for the Rural town archetype. Given that a generic operational model is used for all cases, the technologies that are not considered in one archetype are simply not activated as happens with the assets that were not part of the investment decisions made. In the following paragraphs, a brief explanation of the modelling approach used for each energy asset is given while the specific mathematical formulation can be found in Annex 2.

Solar PV and wind turbines. No further explanation is given as they are represented as in the investment model using the load factors applicable to each technology and location and the installed capacity, which in this case is not a variable but a given input.

V2G charging stations. To model a charging point with V2G capabilities, the state of charge (SOC) of the EV battery should be included in the operational model as an available and accessible data to be able to decide when the EV battery should be charged or discharged to meet both the EV owner needs and Energy community interests. The charging and discharging modes are decided using binary variables to model the bidirectional operation of these chargers, and when a binary variable is introduced, the model becomes a combinatorial problem with a harder computational requirement. This is not a problem per se, except when a large number of charging points are considered as the computational time required to find the optimal solution might be too large to be feasible. To avoid this problem, the operation model proposed for MODECO is inspired by the authors of (Quiros-Tortos et al., 2018) that suggest using an aggregated solution in order to reduce the number of binary variables in the operational model.

The assumptions made for V2G charging points model following this approach are listed below:

- All electrical vehicles are aggregated to form a single pool of electrical batteries that act as a storage unit, hence the energy and power capacities of the EVs are also aggregated by category. This includes all types of EVs considered in each archetype. Thus, the number of EVs per type connected at the V2G points must be known to calculate the aggregated batteries capacity available for every single hour.
- The optimization model decides the behaviour of the aggregated pool for every time step. The time steps have been defined on an hourly basis according to the specifications made for both the operational and the investment models. Then, if the pool starts charging or discharging at the beginning of a time interval with a determined power value, it is supposed that this operation point is the same during the whole hour.
- The battery capacity values will be in line with the values defined for the reference models described in Table 21. The number of vehicles per model is decided following the technological evolution assumed for private charging points. In 2025, mostly EV with low capacities are considered, whereas for future timespans, the number of EVs with larger capacities increments. This is in line with (Gaete-Morales et al., 2021) that states that the typical EV battery size in 2010 was 30 kWh; today 60 kWh is not an exception anymore and by 2030 the battery capacity for new vehicles will be over 80kWh.
- The maximum state of charge and depth of discharge of the entire vehicle pool, as well as the efficiencies remain constant. These maximum states of charge and depth of discharge will be calculated as the average of the current values for this technology, since they are quite stable values over time, whereas efficiencies will be considered 95% as for private charging points.
- Corchero Garcia (2015) reported statistical data from several European electric vehicles and charging points monitored during three years. Based on their results for EVs of private use, it can be assumed for this work that the initial SOC for every electrical vehicle connecting to the charging station at every time is considered to be 58% and the request SOC at departure time is considered to be 84% (Corchero García, 2015).

Apart from assumptions and parameters values, the model has some constraints explained below whose mathematical formulation can be consulted in Annex 2:

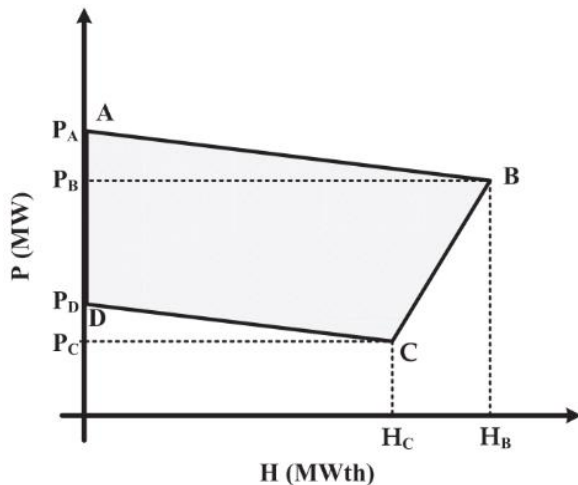
1. Two constraints aggregating all available energy and the power capacities of all EVs in a particular time. Specifically, the capacity of each EV type is multiplied by the number of this EV type connecting in each hour.
2. All EVs that arrive or depart at time interval t are assumed to do so at the start of the interval and remain in that state without any further cars arriving or departing until the start of the next period. Note that the main input for this model is the number of electrical vehicles of each considered type arriving or departing at every period of time.
3. The energy balance equation of the aggregated battery pool illustrates the fact that all the EVs connecting or disconnecting at a certain time period have the same energy levels across their batteries.
4. The energy level of the pool is not allowed to surpass the maximum SOC defined, or be inferior to the minimum SOC established.
5. The last set of constraints ensure that the upper and lower power limits for charging and discharging at every time step cannot be surpassed.

Electrical storage. As the electrical storage capacity is known from the start, batteries can be modelled using the typical approach shown in Eq. 24 without any particular assumptions needed. Nonetheless, the following set of constraints must be taken into consideration:

- The energy level of charging and discharging cannot surpass the battery's upper operational limit. This ensures safety operation and expands the battery' life expectancy.
- Discharge and charge cannot be performed simultaneously. A real battery can only perform one action at a time.
- The electrical storage SOC fluctuates according to the operational needs but cannot exceed the maximum and minimum operational levels. These limits are defined based on the batteries' technical characteristics and can be consulted in the Annex database.
- Efficiency losses are incorporated when charging and discharging the battery, this represents that some energy is lost when using the battery as happens in real storage systems.
- Final SOC is considered equal to the battery's initial SOC. Without this constraint, the model will empty all the batteries to sell electricity before the day is over and no battery capacity will be available for the next start.

Combined Heat and Power (CHP). As the installed CHP capacity is known, more complex approaches can be used to represent the features of this equipment in the operational model. In this case, the heat and power production of the CHP unit is not defined through linear relations but by the equipment's feasible operating region, which is represented through a trapezoid (Figure 15) delimited by four operational points (A, B, C, D). Although other approaches are found in the literature, for instance using more operational points, the feasible operating region considered in MODECO is the same as suggested by the authors of (Mansouri et al., 2020).

Figure 15. Feasible operational region for a CHP unit given four operational points



Source: (Mansouri et al., 2020)

As explained before, the CHP units can be operated using gaseous fuels – natural gas or hydrogen – or biomass (pellets). In both cases, the same modelling approach is applied although the values used to define the operational points are specific to each fuel category (gases, biomass). The general constraints considered for this technology are:

A set of constraints representing the operational points forming the unit's feasible operating region and the relation between heat and power conversion at each point:

- An upper and lower limit for energy and heat production that cannot be surpassed. These are related to the operational points and are defined to ensure safety operational boundaries and avoid negative impacts on the units' useful life expectancy.
- An upper limit for power and heat related to the gas, hydrogen and biomass consumed. As explained before, these constraints vary depending on the CHP used, the parameters of each raw material consumed is different.
- As done in the investment model, the operational model contemplates the possibility to shut down the equipment if their operation is not economically feasible and restart it at a later period. However, in this case, minimum up and down times are considered to restrict the number of times this can happen in a day in addition to the shutdown costs.

Additionally, the proposed model permits to take into account the costs associated with the shut down and following restart of the machine ($Cost_{CHP}$). The CHP's shutdown is assumed to have null costs but the start-up costs are valued as equal to the costs of the extra fuel required to warm-up the engines, which is calculated as the required fuel to operate the machine during 10 minutes at nominal power.

Electrolyzer. This equipment produces hydrogen through a chemical reaction initiated by electrical current. This hydrogen produced is able to fill the hydrogen tank or be used as a raw material for the CHP. The constraints applied are:

- An upper and lower limit for the hydrogen produced. This equation is to ensure safety and ensure the electrolyzer maintains its useful life expectancy.
- The maximum power cannot exceed the renewable energy production. It must be noted that the electrolyzer is assumed to be only powered by renewable energy as only green hydrogen usage is considered in MODECO's energy communities.
- A loss of efficiency production is considered. These losses reflect on less hydrogen produced per energy consumed.

Hydrogen storage tank. The hydrogen tank can be filled with the hydrogen produced by the electrolyzer and be later used as fuel in the CHP or boiler units. The considered constraints for this technology are:

- An upper and lower limit for the storage of the hydrogen. It's not feasible to fill the tank more than the tank capacity. This constraint guarantees that the hydrogen doesn't exceed the capacity.
- An upper and lower limit of charging and discharging storage. This equation is to ensure safety and make the hydrogen tank have a longer life expectancy of use.
- The gas pressure inside the tank cannot exceed an upper limit. This equation is also to ensure safety and prolong the life expectancy of the tank.
- The final pressure of the tank must be the same as the initial pressure. Without this constraint, the model will empty the tank and no hydrogen will be available to use after the last time step.
- A hydrogen balance equation, between the tank, the boiler, the CHP, the hydrogen available in the tank and the charging and discharging hydrogen.

Boilers. Boilers, regular and industrial, are included in the operational model following a similar approach to the investment module. The only difference is that the total thermal capacity installed is not a variable but a given input.

Demand response. Demand response is modelled as in the investment model as no investment decisions are made through the optimization model. Instead, the parameters associated to this feature are defined exogenously as done for the investment model.

4.3.4 Calculation of CO₂ emissions

The emissions from the operation of the local generation assets is calculated considering the emissions factors associated to each available fuel (Table 26). From the considered energy assets, only CHP lead to CO₂ emissions when operated with natural gas or biomass. As the operational model outputs the hourly electrical generation per asset, the aggregated annual values are used to calculate the CO₂ emissions associated to local generation by multiplying the electrical production by the corresponding emission factor. In the Industrial polygon, which considers the usage of green hydrogen, it is assumed that the gas-fuelled CHP uses natural gas and hydrogen in the same proportion as the entire community's balance, as the model outputs the total fuel consumption for all the community assets, including boilers.

Table 26 CO₂ emission factors associated to natural gas, hydrogen and biomass combustion

| Fuel | kg CO ₂ /MWt |
|--------------------|-------------------------|
| Natural gas | 201.94 |
| Hydrogen | 0.00 |
| Biomass | 10.53 |

Source: Own elaboration with data from UK Department for Business, Energy and Industrial Strategy (2023) and Chernova (1966)

5 Energy communities' description

The electricity and heat loads obtained for each Energy community case study are presented in this section, highlighting the regional differences between Germany and Spain, as well as the observed evolution during the studied period (2025-2040). It must be remembered that the demand from smart EV charging points is not yet included as its installation will be decided by the investment model. Also, the final behaviour from the heat pumps fleet might be different in the final results due to changes induced by the DSR program considered.

5.1 Business park

The Business park archetype is also located within an urban context, but contrary to the Urban district case, practically **all energy loads are driven by Non-residential buildings**, with a high presence of office buildings and associated services. In particular, 35 dwellings are considered to be part of this community, but only seven are Mixed buildings with some floors dedicated to residential spaces, which results in a lower number of households than in the Urban district case. In the ground floors of these dwellings, services such as restaurants and coffee shops can be found. From the rest of buildings, sixteen correspond to offices, four to hotels, three banks, two supermarkets, two fitness centres and one kindergarten. All services are thought to serve an urban space with a large presence of employed people.

Table 27 Business park indicators

| Indicator | Germany | | | Spain | | |
|---|---------|--------|--------|--------|--------|--------|
| | 2025 | 2030 | 2040 | 2025 | 2030 | 2040 |
| Total number of dwellings | 35 | 35 | 35 | 35 | 35 | 35 |
| Number of MFB | 0 | 0 | 0 | 0 | 0 | 0 |
| Number of SFB | 0 | 0 | 0 | 0 | 0 | 0 |
| Number of NRB | 28 | 28 | 28 | 28 | 28 | 28 |
| Number of MB | 7 | 7 | 7 | 7 | 7 | 7 |
| Number of IB | 0 | 0 | 0 | 0 | 0 | 0 |
| Total rooftop area [m²] | 15,700 | 15,700 | 15,700 | 15,700 | 15,700 | 15,700 |
| Total land area [m²] | - | - | - | - | - | - |
| Number of households | 150 | 150 | 150 | 150 | 150 | 150 |
| Non-smart charging points | 24 | 28 | 49 | 24 | 28 | 49 |
| Annual electricity demand [GWh] | 9.22 | 9.43 | 9.88 | 9.95 | 10.08 | 10.42 |
| Annual heat demand [GWh] | 17.32 | 17.05 | 16.69 | 16.56 | 16.46 | 16.34 |

Source: Own elaboration based on MODECO's methodology and assumptions

Table 28 CO₂ emissions associated with energy usage in the Business park archetype

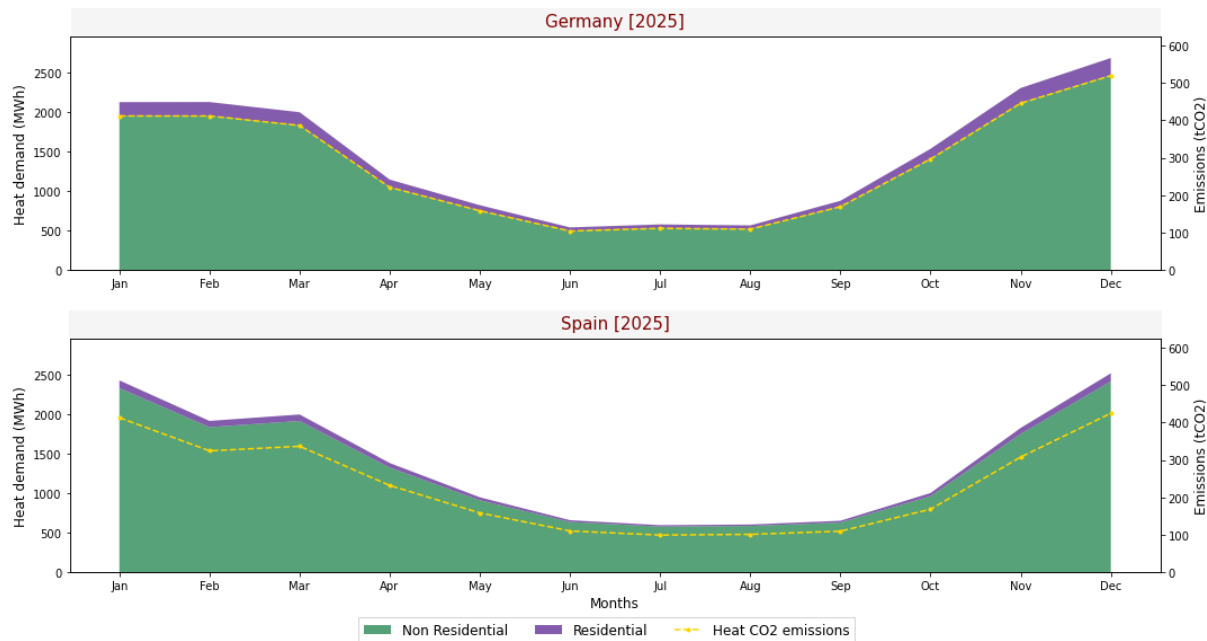
| CO ₂ emissions [ton/year] | Germany | | | Spain | | |
|--------------------------------------|---------|---------|---------|---------|--------|---------|
| | 2025 | 2030 | 2040 | 2025 | 2030 | 2040 |
| Total | 4301 | 3969.27 | 3685.92 | 3084.35 | 2778.6 | 2622.22 |
| Electricity usage [%] | 22.69 | 22.25 | 28.01 | 11.99 | 9.35 | 18.35 |
| Boiler usage [%] | 77.31 | 77.75 | 71.99 | 88.01 | 90.66 | 81.65 |
| Displaced by heat pumps | 145.88 | 345.07 | 717.59 | 630.93 | 827.9 | 1188.72 |

Source: Own elaboration based on MODECO's methodology and assumptions

5.1.1 Business park: Heat demand

The large presence of Non-residential buildings is evident in the distribution of monthly heat demand per sector, as heat demand from residential is minimal inside the community, even in the German region (Figure 16) where the larger heat demand considered per household makes its presence more evident in the Urban district and Rural town archetypes. Furthermore, fewer differences are observed between the Spanish and German cases as heat demand among Non-residential buildings in both regions is less distant than per residential users. Still, heat demand in the German Business park is significantly larger, particularly driven by higher requirements in the winter months, with the exception of January, when Spanish Non-residential buildings demanded more heat due to an especially cold winter. This trend is also observable in other archetypes, as all use the same temperature data as reference.

Figure 16. Monthly heat demand per sector in the Business park archetype in 2025

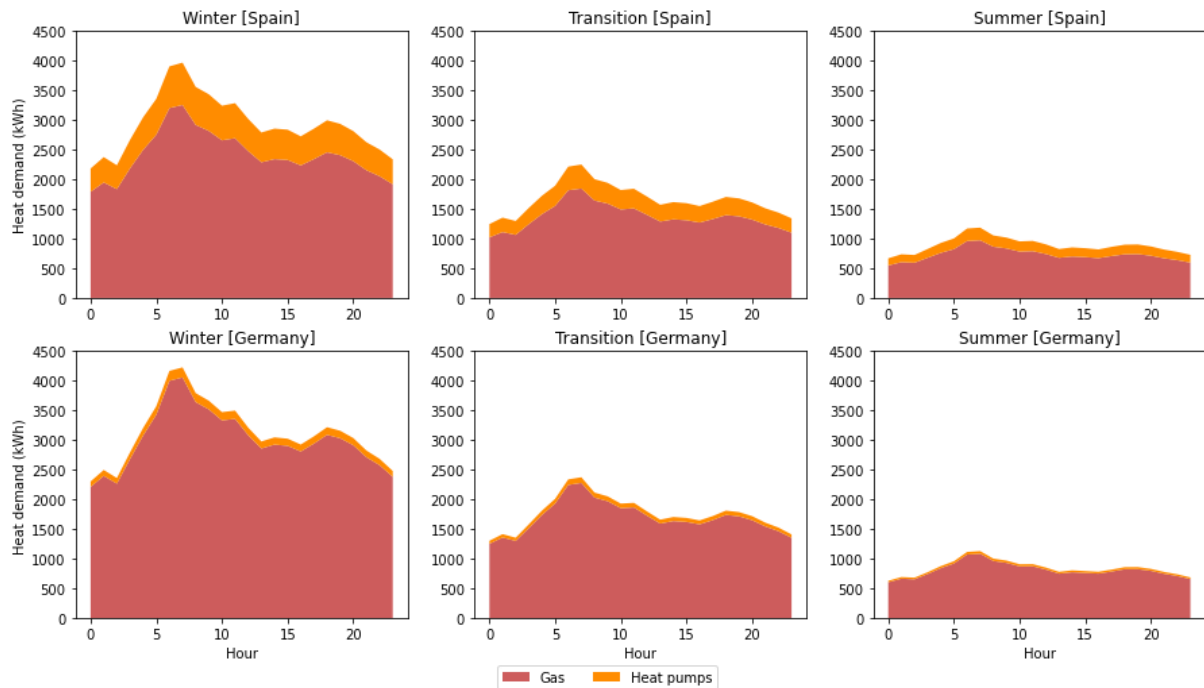


Source: Own elaboration based on MODECO's methodology and assumptions

The observed hourly demand (Figure 17) for this archetype follows a similar shape to the Urban district archetype, but indicates a steeper peak during morning hours (around 7:00 am). This can be explained by the large number of dwellings with business hours' operations such as banks and offices. The winter evening peak is also more visible here than in the Rural town archetype, following a similar shape to the Urban district case.

This peak practically disappears in the transition period and is nonexistent in the summer, where evening heating is not required and people tend to spend more time outside.

Figure 17. Mean heat consumption reported in 2025 in the Business park archetype in Germany and Spain

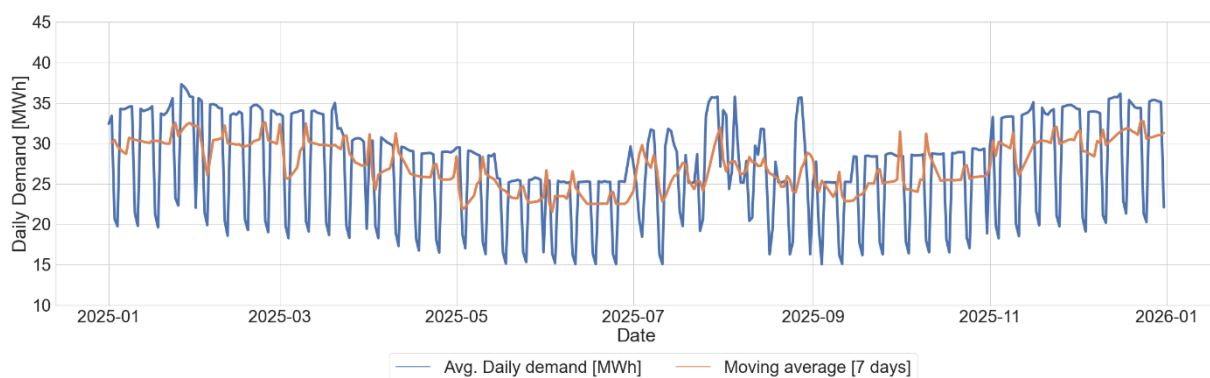


Source: Own elaboration based on MODECO's methodology and assumptions

5.1.2 Business park: Electrical demand

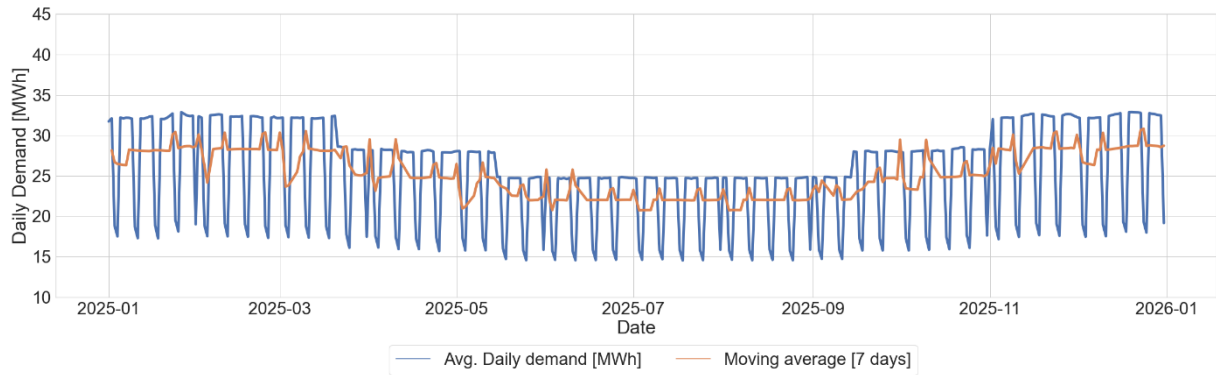
The daily electricity demand in the Business park follows a similar shape to the Urban district, but it must be noted that demand is far larger in this archetype than in the previous two cases. In the Spanish region, it is also relevant that the peak winter demand is practically at the same level as the summer peak demand (Figure). In the Urban district case, the summer peak demand – mostly driven by space cooling requirements – represents the highest daily demand in the year. This is also due to the higher heating requirements from Spanish Non-residential buildings than from residential users, more relevant in previous archetypes, which translates into higher electricity demand in the winter thanks to the 18% heat pumps usage considered in this region. In Germany (Figure), on the contrary, less differences are observed among the Urban district and Business park load shapes.

Figure 18. Daily electricity demand per sector in the Business park archetype in Spain [2025]



Source: Own elaboration based on MODECO's methodology and assumptions

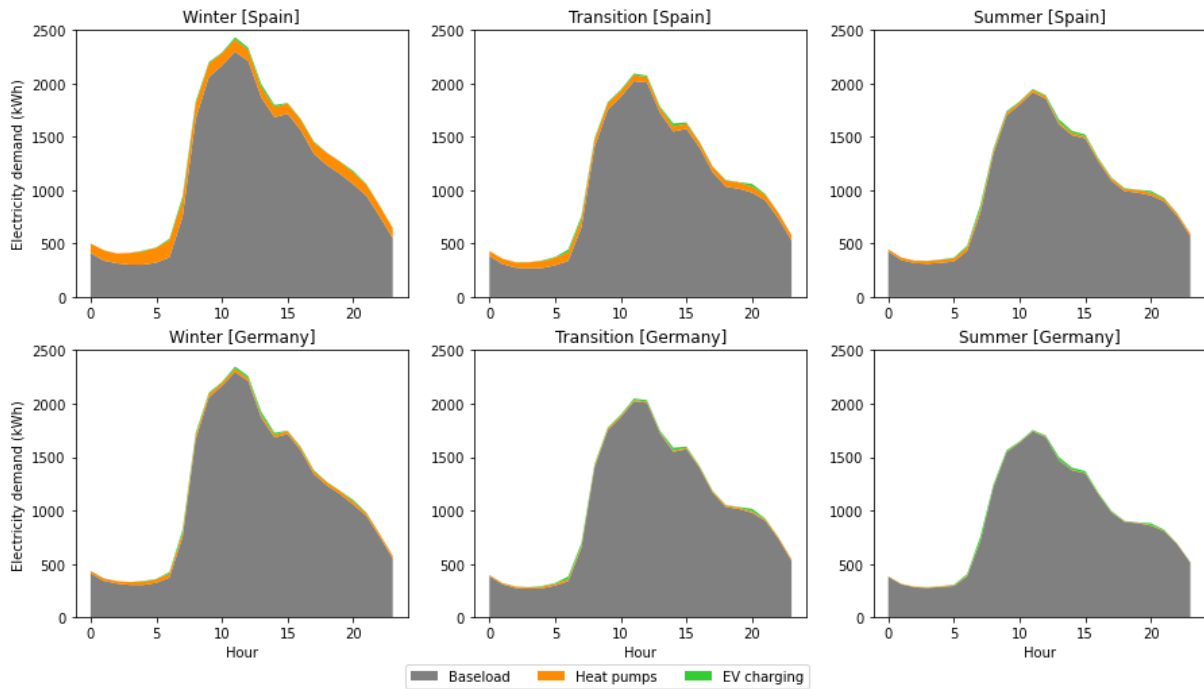
Figure 19. Daily electricity demand per sector in the Business park archetype in Germany [2025]



Source: Own elaboration based on MODECO's methodology and assumptions

As happened with heat demand, electricity consumption in the Business park peaks during morning hours (around 11:00 am) but a few hours later than for heat. Electricity demand starts increasing rapidly after 7:00am, which coincides with the observed heat demand and aligns with the business hours' operations of Non-residential buildings from the sectors considered in this archetype. It is relevant to observe that the summer demand in Spain remains practically the same than in the transition season, whereas in Germany, summer electricity demand is clearly lower in the Summer. This can be explained by the space cooling requirements that are particular to the Spanish case and take place during the summer months.

Figure 20. Mean electricity consumption reported in 2025 in the Business park archetype in Germany and Spain



Source: Own elaboration based on MODECO's methodology and assumptions

The number of EV charging points considered in the Business park is larger than for the two previous cases, but its contribution to the community's total electrical load is insignificant given the presence of large energy users such as hotels. The annual heat and electricity demand evolution follow a similar shape to the Urban district archetype, with annual reductions in the community's heat demand in addition to larger usage of electrical heat pumps, and can be consulted in the attached database.

5.2 Industrial polygon

The industrial polygon archetype presents a series of characteristics that are particular to this case. For instance, the use of a different member classification (Type 1: Ambient temperature dependent; Type 2: Ambient temperature independent) instead of the residential and non-residential categories used so far for the previous archetypes. However, this does not mean that Non-residential buildings are not present in this case as some of the Type 1 members can be classified as such (for instance, warehouse or industrial offices). Still, as a different approach is used, the Type 1 and Type 2 classification is preferred.

Table 29 Industrial polygon indicators

| Indicator | Germany | | | Spain | | |
|---|---------|--------|--------|--------|--------|--------|
| | 2025 | 2030 | 2040 | 2025 | 2030 | 2040 |
| Total number of dwellings | 50 | 50 | 50 | 50 | 50 | 50 |
| Number of Type 1 buildings | 39 | 39 | 39 | 39 | 39 | 39 |
| Number of Type 2 buildings | 11 | 11 | 11 | 11 | 11 | 11 |
| Total rooftop area [m²] | 33,800 | 33,800 | 33,800 | 33,800 | 33,800 | 33,800 |
| Total land area [ha] | 50 | 50 | 50 | 50 | 50 | 50 |
| Non-smart charging points | 25 | 25 | 25 | 25 | 25 | 25 |
| Annual electricity demand [GWh] | 373.48 | 373.48 | 373.46 | 372.96 | 372.96 | 372.94 |
| Annual heat demand [GWh] | 782.49 | 782.49 | 782.48 | 770.67 | 770.67 | 770.65 |

Source: Own elaboration based on MODECO's methodology and assumptions

Table 30 CO₂ emissions associated with energy usage in the Industrial polygon archetype

| CO ₂ emissions [kton/year] | Germany | | | Spain | | |
|---------------------------------------|---------|--------|--------|--------|--------|--------|
| | 2025 | 2030 | 2040 | 2025 | 2030 | 2040 |
| Total | 195.87 | 195.87 | 195.87 | 166.91 | 166.91 | 166.91 |
| Electricity usage [%] | 21.81 | 21.81 | 21.81 | 9.22 | 9.22 | 9.22 |
| Boiler usage [%] | 78.19 | 78.19 | 78.19 | 90.78 | 90.78 | 90.78 |
| Displaced by heat pumps | 3.71 | 3.71 | 3.71 | 2.89 | 2.89 | 2.89 |

Source: Own elaboration based on MODECO's methodology and assumptions

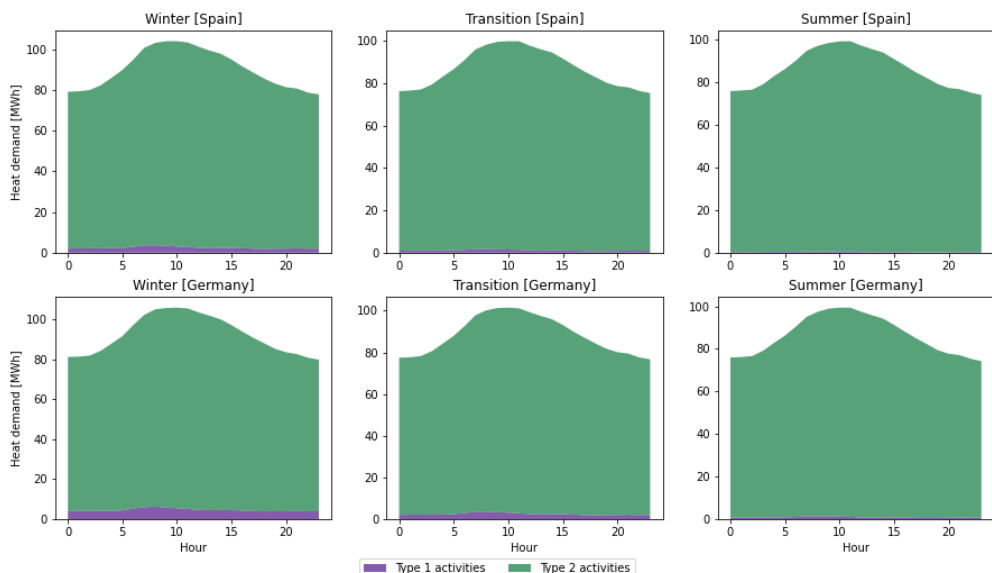
As shown in Table 29, 39 out of the 50 industrial users belong to the Type 1 category, which means that their heat load is related to the ambient temperature, and thus, presents regional differences. From these, only six have a 5-days working schedule, whereas the rest operates all week. The type of industries represented within this group varies among manufacturing of motor vehicles, electrical equipment, furniture and machinery; wholesale and retail trade; transportation companies; and warehousing. The full list of industries can be consulted in the associated database.

From the eleven industrial users belonging to the Type 2, three belong to the chemical sector, three to the food industry, two produce glass, and the rest three iron, paper and vehicles. It is important to note that despite being outnumbered by the Type 1 users, this group represents over 90% of the electrical demand in the Industrial polygon and a similar share of the total heat demand. Thus, few regional differences are observed in this case even at the hourly level as will be explained in the following sections. Also, electrical demand from heat pump usage is minor as most heat demand in the Industrial polygon corresponds to process heat, in particular, high temperature heat (>400 °C).

5.2.1 Industrial polygon: Heat demand

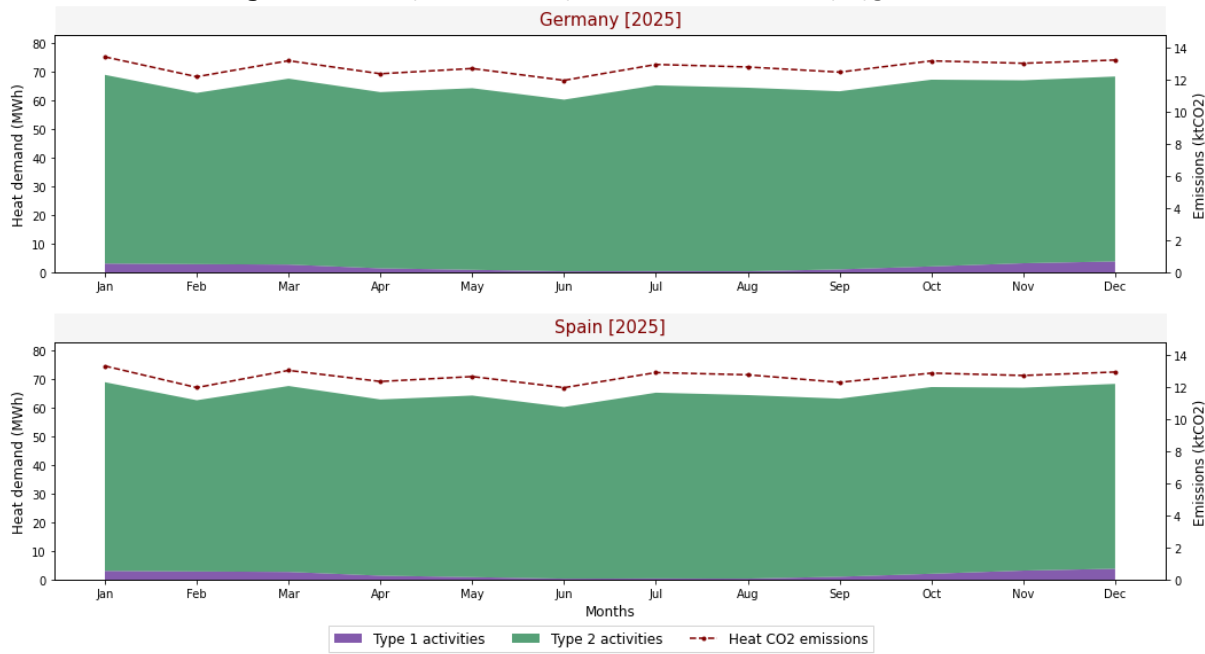
As observed in Figure 21 heat demand from Type 2 members represents the main heat consumption in the industrial polygon. As the consumption from these industries is not directly related to ambient temperature, a similar mean hourly consumption is maintained across seasons. Heat demand starts to increase at 4:00 and shows a peak consumption between 10:00 and 11:00 in the morning during winter, transition and summer periods. Although hardly visible due to its small share in comparison to Type 2 load, the consumption of Type 1 users is at its minimum in summer, when higher temperatures are reached, and maximum during winter. Furthermore, the difference between regions only impacts Type 1 load, which is higher in Germany than Spain. Looking at monthly data per industrial user category (Figure 22), it is also observed that Type 1 heat demand follows a more pronounced seasonal pattern than that of Type 2 users, but here is still some impact of season on Type 2 demand, being slightly higher in winter than summer months. This is due to the fact that even Type 2 users use heat for space and water heating purposes, although the main share goes to other applications related to their own industrial processes. As an example, the monthly results for the German case in 2025 are shown in Figure 22. The Spanish industrial polygon behaves pretty similarly. The results can be consulted in the associated database.

Figure 21. Mean heat consumption reported in 2025 in the Industrial polygon archetype



Source: Own elaboration based on MODECO's methodology and assumptions

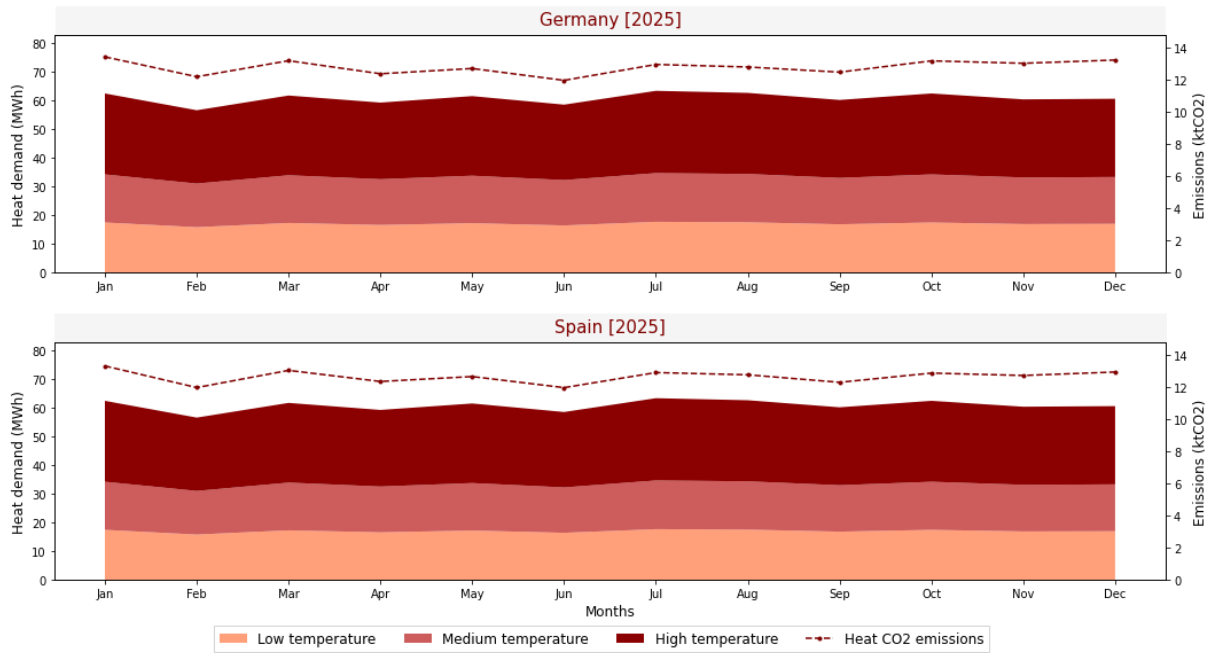
Figure 22. Monthly heat demand per sector in the industrial polygon in 2025



Source: Own elaboration based on MODECO's methodology and assumptions

In Figure 23, the process heat from the German case is divided per temperature range, using the applicable shares per industry. Given the industry mix defined, the resulting shares are similar between low ($<100^{\circ}\text{C}$), medium (100-400 $^{\circ}\text{C}$) and high heat ($>400^{\circ}\text{C}$) temperature ranges. As part of MODECO initiative, it would be assumed that only heat demand for space and water heating can be supplied by electrical heat pumps. Process heat could only be supplied by burning natural gas or green hydrogen at the industrial site.

Figure 23. Monthly heat demand by temperature level in the Industrial polygon in 2025

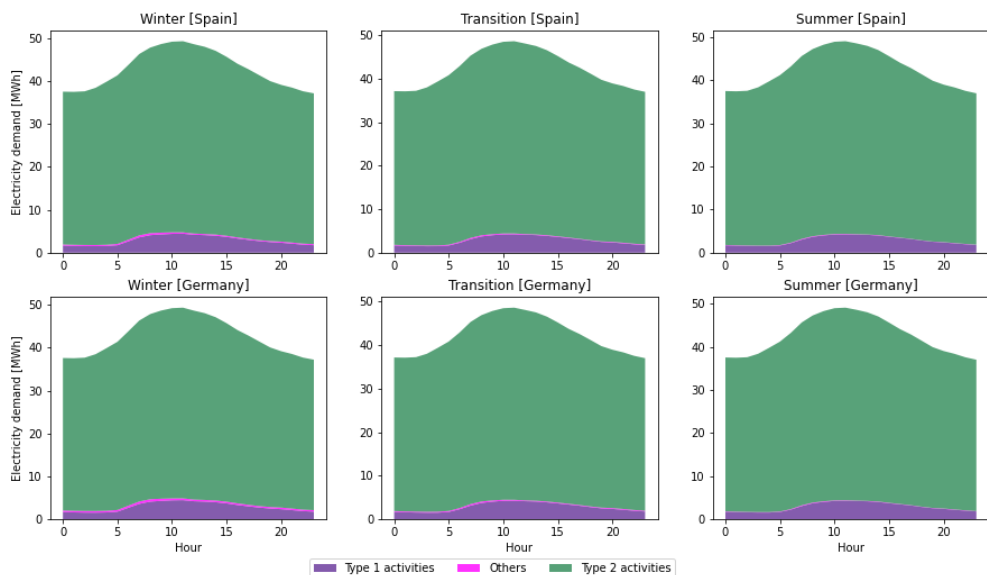


Source: Own elaboration based on MODECO's methodology and assumptions

5.2.2 Industrial polygon: Electrical demand

Contrary to industrial heat demand, which is partially affected by ambient temperature and thus presents regional differences, electrical load is practically the same for both target regions (Figure 24). Although there is some demand for heat and space cooling, this goes unnoticed due to the larger demand from Type 2 industrial consumers, whose processes have high electricity usage intensity. Similarly, no visible difference is observed across seasons, which is expected as electrical demand associated with heat pumps is also negligible when compared to the processing electrical demand. The demand associated with EV charging is as well negligible when compared against the users' baseload.

Figure 24. Mean electricity consumption reported in 2025 in the Industrial polygon archetype (Others include EV and heat pump electrical consumption)



Source: Own elaboration based on MODECO's methodology and assumptions

5.3 Rural town

The Rural town archetype is characterized by the presence of **single-family residential dwellings**, as 48% of the buildings in this community are classified as such (with rooftop area of 90 m²). As shown in Table 32, this means that there is a larger number of dwellings than in the Urban archetype but a lower number of households, making more significant the energy demand from Non-residential buildings. The presence of Single-family buildings also reflects in the rooftop space area, whose average value per dwelling is lower than in the Urban archetype. In addition to the 34 Single-family buildings, there are 19 Multi-family buildings, 7 Mixed buildings and 11 Non-residential buildings. The commercial and services considered in this archetype are similar to those found in the Urban district (supermarket, drugstore, bakery, etcetera), but sizes are in general smaller. The only exception are four buildings where farming activities are carried out, as this are particular of the Rural town archetype. In this case, only six charging points are considered for the starting year (2025), two for household users and four for business usage.

Table 31 Rural town indicators

| Indicator | Germany | | | Spain | | |
|-----------|---------|------|------|-------|------|------|
| | 2025 | 2030 | 2040 | 2025 | 2030 | 2040 |
| | | | | | | |

| Indicator | Germany | | | Spain | | |
|---|---------|--------|--------|--------|--------|--------|
| Total number of dwellings | 71 | 71 | 71 | 71 | 71 | 71 |
| Number of MFB | 19 | 19 | 19 | 19 | 19 | 19 |
| Number of SFB | 34 | 34 | 34 | 34 | 34 | 34 |
| Number of NRB | 11 | 11 | 11 | 11 | 11 | 11 |
| Number of MB | 7 | 7 | 7 | 7 | 7 | 7 |
| Number of IB | 0 | 0 | 0 | 0 | 0 | 0 |
| Total rooftop area [m²] | 16,060 | 16,060 | 16,060 | 16,060 | 16,060 | 16,060 |
| Total land area [ha] | 100 | 100 | 100 | 100 | 100 | 100 |
| Number of households | 151 | 151 | 151 | 151 | 151 | 151 |
| Non-smart charging points | 6 | 10 | 31 | 6 | 10 | 31 |
| Annual electricity demand [GWh] | 2.57 | 2.66 | 2.87 | 2.78 | 2.84 | 3.02 |
| Annual heat demand [GWh_{thermal}] | 7.19 | 6.72 | 6.09 | 5.85 | 5.70 | 5.49 |

Source: Own elaboration based on MODECO's methodology and assumptions

Table 32 CO₂ emissions associated with energy usage in the Rural town archetype

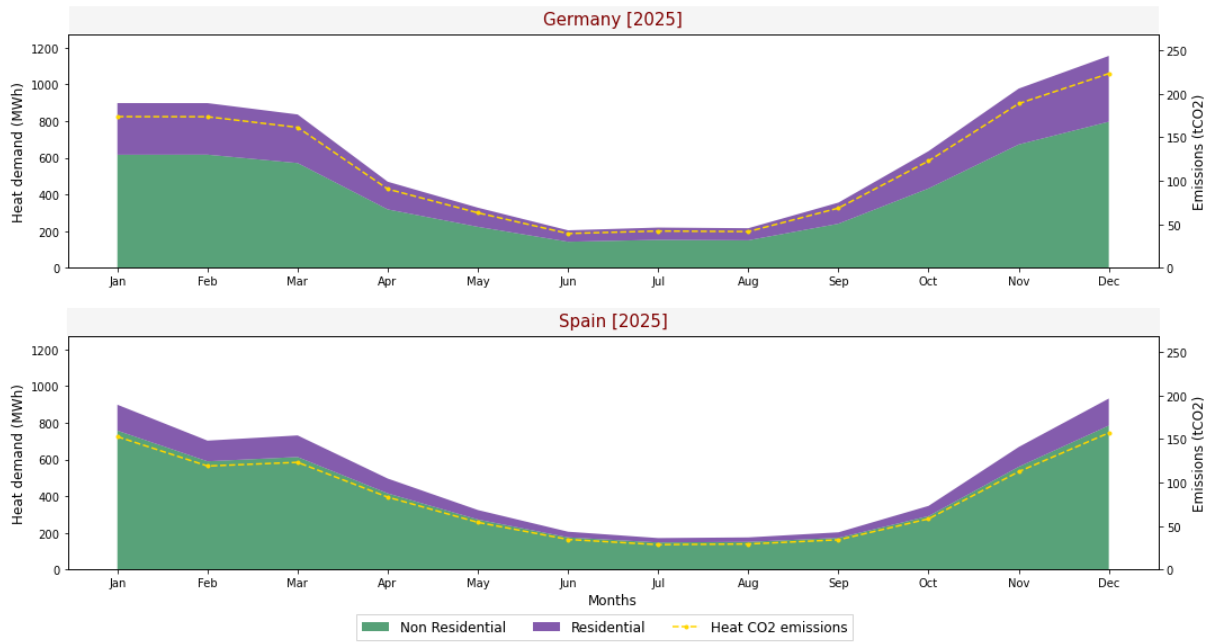
| CO ₂ emissions [ton/year] | Germany | | | Spain | | |
|--------------------------------------|---------|---------|---------|---------|--------|--------|
| | 2025 | 2030 | 2040 | 2025 | 2030 | 2040 |
| Total | 1672.19 | 1490.57 | 1308.25 | 1071.74 | 957.24 | 897.58 |
| Electricity usage [%] | 17.43 | 18.34 | 25.94 | 10.41 | 8.87 | 19.82 |
| Boiler usage [%] | 82.57 | 81.66 | 74.06 | 89.59 | 91.13 | 80.18 |
| Displaced by heat pumps | 60.36 | 135.46 | 260.06 | 222.14 | 285.07 | 396.18 |

Source: Own elaboration based on MODECO's methodology and assumptions

5.3.1 Rural town: Heat demand

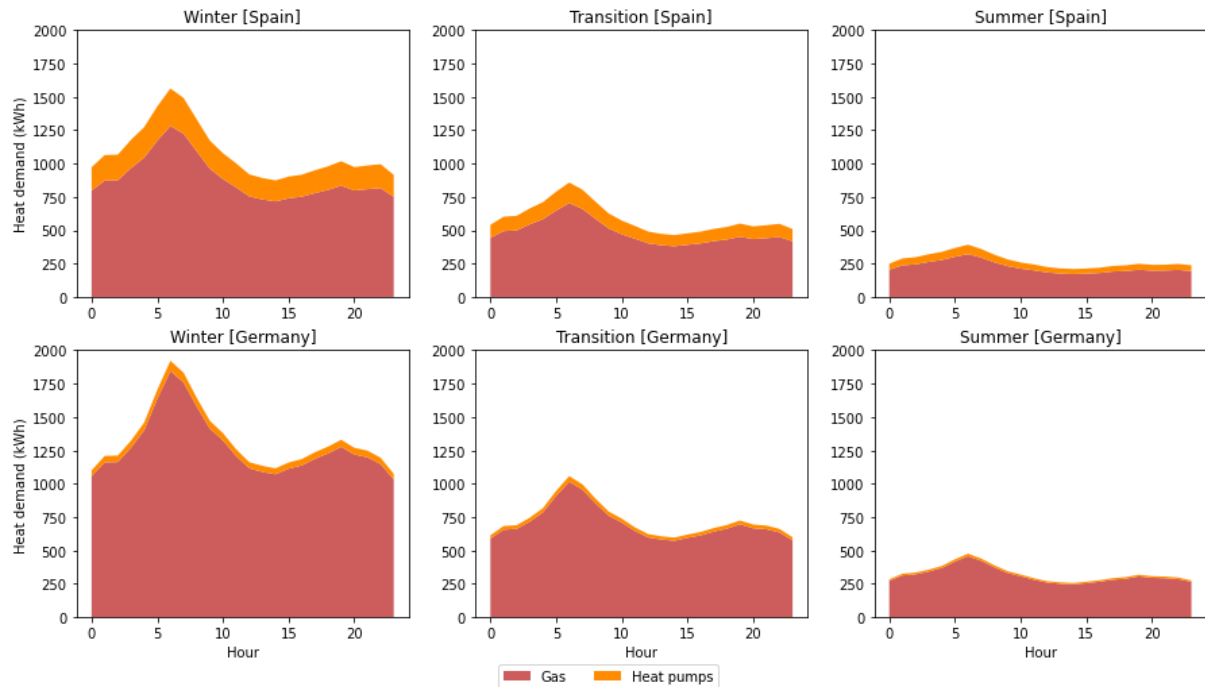
In the Rural town archetype, heat demand from Non-residential buildings is more significant in the community's total load. As expected, heat demand is larger in winter months than in warmer seasons, and is larger in Germany than in Spain. When observing hourly heat demand per final usage, the same trend as in the Urban district is observed regarding heat pump usage, as the adoption rate is also assumed to be larger in Spain (18%) than in Germany (4%). However, in this archetype, the heat demand peak registered at morning hours is more pronounced than in the Urban district archetype, which is related to the dairy farms considered in this energy community type and that have a considerable demand for water and space heating.

Figure 25. Monthly heat demand per sector in the Rural town archetype in 2025



Source: Own elaboration based on MODECO's methodology and assumptions

Figure 26. Mean heat consumption reported in 2025 in the Rural town communities in Germany and Spain



Source: Own elaboration based on MODECO's methodology and assumptions

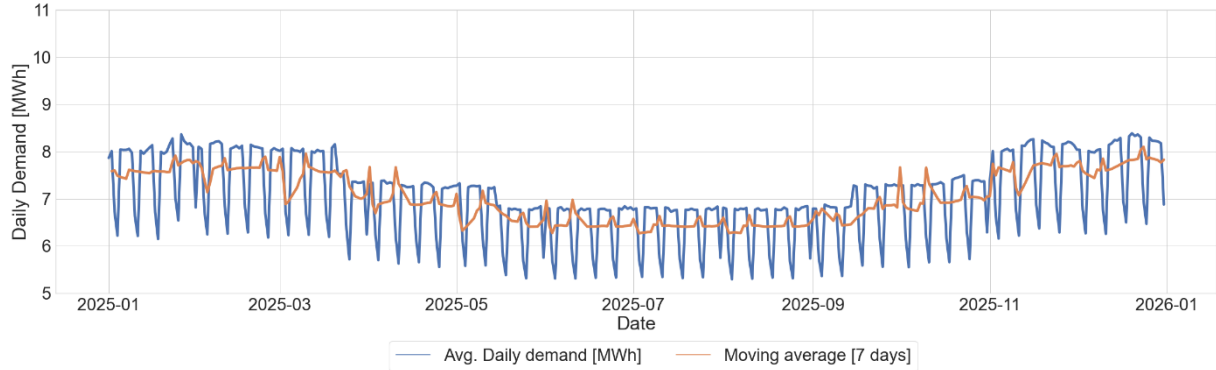
The annual changes in heat demand throughout the studied period behave similar to the Urban district, so these graphics are not shown but can be found in the associated database.

5.3.2 Rural town: Electrical demand

In terms of electricity consumption, similar trends are observed in the daily demand curves for Germany (Figure 27) and Spain (Figure 28), being flatter in the first case. The demand for space cooling is identifiable in the energy communities' Spanish archetypes, as well as the slightly higher demand in winter associated

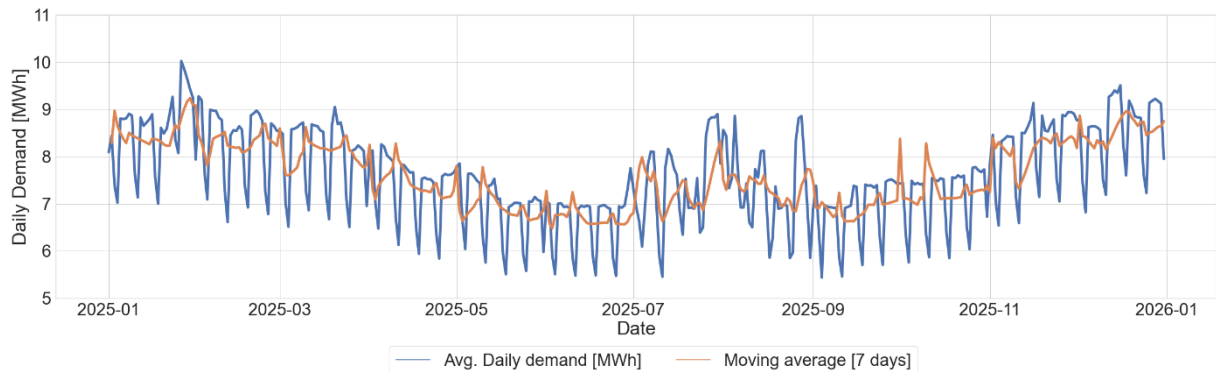
with the heat pump operations. As happened with heat demand, the electricity consumption peaks registered at morning and evening times are more noticeable in this archetype than in the Urban district, due to the presence of agricultural activities. Electrical demand from EV charging is less significant than in the Urban district, which was expected as the number of charging points is lower (Figure 29). As happens with heat demand, the evolution of the electrical demand from 202 to 2040 behaves similarly to the Urban district, with progressive increments associated with heat pumps increasing usage and more EV charging units installed.

Figure 27. Daily electricity demand per sector in the Rural town archetype in Germany [2025]



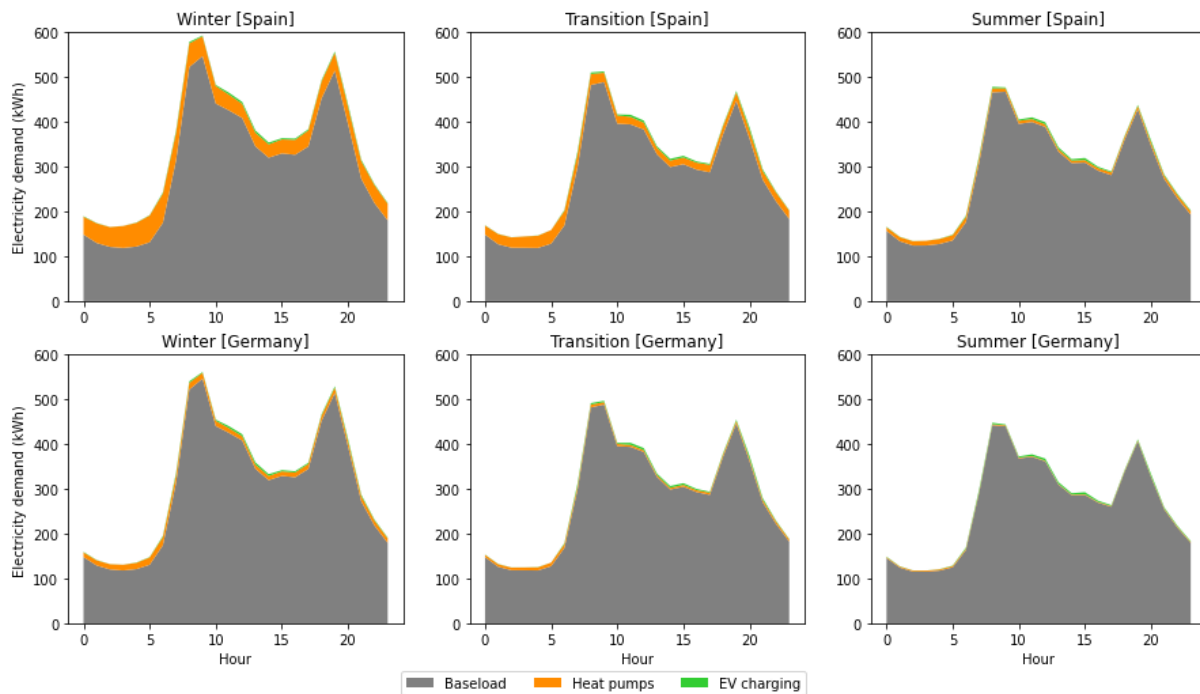
Source: Own elaboration based on MODECO's methodology and assumptions

Figure 28. Daily electricity demand per sector in the Rural town archetype in Spain [2025]



Source: Own elaboration based on MODECO's methodology and assumptions

Figure 29. Mean electricity consumption reported in 2025 in the Rural town communities in Germany and Spain



Source: Own elaboration based on MODECO's methodology and assumptions

5.4 Urban district

The **Urban district archetype is formed by 35 dwellings, 18 of which are residential (Multi-family), 10 Mixed buildings and 7 Non-residential** buildings representing different services and businesses that can be found in urban neighbourhoods. In the ground floors of the Mixed buildings, the following **services** are found: one bakery, one drugstore, one hair salon, one bank, two restaurants, two offices, and two retail shops. In the Non-residential buildings there are three offices, a healthcare clinic, a library, a fitness centre and a supermarket. Sixteen of these buildings are small-sized, sixteen mid-sized and three large-sized, adding a total of 12,300 m² of rooftop space. The total households living in the residential and Mixed buildings are 426, and 5 of them own an EV and its corresponding charging point. Additionally, seven EV charging stations, with two charging points each, are installed in the supermarket and used for its delivery vehicles. A summary of the Urban district archetype is presented below.

Table 33 Urban district indicators

| Indicator | Germany | | | Spain | | |
|----------------------------------|---------|------|------|-------|------|------|
| | 2025 | 2030 | 2040 | 2025 | 2030 | 2040 |
| Total number of dwellings | 35 | 35 | 35 | 35 | 35 | 35 |
| Number of MFB | 18 | 18 | 18 | 18 | 18 | 18 |
| Number of SFB | 0 | 0 | 0 | 0 | 0 | 0 |
| Number of NRB | 7 | 7 | 7 | 7 | 7 | 7 |
| Number of MB | 10 | 10 | 10 | 10 | 10 | 10 |
| Number of IB | 0 | 0 | 0 | 0 | 0 | 0 |

| Indicator | Germany | | | Spain | | |
|---|---------|--------|--------|--------|--------|--------|
| Total rooftop area [m²] | 12,300 | 12,300 | 12,300 | 12,300 | 12,300 | 12,300 |
| Total land area [ha] | - | - | - | - | - | - |
| Number of households | 426 | 426 | 426 | 426 | 426 | 426 |
| Non-smart charging points | 19 | 23 | 44 | 19 | 23 | 44 |
| Annual electricity demand [GWh] | 3.16 | 3.25 | 3.46 | 3.42 | 3.47 | 3.63 |
| Annual heat demand [GWh] | 8.22 | 7.47 | 6.44 | 6.05 | 5.80 | 5.46 |

Source: Own elaboration based on MODECO's methodology and assumptions

Table 34 CO₂ emissions associated with energy usage in the Urban district archetype

| CO ₂ emissions [ton/year] | Germany | | | Spain | | |
|--------------------------------------|---------|---------|---------|---------|--------|--------|
| | 2025 | 2030 | 2040 | 2025 | 2030 | 2040 |
| Total | 1924.28 | 1671.07 | 1410.73 | 1123.62 | 983 | 906.9 |
| Electricity usage [%] | 17.91 | 19.12 | 27.42 | 11.69 | 9.72 | 21.1 |
| Boiler usage [%] | 82.09 | 80.88 | 72.58 | 88.31 | 90.28 | 78.9 |
| Displaced by heat pumps | 68.97 | 150.51 | 275.4 | 229.26 | 290.19 | 394.89 |

Source: Own elaboration based on MODECO's methodology and assumptions

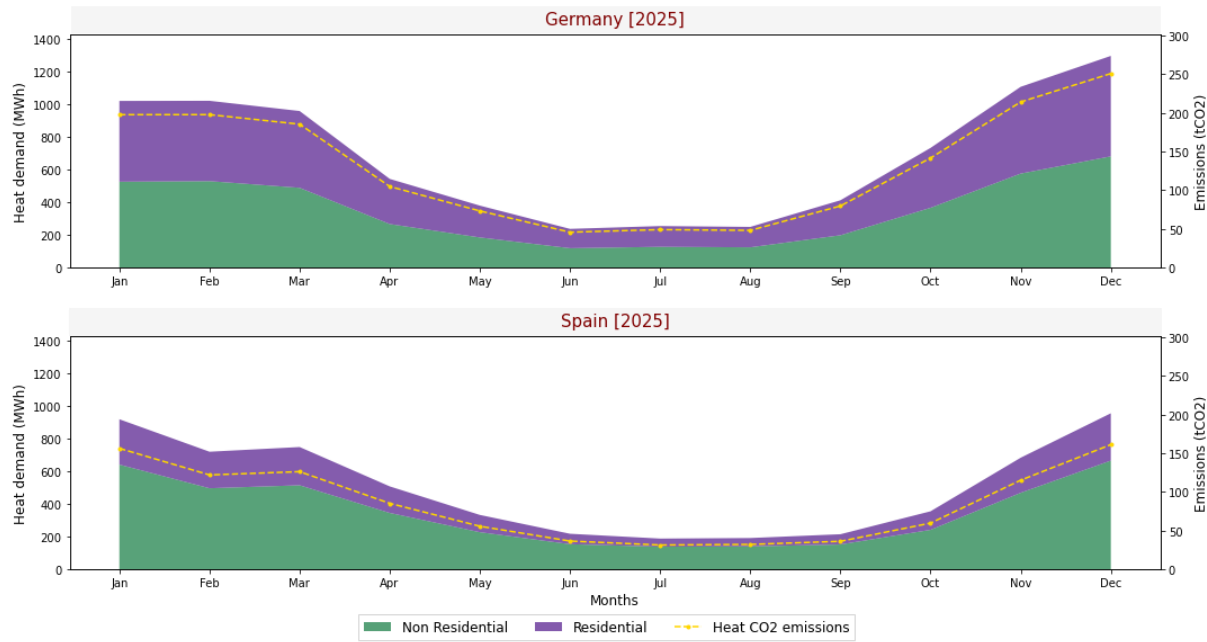
5.4.1 Urban district: Heat demand

In the German case (Figure 30), the urban district distinguishes for a similar representation from residential and non-residential heat consumption, being slightly higher for residential users as the heat demand per household in this region is high and residential dwellings are more numerous than Non-residential buildings. In the Spanish region (Figure 30), Non-residential members consume more heat than residential users as they have higher energy intensity per square meter for space heating purposes. Comparing both regions, it is noticeable that heat demand in the summer is similar for both regions as it is practically associated with domestic water heating consumption. Nonetheless, in winter, it is clear that in German households, heat consumption is much larger than in the Spanish case.

Looking at the heat consumption per season and source (Figure 31), the gradual decrease in heat demand as temperature gets higher is observed in both regions. Also, it is clear that heat demand is higher in the morning, mostly driven by Non-residential buildings, although another peak is identified in the evening. The heat share covered by heat pumps is considerably lower in the German Urban district, despite the higher overall heat demand, as heat pumps usage share is significantly lower in Germany (4%) than Spain (18%).

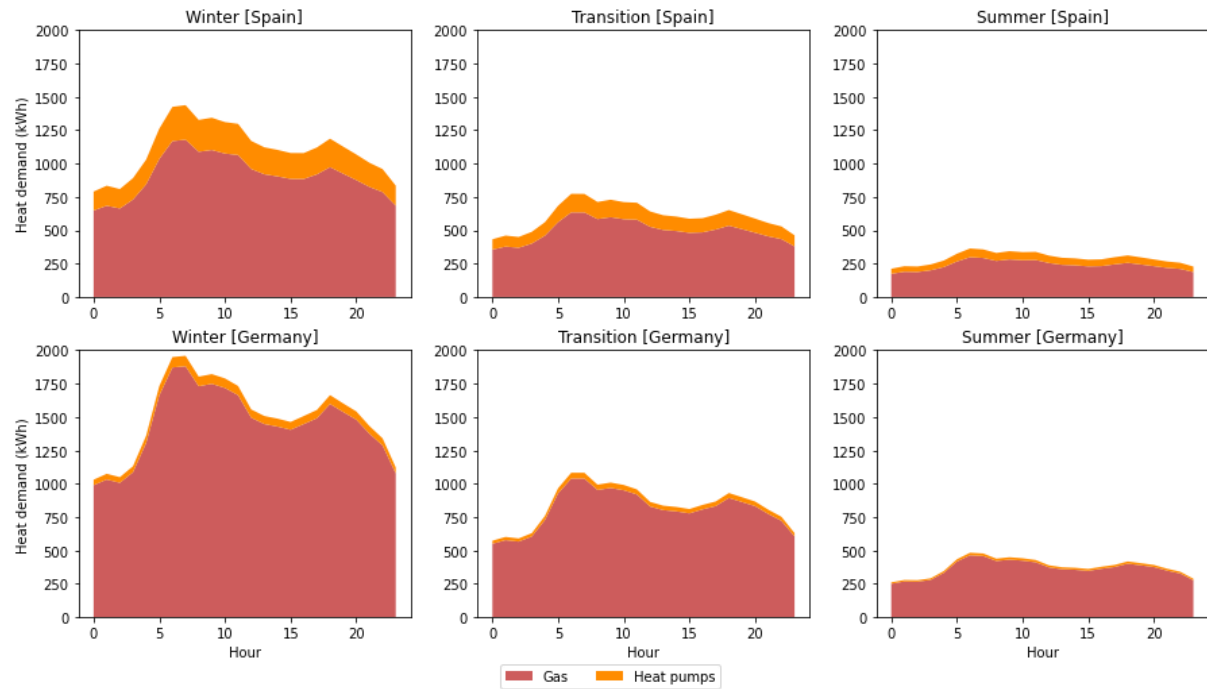
The refurbishment rate considered for the Urban district community reflects lower heat demand in future years in comparison with 2025 for both target regions (Figure 32). Similarly, the higher heat pumps usage rate assumed for both regions, results in a larger heat share supplied by these technologies. As will be explained in the following section, this also reflects in larger electrical consumption associated with heat pumps operation.

Figure 30. Monthly heat demand per sector in the Urban district archetype in 2025



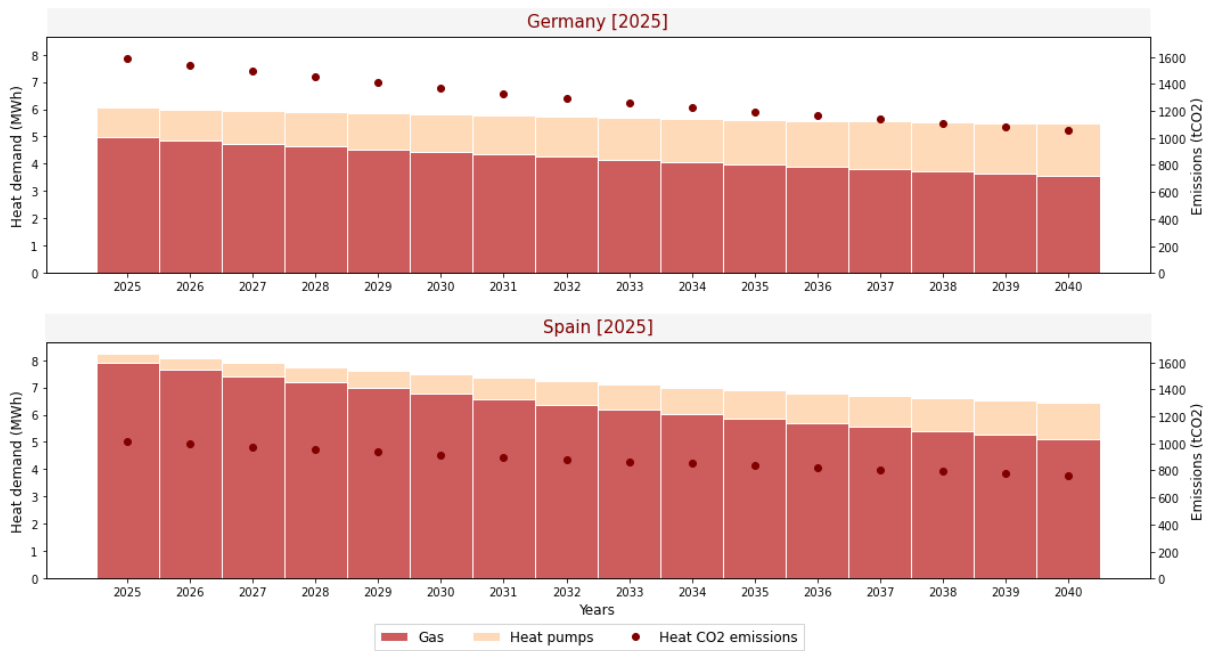
Source: Own elaboration based on MODECO's methodology and assumptions

Figure 31. Mean heat consumption reported in 2025 in the Urban district communities in Germany and Spain



Source: Own elaboration based on MODECO's methodology and assumptions

Figure 32. Annual heat consumption and associated CO2 emissions for the Urban district archetype

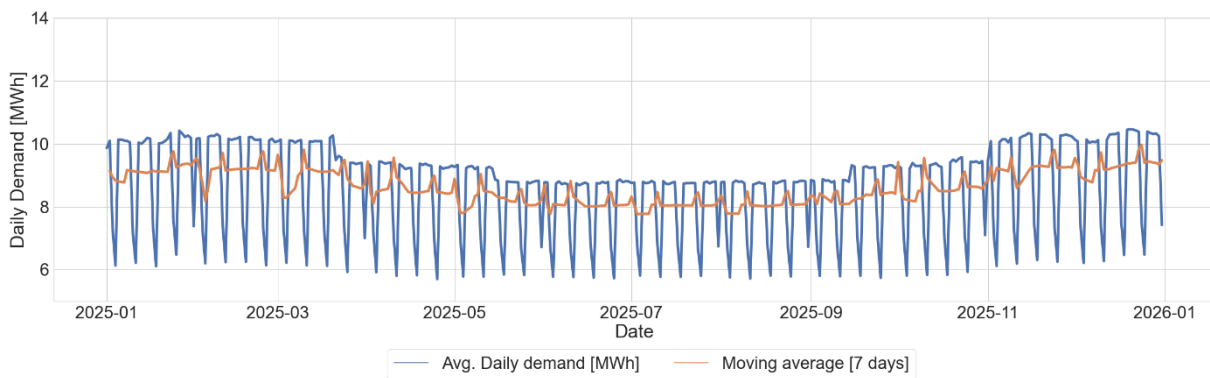


Source: Own elaboration based on MODECO's methodology and assumptions

5.4.2 Urban district: Electrical demand

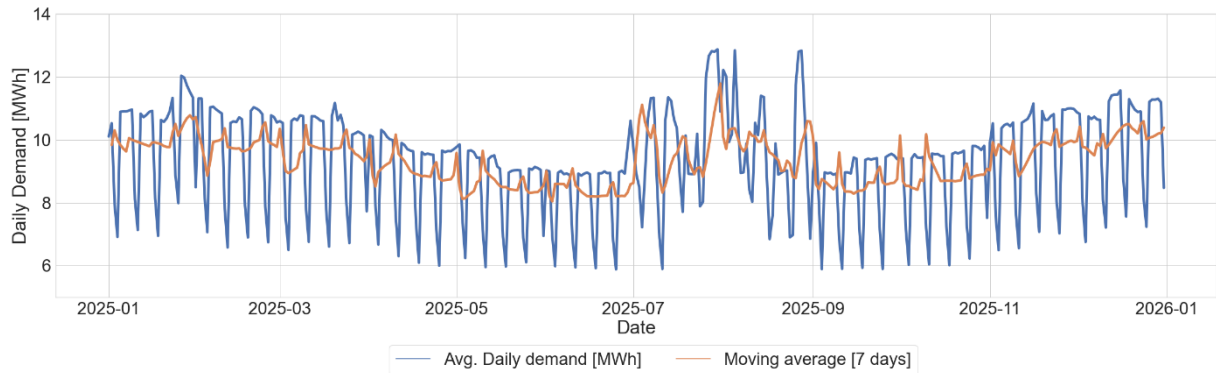
Regarding electricity consumption, residential and Non-residential buildings contribute similar shares to the community total demand in both regions. In Germany (Figure 33), electrical load has a flat behaviour throughout the year, with slightly higher consumption in winter. This is expected as no cooling demand is considered and space heating is mostly supplied by natural gas equipment. On the other side, increased electricity demand for space cooling is observable in the Spanish Urban district during the summer months (Figure 34). Similarly, a higher demand in winter is observed in this region in comparison with other seasons and with the German case (Figure 35). This is due to the consideration of a larger share of heat pumps' usage for space heating applications, which transforms into higher electricity demand in winter. Electricity consumption from EV charging is low in comparison to baseload demand as few charging points are available in the starting year (2025).

Figure 33. Daily electricity demand per sector in the Urban district archetype in Germany [2025]



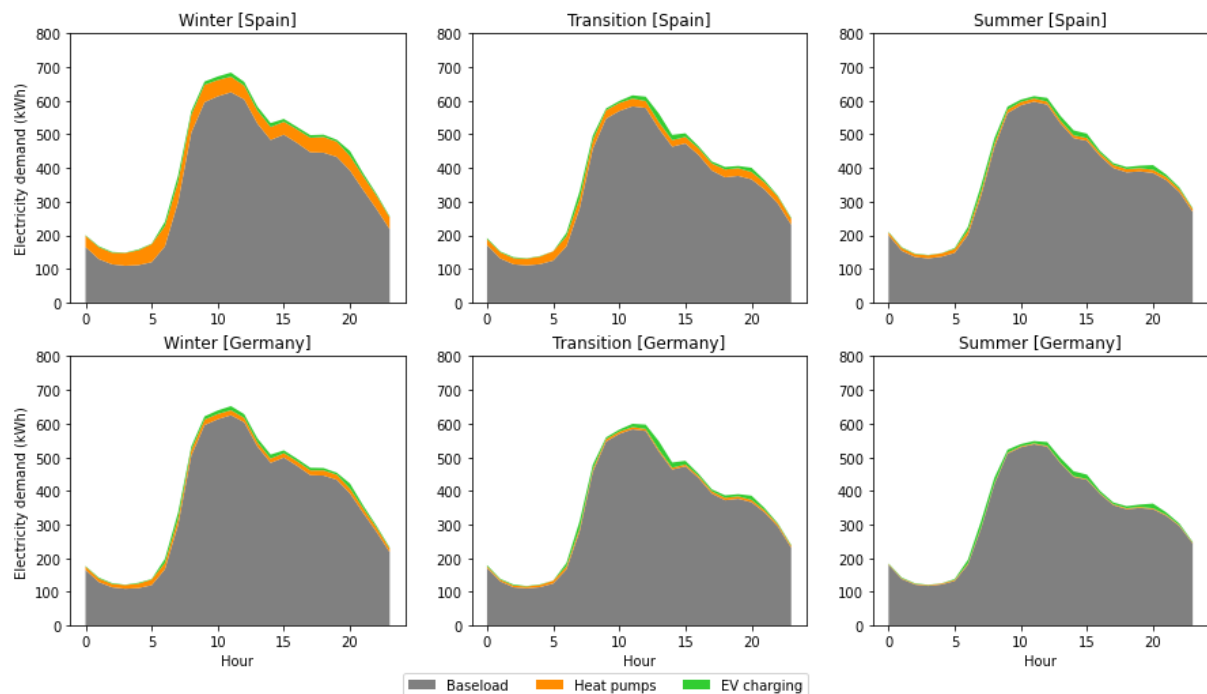
Source: Own elaboration based on MODECO's methodology and assumptions

Figure 34. Daily electricity demand per sector in the Urban district archetype in Spain [2025]



Source: Own elaboration based on MODECO's methodology and assumptions

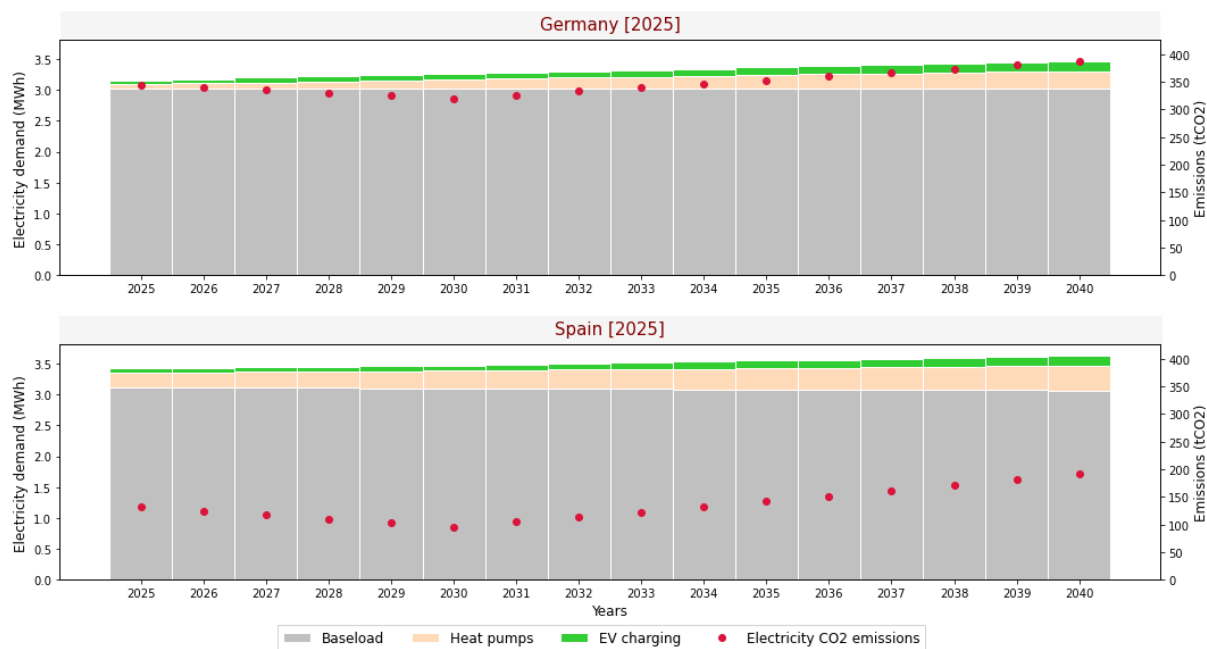
Figure 35. Mean electricity consumption reported in 2025 in the Urban district communities



Source: Own elaboration based on MODECO's methodology and assumptions

In the evolution of the Urban district's electricity demand, the increasing electrical demand from heat pumps' operations is observable as expected by the larger share of heat that is supplied by this technology as the usage rate increases in both regions. To a lesser extent, the electrical demand associated to EV charging also increases with time, although its contribution to the community's total demand is still minimal, even in 2040. As observed from the following figures, annual electricity demand in the Spanish case is higher than in Germany, which is associated to space cooling and space heating needs supply via heat pumps.

Figure 36. Annual electricity consumption and associated CO₂ emissions for the Urban district archetype



Source: Own elaboration based on MODECO's methodology and assumptions

5.5 Virtual community

Similar to the Business park case, the Virtual community shares **common traits with the Urban district archetype**, as it is located within an urban context and has members with similar characteristics to those included in the Urban district case. Nonetheless, the Virtual community lack of vicinity boundaries permit to include a larger number of members than in the other Energy community archetypes. The higher number of members is observable in the annual electricity demand reported in this case, which is more aligned to the Business park case, even though, residential dwellings are the most numerous group in this case. Heat demand is even larger in the Virtual community than in the Business park, but this demand cannot be supplied by a shared asset as members are located on different points and heat cannot be shared "virtually" as electricity can.

As mentioned before, residential dwellings are the most common within the Virtual community members as 53 out of 100 members are Multi-family dwellings, 24 are Mixed buildings and just 23 are Non-residential buildings. Among the last group, there are banks, offices, cinemas, fitness centres, museums, libraries, hotels, primary schools, secondary schools, shopping malls, supermarkets and universities. As happens with the members' number, the lack of geographical boundaries also permits more diversification in the type of members included in the community. The number of EV charging points is also more significant as it is not restricted to a specific area but can include charging stations located in any point of the city.

Table 35 Virtual community indicators

| Indicator | Germany | Spain |
|-----------|---------|-------|
|-----------|---------|-------|

| Indicator | Germany | | | Spain | | |
|---|---------|--------|--------|--------|--------|--------|
| | 2025 | 2030 | 2040 | 2025 | 2030 | 2040 |
| Total number of dwellings | 100 | 100 | 100 | 100 | 100 | 100 |
| Number of MFB | 53 | 53 | 53 | 53 | 53 | 53 |
| Number of SFB | 0 | 0 | 0 | 0 | 0 | 0 |
| Number of NRB | 23 | 23 | 23 | 23 | 23 | 23 |
| Number of MB | 24 | 24 | 24 | 24 | 24 | 24 |
| Number of IB | 0 | 0 | 0 | 0 | 0 | 0 |
| Total rooftop area [m²] | 34,100 | 34,100 | 34,100 | 34,100 | 34,100 | 34,100 |
| Total land area [ha] | 300 | 300 | 300 | 300 | 300 | 300 |
| Number of households | 1,118 | 1,118 | 1,118 | 1,118 | 1,118 | 1,118 |
| Non-smart charging points | 63 | 67 | 88 | 63 | 67 | 88 |
| Annual electricity demand [GWh] | 8.95 | 9.18 | 9.60 | 9.60 | 9.72 | 10.01 |
| Annual heat demand [GWh] | 21.23 | 19.24 | 16.55 | 15.52 | 14.87 | 13.98 |

Source: Own elaboration based on MODECO's methodology and assumptions

Table 36 CO₂ emissions associated with energy usage in the Virtual community archetype

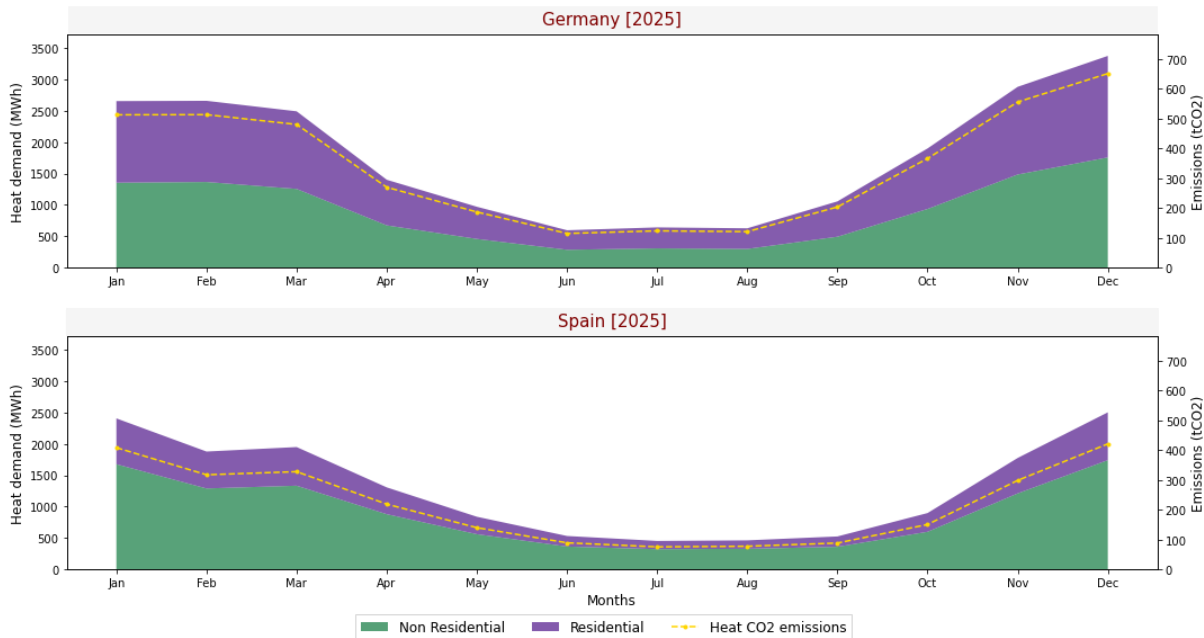
| CO ₂ emissions [ton/year] | Germany | | | Spain | | |
|--------------------------------------|---------|---------|---------|---------|--------|---------|
| | 2025 | 2030 | 2040 | 2025 | 2030 | 2040 |
| Total | 5043.17 | 4369.64 | 3677.16 | 2911.48 | 2537.8 | 2336.16 |
| Electricity usage [%] | 19.15 | 20.29 | 28.46 | 12.56 | 10.37 | 21.61 |
| Boiler usage [%] | 80.85 | 79.71 | 71.54 | 87.44 | 89.63 | 78.39 |
| Displaced by heat pumps | 177.98 | 387.6 | 706.97 | 587.7 | 743.2 | 1009.53 |

Source: Own elaboration based on MODECO's methodology and assumptions

5.5.1 Virtual community: Heat demand

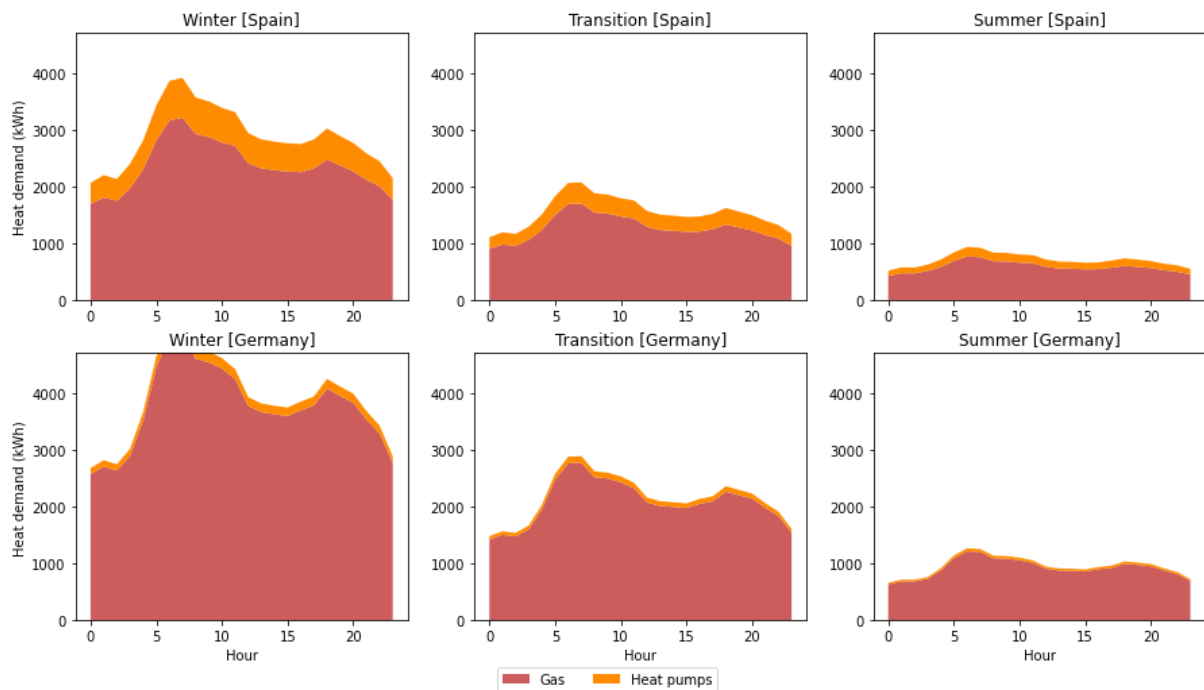
As observed in Figure 37, heat demand from residential users is the most relevant load in the German Virtual community, whereas in Spain, Non-residential buildings represent the principal heat consumers. As happened in other archetypes, there are few differences at the monthly scale between one archetype and other regarding the curve shape. Nonetheless, at the hourly level (Figure 38), it is possible to identify different trends. However, this archetype's behaviour is highly similar to that of the Urban district, as the main difference between these two is not the type of dwellings but the number and absence of physical constraints, which will strongly influence the investment decisions of the Virtual community in comparison with the other urban archetypes.

Figure 37. Monthly heat demand per sector in the Virtual community archetype in 2025



Source: Own elaboration based on MODECO's methodology and assumptions

Figure 38. Mean heat consumption reported in 2025 in the virtual community archetype in Germany and Spain

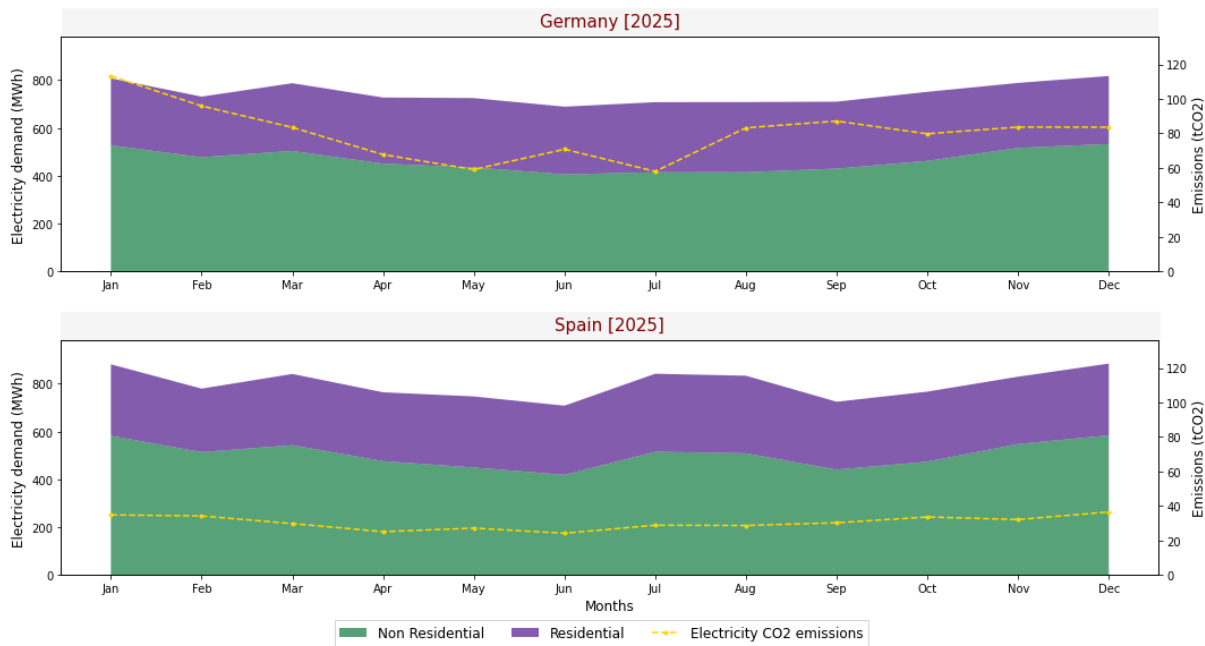


Source: Own elaboration based on MODECO's methodology and assumptions

5.5.2 Virtual community: Electrical demand

The daily electricity demand from the Virtual community follows a similar trend to the Urban district, although with a larger overall demand. Instead, the monthly electrical loads are shown to highlight the flatter shape of the German case, which is also observed in previous archetypes. Also, it is relevant to observe that in terms of electricity consumption, residential and Non-residential buildings follow a similar trend and show less differences in volume than in heat demand.

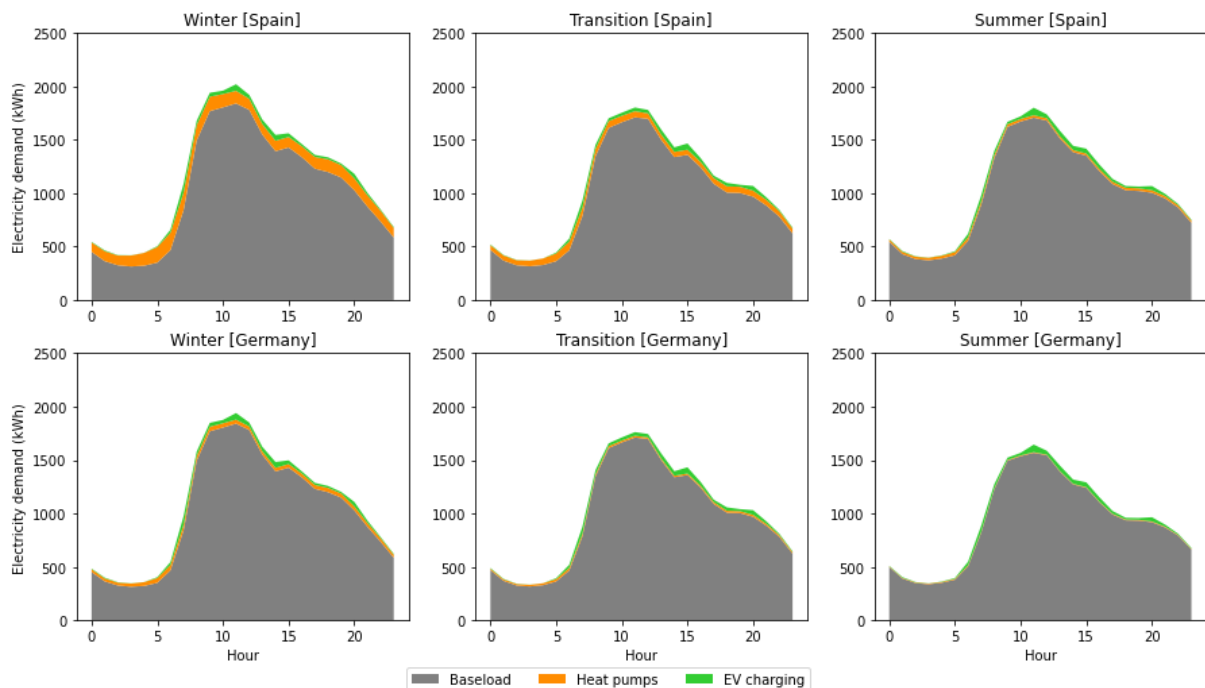
Figure 39. Monthly electricity demand per sector in the Virtual community archetype in 2025



Source: Own elaboration based on MODECO's methodology and assumptions

At the hourly level (Figure 40), some differences are observed between the Virtual community and Urban district load shapes, as the first has a more pronounced peak during the morning, looking more similar to the Business park archetype in this sense. Finally, the demand from EV charging remains more visible in this case for both studied regions, this might be due to the high presence of offices and banks in this case than in the Urban district.

Figure 40. Mean electricity consumption reported in 2025 in the Virtual community archetype



Source: Own elaboration based on MODECO's methodology and assumptions

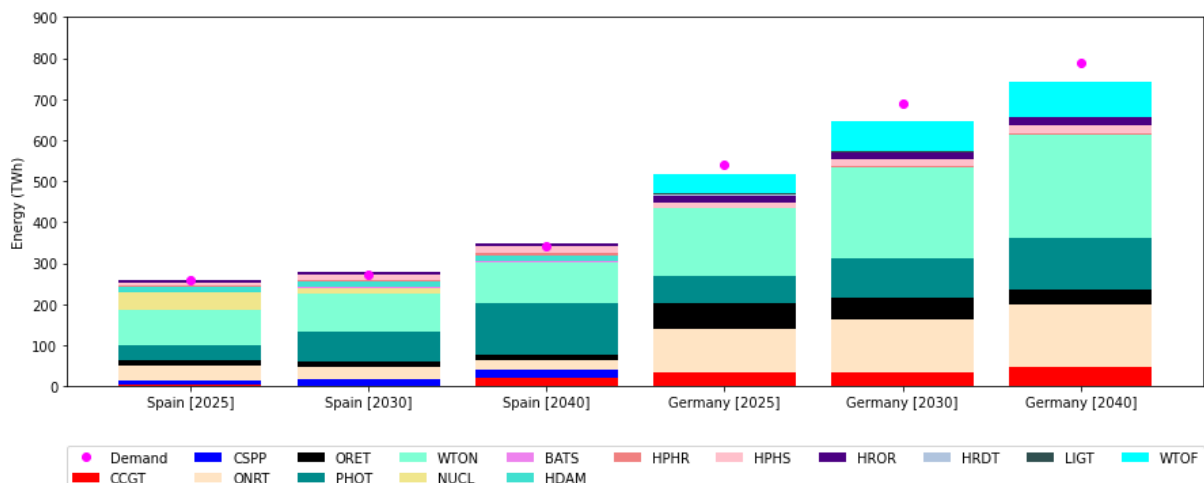
6 Energy price scenarios

The marginal prices obtained from the first round execution of the UCED model are discussed in this section, as well as the **energy tariffs** formed from them by adding the taxes and Use-of-Network charges applicable to each scenario. A **brief overview of the power system's behaviour** – demand and energy dispatched per type of technology – leading to these prices is also presented, including the key indicators shown in Figure 14: Energy Not Served, CO₂ emissions and renewables curtailment.

6.1 Power system indicators

As seen in Chapter 2, the considered reference scenario for the evolution of the European power system considers a gradual phase out of fossil-fuelled technologies and a considerable growth in variable renewable energies (solar and wind) and energy storage, with specific technological trends for each geographical location. As shown in Figure 41, which summarizes the amount of energy dispatched per technology in Germany and Spain during the target years executed, the demand for the two countries analysed increments from 2025 to 2040. In Germany, the increase from 2025 to 2030 is similar to that observed from 2030 to 2040, which means that in the latter years, demand growth happens at a slower rate. On the contrary, demand in Spain remains fairly the same from 2025 to 2030, incrementing an average of just 2.3 TWh per year, whereas from 2030 to 2040 it grows at a faster pace, augmenting in average 7.0 TWh each year.

Figure 41. Annual demand versus energy dispatched per technology and year in Germany and Spain



BATS: Batteries; CCGT: Combined Cycle Gas Turbines; FCEL: Fuel Cell; GAST: Gas Turbines; HDAM: Hydro-reservoirs; HPHR: Open-loop hydro pumped storage; HPHS: Closed-loop hydro pumped storage; HRDT: Hard coal-fuelled generators; HROR: Hydro Run-of-River; LIGT: Lignite-fuelled generators; OCGT: Open Cycle Gas Turbines; OILT: Oil-fuelled generators; ORES: Other Renewables; OTHT: Other non-renewables (combined heat and power); PHOT: solar photovoltaics; WTOF: wind offshore; WTON: wind onshore.

Source: Own elaboration from the UCED's model first executions

As observed in the graph above, **annual demand in Spain is always below the total generated energy**, as part of the produced energy is exported to neighbouring countries. Germany, on the contrary, relies on energy imports to cover its demand in the three analysed years as the total national production is below consumption requirements. In **2040, Germany's** demand gets significantly larger than the produced energy, complicating meeting demand at all hours. In fact, **lost load events take place in this year and country** during 19 hours reported in four particular **winter** days¹², meaning that the system is not able to meet demand with its own generation or with imported energy at that time. The volume of Energy Not Served (ENS) in 2040 accounts for 15.39 GWh. No other year in Germany and Spain presents ENS under the modelled conditions.

¹² The dates and times in which ENS is reported are: 22 January 2040 (18:00-23:00), 13 February (20:00-23:00), 16 February (19:00-23:00), 18 December (20:00-23:00).

Wind and solar technologies have a prominent role in both analysed countries as expected due to the evolution of the reference power system scenario, gaining more relevance in 2040 when these technologies account for 62% and 70% of the total energy generated in Germany and Spain, respectively. Even by 2025, these generators already account for half the energy produced in both countries, which impact on the dynamics of the obtained marginal prices that will be presented in the next section, particularly in hours with high solar irradiation. This is particularly important in **Spain**, where **solar technologies** (concentrated solar power and photovoltaics) account for 19% of the total energy generated in 2025, but go up to 42% in 2040. Spanish wind farms represent the largest generation in 2025 (32%) but are relegated to a second place in the **future years**, when they are responsible for 29% of the total energy produced in the Mediterranean country.

In the case of **Germany**, **wind is the dominant technology**, representing 40% of the total energy generated in 2025 and 45% in 2040, while solar photovoltaics account for just 13% and 17% of the energy produced in those years. It is also relevant to point out the intensive usage of gas-fuelled generators, particularly in the form of Combined Cycle Gas Turbines (CCGT) and combined heat and power units, which are represented by the Other Non-Renewable (ONRT) category shown in Figure 41.

The CO₂ emissions associated with energy generation in each case are presented in Table 37. Germany has much higher carbon emissions than Spain due to a more intensive usage of combined cycle units. In 2025 and 2030, a portion of the emissions is also related to the utilization of lignite (LIGT) and hard carbon (HRDT) plants. In 2030, Germany's emissions decrease in comparison to 2025 even as gas generation grows, due to the almost phase out of carbon-based power plants, which pass from generating 5.2 TWh in 2025 to 1.7 TWh in 2030. Their usage is completely eliminated in 2040, but the increment in gas generation is more significant, which raises total emissions in 2040 above 2025 levels. In Spain, carbon emissions are purely associated with combined cycle units. From 2025 to 2030 the energy generated from these plants decreases from 2.6 TWh to 0.6 TWh, which results in less carbon emissions. Nonetheless, it increases up to 20.8 TWh in 2040 when nuclear facilities are no longer in operation, raising significantly the carbon emissions registered in Spain.

Table 37 Annual volume of CO₂ emissions associated to power generation in Germany and Spain

| Year | CO ₂ emissions [kton] | |
|-------------|----------------------------------|----------|
| | Germany | Spain |
| 2025 | 8,498.06 | 529.66 |
| 2030 | 7,889.67 | 113.08 |
| 2040 | 9778.93 | 4,198.31 |

Source: own elaboration with results from the UCED model execution.

6.2 Marginal prices

The first set of marginal prices used for the construction of the tariff scenarios described in Section 2.3 are obtained from adapting the UCED model to the ESES reference scenario (see Section 4.1.1). As observed in Table 38, the mean annual marginal prices obtained for Germany are overall higher than for Spain during the entire studied period. The largest difference between the two countries is observed in 2030, when the mean annual price in Germany is 157% higher than in Spain. In 2040, this gap narrows, as prices in Spain nearly tripled from 2030 to 2040 whereas in Germany 2040 prices increase only 42% in comparison to 2030, resulting in Germany's prices being just 17% higher than Spain at 2040. In summary, for the modelled scenario, it is observed that Germany has larger prices than Spain and experiences a sustained growth throughout the 16-year period, while Spain experiences a slight decrease (6%) in prices from 2025 to 2030 to later increase at a rapid pace till the end of the analysed timeframe.

As observed in Figure 42, rising prices in Germany are mostly led by the winter season, which maintains a steady increasing trend for the whole analysed period. German prices in summer and transition seasons rise almost as fast as in winter from 2025 to 2030, but it then slows down. In Spain, winter prices also follow an increasing trend during the evaluated period, but it speeds up after 2030. For summer and transition seasons,

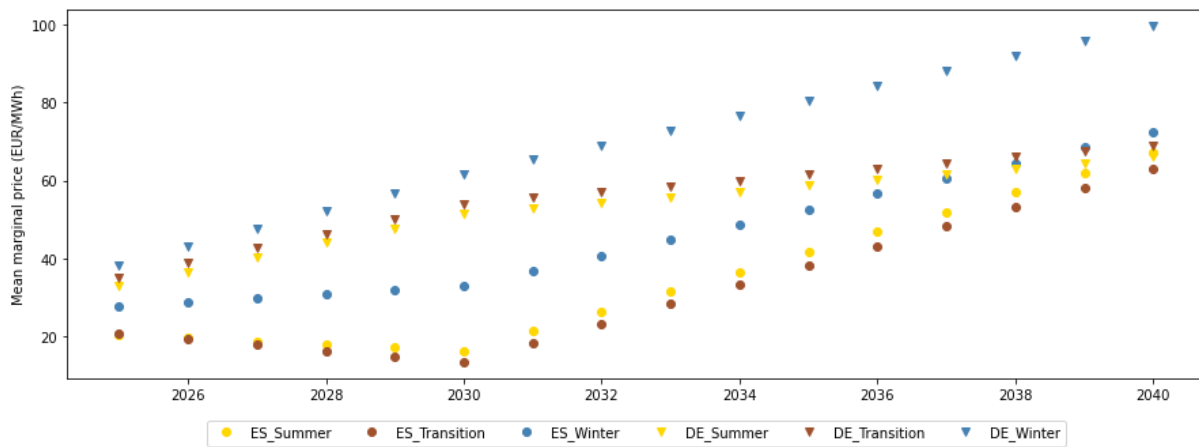
prices actually go down between 2025 and 2030, but then rise quickly, reaching a mean marginal price similar to that reported for Germany during the same seasons, or in winter in Spain.

Table 38 Mean annual marginal price registered in Germany and Spain for each target year

| Year | Mean annual marginal price [EUR/MWh] | |
|-------------|--------------------------------------|-------|
| | Germany | Spain |
| 2025 | 35.62 | 23.30 |
| 2030 | 55.99 | 21.82 |
| 2040 | 79.69 | 68.02 |

Source: own elaboration with results from the UCED model execution.

Figure 42. Mean marginal price per season and year registered in Spain and Germany

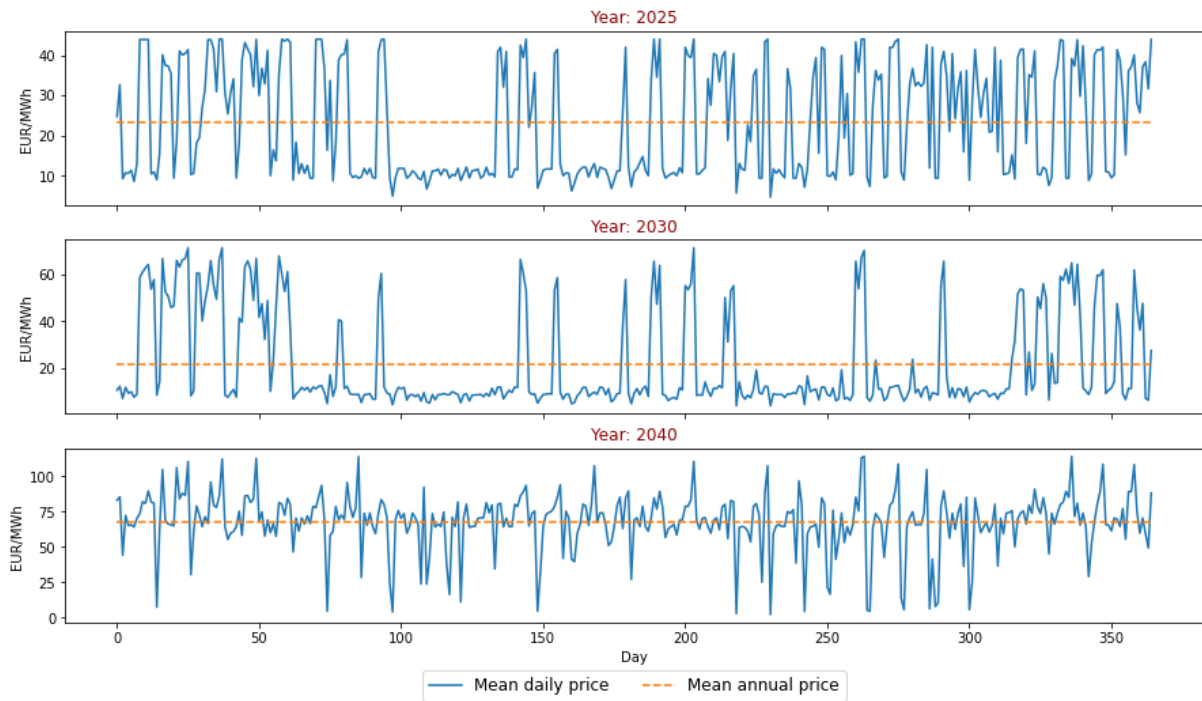


Source: Own elaboration from the UCED's model first executions

When looking at the mean daily prices, it is identified that marginal prices in Spain do not follow an established pattern throughout the year, as there are certain periods in which daily prices remain low (< 20 EUR/MWh) for a sustained number of days in 2025 and 2030 (Figure 43). In the starting year, this happens from 07 April to 14 May, while in 2030, the low-priced period extends 10 more days from 05 April to 22 May and similar events are observed from 07 August to 17 September, 22 September to 17 October, and 20 October to 11 November. Such low daily prices are reflected in the mean seasonal prices reported for the summer and transition periods in Spain at 2025 and 2030 (Figure 42). As observed in the graph below, the sustained low-priced periods disappear in 2040, leading to an increase in the mean price reported for all seasons in the years between 2030 and 2040. Nonetheless, some days with extremely low prices (< 6 EUR/MWh) are maintained around these same dates, accounting for the valley mean daily prices observed in 2040.

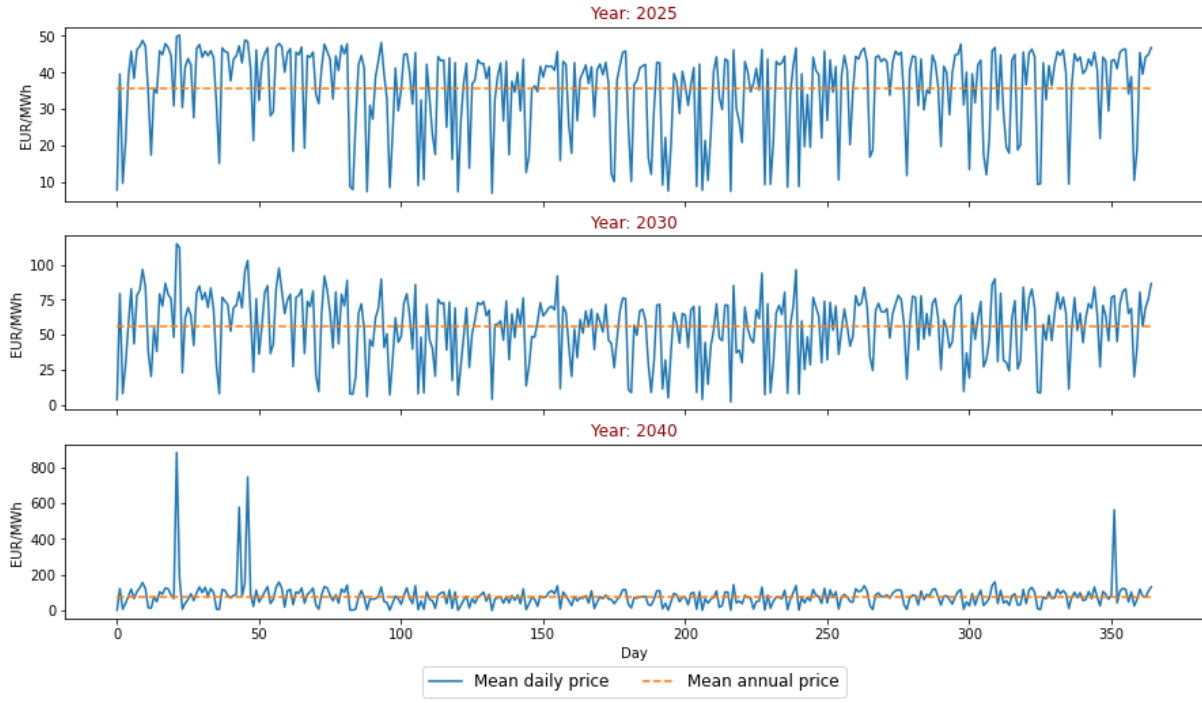
In Germany, mean daily prices raise evenly throughout the years, except for valley priced days (< 20 EUR/MWh), concentrated mostly in summer and transition periods, in which prices actually tend to decrease from 2025 to 2040. (Figure 44) As noted, a particular set of days in which prices rise above 560 EUR/MWh are registered in 2040 (22 January, 13 and 16 February, and 18 December). These correspond to days in which lost load events take place and are the main cause between the high increase in the mean winter prices registered for Germany after 2031. Nonetheless, the rest of 2040 prices tend to go up in comparison to 2030 values but maintain a similar daily trend to the former years, with valley prices going down or slightly up, but prices above the annual average mostly increasing significantly, thus raising the annual mean value expected for future years.

Figure 43. Mean daily marginal price registered in Spain in 2025, 2030 and 2040.



Source: Own elaboration from the UCED's model first executions

Figure 44. Mean daily marginal price registered in Germany in 2025, 2030 and 2040.

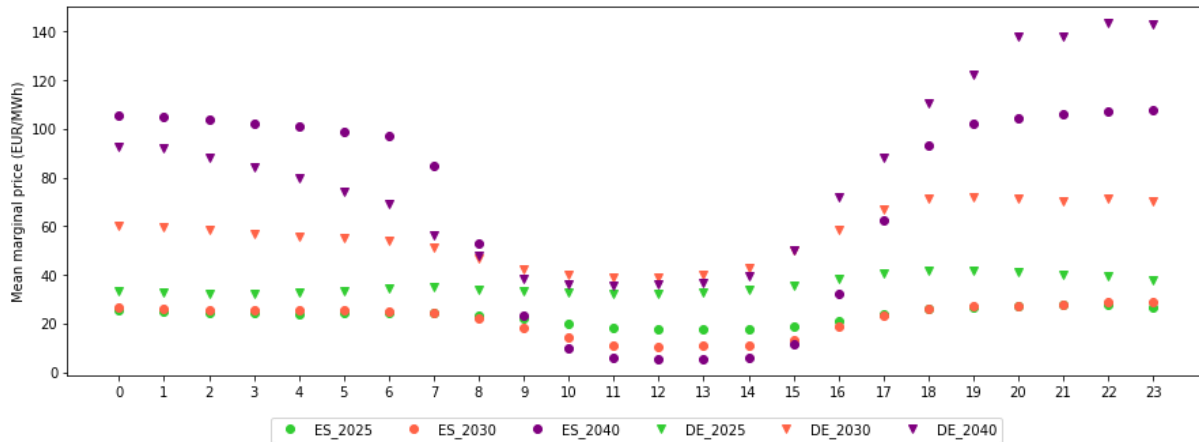


Source: Own elaboration from the UCED's model first executions

As shown in the next figure, hourly peak prices for both regions are concentrated in late night and early morning hours. However, the highest prices for Germany are reported at night whereas in Spain these are observed during early morning hours. During peak hours, prices increase for both countries towards the future. However, at low prices periods (8:00-15:00), marginal prices in Spain actually tend to decrease from 2024 to 2040, while in Germany prices go up from 2025 to 2030 but decrease slightly from 2030 to the end of the

period. The low prices registered at this timeslot are linked to the high amount of solar energy generated¹³ in these hours, which correspond to the times with the highest solar radiation registered in both regions (see Figure 6). This low cost energy adds to the high volumes of wind energy also available at this time, bringing marginal prices down. On the contrary peak prices are due to high demand requirements at times in which solar resources are not available and low cost technologies (renewables and fossil fuel-based) do not have enough capacity to supply all of it, thus requiring the usage of expensive units. As explained before, for some hours in the German 2040 scenario, not even these are enough to meet peak demand in winter nights, which results in lost load events, valued at €3,000 in MODECO's scenarios.

Figure 45. Mean marginal price per hour and year registered in Spain and Germany



Source: Own elaboration from the UCED's model first executions

Box 3. Key trends from the modelled energy prices under a power system evolution led by distributed energy

- Marginal prices in Germany are overall higher than in Spain for the entire period. In both regions, prices tend to increase towards the future, but more significantly in Spain.
- Seasonally, summer and transition prices decrease in Spain from 2025 to 2030, and increase after 2030. Winter prices grow constantly but much faster after 2030. In Germany, summer and transition grow mostly from 2025 to 2030, slightly increasing afterwards. Winter prices maintain a linear increase during the 16-year period.
- For both countries, winter marginal prices are the highest. However, the difference between this season and the rest is widest for Germany 2040.
- In Germany, four days in 2040 register extremely high prices due to lost load events.
- Peak prices occur at night and early morning hours in both countries. However, in Germany the highest are registered at night and in Spain before dawn.
- A price increase is observed during peak price hours, whereas the rest of the day prices actually tend to decrease due to higher solar energy availability.

6.3 Energy tariffs

The applicable taxes and Use-of-Network charges are applied to the marginal prices obtained from the UCED model to form the energy tariffs used in the scenarios defined in Section 2.3. The prices obtained for the scenarios with TOU charges are shown in Figure 46 for Germany and Figure 47 for Spain. As explained before, the charges applicable to low and medium voltage users are different (see Table 10 and Table 11) as the first imply a more intensive use of the network infrastructure. Thus, different tariffs are obtained for low and

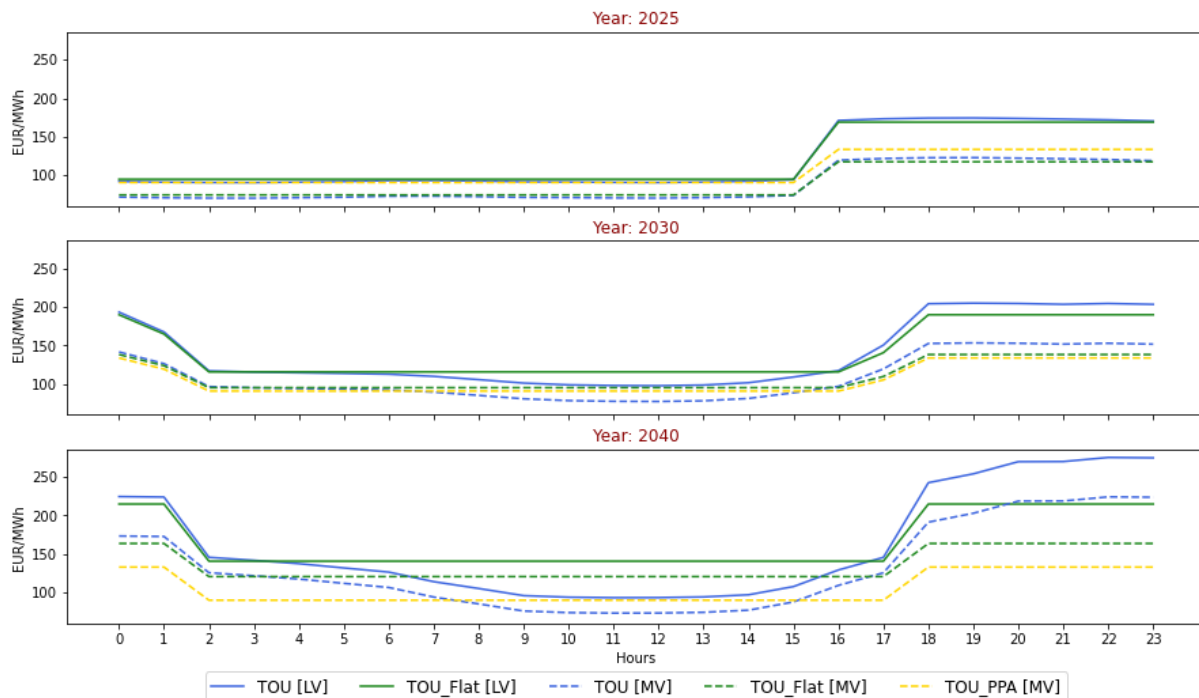
¹³ Solar energy is produced via solar PV in Germany, and via solar PV and concentrated solar power plants in the case of Spain.

medium voltage users in scenarios with dynamic and flat energy prices. As observed in the following figures, medium voltage tariffs are lower than their low voltage counterparts, which reflects each users' usage from the network. The scenario with a PPA energy price (TOU_PPA) is only shown for medium voltage users as it is only evaluated within the industrial polygon archetype. Finally, the values for the scenario with no charges (No Charges) are also included for comparison.

The energy costs obtained for the Peak power and Bandwidth models are not shown as they follow the same trend as the No Charges case, except that values are slightly higher due to the inclusion of the applicable electricity taxes. In these cases, the Use-of-Network charges are recovered through the capacity-based fees shown in Table 10 for the peak power-based model and in Table 11 for the bandwidth case. All archetypes except the industrial polygon, which is interconnected to the medium voltage grid, are subjected to the low voltage fees.

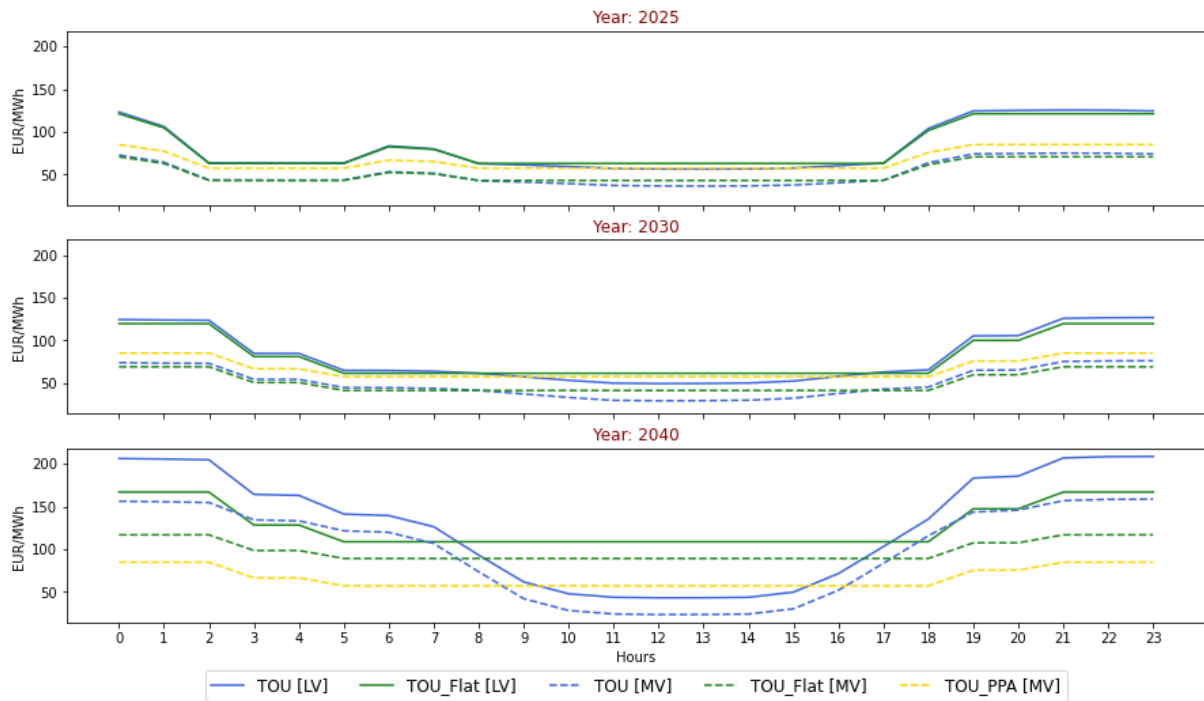
In 2025, the mean hourly values obtained for the dynamic (TOU [LV], and TOU [MV]) and flat rate (TOU_Flat [LV] and TOU_Flat [MV]) scenarios are practically the same for both countries and voltage levels. In future years, however, the mean hourly values for the dynamic tariff scenarios get lower than for the flat prices cases around midday, when marginal prices are at their lowest (see Figure 45). On the contrary, during night peak hours, the dynamic price tariffs get higher than in the flat rate scenario. This difference is particularly noticeable in 2040. For Spain, dynamic tariffs are also significantly higher than in the flat rate case before dawn, which is related to the marginal prices dynamic discussed in the previous section.

Figure 46. TOU energy tariffs applicable to Energy communities in Germany



Source: Own elaboration from the UCED's model first executions

Figure 47. TOU energy tariffs applicable to Energy communities in Spain



Source: Own elaboration from the UCED's model first executions

Following the methodology defined in Section 2.3.2.1, the peak and off-peak hours are defined per each season and year based on the residual load values identified according to the energy system characteristics defined for each country. The final classification is summarised in Table 39. Then, the applicable Use-of-Network charges are applied to off-peak and peak hours, respectively. As the latter are higher, energy costs for users are always more expensive at peak hours in the TOU scenarios, although the difference between peak and off-peak hours gets more significant in the future for the dynamic price cases as could be observed in the previous graphs. Such differences would influence investment decisions as will be explained in the next chapter.

Table 39 Hours classified as peak in each country, year and season

| Year | Germany | | | Spain | | |
|------|---------------------------|---------------------------|---------------------------|--|--|---------------------------|
| | Summer | Transition | Winter | Summer | Transition | Winter |
| 2025 | 16:00-00:00 | 16:00-00:00 | 16:00-00:00 | 00:00-2:00 6:00-7:00 19:00-00:00 | 00:00-1:00 7:00-8:00 18:00-00:00 | 00:00-2:00 18:00-00:00 |
| | 00:00-1:00 17:00-00:00 | 00:00-2:00 18:00-00:00 | 00:00-2:00 18:00-00:00 | 00:00-5:00 21:00-00:00 | 00:00-3:00 19:00-00:00 | 00:00-3:00 19:00-00:00 |
| | 00:00-2:00 18:00-00:00 | 00:00-2:00 18:00-00:00 | 00:00-2:00 18:00-00:00 | 00:00-5:00 21:00-00:00 | 00:00-3:00 19:00-00:00 | 00:00-3:00 19:00-00:00 |

Source: own elaboration with results from the UCED model execution.

7 Investment model results

The use of different tariff structures influences the investment choices of Energy communities in different manners. However, attention must also be paid to regional differences regarding marginal prices, demand patterns, resource availability and climatic conditions, as well as the archetypes' intrinsic characteristics. In Section 7.1, the results for the main Use-of-Network tariff structures – No charges, Time-of-Use, Bandwidth and Peak power – are discussed, highlighting the effect of this in the obtained results, as well as the influence of other relevant variables. In Section 7.2.1, the key findings from using different energy prices – dynamic, flat and PPA (the latter only in the Industrial polygon) – under a TOU structure are presented. Finally, a sensitivity analysis using different discount rates is done and discussed in Section 7.2.2.

7.1 Tariff structures: TOU, Peak power, Bandwidth

The objective function values obtained for the base tariff scenarios are presented in the table below. As observed, all values are positive, which indicate that the costs associated with the assets installation, operation and maintenance, as well as those related to demand response operation and electricity and fuel purchases incurred by the communities in the 16-year period are in aggregated higher than the benefits obtained from excess electricity selling and the provision of smart EV charging services. The largest values are reported for the Industrial polygon archetype as its large electrical demand complicates reaching high self-consumption values through local generation, given the space and other constraints. In almost all cases the lowest value is reported for the No Charges scenario and the highest for the Bandwidth model. The only exceptions are the German Rural town, in which the TOU Scenario presents the lowest results, and the Spanish Virtual community, in which the highest value is reported for the TOU tariff. The reasons behind such results will be discussed in the following sections in which each archetype's investment decisions will be analysed individually.

Table 40 Value of the objective function obtained for each case in million euros [M€]

| Archetype | Germany | | | | Spain | | | |
|---------------------------|---------|--------|--------|--------|--------|--------|--------|--------|
| | NC | TOU | BW | PP | NC | TOU | BW | PP |
| Business park | 4.32 | 6.59 | 14.05 | 7.34 | 3.71 | 5.75 | 8.73 | 5.33 |
| Industrial polygon | 161.86 | 264.60 | 367.14 | 294.36 | 109.07 | 137.08 | 210.04 | 143.21 |
| Rural town | 0.19 | 0.09 | 2.66 | 0.66 | 0.92 | 1.25 | 2.08 | 1.21 |
| Urban district | 0.94 | 1.53 | 3.95 | 1.62 | 10.92 | 11.47 | 12.51 | 11.34 |
| Virtual community | 2.22 | 10.16 | 11.36 | 8.8 | 2.22 | 8.33 | 6.95 | 4.30 |

Source: own elaboration with results from the UCED model execution.

All the cases evaluated in this section obtained the defined gap value (<1%), except for the Rural town and Virtual community under the No Charges tariff, the Business park under the Bandwidth scenario, and the Rural town with a TOU tariff. The latter, however, was the only case with a gap value higher than 1%. The specific gap values obtained can be consulted in Annex 4.

7.1.1 Business park

The total investments made by the Business park communities in Germany and Spain are shown in Figure 48. In general terms, the Spanish Business park undergoes larger investments than the German community, but the differences are more significant in the No Charges and Bandwidth cases, whose results seem to be more sensitive to the regional variations. The Bandwidth scenario results in the largest total investments in Spain (7.8 M€) although just slightly below those reported under No Charges (7.55 M€). In Germany, both cases also result in similar investments, but the total amount is 2% larger in the No Charges than in the Bandwidth scenario. The least total investments are found in the TOU and Peak-power tariff structures for both regions, with investments in the latter being slightly below (2-3%) those in the TOU case. In all tariff structure scenarios, the Business park communities invest in gas-fuelled CHP, rooftop solar photovoltaics, V2G charging

stations and batteries. This archetype was assumed to have no land space available for ground-mounted solar and wind installations, so these options are not eligible investments.

Figure 48. Investments performed in the Business park archetype under different Use-of-Network structures

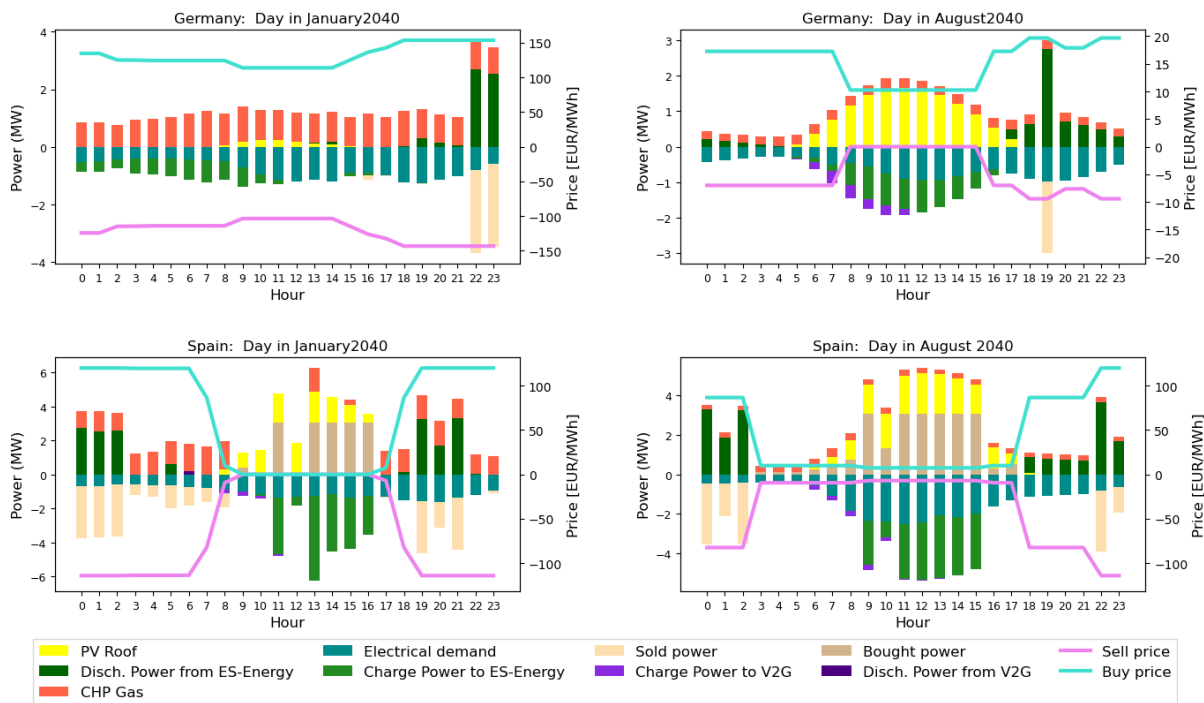


Source: Own elaboration with results from MODECO's investment model

The results for the **German Business park** show little variation between the No Charges and Bandwidth cases. **The installed CHP capacity is 1.86 MWe** (3.38 MWt) in both cases, which is 25% above the mean thermal demand (2.70 MWt) registered for this archetype in winter but below the maximum peak demand (7.10 MWt), which suggest a correct sizing. The **storage power considered is 14.12 MWh and 13.15 MWh** in the No Charges case and Bandwidth models, respectively, and corresponds to energy-based batteries only. Additionally, **27 V2G chargers are installed when No Charges is considered, and 33 when using the Bandwidth restrictions**. As seen in Figure 49, where the electrical balance for two representative days in the Bandwidth scenario is shown, the installed batteries in the German Park are used to store excess CHP and solar production in low-priced windows and sell it back when prices get higher. The PV solar rooftop installed in both scenarios corresponds to the maximum possible given the available area. As seen in the figure below, this results in some excess production during summer, which is used to charge batteries.

In **Spain**, these two scenarios also lead to similar investment decisions. The **installed CHP capacity is the same for the No Charges and Bandwidth tariffs** (3.75 MWe, 6.83 MWt) and higher than in the German region despite that the Spanish Business park has a thermal demand 12% lower. Looking at the annual investments made by the Spanish park under these scenarios, it is observed that the largest CHP capacities are installed in Spain in 2025 and 2040 (see the Bandwidth model example in Figure 50). The cogeneration capacity installed in 2025 is pretty similar to that made in the German region. Moreover, the CHP operates at partial load practically all the time, which is why the new CHP power installed in 2040 does not make operational sense. It is just included to justify larger storage capacity without violating the model restrictions.

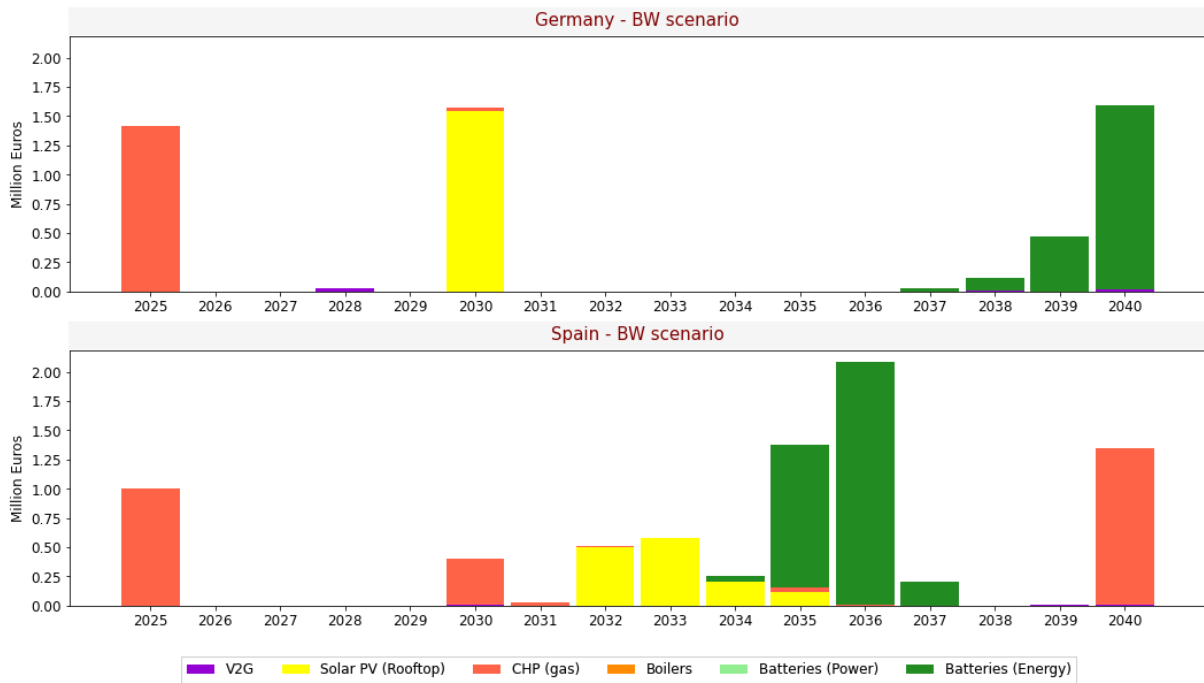
Figure 49. Electrical balance for the Business park communities under a Bandwidth tariff in two representative days in January and August 2040 [Maximum Ω]



The selected representative days are January 11th (Ω : 24) and August 25th (Ω : 20) for Germany and January 31st (Ω : 27) and August 28th (Ω : 19) for Spain. In all cases, the days with the highest weight (Ω) per month were selected.

Source: Own elaboration with results from MODECO's investment model

Figure 50. Annual investments performed in the Business park archetype under the Bandwidth tariff case



Source: Own elaboration with results from MODECO's investment model.

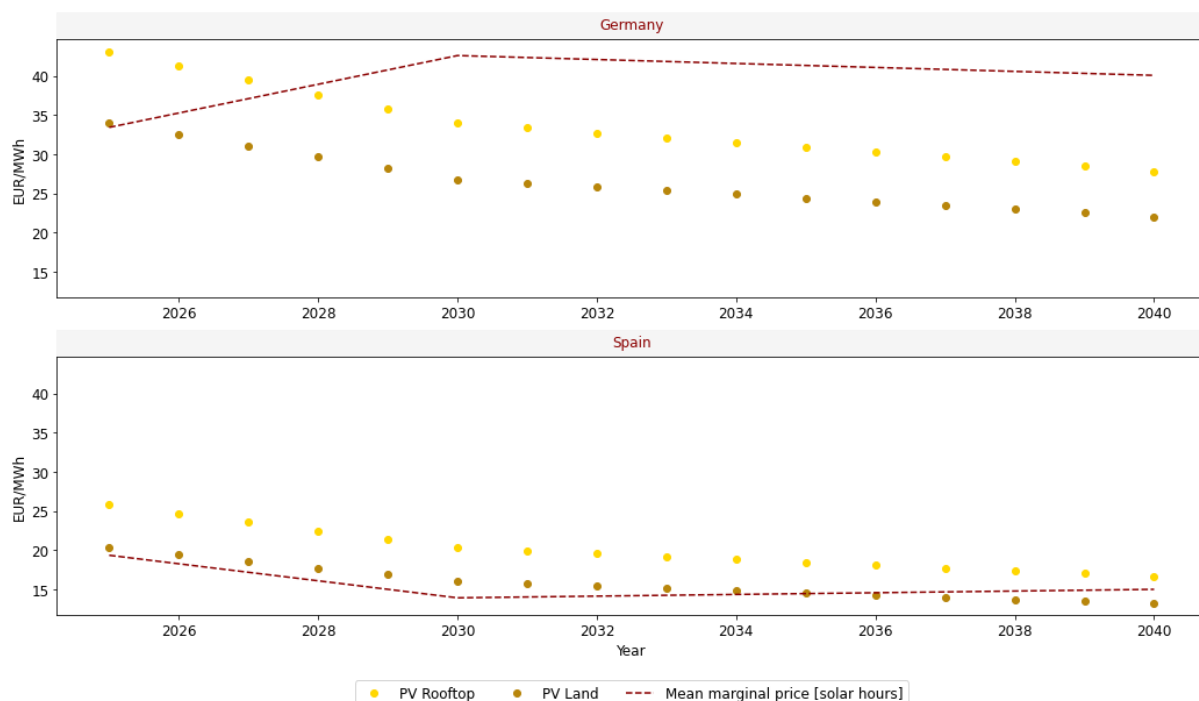
The **storage power installed in the Spanish park under the No Charges and Bandwidth cases** (3.75 MWh) **doubles that considered under the same tariffs in the German region**. As observed in the electrical balance for the Bandwidth model shown in Figure 49, at some hours, the **purchase prices**

considered in the Spanish Business park are close to zero, which permits charging batteries with grid electricity on top of excess energy and selling it later to obtain a profit. Given the considerable price spreads, these obtained revenues are high enough to justify installing excess CHP at the end of the period just to ‘trick’ the model into accepting larger investments in energy-based batteries.

As explained before, the model limits the storage capacity to the installed power capacity to avoid overinvestments in batteries solely for energy arbitrage purposes, which derives from the definition of energy communities as non-for-profit entities. However, under this context, revenues associated with energy arbitrage are large enough to support the installation of more CHP than actually needed to meet the community’s thermal or electrical demand. This extra CHP capacity is acquired at the end of the period to minimize the fixed operational and maintenance costs associated with this technology in the computation of the 16-year total operational costs.

PV solar rooftop capacity is below the maximum permissible in both cases, but the installed capacity is lower in the No Charges (2.85 MW) than in the Bandwidth (2.97 MW), as marginal prices are lower in the first as taxes are not considered, and no opportunity to save any further costs are present as no Use-of-Network tariffs are considered. As explained in Section 6.2, **marginal prices in Spain are low in high peak solar production hours** (9:00 – 16:00) and get even lower in the future, which makes solar a less attractive investment despite the lower LCOE offered by these technologies in Spain. In Germany, lower solar radiation increases the value of LCOE, but this is still competitive before 2030 due to the larger marginal prices registered in this region (Figure 51). Solar LCOE in Germany and Spain versus mean marginal price during high solar radiation hours (Figure 51). For this reason, when looking at the annual investments made by the communities, **solar power is installed earlier in Germany than in Spain** (see for instance the Bandwidth model results shown in Figure 50). Notably, no penalizations for bandwidth excess usage is reported for the German or Spanish Business park under the proposed investment strategy.

Figure 51. Solar LCOE in Germany and Spain versus mean marginal price during high solar radiation hours

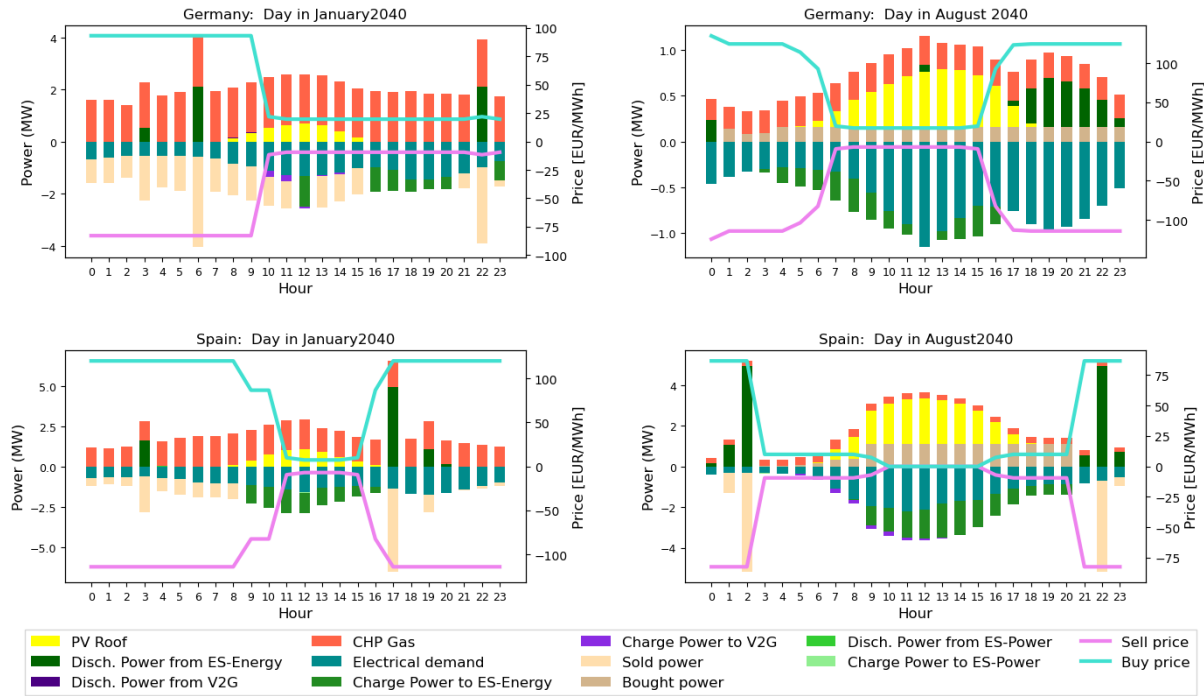


Source: Own elaboration with results from MODECO’s investment model.

The **Peak power** scenario results in slightly larger cogeneration (1.93 MWe, 3.51 MWt) capacity being installed at the German Business park than under the rest of tariffs. However, the storage capacity considered is lower (5.98 MWh) as well as the number of V2G points (21). As in the other cases, PV solar rooftop is kept to the maximum possible. Although on most days, batteries are charged with excess local generation, at some hours, batteries need to use grid electricity as support (see the representative days shown in Figure 52 for the Peak power case). Electricity grid charging is economically penalized under the Peak power tariff when it

contributes to increasing demand peaks, reducing the times in which it can be done up to a certain level without incurring in extra costs. For instance, on the August day shown in Figure 52, batteries stop charging at 12:00 when the highest demand is presented. On the contrary, when using the No Charges scenario, batteries charge large energy volumes at low-priced periods. The lowest number of V2G points (21) are installed in the Business park under this tariff.

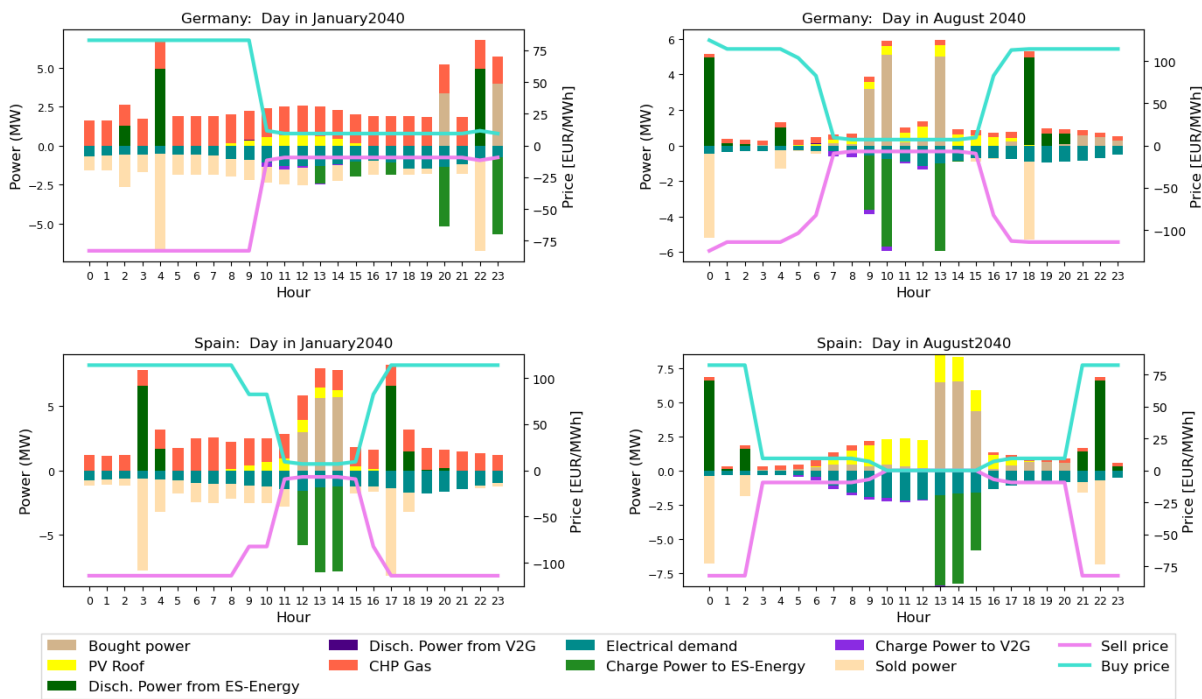
Figure 52. Electrical balance for the Business park communities under a Peak power tariff in two representative days in February and August 2040 [Minimum Ω]



The selected representative days are January 25th (Ω : 7) and August 11th (Ω : 11) for Germany and January 24th (Ω : 4) and August 16th (Ω : 12) for Spain. In all cases, the days with the minimum weight (Ω) per month were selected.

Source: Own elaboration with results from MODECO's investment model

Figure 53. Electrical balance for the Business park communities under a No Charges tariff in two representative days in February and August 2040 [Minimum Ω]



The selected representative days are January 25th (Ω : 7) and August 11th (Ω : 11) for Germany and January 24th (Ω : 4) and August 16th (Ω : 12) for Spain. In all cases, the days with the minimum weight (Ω) per month were selected.

Source: Own elaboration with results from MODECO's investment model

In **Spain**, the installed cogeneration capacity (1.90 MWe, 3.45 MWt) under the Peak power is larger than in the TOU but lower than in the No Charges and Bandwidth scenarios (where it was oversized). The **installed CHP size is aligned with the community's thermal demand** (demand peak of 6.3 MWt). Storage capacity is also lower (14.09 MWh) than in the previous cases for the same reasons explained for the German community. This is the only case in which the Business park installs power-based batteries (C-rate 2) instead of just energy-based units (C-rate 0.35). The storage capacity, however, is pretty low (30,2 kWh) for this battery type. As happened in Germany, the **Power peak tariff results in the least number of V2G chargers (18) installed**.

Under the TOU tariff, the same CHP capacity as in the No Charges and Bandwidth models is installed in the German community. PV solar rooftop is also kept to the maximum power possible. Storage capacity (7.01 MWh), nonetheless, is lower than in these scenarios but higher than in the Peak power. In the TOU scenario, **battery grid charging is also costlier than in the Bandwidth (up to a certain limit) and the No Charges model, particularly at peak hours, which makes energy arbitrage less profitable for batteries, reducing its economic viability**. The number of V2G stations (34) is similar to that installed in the Bandwidth case (33). However, it must be noted that the representative days are different for this tariff as the Use-of-Network tariffs result in a different price curve.

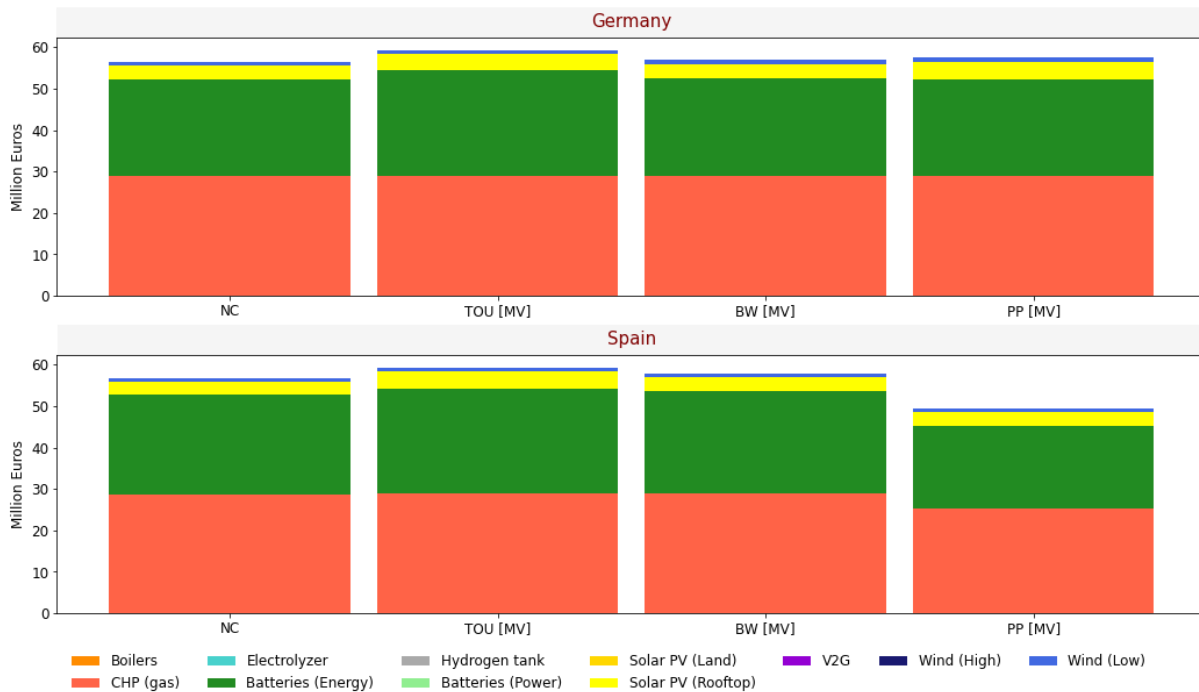
In Spain, the **cogeneration** (1.63 MWe, 2.96 MWt) and **storage** (13.45 MWh) capacity **are the lowest in this scenario**. The values, however, are not that far from those reported in the Peak power case even though different representative days are used. As in most cases, only energy-based batteries are installed. The **number of V2G charging points installed are the highest (36) as in the German region**.

7.1.2 Industrial polygon

The **industrial polygon** is the archetype in which **less regional differences are observed regarding electrical and heat demand** in the German and Spanish cases, as energy needs are more process than climate driven (see Section 3.1.2). Thus, investment choices in this archetype remain practically unaffected by this variable. As shown in Figure 54, the results from the investment model consider installations in CHP, energy-based storage, V2G charging stations, solar PV rooftop and low-capacity wind turbines. The

investments done in solar PV rooftop and low-capacity wind turbines are the same for all cases and correspond to the maximum allowed given the available rooftop and land spaces.

Figure 54. Investments performed in the Industrial polygon under different Use-of-Network structures

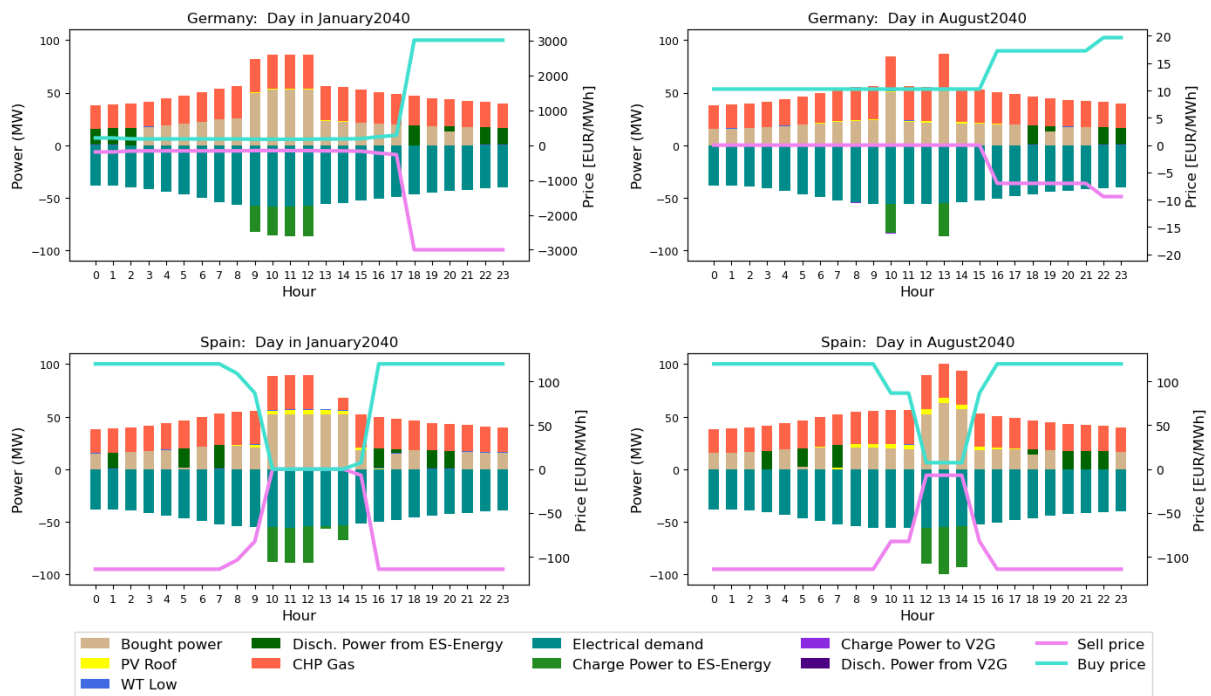


Source: Own elaboration with results from MODECO's investment model

No significant differences are observed in the total amount invested by the German or Spanish communities **under the TOU, No Charges and Bandwidth cases**. The German community also results in the same investment decisions when considered the Peak power tariff. In all these scenarios, the same CHP capacity is installed (37.52 MWe, 68.22 MWt), which corresponds to 15% above the thermal demand peak registered in the Industrial polygon. The average thermal demand in the Industrial polygon is 45.8 MWt, and values are above that threshold just 50% of hours in the 16-year period, which means that the CHP unit operates most of the time at partial load. Still, the maximum allowed cogeneration capacity is installed to justify installing larger storage capacity to perform energy arbitrage. The storage capacity installed in all of these cases is 128.24 MWh, and corresponds to energy-based batteries (C-rate 0.35) only. The number of V2G points installed vary slightly among scenarios. The only exception is the German polygon under the Peak power tariff when only four stations are installed, while the average in the rest of cases is 38.

In all these cases, the installed power of PV solar rooftop (6.63 MWe) and low-capacity wind turbines (0.74 MWe) correspond to the maximum possible given the available land and rooftop space. Compared to the rest of technologies wind influence is barely noticeable as shown in the electrical balance for the two representative days in the Bandwidth scenario (Figure 55). PV solar production is more significant in Spain as solar radiation is higher. As the representative days and price curves vary between regions, some difference in the asset's operation can be observed. Still, these do not reflect in different investment decisions.

Figure 55. Electrical balance for the Industrial polygon communities under a Bandwidth tariff in selected representative days in January and August 2040 [Maximum Ω]



The selected representative days are January 22nd (Ω : 22) and August 29th (Ω : 22) for Germany and January 23rd (Ω : 22) and August 29th (Ω : 23) for Spain. In all cases, the days with the highest weight (Ω) per month were selected.

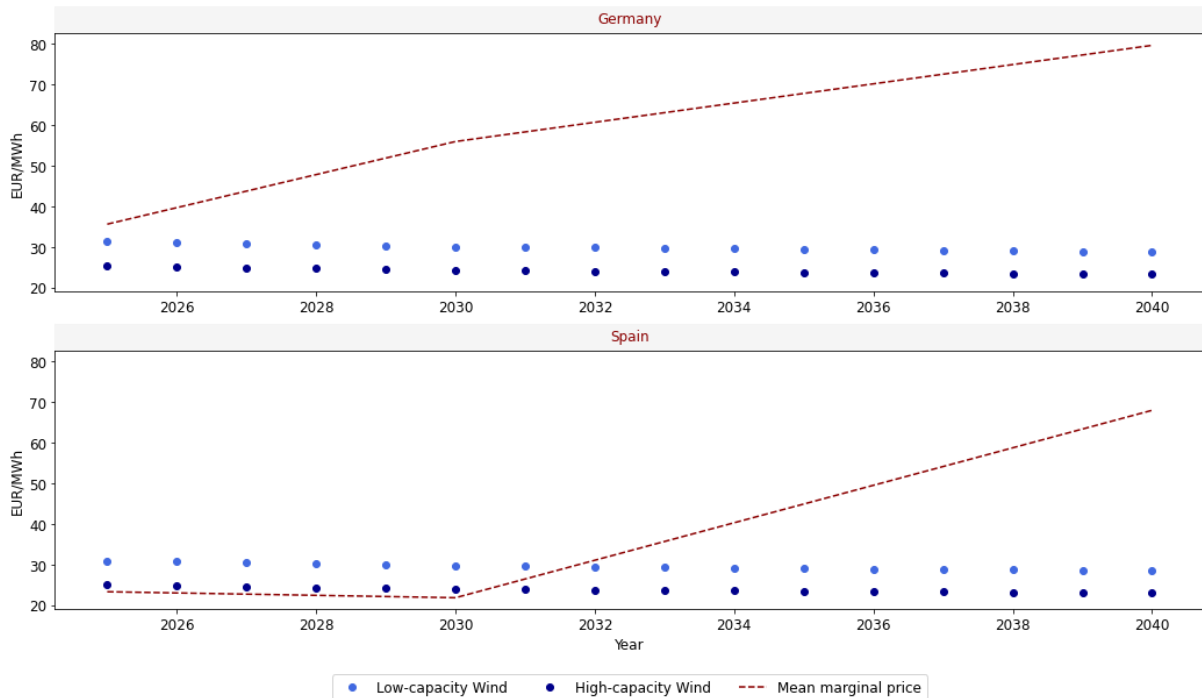
Source: Own elaboration with results from MODECO's investment model

The investment made in solar and low-capacity wind turbines are influenced by the technologies' LCOE and the available area at the archetype. The selected wind turbines have a higher LCOE than the high-capacity wind turbines or the ground-mounted PV solar, but they occupy the least area per installed Megawatt from all the renewable energies considered. As the available land is limited in this archetype, the model chooses the technology that permits installing the largest capacity. It must be noted that despite having larger LCOE than the other alternatives, it is still competitive against the electricity grid prices.

As happens with solar, the year in which wind farms are installed varies across regions. In Germany, wind is installed earlier as low-capacity turbines are competitive in price since the start of the evaluation period (Figure 56), while in Spain this equipment's LCOE gets below the mean marginal prices until 2032. As seen in the annual investments reported under the Bandwidth scenario (Figure 57), the German polygon installs low-capacity wind turbines in 2025 whereas the Spanish community does it until 2032.

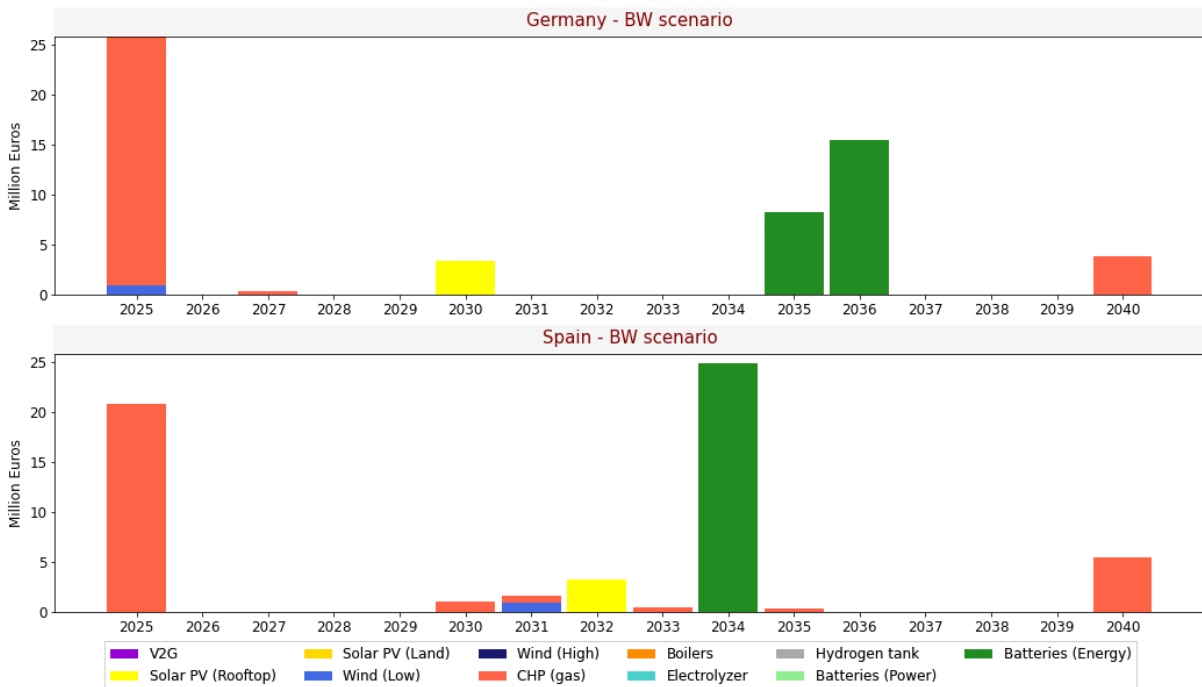
As PV solar rooftop does not compete against the rest of wind and solar technologies over land space, and its LCOE is competitive against marginal prices in both countries, the maximum possible is always installed. The investments in Germany and Spain are done at different points as LCOE becomes competitive against marginal prices after different years as explained in the previous archetype (see Figure 56). In general, these investments are done at earlier years in Germany than in Spain.

Figure 56. Wind LCOE in Germany and Spain versus mean marginal price



Source: Own elaboration with results from MODECO's investment model.

Figure 57. Annual investments performed in the Industrial polygon archetype under the Bandwidth tariff case



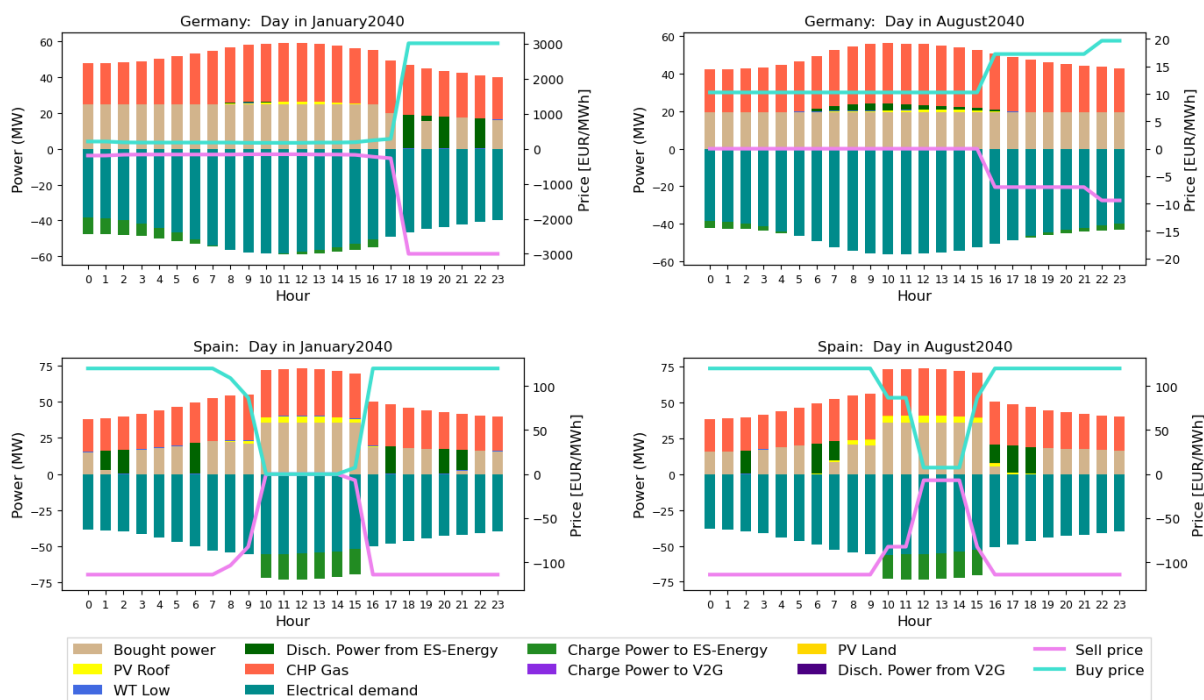
Source: Own elaboration with results from MODECO's investment model

It is relevant to note that in this archetype, **the Spanish community does incur in some penalizations for excess energy withdrawal under the Bandwidth model**. These start in 2034 and continue until the end of the period, representing average annual costs of 11,846 €. In the German community no penalizations are reported. As observed in the Bandwidth electrical balance for two representative days in 2040 (Figure 55), in both days, the Spanish polygon charges batteries around midday, when prices are low, to discharge at night and dawn when selling prices reach over 100 EUR/MWh. However, **in the August day, it surpasses its**

established limit (52.44 MWe) as the low-priced window is narrower and the potential economic benefits to sell that energy back later permits to afford such penalties. The rest of the time, the model prefers to maintain demand up to the maximum possible without causing penalizations.

The Spanish polygon shows some difference with the rest of scenarios when using the **Peak Power** tariff. First, the installed CHP capacity is slightly below the other scenarios (32.47 MWe, 59.04 MWt), as is the wind power (0.65 MWe) and energy-based batteries installed (114.13 MWh). PV solar rooftop power is the same as in all other scenarios, but **ground-mounted solar** (0.19 MWe) is also installed in this particular case. Still, the installed amount is small given the limited land space considered for this archetype. As shown in Figure 58, **solar investments are encouraged in the Spanish polygon** as its profile coincides with the community's demand peaks, contributing to decrease costs associated with capacity-based network charges. In Germany, this is also the case, but the lower solar radiation available in this region makes this technology less attractive as an investment even under a Peak power tariff, which is why wind is preferred on land and PV solar is constrained to the rooftop area.

Figure 58. Electrical balance for the Industrial polygon communities under a Peak power tariff in selected representative days in January and August 2040 [Maximum Ω]



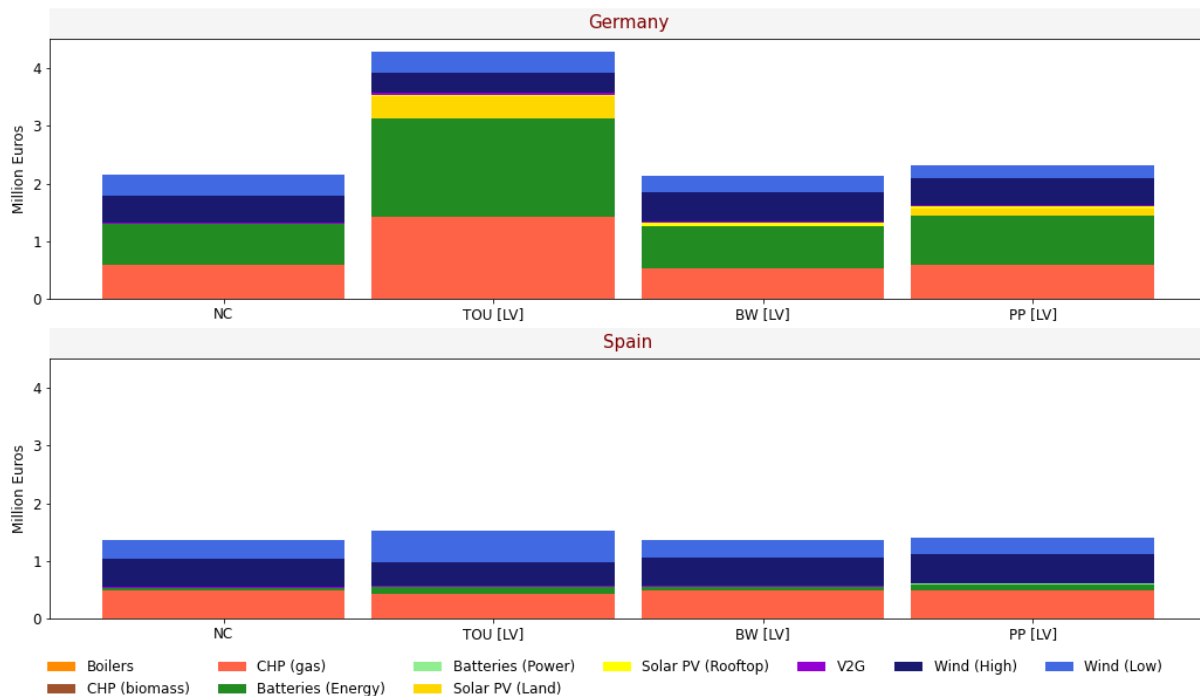
The selected representative days are January 22nd ($\Omega: 22$) and August 29th ($\Omega: 22$) for Germany and January 23rd ($\Omega: 22$) and August 29th ($\Omega: 23$) for Spain. In all cases, the days with the highest weight (Ω) per month were selected.

Source: Own elaboration with results from MODECO's investment model

7.1.3 Rural town

The **Rural town communities invest in wind, solar, gas-fuelled CHP, batteries and V2G charging points.** In this case, however, a combination of ground-mounted solar, low and high-capacity wind turbines are used depending on the tariff case evaluated. In this archetype, the investments done by the Spanish community present less variations among tariff scenarios, whereas in Germany the **TOU case reports the largest investments, mostly related to CHP and storage installations** (Figure 59).

Figure 59. Investments performed in the Rural town under different Use-of-Network structures

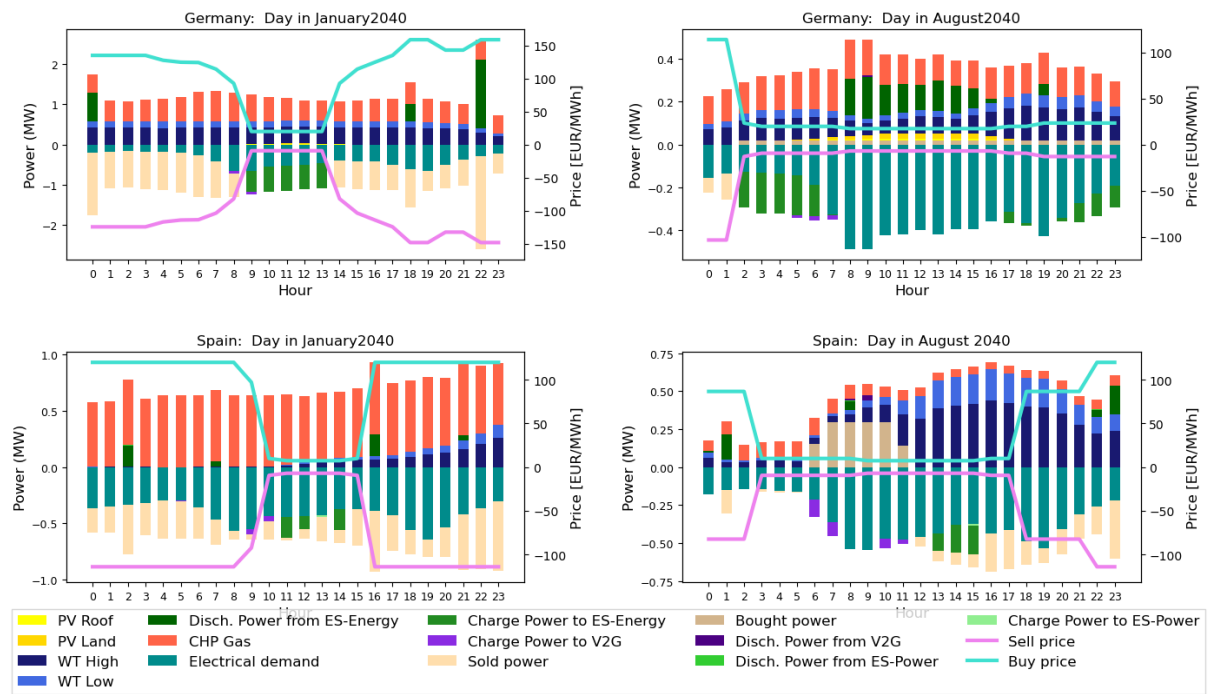


Source: Own elaboration from the UCED's model first executions

The CHP capacities installed in the German Rural town under the No Charges, Bandwidth and Peak power are aligned with the community's heat requirements, considering that in Germany an average thermal power demand of 1.07 MWe is reported during the winter season. The cogeneration power ranges from 0.68 MWe (1.24 MWe) in the Bandwidth to 0.75 MWe (1.36 MWe) in the No Charges case. The **storage capacity considered are also pretty similar in the No Charges and Bandwidth tariffs** (4.33 MWh and 4.43 MWh). Under a Peak power tariff, significantly higher storage is installed (4.88 MWh). As seen in the representative day show for August 2040 in Figure 60, in Germany, batteries are needed to reduce the demand peaks reported at 8:00 and 9:00 hours for this archetype, as local generation at this time is limited. The number of V2G charging points is the same (14) for the No Charges and Bandwidth cases. In the Peak power scenario, two extra charging points are considered.

In all these tariffs, **low and high-capacity wind turbines are installed in similar proportions in the German region**. The largest wind capacity (0.77 MWe), nonetheless, is found at the **No Charges scenario**, in which **no solar investments** – rooftop or land – are done. In the Bandwidth model, slightly less wind capacity is installed (0.73 MWe), but solar PV rooftop (0.13 MWe) is also included in the local generation mix. Finally, in the Peak power scenario, part of potentially installed wind capacity is sacrificed (reaching 0.6 MWe) to instead include ground-mounted solar (0.22 MWe). As seen in the figure below, solar helps reducing peak demands and, therefore, capacity-based network charges. The investment decisions over wind and solar technologies are based upon the technologies costs, the curve prices and the land available as discussed previously for the Industrial polygon.

Figure 60. Electrical balance for the Rural town communities under a Peak power tariff in selected representative days in January and August 2040 [Maximum Ω]



The selected representative days are January 29th ($\Omega: 23$) and August 19th ($\Omega: 21$) for Germany and January 8th ($\Omega: 25$) and August 6th ($\Omega: 19$) for Spain. In all cases, the days with the highest weight (Ω) per month were selected.

Source: Own elaboration with results from MODECO's investment model.

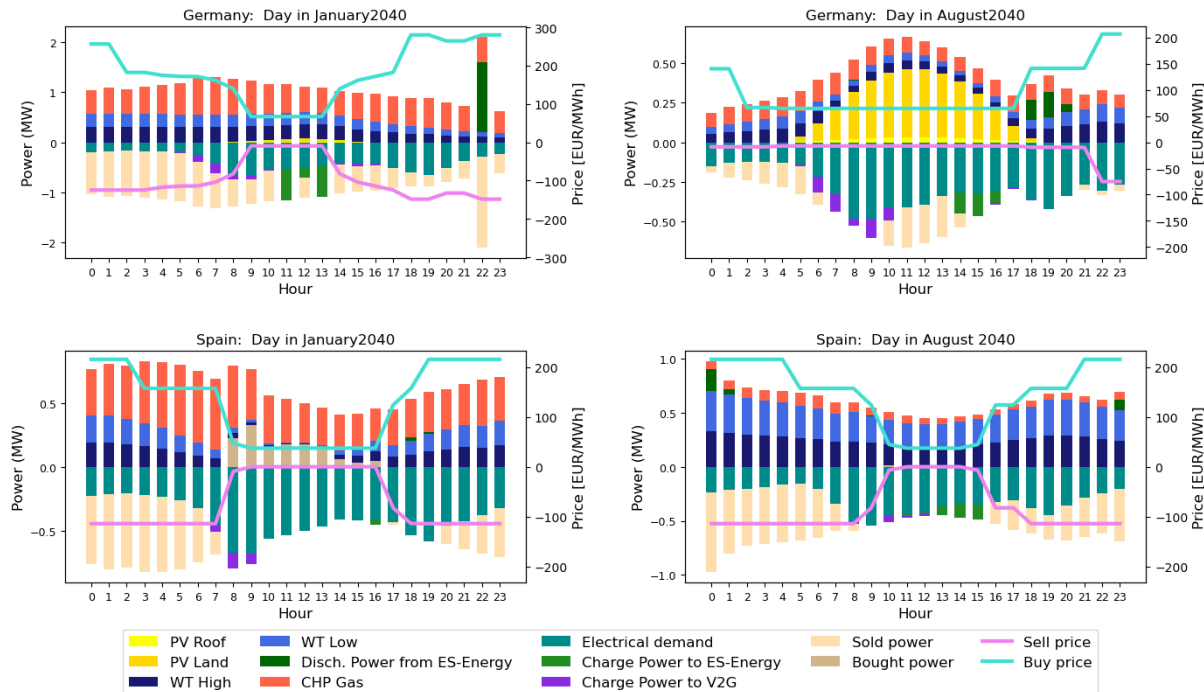
In Spain, the installed **cogeneration capacity** is practically the same (0.63 MWe, 1.15 MWt) for the No Charges, Bandwidth and Peak Power scenarios. As in the German region, this capacity is **adjusted to the community's thermal demand**. Wind installations are also pretty similar in the three cases, with average high and low-capacity wind power of 0.49 MWe and 0.25 MWe, respectively. No solar is installed in any case. The installed storage capacity is the lowest in the No Charges case (0.25 MWh) and highest in the Peak power scenario (0.54 MWh). The latter is also the only case in which the Rural town installs power-based batteries (C-rate 2) and not only energy-base units (C-rate 0.35). However, as happened in the Business park archetype, the installed power-based capacity is low (13 kWe). As shown above, **under the Peak power tariff, batteries are used in the Spanish town to store excess wind energy at times in which demand and prices are low to discharge at higher-priced hours (1:00 and 23:00) or when demand peaks occur (8:00)**. Still, in all cases, the storage capacity installed in Spain is significantly lower than in Germany as the wind generation profile has a high coincidence to high-priced and demand periods, which makes batteries usage less attractive.

The results obtained for the **German Rural town under the TOU tariff present significantly higher investments when compared with the rest of cases**. The CHP capacity installed (1.91 MWe, 3.47 MWt) corresponds to the **maximum allowed investment given the community's peak demand** (3.18 MWt). The CHP, nonetheless, was already utilized at partial load for practically all hours after 2025, so new investments in CHP are not justified in 2040 except for allowing higher storage instalments. As can be seen in Figure 61, in the selected days for the German Rural town there are higher selling prices than in other archetypes, reaching over 100 EUR/MWh in several days, such as in the chosen day for January 2040 at 22:00 hours. This mix of conditions results in significantly larger storage capacity being added in the German town under the TOU tariff (9.38 MWh) than with the rest of tariffs in which the total storage capacity installed averages 4.55 MWh. This, in turn, leads to extra CHP capacity installed to obey the model rules. Wind installations in this case (0.65 MWe) are similar to the Peak power case. Both, PV solar rooftop (0.05 MWe) and land (0.67 MWe) are also considered in this case, which represents the largest solar investments made in the German Rural town. The number of V2G points (18) are larger than for the rest of archetypes.

On the contrary, in Spain, **the lowest CHP capacity is installed under the TOU tariff** (0.56 MWe, 1.02 MWt). Storage capacity (0.57 MWh) is higher than in the rest of tariff scenarios. As seen in Figure 61,

batteries in this case are used similarly to the other cases; their purpose is to store excess wind energy during low-priced periods to be later sold at a higher price. As the TOU uses different selected days than the rest of archetypes, the resulting price curves have a strong influence over the results obtained in this case. As can be seen in the figure below, the peak prices reported in the chosen representative day for August 2040 doubles the prices applicable to the Spanish town in the rest of scenarios, which reflects in more installed batteries as energy arbitrage becomes more profitable. Still, the storage capacity installed continues being significantly lower than for Germany, as wind production in Spain fits better the demand and price curves used, making batteries less useful.

Figure 61. Electrical balance for the Rural town communities under a TOU tariff in selected representative days in January and August 2040 [Maximum Ω]



The selected representative days are January 29th ($\Omega: 23$) and August 19th ($\Omega: 21$) for Germany and January 8th ($\Omega: 25$) and August 6th ($\Omega: 19$) for Spain. In all cases, the days with the highest weight (Ω) per month were selected.

Source: Own elaboration with results from MODECO's investment model.

Low and high capacity wind turbines are also considered in the TOU case. High capacity installations are favoured earlier as they offer a lower LCOE than the low-capacity types (see Figure 56). In the Spanish town, the land-prices-technology dynamics imply not installing any PV solar on land as prices during solar irradiation hours are fairly low, and self-consumption is already covered by wind production. Despite not competing over the same area availability, no PV solar rooftop is installed in the Spanish community under a TOU or any other tariff tested for the same reason that PV solar on land is disregarded: prices during solar radiation hours are not competitive. As in the Industrial polygon, for land installations, the model finds the technological combination that permits to maximize benefits, considering the prices curves, generation profiles and technologies' costs and features, such as land usage.

7.1.4 Urban district

In the **Urban district archetype**, communities invest in **gas-fuelled CHP, batteries, solar PV rooftop and V2G charging points** (Figure 62). Ground mounted solar and wind farms are not possible investments due to land usage restrictions. The scenarios that prompt the largest investments are the No charges for Spain and the TOU for Germany, although just slightly above the No charges case. As happens in the previous archetypes, **the major differences** are mostly due to the **decisions taken regarding investments in CHP and batteries**. In this case, however, significant differences are observed regarding the amount of PV solar rooftop installed in each region, and among the tariff structures evaluated in the Spanish Urban district.

Figure 62. Investments performed in the Urban district under different Use-of-Network structures



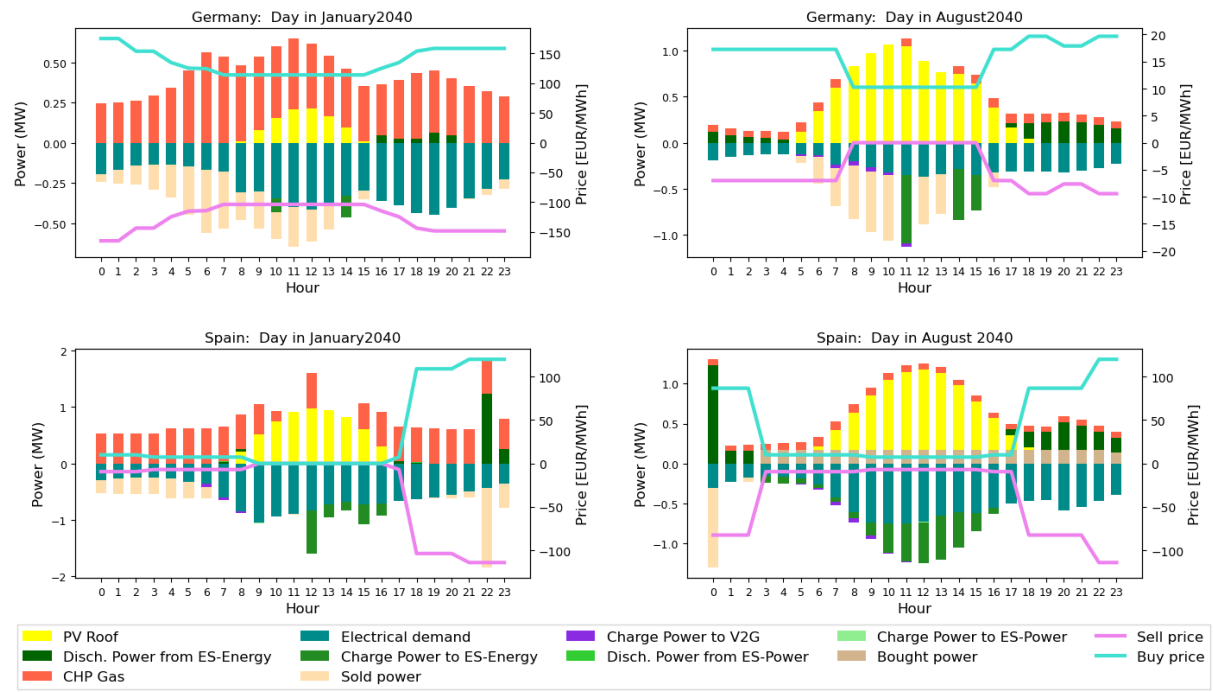
Source: Own elaboration from the UCED's model first executions

For the German district, the lowest amount invested (4.31 M€) is registered in the No Charges scenario. The difference, however, is narrow when compared to the rest of tariff analysed. The installed CHP capacity (1.58 MWe, 2.87 MWt) is just below the community's peak thermal demand (3.51 MWt). As in previous archetypes, this means that the cogeneration unit operates at partial loads most of the time. The **installed batteries (10.89 MWh) are the lowest considered for the German Urban district, but are large enough to need extra CHP installed to obey the model rules**. PV solar rooftop capacity is also at its lowest in this scenario (2.24 MWe) as no Use-of-Network charges can be avoided as in other tariffs. The number of V2G stations installed (5) is practically the same as for all other scenarios.

In the Spanish region, the opposite trend is observed as the **No Charges case is the one with the largest amount of money invested** (2.09 M€). While the PV solar rooftop installed is lower than for other cases (1.15 MWe), the installed CHP capacity is far higher (1.41 MWe, 6.44 MWt) than for the rest of the tariffs, which result in cogeneration sizes of around 0.64 MWe (2.56 MWt) for the Spanish district. As happened with the German district, an oversized CHP is installed to justify investments in energy-based batteries (C-rate 0.35). The storage capacity considered in this scenario (7.29 MWh) is below that installed for the German district, but it is significantly higher than that installed in the Bandwidth and Peak power models, which use the same representative days as the No Charges case.

The CHP capacity installed in the German district under the Bandwidth and Peak power cases is equal to that installed in the No Charges case. Storage capacities, nonetheless, are higher under these tariffs, and in both cases round 11.3 MWh. As shown in Figure 63, batteries under the Peak power tariff are used to store excess solar and CHP electricity in low-priced periods to be consume later when purchase price are higher. The installed solar PV rooftop is also larger as the Bandwidth and Peak power offer some further opportunities to reduce costs by avoiding Use-of-Network tariffs through self-consumption. The solar power in the Bandwidth (2.36 MWe) is below that considered in the Peak power case (2.41 MWe), which corresponds to the maximum allowed given area restrictions. This as in the latter cost saving opportunities through peak shaving offer higher benefits; for instance, see the electrical balance for the representative day in January 2040 shown in Figure 63.

Figure 63. Electrical balance for the Urban district communities under a Peak power tariff in selected representative days in January and August 2040

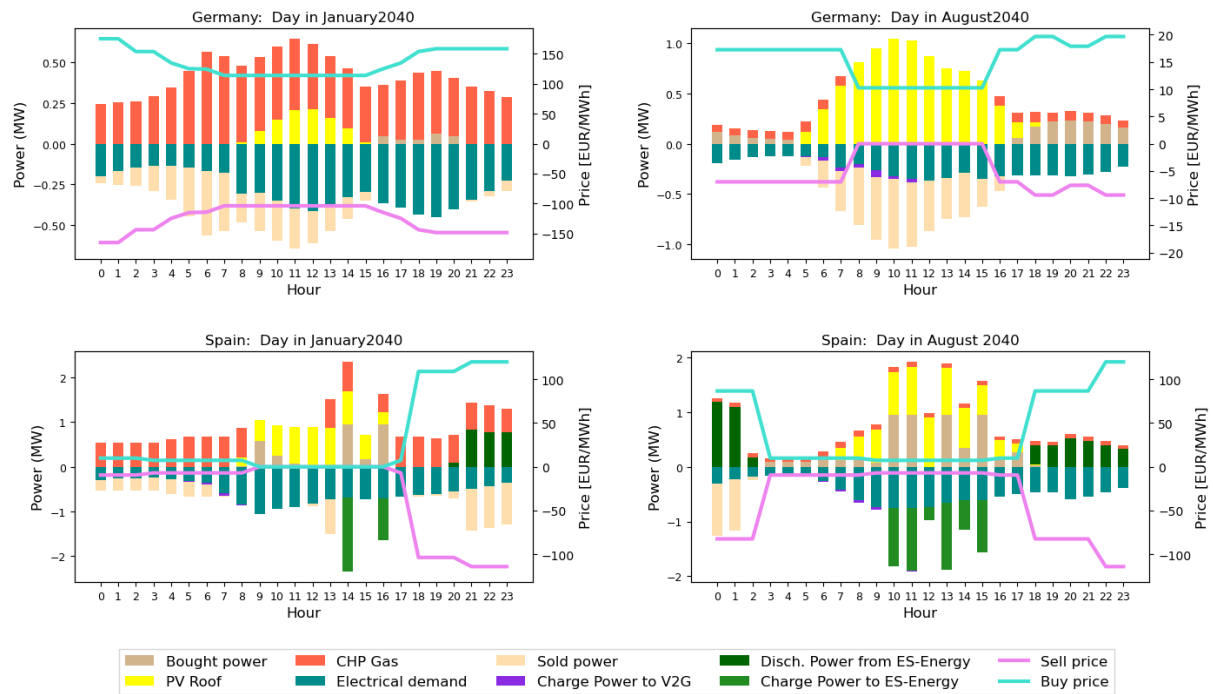


The selected representative days are January 18th ($\Omega: 23$) and August 25th ($\Omega: 24$) for Germany and January 27th ($\Omega: 23$) and August 28th ($\Omega: 19$) for Spain. In all cases, the days with the highest weight (Ω) per month were selected.

Source: Own elaboration with results from MODECO's investment model

In the Spanish district, the installed cogeneration capacity is at a similar level for both the Bandwidth (0.67 MWe, 1.22 MWT) and Peak power (0.62 MWe, 1.13 MWT) tariffs. This is sized to the community's thermal requirements (mean winter thermal demand of 0.77 MWT). However, the storage capacity installed is more significant in the Bandwidth (5.62 MWh) than in the Peak power (3.53 MWh). As seen in Figure 63, under a Peak power structure, batteries are mostly charged with excess solar that is discharge at night, when no solar is produced, to supply demand and avoid electricity purchases at high-priced hours. In the Bandwidth scenario, however, batteries are also charged through the grid (Figure 64). Notably, **in any case the maximum PV solar rooftop capacity (2.41 MWe) is installed in the Spanish district, the energy prices are so low during high solar production hours that is more convenient to consume directly from the grid**. In the Bandwidth scenario the PV solar rooftop considered is 1.29 MWe while in the Peak power this is slightly larger. V2G stations installed are 4 and 5, respectively.

Figure 64. Electrical balance for the Urban district communities under a Bandwidth tariff in selected representative days in January and August 2040

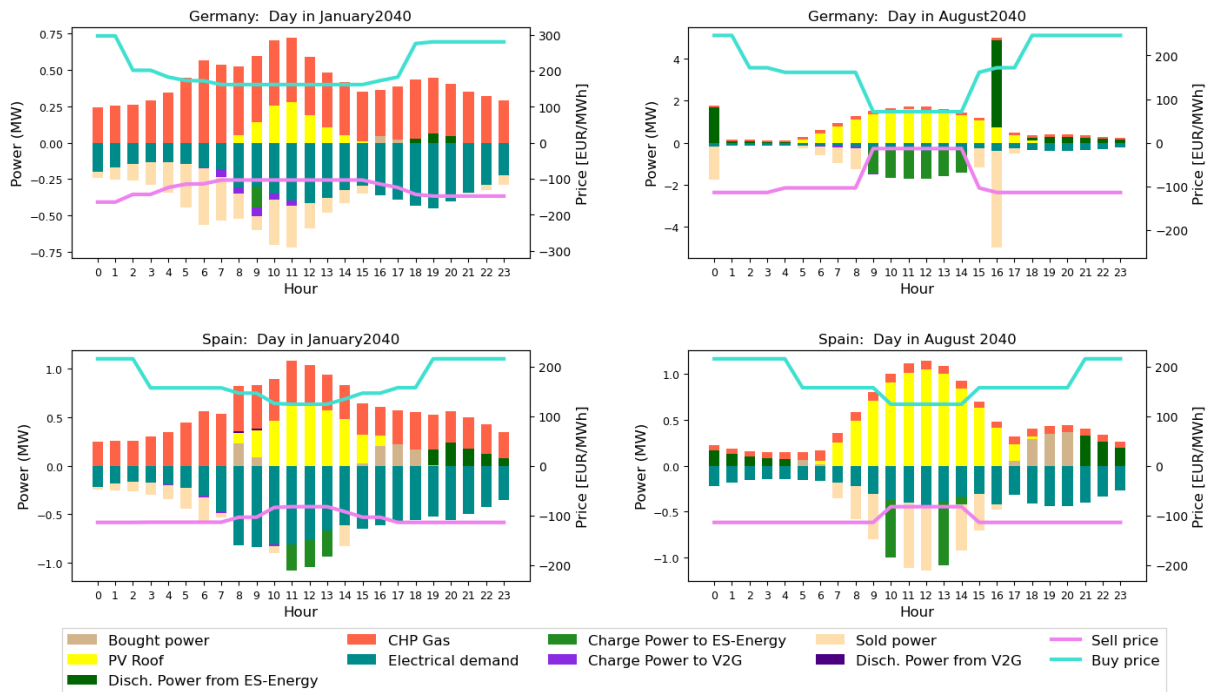


The selected representative days are January 18th (Q: 23) and August 25th (Q: 24) for Germany and January 27th (Q: 23) and August 28th (Q: 19) for Spain. In all cases, the days with the highest weight (Q) per month were selected.

Source: Own elaboration with results from MODECO's investment model

The results obtained for the TOU scenario show similar dynamics to those described for other archetypes. In **Germany, investments in batteries (12.26 MWh) are larger than in Spain (3.81 MWh)** as price spreads are not as pronounced in the latter (see Figure 65). For Germany, this encourages installing **extra CHP capacity** in 2040 (totalling 1.88 MWe, 3.42 MWT) to allow further batteries instalments, even when the equipment's full load operation is not required most of the time. In Spain, a CHP size (0.6 MWe, 1.1 MWT) more aligned to the district heat demand (mean winter thermal demand equal to 0.8 MWT per hour) is installed. In this case, the German Urban district installs the maximum PV solar rooftop capacity possible due to space restrictions (2.41 MWe). This is decided based upon the regional electricity prices and the technology's LCOE (See Figure 51). However, the Spanish district only installs 62% of this capacity as marginal prices during solar radiation hours are low, and get even lower in future years. The installed V2G charging points are similar for both regions (5 in Germany and 6 in Spain).

Figure 65. Electrical balance for the Urban district communities under a TOU tariff in selected representative days in January and August 2040 [Maximum Ω]



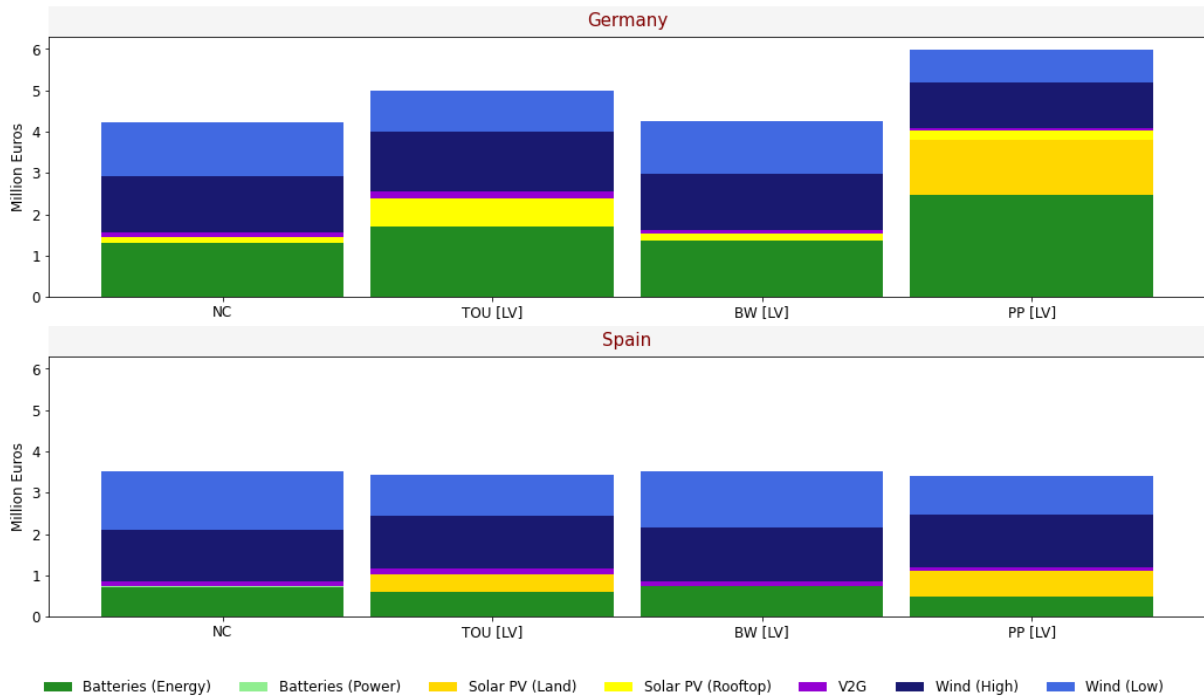
The selected representative days are January 18th (Ω : 23) and August 18th (Ω : 21) for Germany and January 22th (Ω : 25) and August 18th (Ω : 17) for Spain. In all cases, the days with the highest weight (Ω) per month were selected.

Source: Own elaboration with results from MODECO's investment model

7.1.5 Virtual community

The total investments made in the Virtual community cases are shown in Figure 66. As in this case the community members are not within the same location, **CHP installation is not considered feasible**. Moreover, this is the only case in which energy-based Use-of-Network tariffs are associated with self-consumption. The Virtual community members still save money as self-consumption avoids paying the entire tariff costs, and just a fraction is charged. In this archetype, **the communities invest in batteries (mostly energy-based), solar PV, low and high-capacity wind turbines, and V2G charging points**. Overall, investments in Germany are higher than in Spain. **The largest investments are reported for the Peak power case** (6 M€) followed by the TOU tariff (5 M€), while in the two other scenarios the amount of money invested is 4.2 M€. In Spain, there are less differences among scenarios regarding the total amount invested, going from 3.53 M€ in the Bandwidth model to 3.40 M€ in the Peak power case.

Figure 66. Investments performed in the Virtual community under different Use-of-Network structures

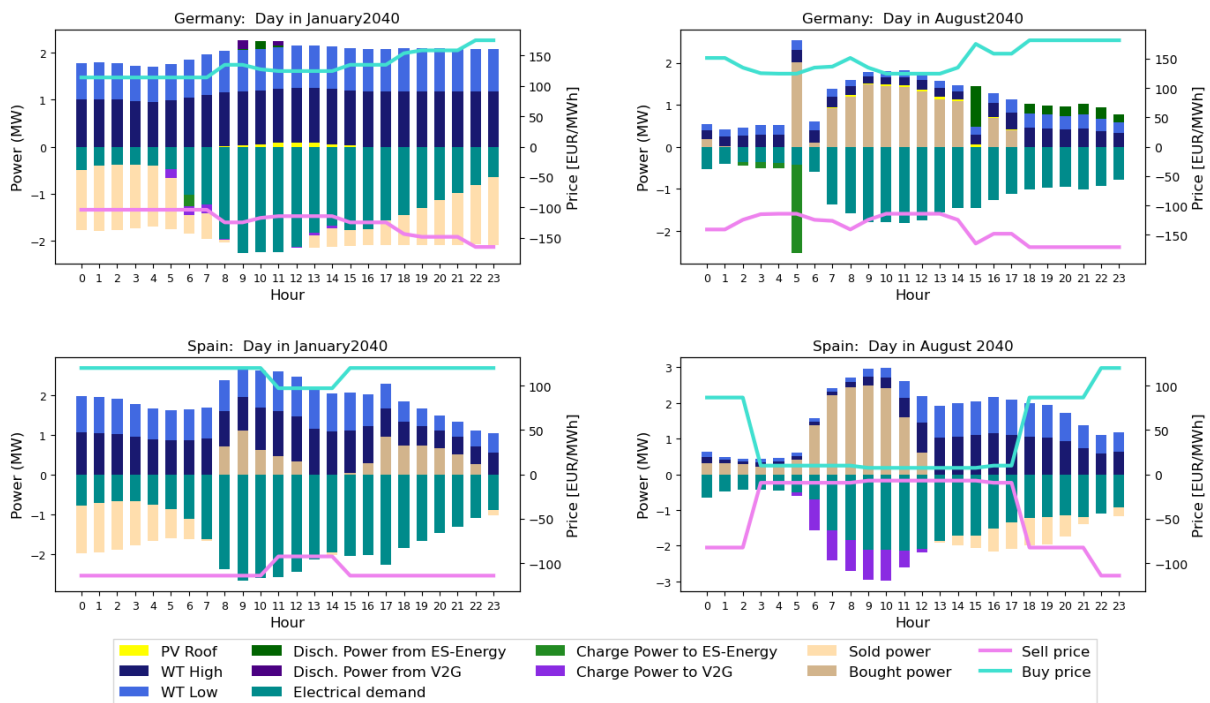


Source: Own elaboration from the UCED's model first executions

In Germany, the No Charges scenario results in similar investments to the Bandwidth model. In Germany, the available land space is filled with high and low-capacity turbines, with equal installed power for both tariffs (1.36 MWe and 1.05 MWe of high and low-capacity, respectively). **High capacity is preferred over low-capacity** as there is wide land space available and the first wind turbine type offers the lowest LCOE. PV land is not considered even though it offers a lower LCOE than low-capacity wind as it occupies more space and would reduce total renewable production, particularly as solar resources in Germany are less abundant. PV solar rooftop is installed, as it does not compete over land space, with smaller capacity in the No Charges (0.35 MWe) than Bandwidth model (0.44 MWe). A larger solar capacity is installed in the Bandwidth model as the taxes considered in this scenario make self-consumption more beneficial by avoiding these costs even below the penalization limit. Batteries investments are 3% larger for the German Virtual community under a Bandwidth model, but the **No Charges** case results in **more V2G charging points** (89 versus 56 in the Bandwidth model), which can also be **used as storage** as done in the representative days shown in Figure Y for the Bandwidth scenario. The high number of V2G points installed in this archetype are due to the larger influence area considered, which results in a **higher number of electric vehicles circulation**.

In Spain, practically the same investment decisions are taken under the No Charges and the Bandwidth model. The only relevant difference is that in the No Charges case, some power-based storage (C-rate 2) is installed, although the capacity is small (0.08 MWe). As seen in Figure 66, the total amount invested in these scenarios is lower in Spain than in Germany (on average, 17% less). The main difference is the storage capacity, as wind, solar and V2G are installed at similar levels. As happened in the Rural town, the Spanish wind profile results in more wind production during high price periods. This makes **batteries less attractive**. For instance, in the representative days shown in Figure 67, no batteries are used in Spain as during low-priced periods wind excess is used to charge electric vehicles, which represent a fixed income for the community. The rest of the time, excess production is injected to the grid.

Figure 67. Electrical balance for the Virtual communities under a Bandwidth tariff in selected representative days in January and August 2040 [Maximum Ω]



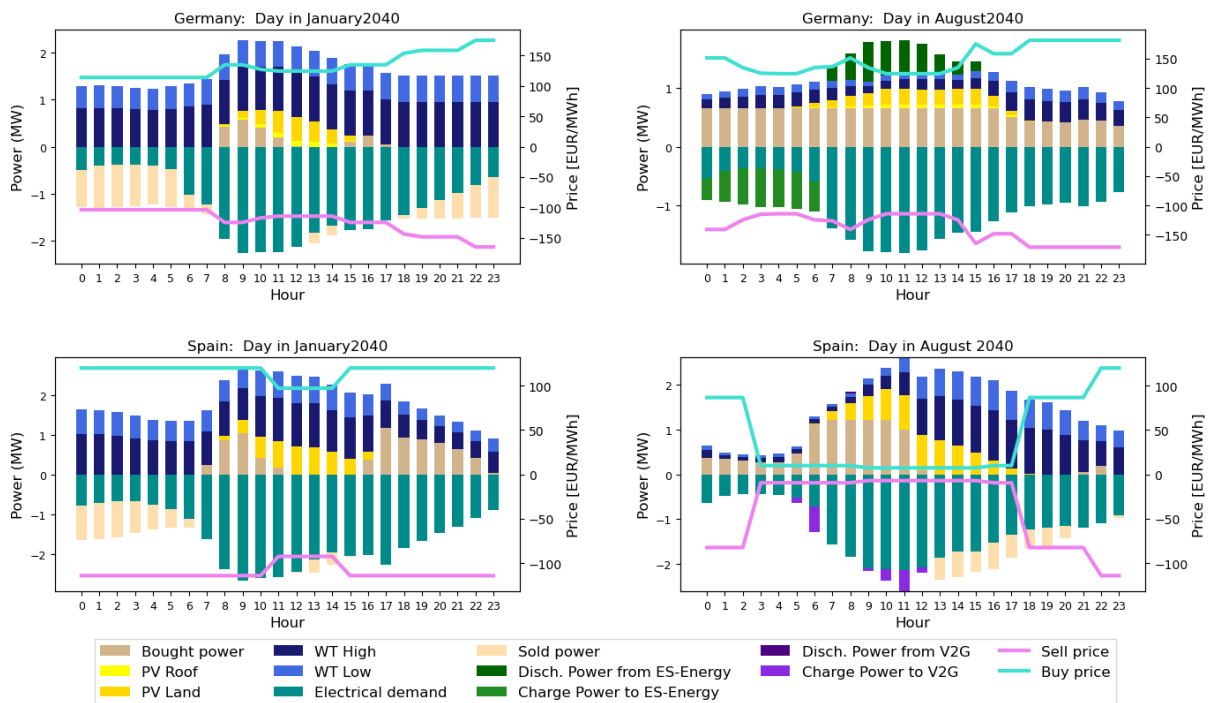
The selected representative days are January 2th (Ω : 25) and August 28th (Ω : 23) for Germany and January 26th (Ω : 27) and August 28th (Ω : 19) for Spain. In all cases, the days with the highest weight (Ω) per month were selected.

Source: Own elaboration with results from MODECO's investment model

Under the **Peak power tariff**, the German community results in the **largest investments** from all Virtual community cases. The main differences are related to **battery investments** as the wind power installed is actually lower than in the previous cases (-27%), and the solar capacity is above the No Charges and Bandwidth, but below the TOU scenario. This is the only case in which the German community **installs PV solar on land** (2.38 MWe). The latter as solar production coincides with the community peak demands, which is why a larger capacity of PV solar rooftop is installed (0.54 MWe) compared to the previous tariff scenarios (0.44 MWe and 0.35 MWe are installed in the Bandwidth and No Charges cases, respectively). The total storage capacity installed in the German Virtual Community is 13.36 MWe, 70% and 60% more than in the No Charges and Bandwidth cases. As observed in the electrical balance shown in Figure 68, batteries are mostly used by the German community **to lower summer demand peaks as wind load factor is lower during this season** (see Figure 7). **Batteries are charged at dawn** when prices are low and discharge between 8:00 and 15:00 when peak demand take place. In the Bandwidth and No Charges scenarios, less storage is installed as less benefits are obtained from using batteries. As seen in the figure above, **batteries are discharged at night when prices are higher**, still the price spread is not as high as the costs avoided through peak shaving. The amount of energy-based storage in this case disincentives the installation of V2G points, which is the lowest in the four scenarios tested.

In the Spanish region, the installed wind capacity is also lower (-17%) than in the No Charges and Bandwidth cases. As in the German community, ground-mounted PV solar (1.14 MWe) is also considered under a Peak power tariff, but no PV solar rooftop is installed. According to MODECO assumptions, solar on land offers a lower LCOE than on rooftop, which is why it is prioritized to supply demand peaks. As happened in the German region, the Peak power tariff results in the least number of V2G charging stations installed. In this case, however, the energy-based batteries capacity is the lowest (2.29 MWh) from the four tariffs analysed. As seen in the representative days shown in Figure 68, during peak demand times there is plenty of wind and solar energy available, which makes less beneficial to install and operate batteries (as shown in Figure 6 and Figure 7, wind resources and solar resources are more stable throughout the year than in Germany). Moreover, excess renewable production during low-priced windows is mostly used for electric vehicle charging.

Figure 68. Electrical balance for the Virtual communities under a Peak power tariff in selected representative days in January and August 2040 [Maximum Ω]



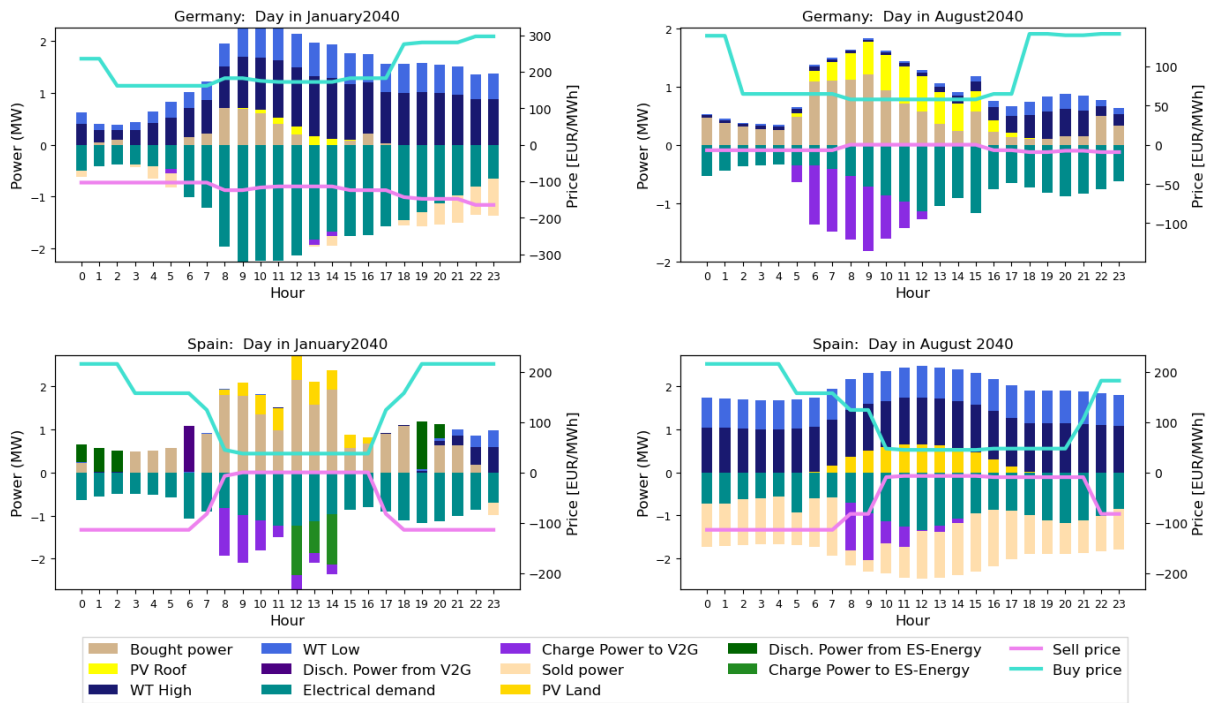
The selected representative days are January 2nd (Ω : 25) and August 28th (Ω : 24) for Germany and January 26th (Ω : 27) and August 28th (Ω : 19) for Spain. In all cases, the days with the highest weight (Ω) per month were selected.

Source: Own elaboration with results from MODECO's investment model

For the German community, the **TOU tariff results in the second largest total investments**. The total wind capacity (2.26 MWe) is higher than in the Peak power tariff but lower than in the rest. In this case, the solar PV rooftop capacity installed is the highest (1.37 MWe), but contrary to the Peak power, no ground-mounted solar is considered. Under a TOU tariff, solar represents higher potential economic benefits than the No Charges and Bandwidth cases as it avoids paying full Use-of-Network charges for consumption at those hours. These potential savings, however, are below those achieved through peak shaving in the Peak power case. The total energy-based batteries installed is 22% lower than in the previous tariff scenario. In this case, the **largest number of V2G points are registered**. As the representative days selected are different for this case, the electrical balance for the TOU tariff is shown in Figure 69. As observed, in both of the shown days, no batteries are operated in the German community, while **V2G points are actively charging during low-priced windows in August**. In this context, batteries are mostly relegated to performing energy arbitrage in days with wide price spreads, which mostly take place towards the end of the 16-year period, when the energy-based storage is implemented (Figure 70). In the rest of tariff scenarios, batteries are installed earlier in Germany, although the largest capacity is always installed at the end evaluation period (2040).

As happened in Germany, the **TOU tariff** results in the **Spanish community** investing in higher wind capacity (2.12 MWe) than in the Peak power but lower than in the rest. **Solar is also favoured** under this tariff, as it is the only case aside from the Peak power in which **ground-mounted solar is installed** (0.91 MWe) in Spain. No solar PV rooftop is installed in the Spanish community under any tariff, as it has a higher LCOE than solar on land, resulting even less competitive given the low energy prices registered at solar radiation hours in Spain. As prices during solar production hours are low, solar production is used as a complement energy source to charge electric vehicles or batteries that will be discharged later when prices get considerably higher (see the January representative day shown Figure 69). The amount of storage installed for this case (3.29 MWh) is lower than in the Bandwidth and No Charges cases, but higher than in the Peak Power. The results, nonetheless, seem to be more impacted by the representative days selected, which contain wider price spreads than the rest of scenarios as shown in the January day in Figure 69.

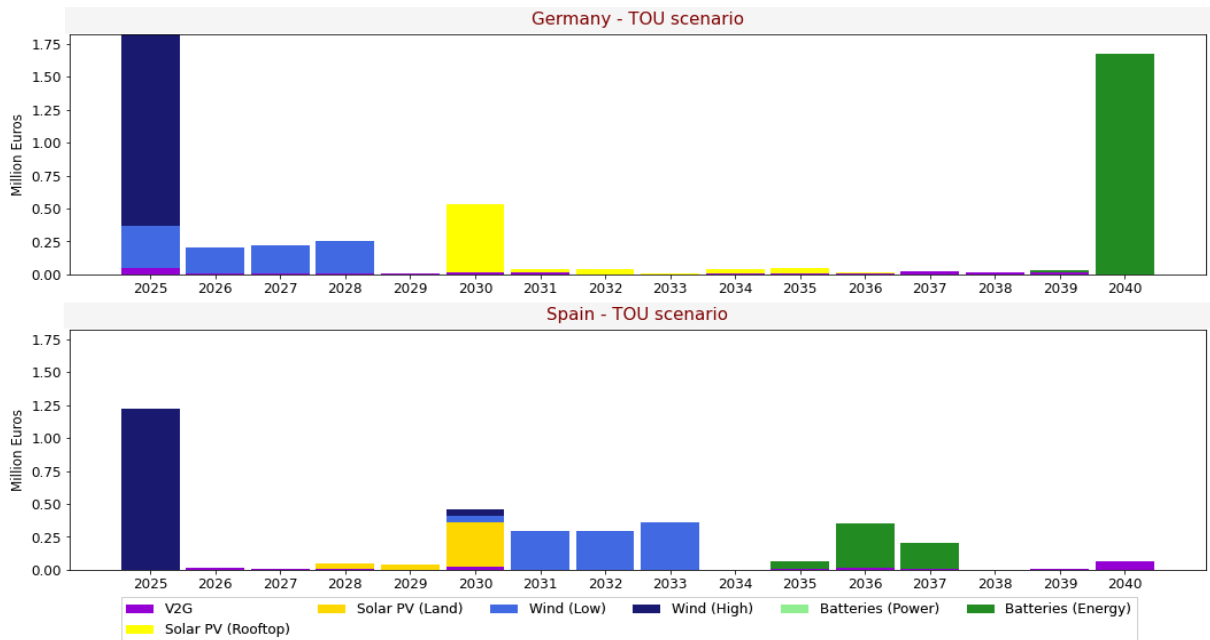
Figure 69. Electrical balance for the Virtual communities under a TOU tariff in selected representative days in January and August 2040 [Maximum Ω]



The selected representative days are January 2nd (Ω: 25) and August 25th (Ω: 22) for Germany and January 18th (Ω: 26) and August 4th (Ω: 17) for Spain. In all cases, the days with the highest weight (Ω) per month were selected.

Source: Own elaboration with results from MODECO's investment model

Figure 70. Annual investments performed in the Virtual community archetype under the TOU case



Source: Own elaboration with results from MODECO's investment model

7.2 Sensitivity tests

In the **TOU tariff scenario**, further tests were run using a **flat rate for the energy purchase price instead of the dynamic price**. The Use-of-Network tariffs are maintained the same as in the base case. For the **Industrial polygon** an additional scenario was analysed using a **fixed price** for the entire 16-year

period, **simulating a PPA/bilateral contract scenario**. As explained in Section 2.3.1, this price was set based on the costs from the generators considered in the power system model for each region.

Using a flat rate with narrower differences between high and low priced hours complicates finding the optimal solution for some cases. Although the model reaches a solution within the established maximum time (6 hours) for all scenarios, this is far from the optimal for some of the archetype-region combinations. As explained in Chapter 4, this is indicated by the gap value reported by the GAMS software. This situation was more often observed in the Spanish region, in which all archetypes except the Virtual community (gap: 6.2%) finalized the optimization process with gap values greater than 9.6%, even when extra restrictions were added¹⁴. For Germany, most of the archetypes managed to get a gap value below 6,0% but only after integrating the additional *positive value constraint*. The only exception was the Business archetype (gap: 37,0%), which was also the case with the highest gap for the Spanish region (gap: 51,0%).

For these reasons only the results for the Industrial polygon (gap: 1.25%), Rural town (gap: 5.7%), Urban district (1.9%) and Virtual community (gap: 0.5%) are discussed in this section, although one of them got gaps below the maximum threshold used for the base case scenarios (<0.1%). For these reasons, the sensitivity test results must be interpreted with caution considering that the proposed investment path is not as close to the optimal solution as those shown in the previous section. A similar situation was encountered for the Industrial polygon when using the 16-year fixed price (TOU_PPA). When the extra *positive value constraint*, the case in Germany managed to reach a gap value of 5,0% but the Spanish community only decrease up to 14%, which is why the Spanish archetypes results are not discussed.

7.2.1 Sensitivity to different price rates

As part of the sensitivity tests run in this study, a **flat rate price** was tested for the German community archetypes under a TOU tariff. The results obtained for the German archetypes with gap values below 6% are shown in Figure 71. As expected, the **resulting investments in energy storage were significantly reduced** as price spreads narrowed down significantly when a mean annual price is used as the base electricity costs. For 2040, when high selling prices are present, the mean average also rises (see Figure 53 in Section 6.2), making it costlier to charge batteries with grid energy and decreasing potential revenues from energy arbitrage activities. For the archetypes with large energy demands (Industrial polygon and Virtual community), using a flat rate resulted in zero storage investments, as local energy production can be mostly consumed directly.

Notably, changing to a flat rate also results in the installation of power-based storage in the Virtual community, a type of investment previously identified only under Peak power scenarios, but the invested sum is barely noticeable as the installed capacity is minimum. The largest reduction in volume storage when using a flat rate are observed in the Industrial polygon in which zero storage capacity is installed. This is followed by the Virtual community (-98%) and Rural town (-96%) archetypes. The least reduction for the flat rate cases is observed in the Urban district (-72%).

For the Industrial polygon, using the 16-year fixed price (**TOU_PPA**) results in 11% reduction in the storage capacity installed compared to the dynamic price case. As could be seen in Figure 53 (Section 6.3), the fixed prices used in 2025 in the TOU_PPA case result in energy tariffs with peak prices slightly above those of the dynamic price scenario (TOU). However, in future years, dynamic prices increase at peak hours and decrease at valley times. These price differences result in batteries being installed in 2033 and 2034 in the dynamic case, while in the PPA scenario, investments are done until the end of the evaluation period (2038 and 2040) when energy-based batteries' costs are low enough to offer some profit. In the flat rate scenario, no investments in batteries are reported despite offering higher prices and a similar trend to the PPA case. It is therefore assumed that the storage investment reported for the PPA scenario might be overestimated given the larger gap value obtained for this scenario.

Investments in CHP are also reduced (around 60% reduction) particularly in those archetypes in which unrequired additional CHP was installed by the end of the period to allow further battery installations (Rural town and Urban district). In the Industrial polygon, CHP installed capacity remains the same for all TOU cases despite the energy price structure. As explained in Section 7.2, the CHP installed in the German polygon under

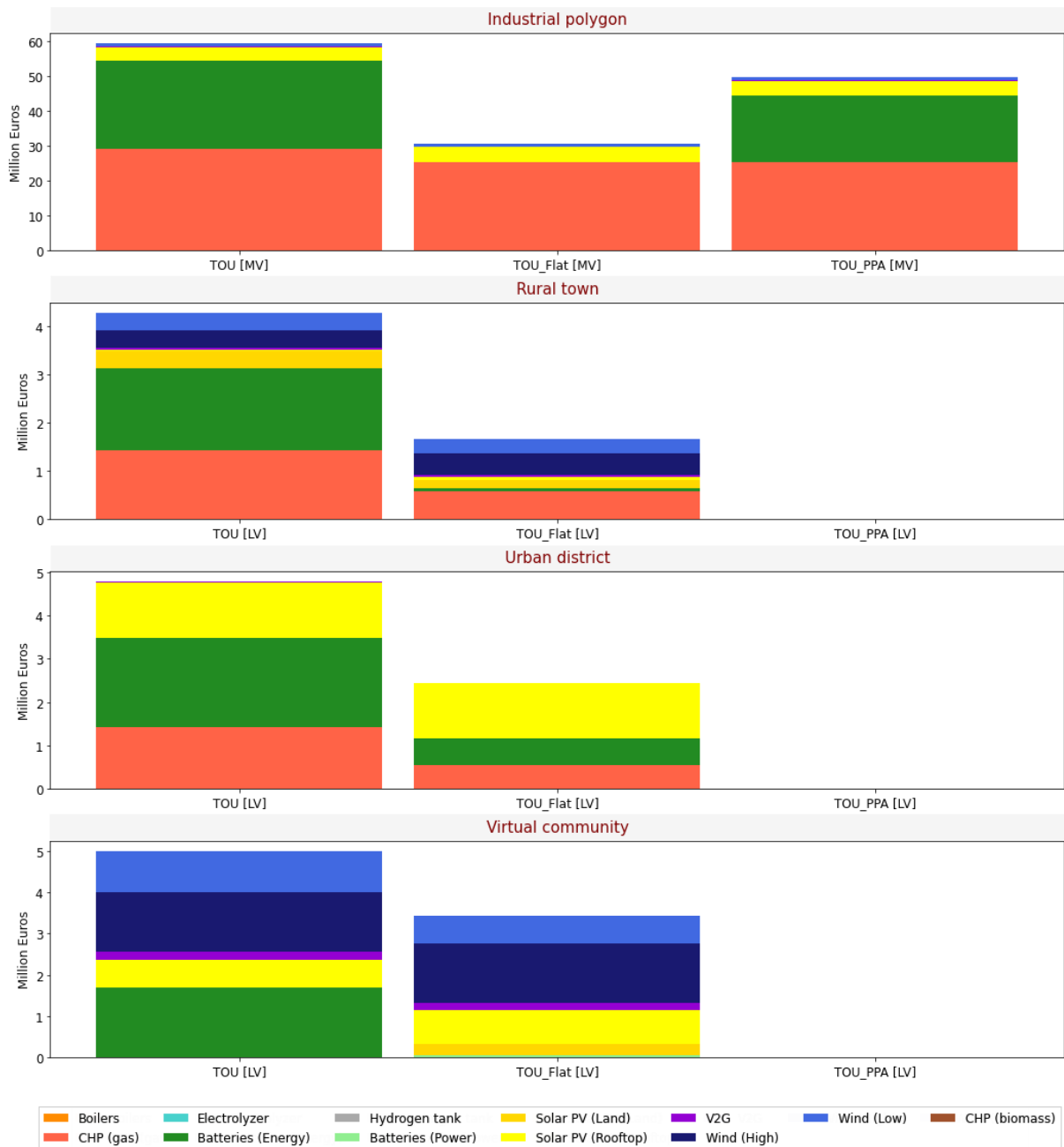
¹⁴ As explained in Section 4.2, those cases that using the standard configuration reached gap values above the desired target (0.1%) were repeated adding a new constraint that limited the objective function to positive values: *positive value constraint*.

these conditions is sized to its thermal demand. It must be noted that CHP investments are not considered an option for the Virtual community archetype.

Regarding the amount of PV solar installed, no changes among tariff scenarios are observed in the Industrial polygon and Urban district. Similarly, in the Industrial polygon, wind investments are maintained equal. In the Rural town, however, ground mounted PV solar capacity (0.3 MWe) is reduced in comparison to the base case (0.6 MWe) as well as low-capacity turbines, which are also decreased but to a lower extent (from 0.29 MWe to 0.25 MWe). On the contrary, high-capacity turbines capacity increased to 0.43 MWe from the 0.36 MWe reported in the dynamic price case. PV solar rooftop, which does not compete over land space, increases in this and the Virtual community archetypes. As new representative days were selected for this scenario, the results are also affected by the behaviour of the energy selling prices, which remain linked to the dynamic prices. Although these were already low on the base case, it gets even lower for the representative days selected for the flat rate scenario, which discourages selling energy, particularly at solar radiation hours. Moreover, the reduced storage investments shifting excess energy to hours with higher prices as done in the dynamic price case, in which high price peaks were profited.

In the Virtual community, the capacity of PV solar on land is increased from zero to 0.5 MWe, while low-capacity wind turbines' capacity is reduced considerably (from 0.81 MWe to 0.55 MWe). High-capacity wind units are just slightly increased (+1%). Overall, the flat price resulted in larger renewable capacity being installed in the Virtual community and lower in the Rural town. For this particular archetype the flat rate means that solar is able to obtain higher benefits during radiation hours as tariffs are in average larger in this timeframe, but it also means paying larger Use-of-Network tariff than in the dynamic case. The extra benefits, however outweighs the burdens. Wind power, on the contrary, loses some of the evening peak prices registered in Germany at evening and night under the TOU with dynamic prices, obtaining in average lower benefits, which are not compensated by the decreased Use-of-Network payments.

Figure 71. Investments performed in German archetypes under a TOU tariff with dynamic, flat and PPA prices



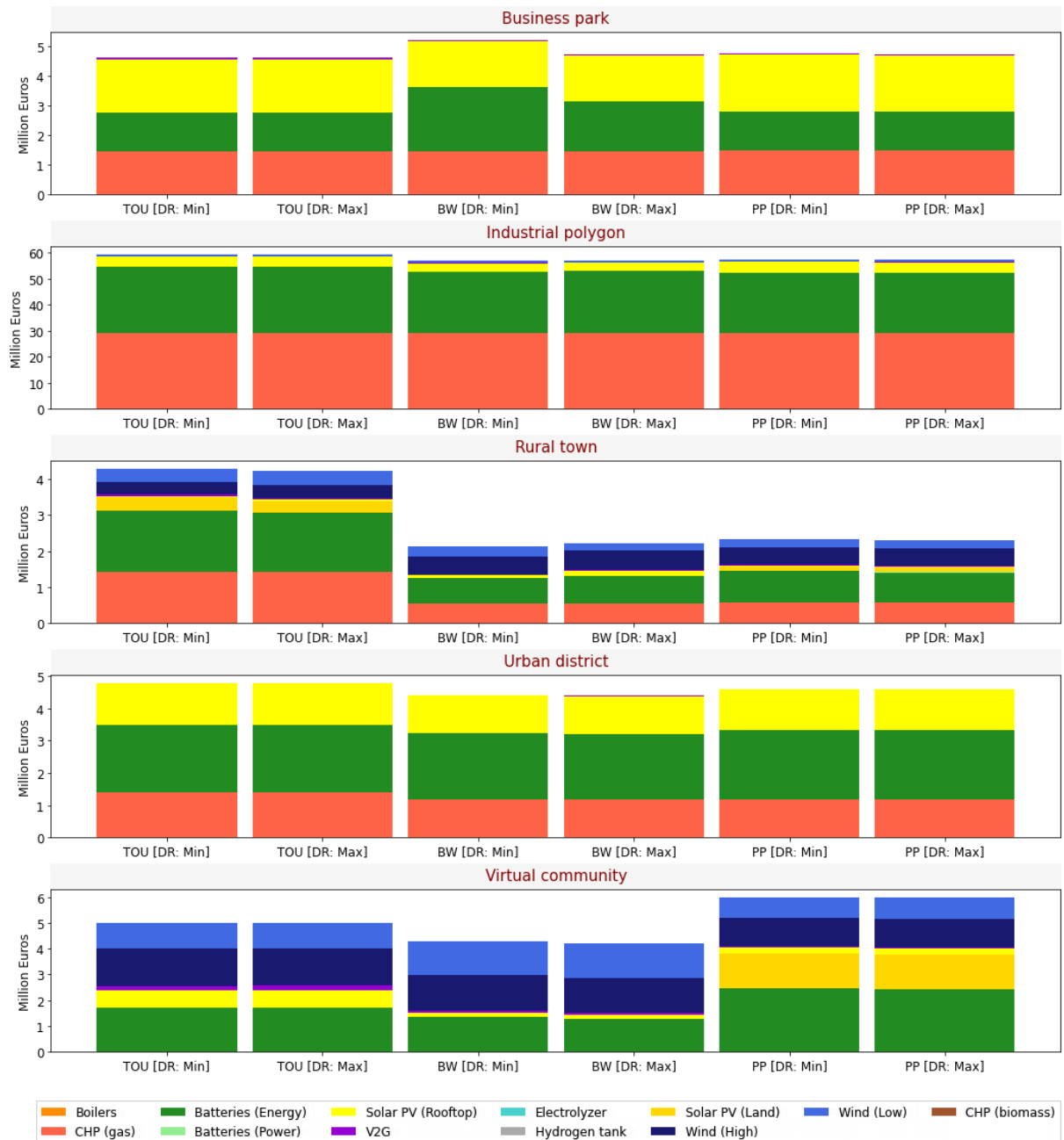
Results for the PPA energy price are deliberately omitted for the Rural town, Urban district and Virtual Community archetypes as this scenario is only considered for the Industrial polygon.

Source: Own elaboration from the UCED's model first executions

7.2.2 Sensitivity to different discount rates

The tariff base cases – TOU, Bandwidth and Peak Power – were repeated using the maximum discount rate for Germany (2.5%) instead of the minimum (1.3%) listed in Table 2. For most scenarios, using the higher discount rate results in lower sums being invested in energy assets, which is expected as future money revenues are reduced when considering the present value of future cash flows. In most cases, however, the differences between using the minimum and maximum discount rate are below 1%. As observed in Figure 72, the case in which the difference between discount rates is more visible is the Business park under the Bandwidth tariff. Using the 1.3% discount rate results in 9.6% more money invested in energy assets than when considering the 2.5% rate. In this case, the largest increment is observed in the investments done in energy-based storage.

Figure 72. Investments performed in German archetypes under the base tariff scenarios considering different discount rates



The minimum discount rate considered is 1.3%, and the maximum 2.5%.

Source: Own elaboration with results from MODECO's investment model

As shown in Figure 49, during the representative days in the summer season, batteries are mostly charged using excess solar production for the German Business park under a Bandwidth model. For both discount rate scenarios, the solar installed capacity is maintained the same (the maximum permissible given the available rooftop area). Given that storage investments are done towards the end of the evaluation period; these investments are more sensible to decrements in the value of future expected revenues. The exceptional scenarios in which the total sum invested is higher when considering the 2.5% discount rate, are the Industrial polygon and Rural town under a Bandwidth model, and the Virtual community under a TOU tariff. In the Virtual community and Industrial polygon cases, the differences obtained for the different discount rates are quite low (< 0.5%). In the Rural town, however, the investments done when using the 2.5% rate are 3.3% higher than with the lower rate. Contrary to the Business park, the Rural town under a Bandwidth model results in much higher investments in energy storage when using the maximum discount rate. Although these

investments are also done towards the end of the evaluation period, they are affected differently given that the investments in variable renewable energy assets (solar, wind) also increment in this case, which was not the case in the Business park archetype.

8 Operational model results

The operational model follows a similar formulation to the investment model, but allowing for further details in some assets and the possibility to optimize the entire year (8760 time steps) instead of selecting representative days. This is possible as the installed capacities are known and each year is optimized individually, which reduces the number of variables and computational time (see Chapter 4). From the case studies discussed in Chapter 7, the optimal operation of the assets installed by the German and Spanish archetypes under the TOU, Bandwidth and Peak power tariffs is analysed for each target year (2025, 2030, 2040), looking at the key indicators evolution following the installation of the energy assets dictated by the investment model. As shown in Figure 14, those key indicators are: the volume of energy dispatched per type of technology and its associated CO₂ emissions, the percentage of demand covered by self-consumption, the amount of energy purchased from the grid, energy costs disaggregated by payment concept, and the revenues associated to energy sales.

8.1 Local generation mix

The annual demand and generation per type of technology is presented in (Figure 80) for German archetypes and (Figure 81) for the Spanish. The technological categories have been narrowed down to: Solar PV, Wind turbines, and Gas-fuelled CHP. Biomass CHP is not included as it is not installed in any region. The annual electricity purchased is also shown as its volume gives hints about the level of energy arbitrage performed in certain scenarios.

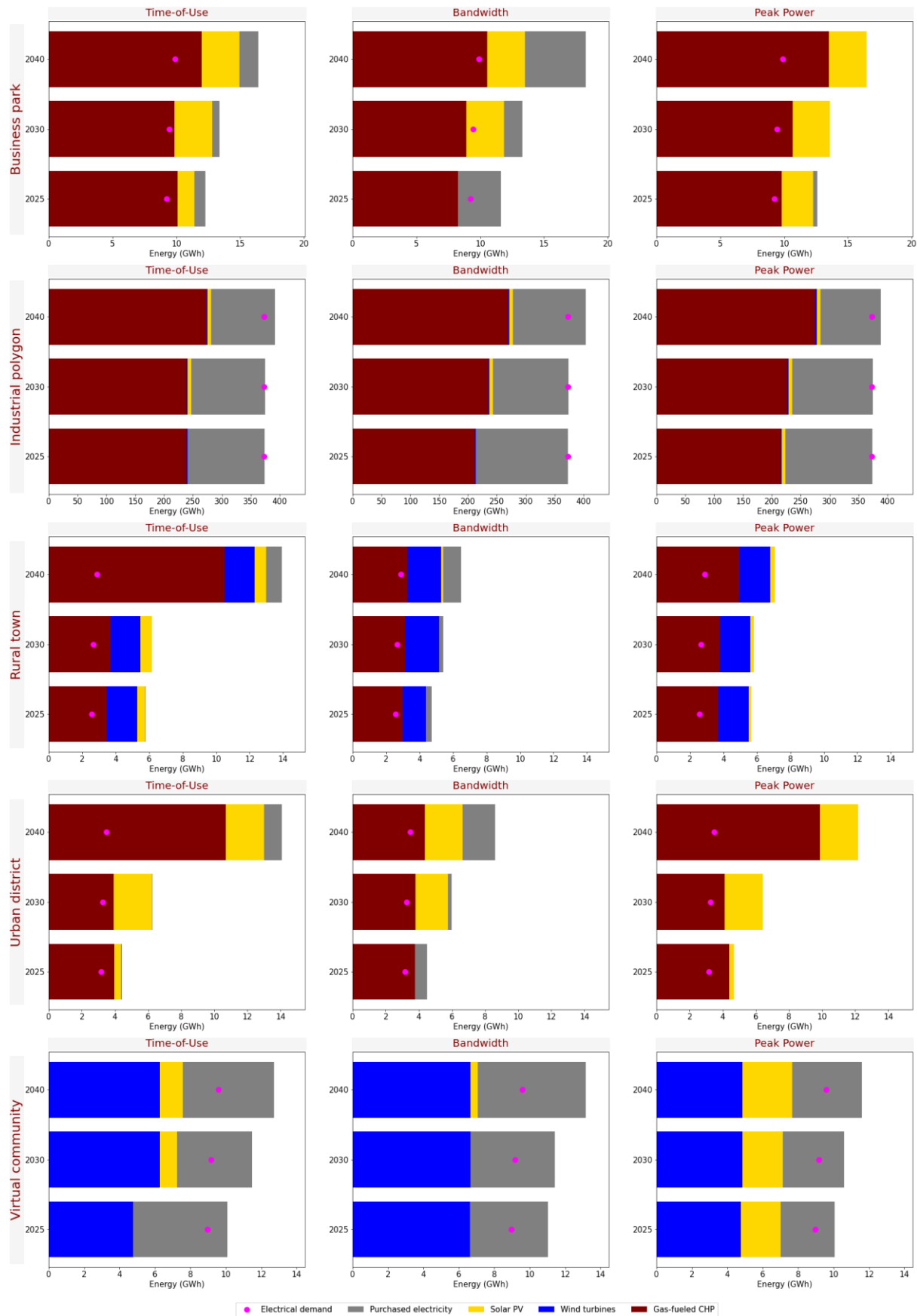
In **Germany**, it is observed that **local generation** (wind, solar, CHP) **surpasses demand in most archetypes**, except for the Industrial polygon (where baseload demand is particularly high) and the Virtual Community (in which Use-of-Network charges are also applied to self-consumption). This indicates that a fraction of the energy generated by the community in these cases (Business park, Rural town, Urban district) is being sold back to the grid at some point. In all German scenarios, the amount of local energy generated grows in 2040, when marginal prices are considerably higher (Figure 45). The highest local generation increases in 2040 are observed in the Rural town and Urban district archetypes under a TOU tariff and in the Urban district when a Peak power is considered. In all cases, the major increase is due to a more intensive CHP usage.

In the German Business park, Rural town and Urban district archetypes, it is observed that the **power production from CHP is equal or larger than the communities' electrical demand** (with the exception of the Business park 2025 under a Bandwidth tariff). However, as shown in Figure 73, **boilers are required in all of scenarios to cover the thermal demand of the German communities**, even in those cases in which CHP power generation increases considerably in 2040. The Industrial polygon is the only German archetype in which practically all thermal demand (low and medium heat) is supplied by CHP in 2040, while in previous years it already covers a large percentage of it (> 93% in all tariffs). For this case, producing all heat through CHP does not translate into higher electricity exports as it is consumed locally given the polygon's large electrical demand.

In the case of **Spain**, which has a lower thermal demand and lower marginal prices, the **local power generation only surpasses electrical demand** in 2025 and 2030 **in specific cases**, which indicates that lower surplus electricity is sold than in Germany in these years. **In 2040**, nonetheless, a **similar trend to the German archetypes** is observed, with local generation being higher than demand in all archetypes and tariffs except the Industrial polygon and Virtual community; and with the largest increase from 2030 to 2040 in the Rural town and Urban district under TOU tariffs and the Urban district under Peak power, being the result of a higher CHP usage. In this region, **boilers play a more significant role** in covering the community's thermal demand. In fact, the only case in which CHP covers all thermal requirements is the Industrial polygon in 2040 under a TOU tariff.

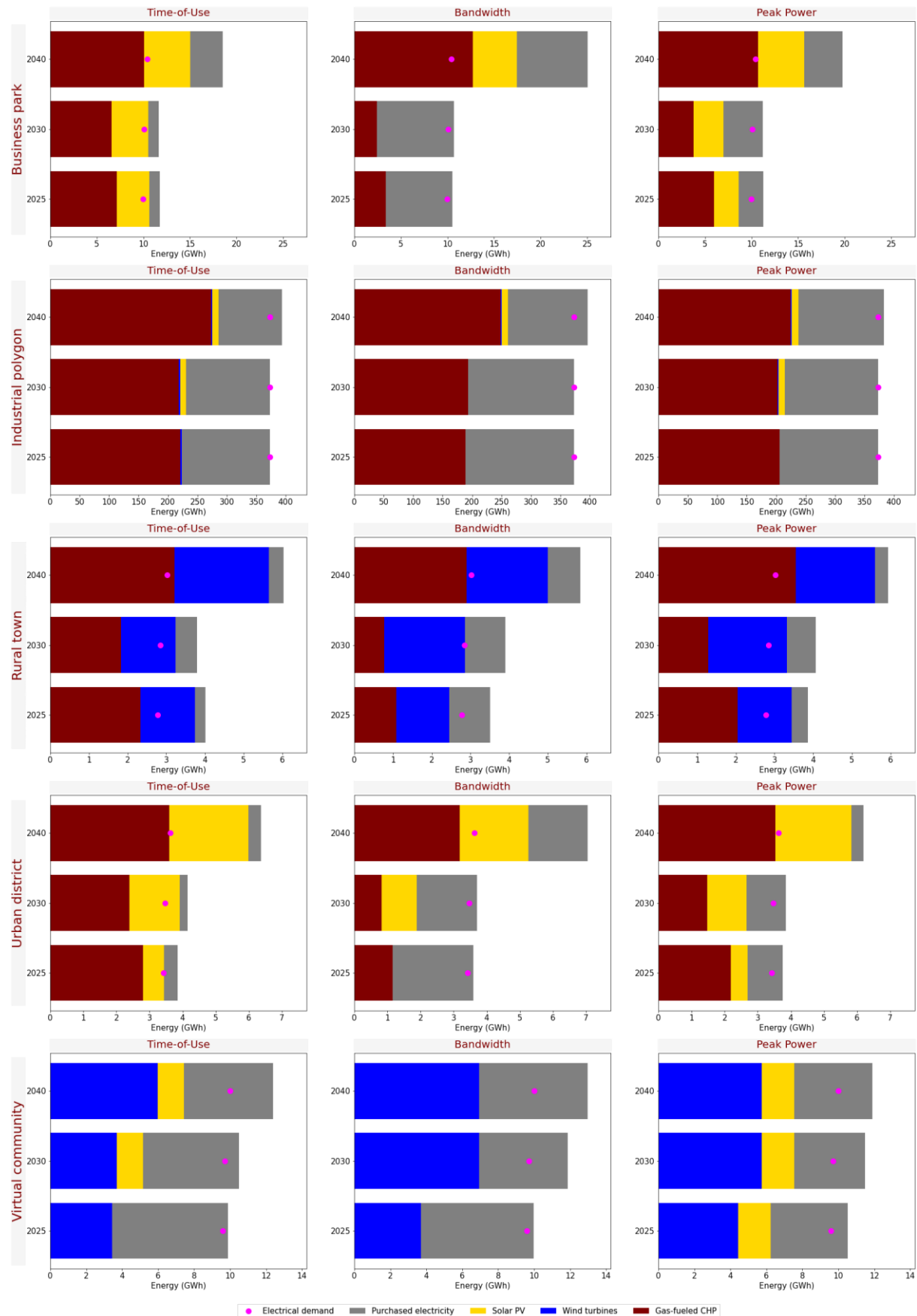
The effect of the tariff structure on the final generation mix is similar for both regions. **The use of a TOU tariff structure reflects in higher local production**, particularly in 2040. This is more evident in those scenarios in which representative days with pronounced peak prices were selected (Urban district and Rural town). The only exceptions are the Industrial polygon, in which the tariff structure seems to have a subtler effect on the community's generation mix, and the Virtual community, where chargers are also applied to self-consumption. **This tariff also reflects on a lower boiler usage**, particularly in 2040. This is especially visible in the Spanish cases as in the German, the Peak power scenarios results in similar shares regarding CHP and boiler usage.

Figure 73. Annual demand, purchased electricity and local generation per type of technology in German cases



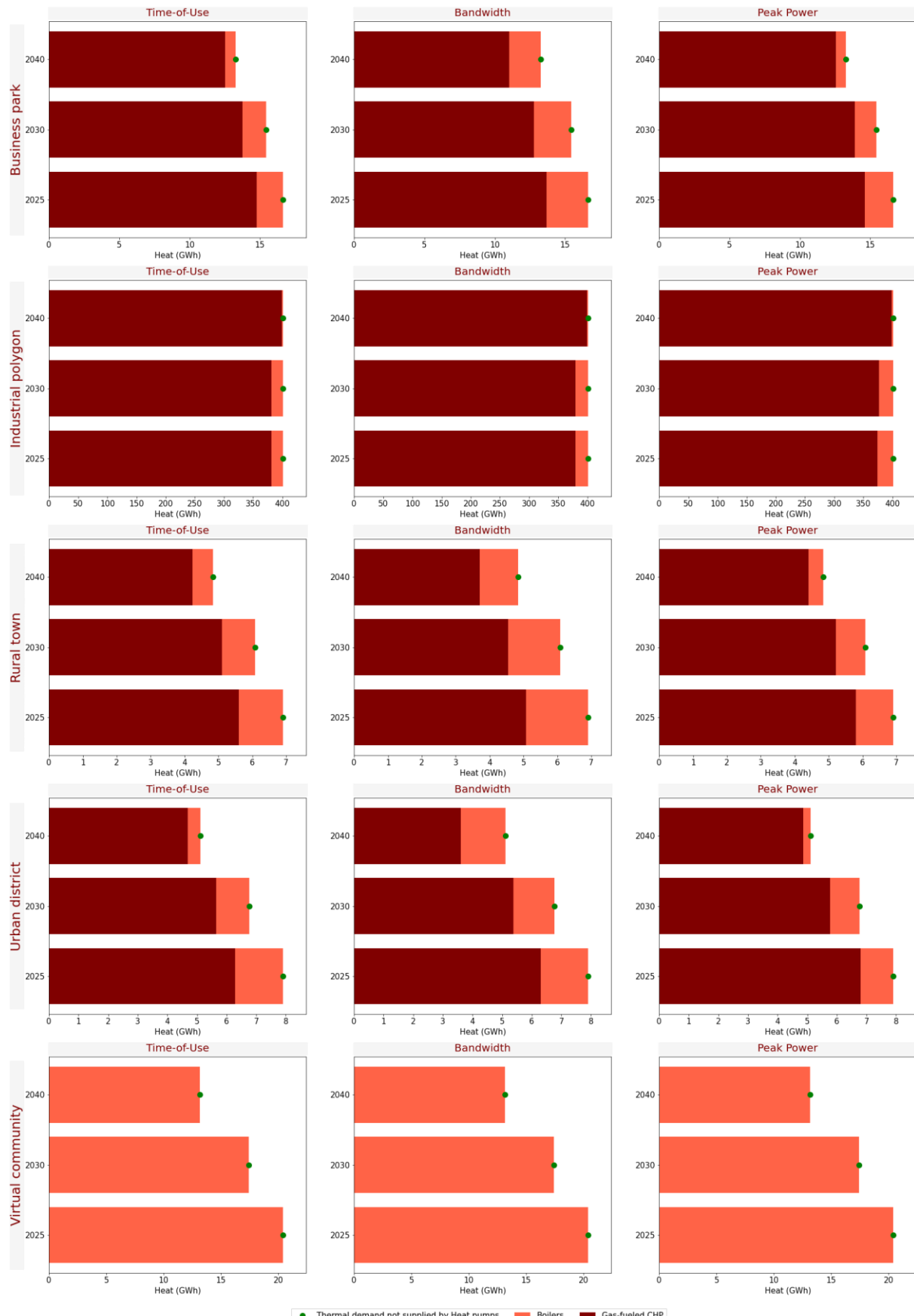
Source: Own elaboration with results from MODECO's operational model

Figure 74. Annual demand, purchased electricity and local generation per type of technology in Spanish cases



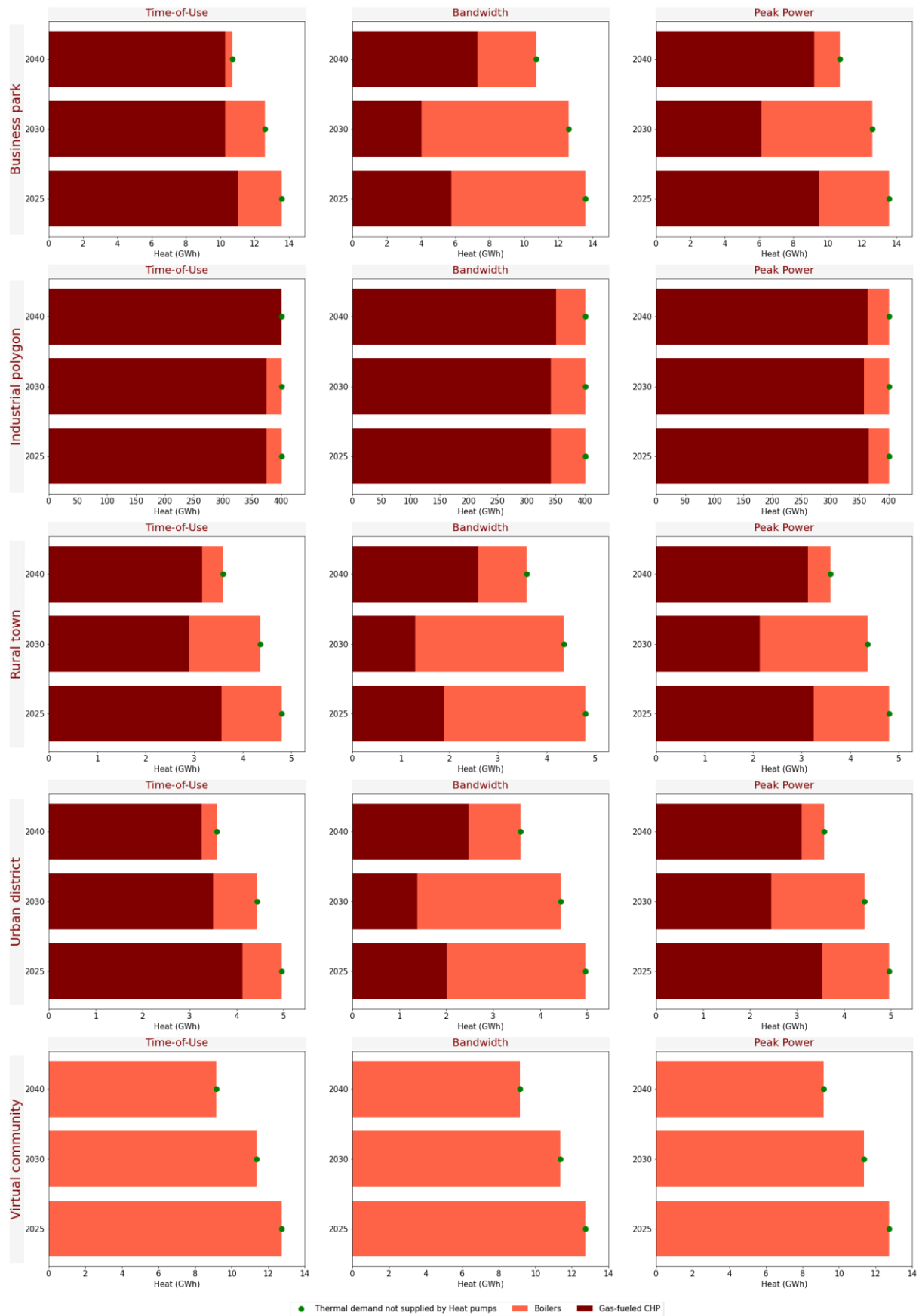
Source: Own elaboration with results from MODECO's operational model

Figure 75. Annual thermal demand and heat generation per type of technology in German cases.



Source: Own elaboration with results from MODECO's operational model

Figure 76. Annual thermal demand and heat generation per type of technology in Spanish archetypes.



Source: Own elaboration with results from MODECO's operational model

The **Bandwidth scenario**, on the contrary, tends to **result in lower local generation and disincentives the usage of solar PV technologies** compared to the other tariffs, especially in the Spanish region. Even in those scenarios in which representative days with high electricity prices are chosen for 2040, resulting in high electricity surpluses being generated, the results for the Bandwidth model show a slight increase when compared to 2030 values. In some cases, however, the **Bandwidth model results in larger electricity purchases**, even beyond the community's need. In Spain, the Bandwidth model also reflects in a significant increase in boiler usage in 2030 as CHP power production is lower even when similar capacities have been installed.

The usage of a **Peak power** tariff results in **larger solar investments**, particularly in the German cases. As explained before, wind power matches better with peak demands in the Spanish archetypes, which makes solar PV usage less attractive for peak shaving purposes under this tariff. In the **archetypes with low and medium demand** (Business park, Rural town, Urban district), this tariff **leads to a significant decrease in the amount of electricity purchased** from the grid, being practically zero in the German region. The share of heat supplied by CHP and boilers is similar to TOU in the German archetypes while in Spain it leads to a lower boiler usage than in the Bandwidth but higher than in the TOU scenarios.

The Industrial polygon is the archetype with the largest heat and electrical demand, and the only in which self-generation does not surpasses consumption at any case (Figure 73 and Figure 74), requiring external sourced electricity to cover the community's demand during the entire evaluated period. Contrary to the other archetypes in which CHP production to supply heat demand translates in electricity surpluses, in the Industrial polygon, the CHP power generation (for low and medium heat) only covers a share of the total electrical demand even when the maximum possible capacity is installed.

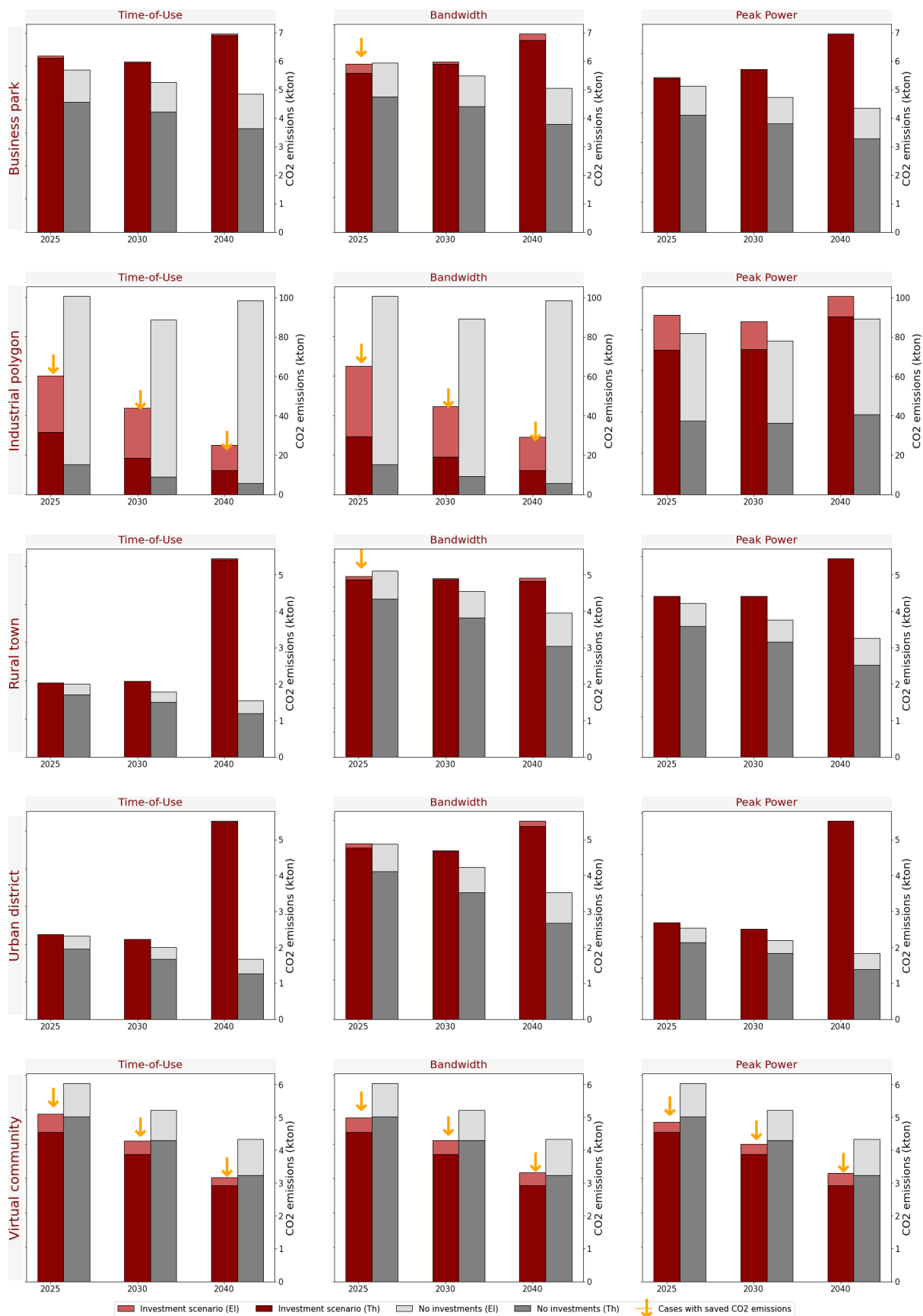
8.1.1 Emitted and avoided CO₂ emissions

The total community emissions after the installation of the selected energy assessment is shown in Figure 81 and Figure 82. Similarly, the baseline emissions from the alternative case (only boilers and grid purchases) are shown with the purpose to identify those scenarios in which the installed energy assets result in lower CO₂ emissions (marked with an orange arrow). As noted in the following figures, **a larger number of cases in which CO₂ emissions are offset through the installation of local power and heat generation assets are reported in Spain than in Germany**. The latter as the **main source of emissions at the community's level are the boilers and CHP units**, whose size and usage is strongly related to the communities' thermal demand, which is considerably higher in Germany than Spain. The second source of emissions is grid electricity, which has a different emissions factor (tonCO₂/MWh) depending on the available generation technologies at each hour, and is significantly higher for Germany than for Spain (see Chapter 6).

Within the evaluated scenarios, the **Bandwidth tariff seems to favoured CO₂ emissions reduction, especially in earlier years** as all archetypes report some savings in 2025 and 2030 – and some even in 2040 – under this tariff in the Spanish region, as well as most of the German archetypes (the only exception is the Urban district that does not report emissions reductions in Germany at any of the evaluated years). As previously discussed, this model results in lower local generation than other tariffs as the model tends to avoid incurring in penalizations for excess electricity injections and, below that limit, self-generation presents less opportunities per cost reduction due to the existence of a fixed charge. Thus, the amount of local energy and heat generated by the communities in this scenario tends to be slightly below that of the Peak Power or TOU cases; such differences are more noticeable in Spain (see for instance the heat volume produced by boilers under this tariff and region in Figure 76).

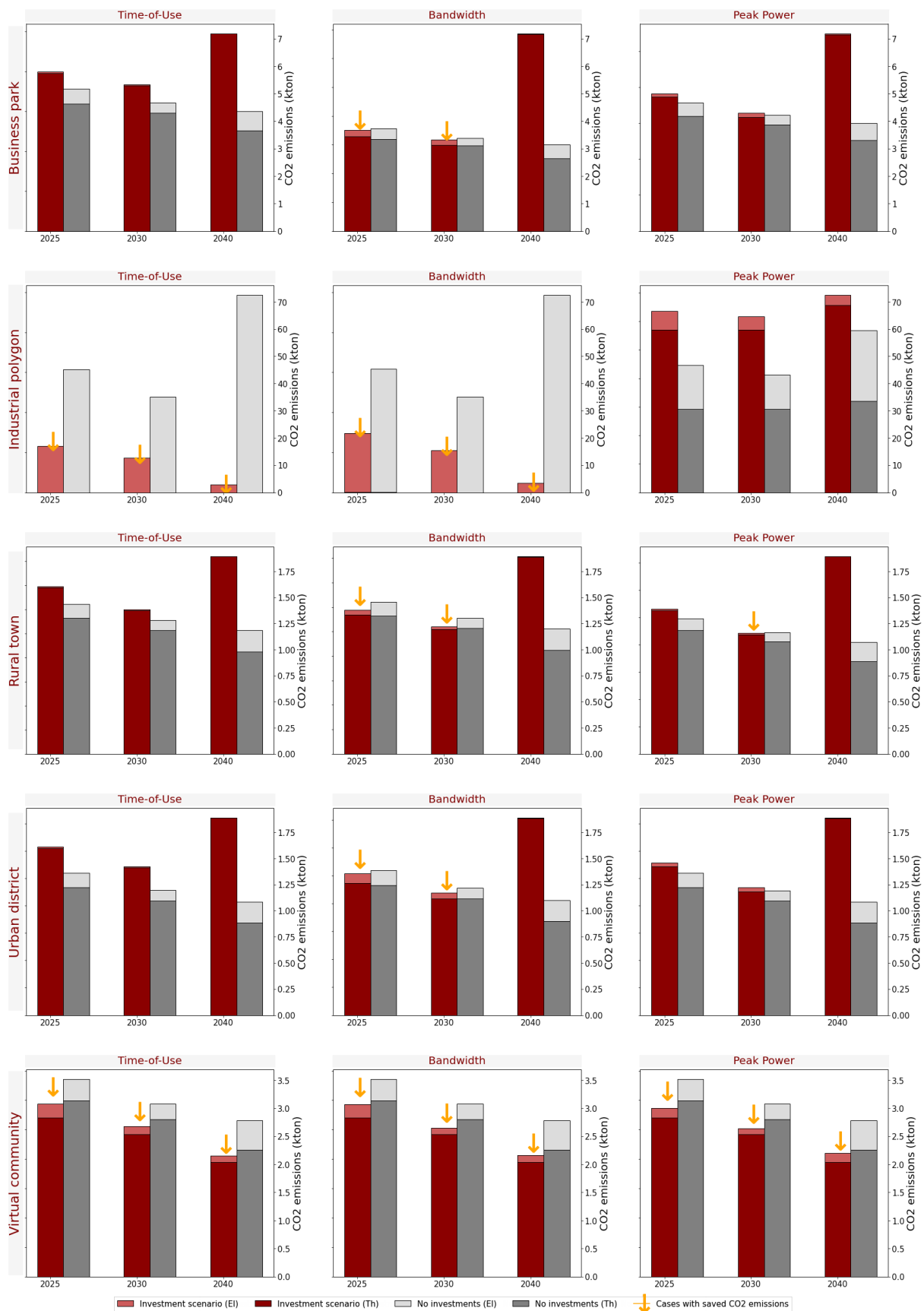
The Peak power and TOU tariff results varies from a case-to-case basis. In the TOU tariff a pair of cases result surprising due to the considerable increment in the community's CO₂ emissions in 2040: The German Urban district and Rural town. As observed in Figure 73, these are related to a high increase in CHP power production, which is used for meeting the community's demand and charge batteries to sold or consume energy at later times when prices are higher. In Spain, less differences are observed between the TOU scenario and the other tariff cases.

Figure 77. CO2 emissions from the operation of installed assets versus base case in the German archetypes



Source: Own elaboration with results from MODECO's operational model

Figure 78. CO2 emissions from the operation of installed assets versus base case in the Spanish archetypes



Source: Own elaboration with results from MODECO's operational model

As explained, CHP power production increases considerably in 2040 in the German Rural town and Urban district archetypes under a TOU tariff. However, the CHP's thermal production decreases for these archetypes in these same years. Within MODECO, it is assumed that CHP units can shift their production modes to prioritised electrical instead of heat production as happens in real operation. These functional modes are represented in the optimization model through the polygon area described in Section 4.3.3 while the assumed values can be consulted in Annex 3. However, the results obtained for these cases indicate that some adjustments might be needed for the assumed values delimiting the polygon or in the selection of a polygonal shape that better represents the type of CHP units modelled in this project. Relevantly, this operational mode also increases CHP's carbon intensity as it only offsets grid power consumption, which is low carbon at many hours due to the power mix considered in the reference ESES (see Section 6.1) and do not displaces boiler usage.

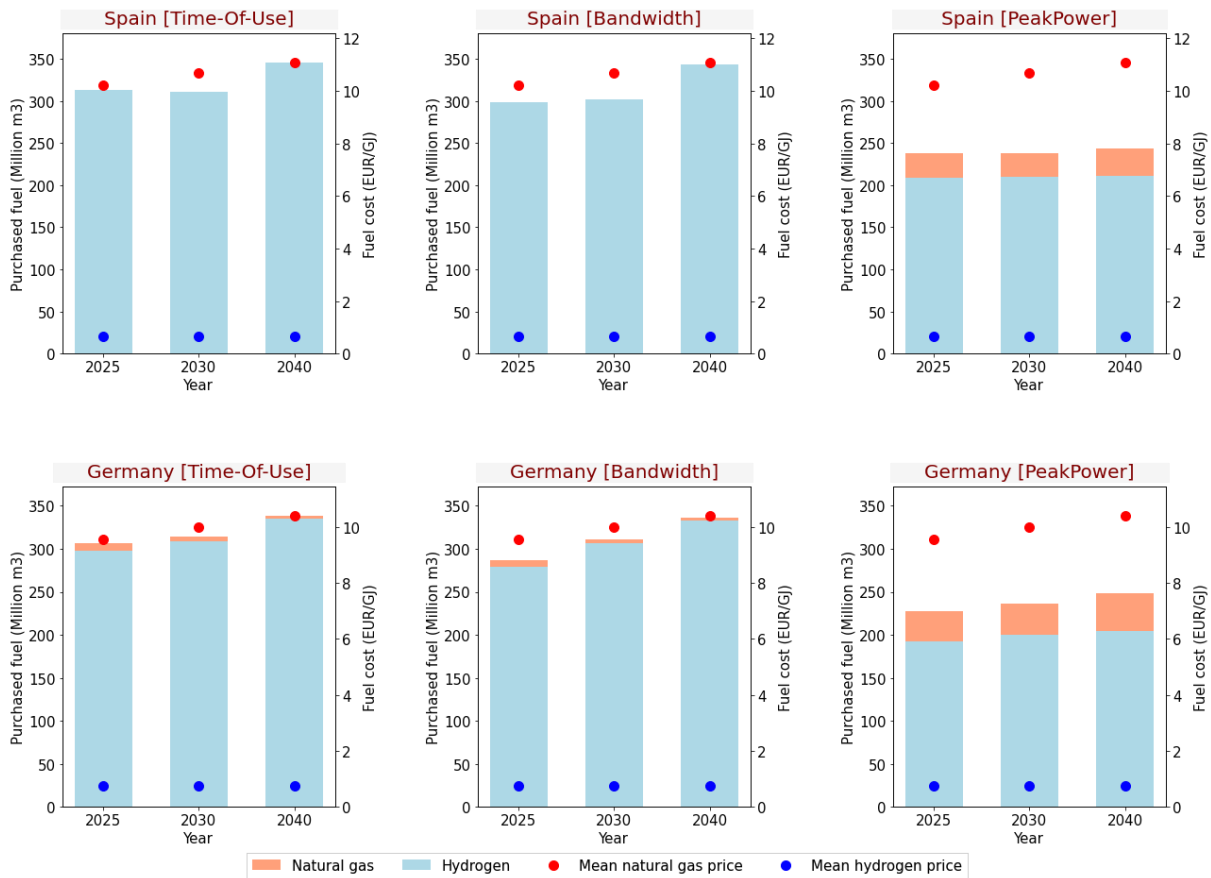
The **Virtual community** is the **only case that reports emissions savings across all years and tariff scenarios in both regions**. This, however, is expected as, under MODECO assumptions, the Virtual community can only invest in renewable or storage assets given the lack of physical proximity among its members, which complicates the installation of CHP units for shared heating systems. For this reason, **this archetype is the only in which a decreasing trend is observed for CO2 emissions from 2025 to 2040, as the electricity produced by the communities are mostly carbon free**. In the rest of archetypes, a slight increase is observed in the emissions registered from 2025 to 2030, but they tend to peak until 2040.

The **Industrial polygon** is the only in which externally sourced green hydrogen is considered as an available fuel. As **green hydrogen is assumed to have no carbon emissions associated to its combustion**, its usage in CHP and boilers reduces the carbon footprint of these assets. In the **TOU and Bandwidth scenarios**, the **investments done result in lower carbon emissions for the German and Spanish polygons**. This as thermal production is all or mostly cover through Hydrogen combustion and a significant share of the consumed electricity is locally generated with renewable energies, resulting in lower emissions than the grid alternative.

In the Peak power, nonetheless, an increase in emissions is reported. As seen in the graphics showing the community's heat and electricity generation per technology (Figure 73 and Figure 75 for Germany, and Figure 74 and Figure 76 for Spain), there are no major differences between the volume of heat or electricity generated by the CHP or purchase from the grid. However, the need to reduce peak demands – which result in significant capacity-based payments – forces the community to generate larger energy at different days and times than in the Bandwidth and TOU tariffs. In some of these days, Natural gas results to be cheaper than Hydrogen, resulting in a larger consumption of this fuel in this tariff (Figure 79). This happens in both Germany and Spain, as although the considered prices are different, the same daily trend is considered.

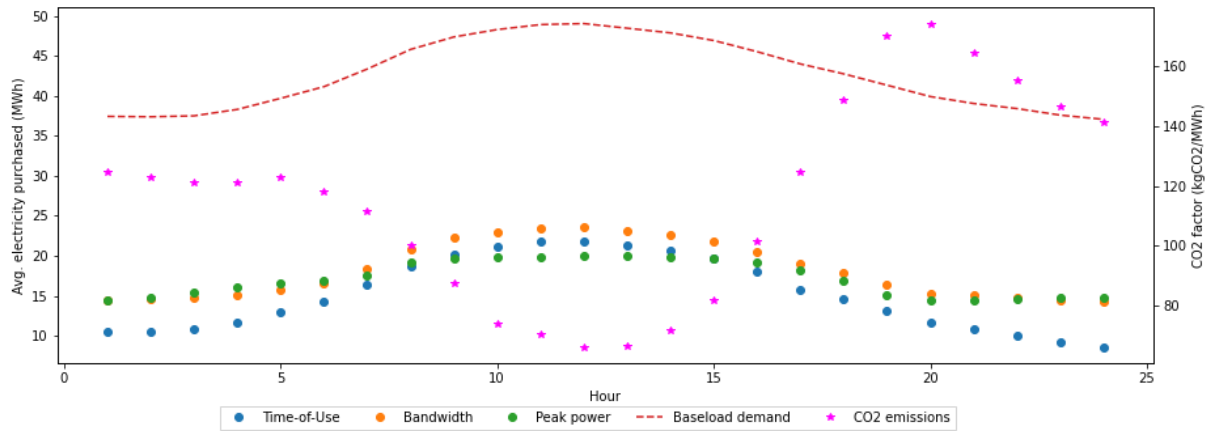
Moreover, when looking at the hourly electricity purchase trends (Figure 80), it is observed that the peak shaving hours, when the polygon reduces demand to avoid power-based costs, coincide with the hours with lower carbon emissions. While at night, when the polygon consumes more to make up for the reduction imposed around midday, it buys energy that has more associated emissions. This not the case for the other archetypes as its demand peaks tend to coincide with high emissions hours, which also tend to be the more expensive as they are produced by fossil-fuel generator, which are costlier than clean energies under MODECO future scenario assumptions.

Figure 79. Mean annual fuel cost and total fuel consumption in the Industrial polygon



Source: Own elaboration with results from MODECO's operational model

Figure 80. CO₂ emissions from the operation of installed assets versus base case in the German archetypes



Source: Own elaboration with results from MODECO's operational model

8.2 Economic benefits

The communities' annual electrical balance is presented in the following figures, considering the total amount of electricity purchased, generated (disaggregated by self-consumed and surplus electricity¹⁵), stored¹⁶ and

¹⁵ Electricity that is locally generated by the community and not used for self-consumption.

sold. The community's demand is also presented, as well as the economic benefits obtained from surplus electricity sales and avoided purchase costs due to self-consumption.

As already mentioned, the electrical balance for the German (Figure 81) and Spanish (Figure 82) archetypes show that the amount of electricity purchased tends to be lower in the Peak power scenario. Moreover, it results in zero purchased electricity for the German Business park, Rural town and Urban district, which cover their demand with local generation since 2025. In most of the evaluated scenarios, the Peak power tariff tend to result in similar economic benefits as those obtained for a Bandwidth model for the high-demand communities (Industrial polygon and Virtual community).

In both regions, the **Peak power scheme results in higher economic benefits when compared to the Bandwidth model, but lower than in the TOU cases, which in general results in the largest economic benefits**. For some cases those benefits are due to higher costs avoided while in others they are the result of higher surplus electricity sales, or both. As explained the Bandwidth model seems to lead to larger electricity purchases, although in the German region the differences are narrower than in Spain. Particularly in the latter, the Rural town and Urban district show larger electricity purchases when considering the Bandwidth tariff rather than the Peak Power or TOU,

In Germany, it is also observed that the **Peak power tariff leads to lower storage usage**, particularly as no grid battery charging is carried out. In Spain, the used tariff does not seem to have a strong impact on storage usage. Furthermore, **in both regions, energy storage tends to be utilized at the end of the evaluation period regardless of the tariff** scenario, as there is a more pronounced difference between valley and peak-priced hours.

In most of the scenarios, **the major economic benefit for the communities is the electricity costs avoided through self-consumption**. In fact, electricity sales revenues are irrelevant in 2025, and low in 2030, and just get significant up to 2040. Moreover, the exceptional cases in which electricity sales are the main economic benefit take place only in 2040 – when the annual mean marginal price rises and difference between seasonal and hourly prices widens (see Chapter 6) – in low and medium demand archetypes. The latter also happens with more frequency in Bandwidth and Peak power scenarios. Only the German Rural town and Urban district present larger benefits associated to electricity sales than costs avoided under a TOU scheme, which is explained by the high electricity costs from the representative days selected for these cases.

8.2.1 Avoided energy costs

As seen in the previous chapter, the major economic benefit to the communities is avoiding electricity costs through self-consumption; the values reported for each case are shown in Figure 83 and Figure 84. In **Spain**, the **major avoided costs are registered in the TOU scenario**, being Use-of-Network **charges the most significant costs** for 2025 and 2030. In **2040, the price of energy becomes the largest cost avoided** through the investments made by the Spanish communities. In the Peak power tariff, a similar trend is observed for this region, although the total costs avoided are always lower than in the TOU case.

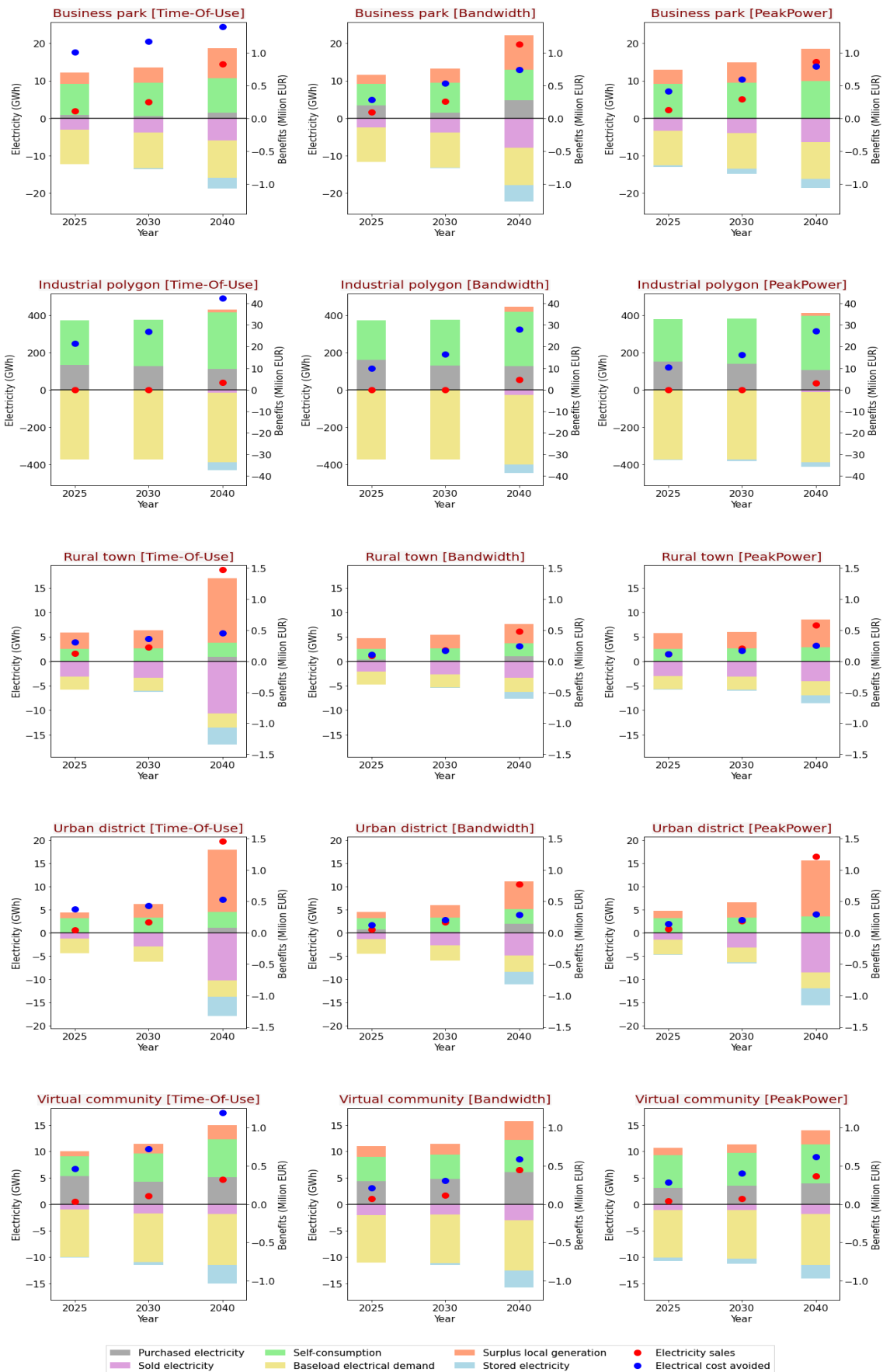
The Bandwidth tariff represents the lowest costs avoided as no Use-of-Charges costs are saved through electricity self-generation and storage. Still, this scenario is not the exception, and in 2040 it results in large economic savings due to the high energy prices avoided through self-consumption. It is important to highlight that the **current investment model does not include the contracted bandwidth value as a variable** which could be an **interesting feature to add** in a future version. Nonetheless, within this tariff, communities can reduce charges costs by avoiding penalizations for exceeding the amount of energy injected or withdraw from the grid.

In Germany, the tariff scenario that **represents the largest savings** is the **Peak power**. In general Use-of-Network charges are higher in Germany than in Spain for all scenarios. It seems, however, that the regional difference between the network costs places on the power-based charge applied in the Peak power case is more significant than the higher peak and off-peak charges applied in the TOU case. In the Bandwidth model, nonetheless, the same trend as in Spain are observed, no Use-of-Network charges are avoided by the installation of the selected energy assets, still the avoided energy prices represent significant economic benefits to the German archetypes in 2040.

¹⁶ Refers to the amount of energy that is stored at the community's energy assets (batteries or EV) at the close of the annual balance. This energy could come from surplus generation or purchased electricity.

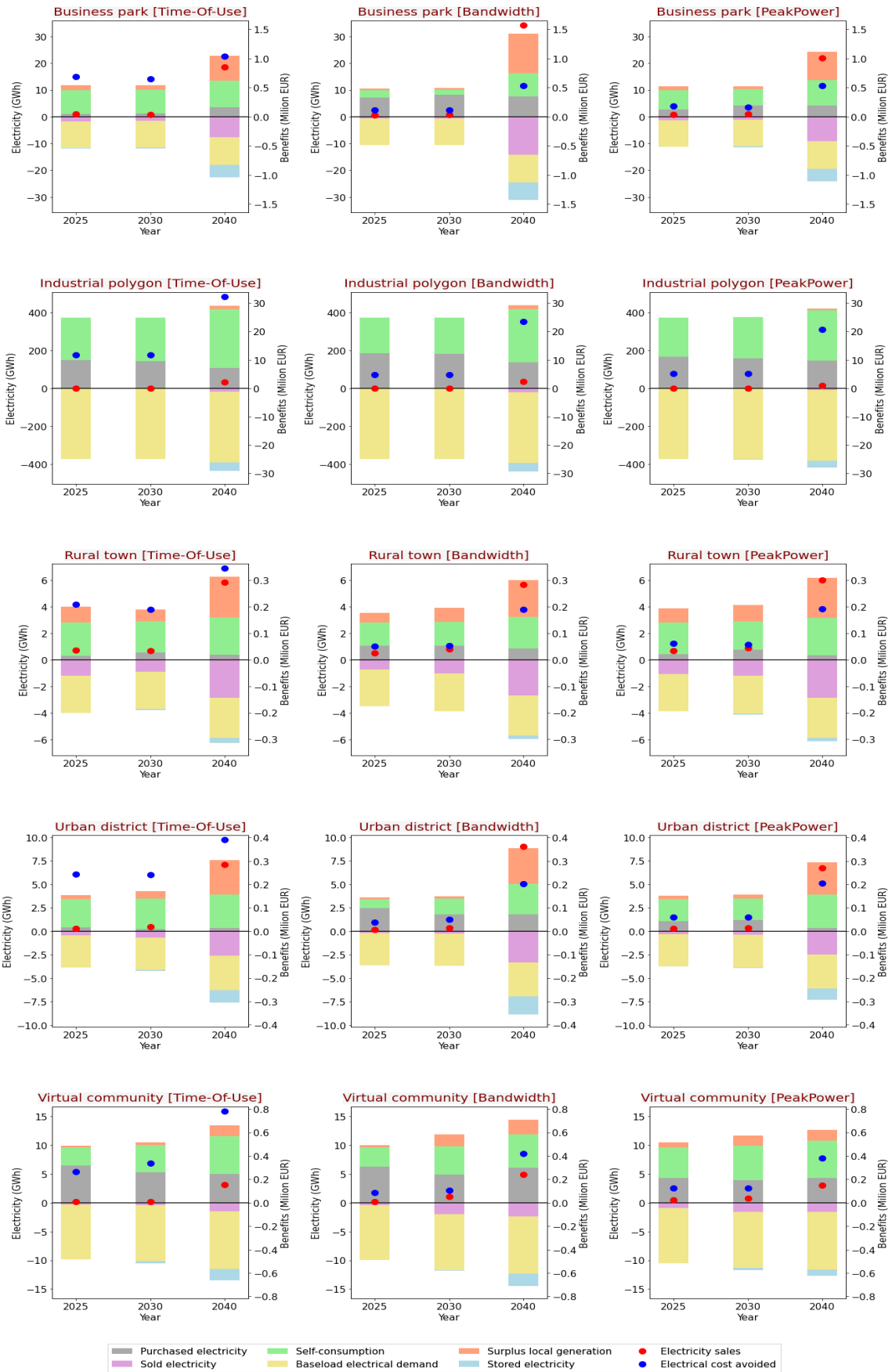
Contrary to Use-of-Network charges, taxes represent the lowest cost share in all tariffs and regions, but are particularly small in the Spanish cases. As explained in Section 2.3.3, Spain uses an *ad valorem* tax, assumed as **5.11%** of the brut energy costs based on the electricity tax currently applied in the country. Nonetheless, **the used percentage probably results in an underestimation of taxes impact on energy costs in Spain**, as in reality the country also applies taxes on contracted and used power. Thus, to better reflect the fiscal burden on electricity consumption, using a higher percentage might be recommendable to account for those network costs that are recover through power consumption taxes and are not part of the 5.11% tax.

Figure 81. Annual electrical balance, energy sales income and electrical cost avoided in German scenarios



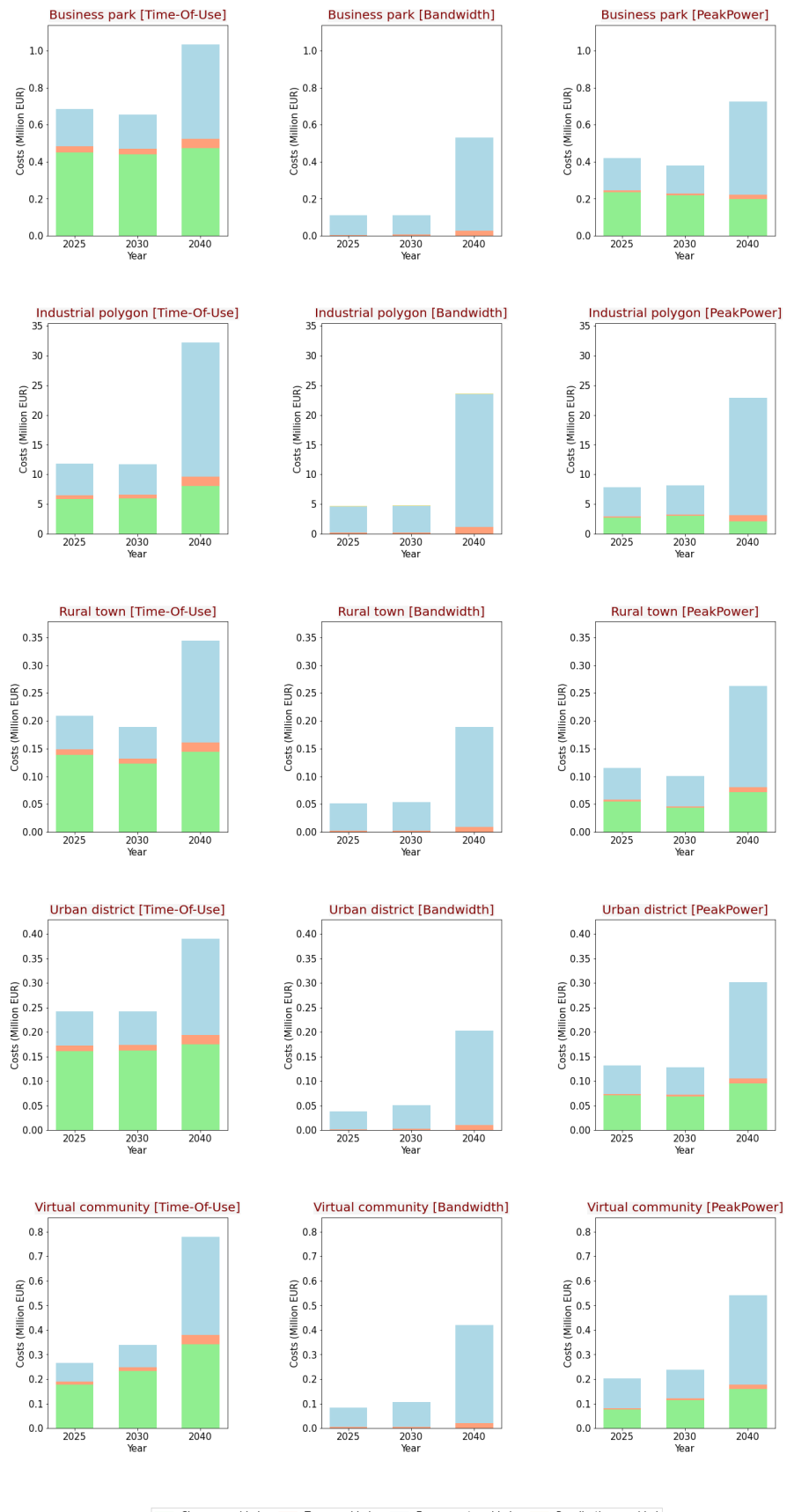
Source: Own elaboration with results from MODECO's operational model

Figure 82. Annual electrical balance, energy sales income and electrical cost avoided in Spanish scenarios



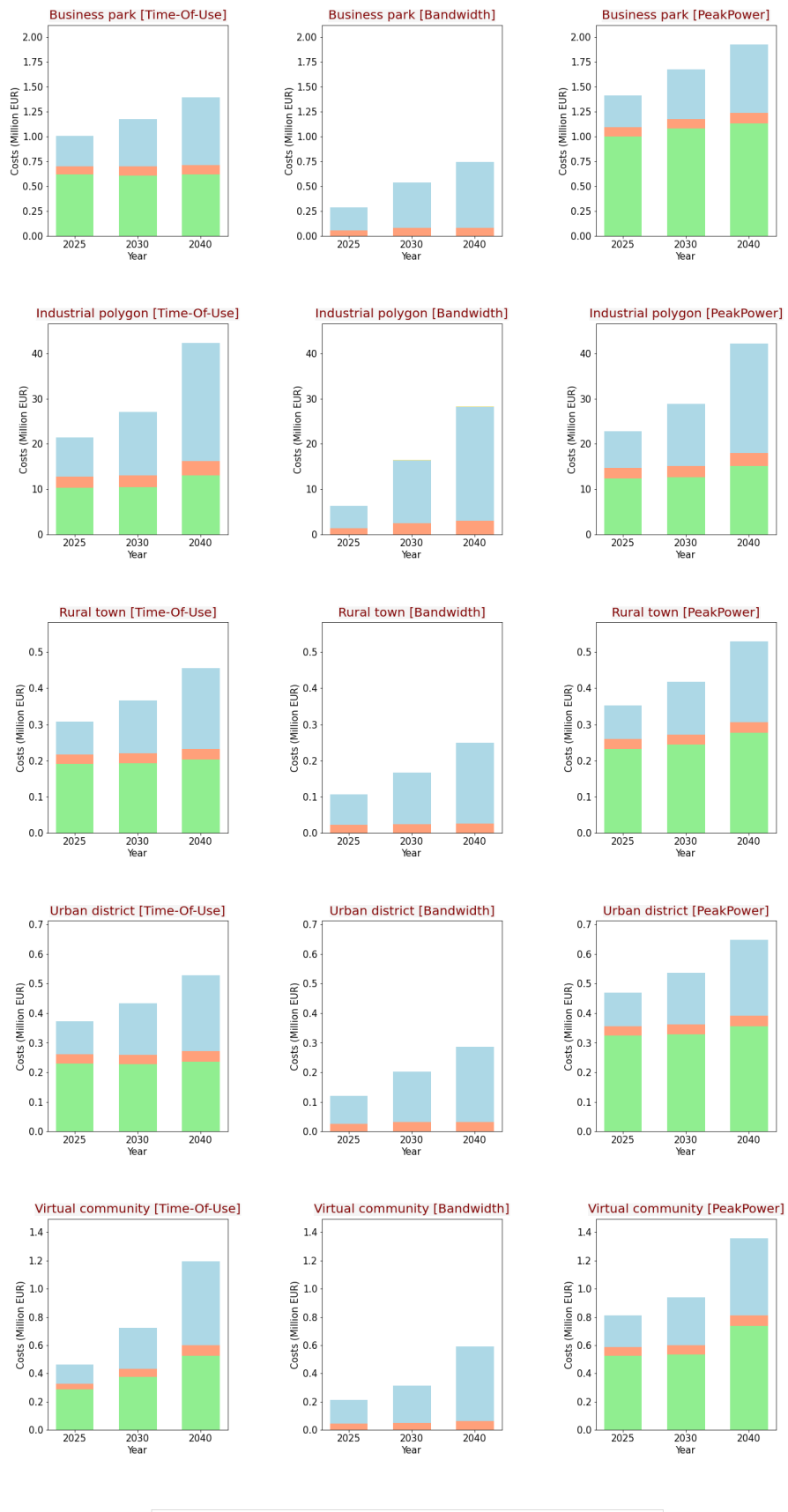
Source: Own elaboration with results from MODECO's operational model

Figure 83. Avoided energy costs in the Spanish scenarios disaggregated by cost component



Source: Own elaboration with results from MODECO's operational model

Figure 84. Avoided energy costs in the German scenarios disaggregated by cost component



Source: Own elaboration with results from MODECO's operational model

8.3 Energy costs

8.3.1 Disaggregated energy payments

The total annual costs associated with the purchase of electricity are shown in Figure 85 (Spain) and Figure 86 (Germany) disaggregated by component: **Use-of Network charges, taxes and energy costs** (marginal electricity prices). For the Bandwidth scenario, the applicable **Penalizations** for exceeding the contracted Bandwidth are represented in a particular category, as they are also part of the Use-of-Network charges, but its visibility provides useful information about the community's behaviour, particularly considering that in most cases, **the community's energy operations tend to avoid incurring in penalizations** for both, energy injections and withdrawal (see Chapter 7).

As observed in Figure 85 and Figure 86, Use-of-Network charges have a high relevance in the total purchased costs boreed by the communities, representing the largest share for all scenarios. Under a **Bandwidth** model, **charges costs are particularly high** in both regions, which is explained by the consideration of a **fixed subscription cost** per contracted kilowatt (Table 41) – calculated monthly – **that cannot be offset through self-generation** under MODECO assumptions. As explained in Section 2.3.2.3, the contracted bandwidth assumed for each community corresponds to 90% of the community's peak demand in the 16-year period which would lead to penalizations in a certain number of hours. The contracted value considered in each case can be seen in the following table.

Table 41 Use-of-Network charges applied in the Bandwidth scenarios by region and voltage level

| Country | Archetype | Contracted bandwidth [kWe] | Subscription price [€/kWh] | Annual subscription costs [k€] |
|---------|--------------------|----------------------------|----------------------------|--------------------------------|
| Spain | Business park | 3060.24 | 10.12 | 371 |
| | Industrial polygon | 52435.85 | 10.11 | 6361 |
| | Rural town | 723.75 | 10.12 | 87 |
| | Urban district | 944.15 | 10.12 | 114 |
| | Virtual community | 2705.06 | 10.12 | 328 |
| Germany | Business park | 2879.95 | 18.50 | 639 |
| | Industrial polygon | 52561.8 | 18.49 | 11662 |
| | Rural town | 692.61 | 18.50 | 153 |
| | Urban district | 888.28 | 18.50 | 197 |
| | Virtual community | 2574.41 | 18.50 | 571 |

Source: own elaboration with methodology from Section 2.3.2.3.

From the tested scenarios, **the only cases in which penalizations cost are significant are the German Rural town and Urban district archetypes**. In both cases the large majority of the penalizations are related to excess energy injections as in these archetypes (which have the lowest demands from all archetypes), the relations among energy prices, and demand and generation profiles, justify exceeding the contracted bandwidth as the obtained revenues greatly surpassed this cost. In the rest of scenarios, energy assets are operated in a way that avoids exceeding the bandwidth at almost all hours.

The charges applied in the **Time-Of-Use scenario** following the methodology described in Section 2.3.2.1 are shown in Table 42. As previously explained, the Medium Voltage costs are used for the Industrial polygon archetype, whereas the Low Voltage costs are applied to the rest. By analysing the data, it can be seen that in the mean value for the full year, the **charges price** account for a **lower proportion to the electricity**

price than the energy price. On the other hand, when one looks at **Figure 85** and **Figure 86**, it can clearly be seen how the charges have in most cases a greater impact in the final electricity purchase cost. This happens because the optimization model **tries to buy energy when it is cheaper**. This happens when the **energy cost is in its lowest values**, and as a consequence, the **charges end up having a greater impact than the energy cost** in most cases. Similarly, the taxes are computed as a fixed proportion of the electricity price in Spain, and as a constant value in Germany, being these values always smaller than the charges and the energy cost.

Table 42 Use-of-Network charges (€/MWh) applicable in the TOU scenario by year, user and voltage level.

| Year | Price category | Spain | | Germany | |
|------|----------------|---------------------|---------------------|--------------------|--------------------|
| | | LV* Charges [€/MWh] | MV* Charges [€/MWh] | LV Charges [€/MWh] | MV Charges [€/MWh] |
| 2025 | Off-peak | 36.22 | 17.24 | 48.27 | 27.97 |
| | Peak | 91.60 | 43.61 | 122.40 | 70.92 |
| 2030 | Off-peak | 36.53 | 17.39 | 48.52 | 28.11 |
| | Peak | 91.91 | 43.76 | 122.65 | 71.06 |
| 2040 | Off-peak | 35.57 | 16.93 | 47.48 | 27.51 |
| | Peak | 90.95 | 43.30 | 121.61 | 70.46 |

*LV: Low Voltage; MV: Medium Voltage.

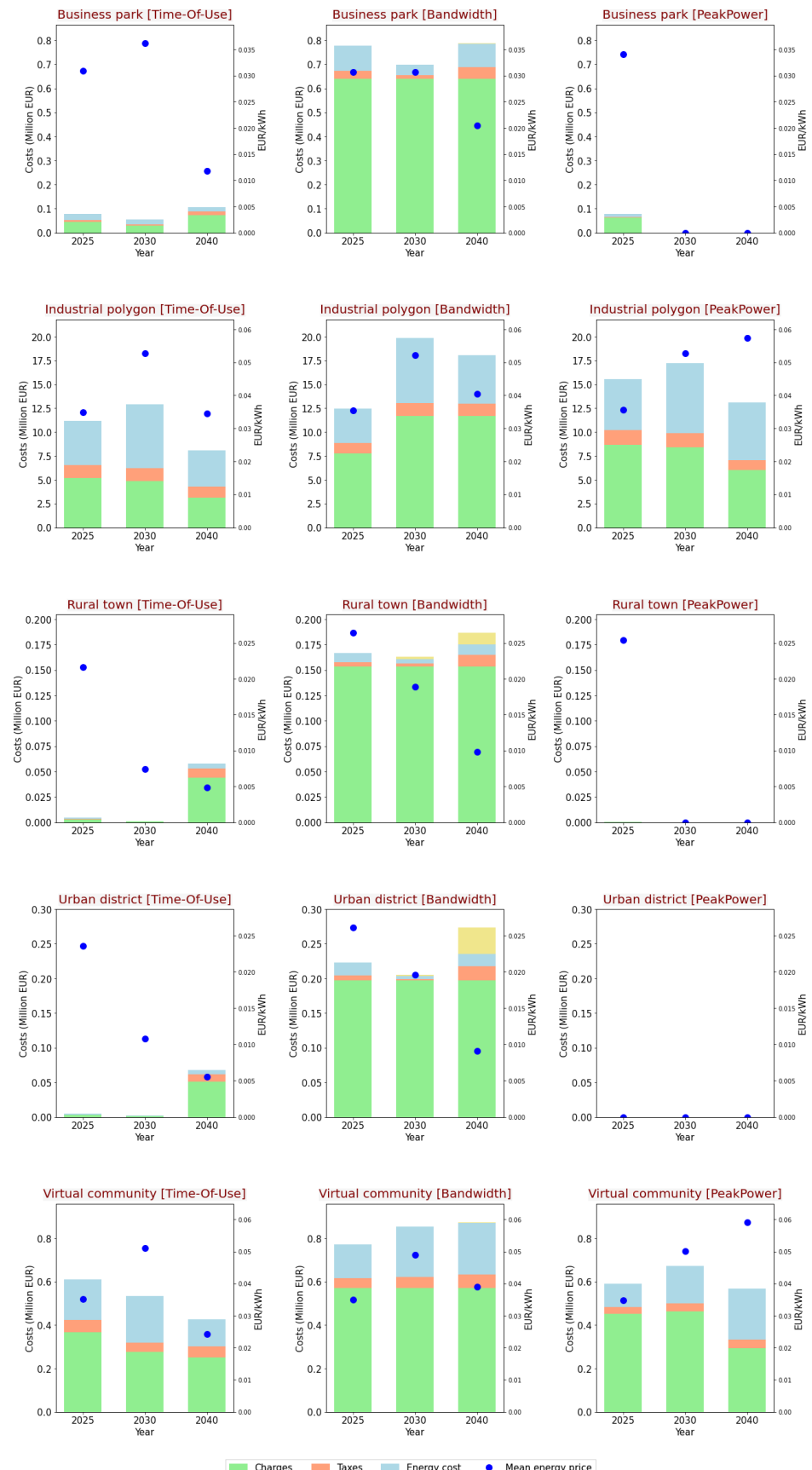
Source: own elaboration with methodology from Section 2.3

From the archetype-specific behaviours, **two interesting cases are Urban district and Rural town in Germany**. In the TOU scenario, both cases buy practically zero energy in 2025 and 2030, which explains the extremely low energy cost shown in Figure 84. However, they experience a dramatic increase in the amount of energy bought, reflecting in a significant rise in the energy costs bore by the community. However, as shown in Figure 81, both archetypes also significantly increase their amount of surplus local generation, sold power, and **stored electricity**. This is an indication of intense energy arbitrage and selling activities, which reflect in significant revenues – particularly related to energy sales – for the community. As explained before, there is not clarity of whether or not these level of energy trading could be still classified as economic benefits and not financial profit generation. This does not happen in the Bandwidth and Peak power model.

In the **Peak power scenario**, the yearly charges are computed based on the considered power cost (7.88 €/kWh and 33.04 €/kWh in Spain and Germany, respectively) which is applied over the community's **maximum demanded power** registered each month. This price is high enough to encourage the communities to invest in assets allowing them to reduce its peak demand as much as possible to minimize charges costs. In fact, this tariff is the only one resulting in zero or nearly zero electricity purchases reported in the three target years (German Business park, Urban district, Rural town) and a substantial decrease in the Spanish low and medium demand archetypes.

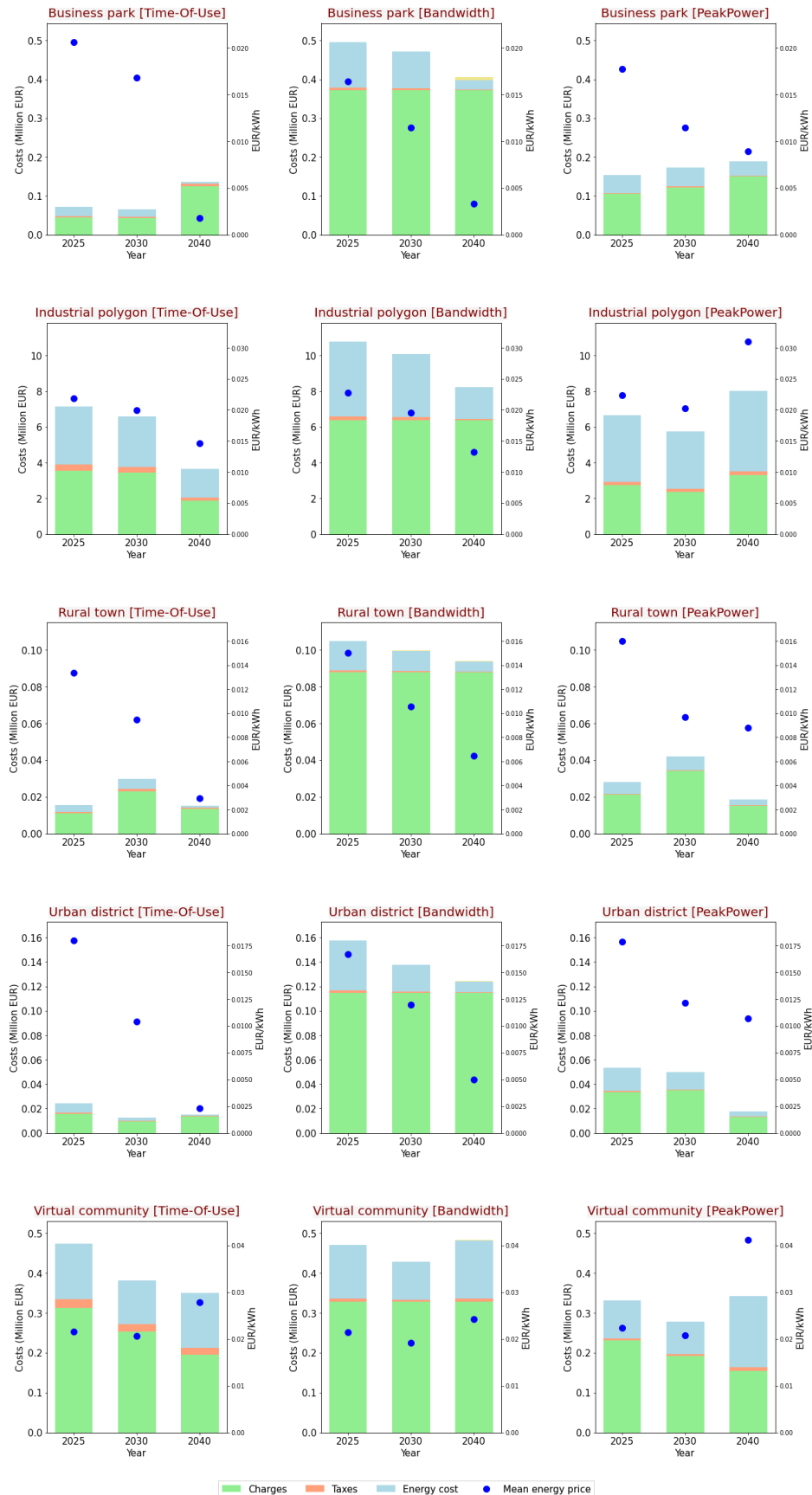
As explained in previous chapters, the Bandwidth model results in the largest energy purchases and thus in the higher buying expenses. Only in the industrial polygon (and less significantly in the Virtual community), the energy costs reported in the Peak power tariff are at the same level as those reported under a Bandwidth tariff. In these archetypes, the energy costs contribution to total purchase expenses get closer to the share reported by Use-of-Network charges. This can be explained by the fact that demand peaks, which are associated to a power-based charge, happens during low-priced hours. Still, reducing the power costs represents a larger benefit for the community so it still reduces demand at these hours to increase it at higher priced periods, increasing energy charges but minimizing power-based costs. This strategy results in costlier electricity as shown by the **weighted average energy price** paid by this archetype and marked with blue dots in Figure 85.

Figure 85. Disaggregated energy payments (price, taxes, Use-of-Network charges) in German scenarios



Source: Own elaboration with results from MODECO's operational model

Figure 86. Disaggregated energy payments (price, taxes, Use-of-Network charges) in Spanish scenarios



Source: Own elaboration with results from MODECO's operational model

In some cases such as the Business park and Rural town in the Bandwidth model, the Rural Town and Urban district in the Peak power, or the Virtual community under a Time-Of-Use tariff, an annual decrease in the weighted average energy costs is observed despite the rising annual marginal prices observed in both regions (Figure 45). This, however, is explained by the growing energy storage and self-generation capacity that takes place in these scenarios towards the end of the evaluation period (see for instance the investment planning laid out for the German Virtual community under a TOU tariff shown in Figure 70). **The communities do not only have more local generation available but can also make smart purchasing through the use of batteries and EV smart charging points.**

9 Conclusions

Energy communities are new players in the European energy market whose participation is expected to take a more prominent role in the upcoming years as the regulatory framework supporting their participation in market activities matures across member countries. Under this context, understanding how economic and regulatory conditions might impact on Energy communities becomes a relevant topic for policy makers looking to advance the energy transition. MODECO contributes to this discussion by providing optimization tools and analysis that permit to find the optimal investment and operational decisions expected from Energy communities under future energy prices and different tariff structures. In particular, this study analysed the investment decisions made by five Energy communities archetypes over a 16-year period and considering two regions (Germany, Spain) and three tariff structures (TOU, Peak Power and Bandwidth). An additional scenario considering no charges or taxes at all is also evaluated for comparison purposes.

Under the considered assumptions, all evaluated tariffs result in similar invested sums for the 16-year period except when representative days with considerably higher peak-priced hours are used. Under these conditions, the TOU model leads to significantly higher investments from Energy Communities, particularly in batteries, as these obtain significant revenues from performing energy arbitrage by charging at low-cost hours and selling the electricity back at these particular high-priced hours. Under the Peak power and Bandwidth model, batteries investments also increase but to a moderate level as increasing energy consumption leads to higher power-based costs in the first, and consumption and injections get penalized above a certain limit in the second.

In other words, communities' storage investments have a higher responsiveness to market price signals under a TOU tariff model. This leads to overinvestments in pricing conditions such as those considered in this study: low prices at high renewable production hours – commonly reaching zero – and extremely high prices at hours in which peak demands coincide with null renewable production. Although higher storage investments seem like a desirable outcome, our results show that a large portion of the batteries installed under a TOU tariff have low utilizations, remaining mostly unused, except when extreme prices are registered, which only happens during a few hours annually. Notably, storage overinvestments take place even when additional restrictions have been added to prevent excessive surplus generation or energy arbitrage given communities' objective to prioritize social, environmental, and economic benefits over financial profit. Still, we obtained these results considering perfect forecasting, where in reality a margin of error would exist. Moreover, this type of investments represents a level of risk that communities are unlikely to assume.

The rest of evaluated technologies – wind turbines, solar PV, CHP, electrolyzer, hydrogen storage tank – are only slightly affected when considering different tariff structures or even, price curves. In particular, the communities' solar and wind investments are led by other factors: investment and operational costs, demand curves, and available area. In particular, we highlight the available area as an important characteristic shaping the modelled communities' investment paths. Moreover, for renewables (wind, solar), using the Peak power tariff tends to favour the technology whose generation profile matches the community's consumption curves even when batteries are also installed. Still, the volume of surplus generation registered by the community does not change significantly; only happens at different times.

In general, communities tend to invest in self-generation assets as long as the investment and operational costs are competitive against average market prices. This becomes clearer when looking at the obtained results for the sensibility analysis using a flat rate instead of the dynamic prices in the TOU tariff scenario. In this case, investments in batteries are significantly reduced whereas investments in other assets remain practically the same as when using the dynamic prices. We suggest running further sensibility tests considering the two other tariffs and varying the investment and operational costs to corroborate these findings, particularly for the electrolyzer and hydrogen storage tank as the assumed costs resulted in zero installed units for all scenarios.

Under future system scenarios with a majority share of renewables, local generation might not always result in carbon offsets if CHP units fuelled by natural gas are installed, even if these displace boiler usage. Nowadays, this is not an issue as grid electricity is still carbon intensive so the operation of CHP results in emissions savings not only when compared to boiler combustion but also to grid electricity consumption. In a future power system like the reference Energy System Evolution Scenario used in MODECO in which most of the time the available electricity is carbon free, the installation of CHP units leads to higher carbon emissions if natural gas is used as combustion fuel. Using hydrogen-fuelled technologies is an interesting alternative in this regard as demonstrated by the Industrial polygon case. In this study, no carbon tax was imposed on CHP electrical generation, but we recommend to consider its inclusion in future studies.

From the communities' gains perspective, the TOU tariff results in the highest economic benefits for the German community archetypes followed closely by the Peak power tariff. In Spain, the Peak power leads to the highest benefits followed by the TOU tariff, with similar values for both tariffs. In the two regions, the Bandwidth model resulted in the lowest benefits even when similar investments as in the other tariffs are made. However, this outcome is likely more favourable if the contracted bandwidth is a variable to be optimized and not a fixed value as assumed in this analysis. We recommend to include this case in further analysis considering some restrictions regarding the maximum number of times that the community can change their selected bandwidth within the 16-year evaluation period.

On the other side, the use of the Bandwidth model results in the most Use-of-Network charges paid by the user due to the existence of a fixed cost per contracted power unit, while in the TOU and Peak power schemes, communities can reduce significantly or even avoid the payment of Use-of-Network charges through self-consumption. Although this feature results in economic gains for the communities, reduces the amount collected for grid cost recovery even when communities make use of grid infrastructure to supply part of their base demand, charge batteries and inject their surplus electricity for other consumers to use. This is important as we found that energy arbitrage and electricity sales could become relevant economic activities for future Energy communities.

Regardless of the tariff or archetype, self-consumption represents the largest economic benefit in 2025 and 2030 for all cases, even when considering the Virtual Community archetype or the Bandwidth tariff cases. Nonetheless, electricity sales take place during the entire evaluated period, meaning that surplus energy sales result in an economically attractive activity up to different levels. The only exception is the Industrial polygon, due to its large electricity demand all local generation is addressed to self-consumption. In 2040 when peak prices rise considerably but off-peak actually fall, energy arbitrage becomes a more significant revenue source for all communities.

From the three analysed tariffs – TOU, Bandwidth and Peak power – only the Subscription Bandwidth model considers a cost beyond energy injections, first implicit in the cost paid for the contracted bandwidth, and second, in the form of penalizations for excess energy injections above the contracted limit. This is a feature that makes this tariff scheme an interesting option for scenarios in which Energy communities actively engaged in energy arbitrage and electricity surplus selling, such as those considered in this study. Nonetheless, we advise to complement this analysis with a study on grid impacts from Energy communities' operation under a Subscription Bandwidth tariff, analysing their imposed cost on the system versus the costs recovered via Use-of-Network charges.

As study follows a cost minimization approach, the modelled communities operate their energy assets in a way that avoids the penalizations associated with excess energy injections and withdrawals beyond the established bandwidth limits. Still, in the scenarios in which days with wide price spreads are used (German Rural town and Business park), the communities choose to bear the penalizations costs in the hours that the selling price is so high that this cost is easily offset. This happens only a few hours, but the volume of injected energy is considerably higher than at other times. In this sense, regulators could consider a scalable penalization fee as the network impact of exceeding the contracted bandwidth by a large percentage does not have the same impact as just for a few kilowatts, even if it is just for a few hours per year.

In the Virtual community archetype, the consideration of partial Use-of-Network charges applied to self-consumption also results in higher grid costs recovery. Nonetheless, the total charges paid by communities in this case are lower than for the Bandwidth model, whose charges remain fixed as the contracted bandwidth does not change. However, our results indicate that the Portuguese regulation, in which partial charges are applied to virtual self-consumption depending on the load and generation location, is an interesting proposal recognizing the benefits of Energy communities with geographically spread members, while also considering their network impacts. Further analysis on these rules impacts on energy communities and grid cost recovery would be advisable.

Overall, the study indicates that none of the evaluated tariff structures poses significant barriers to future expansion of energy communities. As long as investment and operational costs are competitive against energy prices, the installation of self-generation assets (solar PV, wind, CHP) will translate into significant economic benefits for the communities. In all cases, storage installations will be also encouraged to promote energy injections and withdrawals in convenient times for the communities and the power system, maximizing savings and sales revenues. Purely energy-based tariffs (TOU), however, could lead to overinvestments in storage units that would be only used at specific times when prices surpass a given price threshold.

The introduction of power-based charges, e.g. in the Bandwidth and Peak power models, seems to avoid this pitfall even in future power scenarios in which wide price differences are present. In particular, the Bandwidth tariff presents an opportunity to adapt Use-of-Network charges to a future system in which prosumers become more active, reshaping the grid's demand and generation nodes. This becomes especially relevant as the study shows that not only self-consumption, but also energy arbitrage and electricity sales will be relevant activities for future Energy communities. However, we recommend testing additional features when considering this novel tariff such as optimizing the contracted bandwidth, considering scalable penalizations fees, and setting a restriction on the number of times communities can update their contracted bandwidth.

References

- ACEA (European Automobile Manufacturers Association). *European EV Charging Infrastructure Masterplan*, ACEA, Belgium, 2022a. <https://www.acea.auto/files/Research-Whitepaper-A-European-EV-Charging-Infrastructure-Masterplan.pdf>
- ACEA (European Automobile Manufacturers Association). *Vehicles in Use Europe 2022*. ACEA, Belgium, 2022b. <https://www.acea.auto/files/ACEA-report-vehicles-in-use-europe-2022.pdf>
- ACER (European Union Agency for the Cooperation of Energy Regulators). *ACER Report on Distribution Tariff Methodologies in Europe*, ACER, Slovenia, 2021. https://www.acer.europa.eu/Official_documents/Acts_of_the_Agency/Publication/ACER%20Report%20on%20Distribution%20Tariff%20Methodologies.pdf
- Aebischer, B., Catenazzi, G., and Martin, J. Impact of climate change on thermal comfort, heating and cooling energy demand in Europe. *Proceedings ECEEE 2007 Summer Study*, 2007, 859–870. http://www.verozo.be/sites/verozo/files/files/Impact%20ClimateChange_ETH%20Switzerland.pdf
- Algie, C., and Wong, K. P. Reduced cogeneration feasible operating region for combined heat and power scheduling problems. *Fifth International Conference on Power System Management and Control*, 2002, pp. 323–328. <https://doi.org/10.1049/cp.20020056>
- Alipour, M., Zare, K., and Mohammadi-Ivatloo, B. Short-term scheduling of combined heat and power generation units in the presence of demand response programs. *Energy*, No 71, 2014, pp. 289–301. <https://doi.org/10.1016/j.energy.2014.04.059>
- Arybillia, M., Bertram, R., Bolle, A., Corovessi, A., Dembski, F., Fouquet, D., Giňová, P., Księžopolski, K., Mantzaris, N., Ondřich, J., Maćkowiak-Pandera, J., Primova, R., Rüdinger, A., Santini, M., Scheuer, S., Szymalski, W., Torres, J. H., Claude, T., Tsoutsos, T., and Walsh, M. *Energy Atlas 2018 - Facts and figures about renewables in Europe*, Heinrich Böll Stiftung, Friends of the Earth Europe, European Renewable Energies Federation, Green European Foundation, Germany-Belgium-Luxembourg, 2018. https://www.boell.de/sites/default/files/energyatlas2018_facts-and-figures-renewables-europe.pdf.pdf
- BDEW (Bundesverband der Energie- und Wasserwirtschaft). *BDEW / VKU / GEODE- Leitfaden Gas, Abwicklung Von Standardlastprofilen*, BDEW, VKU (Verband kommunaler Unternehmen), GEODE, Germany, 2016. https://www.bdew.de/media/documents/Leitfaden_20160630_Abwicklung-Standardlastprofile-Gas.pdf
- BDEW (Bundesverband der Energie- und Wasserwirtschaft). *BDEW-Strompreisanalyse Januar 2020 Die wichtigsten Ergebnisse im Überblick*, Germany, 2020. https://www.bdew.de/media/documents/20200107_BDEW-Strompreisanalyse_Januar_2020.pdf
- BDEW (Bundesverband der Energie- und Wasserwirtschaft). *Standardlastprofile Strom* [Dataset], Germany, 2017. <https://www.bdew.de/energie/standardlastprofile-strom/>
- BGW (Berufsgenossenschaft für Gesundheitsdienst und Wohlfahrtspflege). *Praxisinformation P 2006/8 Gastransport/Betriebswirtschaft, Anwendung von Standardlastprofilen zur Belieferung nicht-leistungsgemessener Kunden. Praxisinformation P 2006/8 Gastransport/Betriebswirtschaft*, BGW, Germany, 2006. http://www.gwb-netz.de/wa_files/05_bgw_leitfaden_lastprofile_56550.pdf
- Bock, C. *Time Series Analysis on Energy Consumption Data*. Ph.D. dissertation, Informatics Institute, Heinrich-Heine-Universität Düsseldorf, Germany, 2019. https://docserv.uni-duesseldorf.de/servlets/DerivateServlet/Derivate-55305/diss_bock.pdf
- Bolinger, M., Lantz, E., Wiser, R., Hoen, B., Rand, J., and Hammond, R. Opportunities for and challenges to further reductions in the “specific power” rating of wind turbines installed in the United States. *Wind Engineering*, Vol. 45, No 2, 2021, pp. 351–368. <https://doi.org/https://doi.org/10.1177/0309524X199010>
- Brauer, F. *Load profile data of 50 industrial plants in Germany for one year (1.0)* [dataset]. Zenodo. <https://doi.org/10.5281/zenodo.3899018>
- Brown, T., Hörsch, J., and Schlachtberger, D. PYPSA: Python for Power System Analysis. *Journal of Open Research Software*, Vol. 6, No 1, 2018. <https://doi.org/10.5334/jors.188>
- Cagle, A., Shepherd, M., Grodsky, S., Armstrong, A., Jordaan, S. M., and Hernandez, R. Standardized Metrics to Quantify Solar Energy-Land Relationships: A Global Systematic Review. *SSRN Electronic Journal*, 2022. <https://doi.org/10.2139/ssrn.4069060>

Caramizaru, A., and Uihlein, A. *Energy communities: an overview of energy and social innovation*, EUR 30083 EN, Publications Office of the European Union, 2020. <https://doi.org/10.2760/180576>

Chernova, E. A. Stationary combustion. *Journal of Applied Mechanics and Technical Physics*, Vol. 7, No 6, 1966, pp. 69–70. <https://doi.org/10.1007/BF00914340>

COME RES Project. *COME RES Project Website*, 2020. <https://come-res.eu/>

Corchero García, C. European electric vehicle fleet: driving and charging behaviors. *Congreso de La Asociación Española Para La Economía Energética*, 2015, pp. 1–11.

Crespi, A., Terzi, S., Cocuccioni, S., Zebisch, M., Berckmans, J., and Füssel, H.-M. *Climate-related hazards indices for Europe – Technical Paper 1/2020*, European Topic Centre on Climate Change Impacts, Vulnerability and Adaptation (ETC-CCA), Italy, 2020. https://bia.unibz.it/discovery/delivery/39UBZ_INST:ResearchRepository/12236520890001241#132365208800_01241

DAI-Laboratory. *Electric Vehicle Charging Infrastructure Simulator (ELVIS)* [Software], TU Berlin, Germany, 2020. <https://github.com/dailab/elvis>

Dalla Longa, F., Kober, T., Badger, J., Volker, P., Hoyer-Klick, C., Hidalgo, I., Medarac, H., Nijs, W., Politis, S., Tarvydas, D., and Zucker, A. *Wind potentials for EU and neighboring countries: Input datasets for the JRC-EU-TIMES Model*, EUR 29803 EN, Publications Office of the European Union, 2018. <https://doi.org/10.2760/041705>

DECIDE Project. *DECIDE Project Website*. 2020. <https://decide4energy.eu/>

Dimoulkas, I., and Amelin, M. Probabilistic day-ahead CHP operation scheduling. *IEEE Power and Energy Society General Meeting*, September 2015. <https://doi.org/10.1109/PESGM.2015.7285962>

Droutsa, K. G., Balaras, C. A., Lykoudis, S., Kontoyiannidis, S., Dascalaki, E. G., and Argiriou, A. A. Baselines for energy use and carbon emission intensities in Hellenic nonresidential buildings, *Energies*, Vol. 13, No 8, 2020. <https://doi.org/10.3390/en13082100>

Drücke, J., Borsche, M., James, P., Kaspar, F., Pfeifroth, U., Ahrens, B., and Trentmann, J. Climatological analysis of solar and wind energy in Germany using the Grosswetterlagen classification, *Renewable Energy*, Vol. 164, 2021, pp. 1254–1266. <https://doi.org/10.1016/j.renene.2020.10.102>

Duić, N., Štefanić, N., Lulić, Z., Krajačić, G., Pukšec, T., and Novosel, T. *EU28 fuel prices. Heat Roadmap Europe 2050*, Heat Roadmap Europe (HRE4), Croatia, 2017. https://heatroadmap.eu/wp-content/uploads/2020/01/HRE4_D6.1-Future-fuel-price-review.pdf

EDSO. *Lead the Transition – Serve the Customers*, E.DSO, 2020, pp. 1–32. https://www.edsoforsmartgrids.eu/wp-content/uploads/2020/06/EDSO_Customer-White-paper_web.pdf

EFTE (European Federation for Transport and Environment). *Recharge EU: how many charge points will Europe and its Member States need in the 2020s*, European Federation for Transport and Environment, Belgium, 2020. <https://www.transportenvironment.org/wp-content/uploads/2021/07/01%202020%20Draft%20TE%20Infrastructure%20Report%20Final.pdf>

Ember. *EU Carbon Price Tracker*, 2022. <https://ember-climate.org/data/data-tools/carbon-price-viewer/>

Engel, H., Hensley, S., Knupfer, S., and Sahdev, S. *Charging Ahead: Electric Vehicle Infrastructure Demand*, McKinsey & Company – McKinsey Centre for Future Mobility, 2018. <https://www.mckinsey.com/~media/McKinsey/Industries/Automotive%20and%20Assembly/Our%20Insights/Charging%20ahead%20Electric-vehicle%20infrastructure%20demand/Charging-ahead-electric-vehicle-infrastructure-demand-final.pdf>

Ensslen, A., Ringler, P., Dörr, L., Jochem, P., Zimmermann, F., and Fichtner, W. Examining an innovative electric vehicle charging tariff to incentivize customers' provision of load flexibilities. *Energy Research and Social Science*, Vol. 42, 2018, pp. 112–126. <https://doi.org/10.1016/j.erss.2018.02.013>

Entranzo Project. *Interactive online Data Tool* [Dataset], 2008. <https://entranzo.enerdata.net/>

ENTSO-E. *European Resource Adequacy Assessment (ERA) 2021 Climatic Database* [Dataset], 2022 <https://www.entsoe.eu/outlooks/eraa/eraa-downloads/>

ENTSO-E. *TYNDP 2020 - Scenario Building Guidelines. Annex 2: Cost Assumptions for the Investment Modelling*, Annex to TYNDP 2020, ENTSO-E, Belgium, 2020. https://2020.entsos-tyndp-scenarios.eu/wp-content/uploads/2020/07/TYNDP_2020_Scenario_Building-Guidelines_03_Annex_2_Cost_Assumptions_final_report.pdf

ENTSO-E. *TYNDP 2020 Main Report*, ENTSO-E, Belgium, 2021a. https://eepublicdownloads.blob.core.windows.net/public-cdn-container/tyndp-documents/TYNDP2020/Foropinion/TYNDP2020_Main_Report.pdf

ENTSO-E. *TYNDP 2020 scenarios data* [Dataset]. ENTSO-E, 2021b. <https://tyndp.entsoe.eu/maps-data>

ENTSO-E Working Group Economics Framework. *Overview of transmission tariffs in Europe: Synthesis 2019*, ENTSO-E, 2019, Belgium, pp. 1–24. https://docstore.entsoe.eu/Documents/MC%20documents/190626_MC%20TOP%207.2_TTO_Synthesis2019.pdf

ERSE (Entidade Reguladora dos Serviços Energéticos). *Regulamento n.o 8/2021 – Regulamento do Autoconsumo de Energia Elétrica e revoga o Regulamento n.o 266/2020*, Portugal, 2021, pp. 1–46. https://www.erne.pt/media/b5rmusyr/regulamento-erse-n-%C2%BA-8_2021.pdf

EURELECTRIC (Union of the European Electricity Industry). *Power Distribution in Europe – Facts & Figures*, Belgium, 2013, pp. 1–26. https://cdn.eurelectric.org/media/1835/dso_report-web_final-2013-030-0764-01-e-h-D66B0486.pdf

EUROGAS (The European Union of the Natural Gas Industry). *Statistical Report*, EUROGAS, 2011. https://www.ansa.it/documents/1323783543984_Eurogas2011.pdf

European Commission. (n.d.-a). *Energy Communities*. https://energy.ec.europa.eu/topics/markets-and-consumers/energy-communities_en

European Commission. (n.d.-b). *EU Buildings Database* [Dataset]. https://ec.europa.eu/energy/eu-buildings-database_en

European Commission. (n.d.-c). *Renewable energy targets*. https://energy.ec.europa.eu/topics/renewable-energy/renewable-energy-directive-targets-and-rules/renewable-energy-targets_en

Eurostat. *Energy statistics - natural gas and electricity prices (from 2007 onwards)* [Dataset], 2022. https://www.mibgas.es/en/file-access?path=AGNO_2019/XLS

Eurostat. *Combined Heat and Power (CHP) Generation – Directive 2012/27/EU of the European Parliament and of the Council Commission Decision 2008/952/EC (Reporting template)*, 2017. https://ec.europa.eu/eurostat/documents/38154/42195/Final_CHP_reporting_instructions_reference_year_2016_onwards_30052017.pdf/f114b673-aef3-499b-bf38-f58998b40fe6

Eurostat. *Passenger cars per 1000 inhabitants*, 2020. https://ec.europa.eu/eurostat/databrowser/view/road_eqs_carhab/default/table?lang=en

Eurostat. *Heating and cooling degree days – statistics*, 2021. https://ec.europa.eu/eurostat/statistics-explained/index.php?title=Heating_and_cooling_degree_days_-_statistics#Heating_and_cooling_degree_days_at_EU-27_level

Eurostat. *Average household size – EU-SILC survey*, 2022. https://appsso.eurostat.ec.europa.eu/nui/show.do?dataset=ilc_lvph01&lang=en

Eurostat Press Office. *9 out of 10 enterprises in the EU employed fewer than 10 persons.*, November 2015. <https://ec.europa.eu/eurostat/documents/2995521/7076793/4-17112015-AP-EN.pdf/1db58867-0264-45c0-94bf-ab079e62d63f>

Facci, A. L., Andreassi, L., and Ubertini, S. Optimization of CHCP (combined heat power and cooling) systems operation strategy using dynamic programming. *Energy*, Vol. 66, 2014, pp. 387–400. <https://doi.org/10.1016/j.energy.2013.12.069>

Fan, R., Zhang, C., Wang, Y., Ji, C., Meng, Z., Xu, L., Ou, Y., and Chin, C. S. Numerical study on the effects of battery heating in cold climate. *Journal of Energy Storage*, Vol. 26, August 2019. <https://doi.org/10.1016/j.est.2019.100969>

Forest Research. *Tool and Resources - Typical calorific values of fuels*, United Kingdom, 2022. <https://www.forestryresearch.gov.uk/tools-and-resources/fthr/biomass-energy-resources/reference-biomass/facts-figures/typical-calorific-values-of-fuels/>

Frieden, D., Tuerk, A., Neumann, C., D'Herbemont, S., and Roberts, J. *Collective self-consumption and energy communities: Trends and challenges in the transposition of the EU framework*, Compile project, December 2020, pp. 1–50. <https://www.rescoop.eu/uploads/rescoop/downloads/Collective-self-consumption-and-energy-communities.-Trends-and-challenges-in-the-transposition-of-the-EU-framework.pdf>

Gaete-Morales, C., Kramer, H., Schill, W. P., and Zerrahn, A. An open tool for creating battery-electric vehicle time series from empirical data, emobpy. *Scientific Data*, Vol. 8, No 1, 2021, pp. 1–18. <https://doi.org/10.1038/s41597-021-00932-9>

Gambarotta, A., Morini, M., Pomplini, N., and Spina, P. R. Optimization of load allocation strategy of a multi-source energy system by means of dynamic programming, *Energy Procedia*, Vol. 81, 2015, pp. 30–39. <https://doi.org/10.1016/j.egypro.2015.12.056>

German Federal Statistical Office. *Electricity consumption of private households by household size* [Dataset], 2020. <https://www.destatis.de/EN/Themes/Society-Environment/Environment/Material-Energy-Flows/Tables/electricity-consumption-households.html>

Ghaffarpour, R., Mozafari, B., Ranjbar, A. M., and Torabi, T. Resilience oriented water and energy hub scheduling considering maintenance constraint, *Energy*, Vol. 158, 2018, pp. 1092–1104. <https://doi.org/10.1016/j.energy.2018.06.022>

Hecht, C., Das, S., Bussar, C., and Sauer, D. U. Representative, empirical, real-world charging station usage characteristics and data in Germany, *eTransportation*, Vol. 6, 2020. <https://doi.org/10.1016/j.etran.2020.100079>

Heitkoetter, W., Schyska, B. U., Schmidt, D., Medjroubi, W., Vogt, T., and Agert, C. Assessment of the regionalised demand response potential in Germany using an open source tool and dataset. *Advances in Applied Energy*, 2021. <https://doi.org/https://doi.org/10.1016/j.adapen.2020.100001>

HRE4 (Heat Roadmap Europe). *Heat Roadmap Europe HRE4 Cost Database* [Dataset], n.d.

Hu, K., Fang, J., Ai, X., Huang, D., Zhong, Z., Yang, X., and Wang, L. Comparative study of alkaline water electrolysis, proton exchange membrane water electrolysis and solid oxide electrolysis through multiphysics modeling, *Applied Energy*, Vol. 312, February 2022. <https://doi.org/10.1016/j.apenergy.2022.118788>

IEA (International Energy Agency). *Global average levelised cost of hydrogen production by energy source and technology, 2019 and 2050*, IEA, France, 2020. <https://www.iea.org/data-and-statistics/charts/global-average-levelised-cost-of-hydrogen-production-by-energy-source-and-technology-2019-and-2050>

IDAE (Instituto de Diversificación y Ahorro de la Energía). *Consumos del Sector Residencial en España. Resumen de Información Básica*, Eurostat, Ministerio de Industria Energía y Turismo, IDAE, 2014. <https://www.idae.es/uploads/documentos/documentos Documentacion Basica Residencial Unido c93da537.pdf>

Igualada González, L., Corchero García, C., Cruz Zambrano, M., and Heredia, F. Optimal energy management for a residential microgrid including a vehicle-to-grid system. *IEEE Transactions on Smart Grid*, Vol. 5, No 4, 2013. <https://doi.org/10.1109/TSG.2014.2318836>

IRENA (International Renewable Energy Agency). *Time-of-Use Tariffs*. IRENA, Saudi Arabia, 2019, 1–18. https://www.irena.org/-/media/Files/IRENA/Agency/Publication/2019/Feb/IRENA_Innovation_ToU_tariffs_2019.pdf?la=en&hash=36658ADA8AA98677888DB2C184D1EE6A048C7470

IRENA (International Renewable Energy Agency). *Green Hydrogen Cost Reduction: Scaling up Electrolyzers to Meet the 1.5°C Climate Goal*. 2020, IRENA, Saudi Arabia, 2020. https://www.irena.org/-/media/Files/IRENA/Agency/Publication/2020/Dec/IRENA_Green_hydrogen_cost_2020.pdf

IRENA (International Renewable Energy Agency). *Green hydrogen for industry: A guide to policy making*, IRENA, Saudi Arabia, 2022. https://www.irena.org/-/media/Files/IRENA/Agency/Publication/2022/Mar/IRENA_Green_Hydrogen_Industry_2022.pdf

Jesper, M., Pag, F., Vajen, K., and Jordan, U. Annual Industrial and Commercial Heat Load Profiles: Modeling Based on k-Means Clustering and Regression Analysis. *Energy Conversion and Management*, Vol. 10, March 2021. <https://doi.org/10.1016/j.ecmx.2021.100085>

Jesper, M., Pag, F., Vajen, K., and Jordan, U. Heat Load Profiles in Industry and the Tertiary Sector: Correlation with Electricity Consumption and Ex Post Modeling. *Sustainability*, Vol. 14, No 7, 2022. <https://doi.org/10.3390/su14074033>

Koski, A., Järvenpää, J., Salo, J., Järvinen, M., Pylvänäinen, J., and Honkapuro, S. Power-Based Tariff as an Incentive for Distribution System Operator's Customers to Reduce Their Peak Powers, *25th International Conference on Electricity Distribution (CIRED)*, Spain, June 2019, pp. 3–6.

Lapesa Grupo Empresarial. *Pressure tanks for H₂ storage* [Technical Sheet], No. 2201-01, n.d. https://lapesa.es/sites/default/files/ficha_depositos_hidrogeno_h2_2201-01_en.pdf

Li, N., Hakvoort, R. A., and Lukszo, Z. Cost allocation in integrated community energy systems — Performance assessment. *Applied Energy*, Vol. 307, 2022. <https://doi.org/10.1016/j.apenergy.2021.118155>

Lyndon, G., Pomerantz, C., Strange, M., and Donev, J. *Excise tax*, University of Calgary, Canada, 2020. https://energyeducation.ca/encyclopedia/Excise_tax

Mansouri, S. A., Ahmarnajad, A., Javadi, M. S., and Catalão, J. P. S. Two-stage stochastic framework for energy hubs planning considering demand response programs, *Energy*, Vol. 206, 2020. <https://doi.org/10.1016/j.energy.2020.118124>

McCarl, B. A. *McCarl GAMS User Guide Version 24.6*, Texas A&M University, USA, 2016.

McMillan, C. *Manufacturing Thermal Energy Use in 2014* [Dataset], National Renewable Energy Laboratory, USA, 2019. <https://doi.org/10.7799/1570008>

Meenakumar, P., Aunedi, M., and Strbac, G. Optimal Business Case for Provision of Grid Services through EVs with V2G Capabilities. *2020 Fifteenth International Conference on Ecological Vehicles and Renewable Energies (EVER)*, 2020, pp. 1–10. <https://doi.org/10.1109/EVER48776.2020.9242538>

Mercado Ibérico del Gas. *Annual results - MIBGAS-ES index 2019* [Dataset], Spain, 2020. https://www.mibgas.es/en/file-access?path=AGNO_2019/XLS

Ministerio para la Transición Ecológica. *Real Decreto 244/2019, de 5 de abril, por el que se regulan las condiciones administrativas, técnicas y económicas del autoconsumo de energía eléctrica*, España, 2019. <https://www.boe.es/buscar/doc.php?id=BOE-A-2019-5089>

Müller, A., Friedrich, L., Reichel, C., Herceg, S., Mittag, M., and Neuhaus, D. H. A comparative life cycle assessment of silicon PV modules: Impact of module design, manufacturing location and inventory, *Solar Energy Materials and Solar Cells*, Vol. 230, April 2021, <https://doi.org/10.1016/j.solmat.2021.111277>

Nahmmacher, P., Schmid, E., Hirth, L., and Knopf, B. Carpe diem: A novel approach to select representative days for long-term power system modeling, *Energy*, Vol. 112, 2016, pp. 430–442. <https://doi.org/10.1016/j.energy.2016.06.081>

Nastasi, B., Mazzoni, S., Groppi, D., Romagnoli, A., and Astiaso Garcia, D. Optimized integration of Hydrogen technologies in Island energy systems, *Renewable Energy*, Vol. 174, 2021, pp. 850–864. <https://doi.org/10.1016/j.renene.2021.04.137>

Nationale Plattform Elektromobilität. *Ladeinfrastruktur für Elektrofahrzeuge in Deutschland*. Gemeinsame Geschäftsstelle Elektromobilität Der Bundesregierung (GGEMO), Germany, 2015. https://www.bdew.de/media/documents/20151127_Statusbericht-LIS.pdf

Nazari-Heris, F., Mohammadi-ivatloo, B., and Nazarpour, D. Network constrained economic dispatch of renewable energy and CHP based microgrids. *International Journal of Electrical Power and Energy Systems*, Vol 110, 2019, pp. 144–160. <https://doi.org/10.1016/j.ijepes.2019.02.037>

Nojavan, S., and Zare, K. Optimal energy pricing for consumers by electricity retailer, *International Journal of Electrical Power and Energy Systems*, Vol. 102, 2018, pp. 401–412. <https://doi.org/10.1016/j.ijepes.2018.05.013>

Nojavan, S., Zare, K., and Mohammadi-Ivatloo, B. Selling price determination by electricity retailer in the smart grid under demand side management in the presence of the electrolyser and fuel cell as hydrogen storage system, *International Journal of Hydrogen Energy*, Vol. 42, No 5, 2017, pp. 3294–3308. <https://doi.org/10.1016/j.ijhydene.2016.10.070>

Obane, H., Nagai, Y., and Asano, K. Assessing land use and potential conflict in solar and onshore wind energy in Japan, *Renewable Energy*, Vol. 160, 2020, pp. 842–851. <https://doi.org/10.1016/j.renene.2020.06.018>

Observ'ER. *Heat pumps barometer*. EurObserv'ER, Vol. 4–5, 2021, pp. 98–124. <https://www.eurobserv-er.org/heat-pumps-barometer-2020/>

OECD (Organisation for Economic Cooperation and Development). *Taxing Energy Use 2019*. OECD Publishing, France, 2020. <https://doi.org/https://doi.org/10.1787/058ca239-en>

OECD (Organisation for Economic Cooperation and Development). *Taxing Energy Use 2019: Country Note – Germany. Supplement to Taxing Energy Use 2019*, OECD Publishing, France, 2019a. <https://www.oecd.org/tax/tax-policy/taxing-energy-use-spain.pdf>

OECD (Organisation for Economic Cooperation and Development). *Taxing Energy Use 2019: Country Note – Spain. Supplement to Taxing Energy Use 2019*, OECD Publishing, France, 2019b. <https://www.oecd.org/tax/tax-policy/taxing-energy-use-germany.pdf>

Open Power System Data. *Weather Data* [Dataset], 2020. https://doi.org/https://doi.org/10.25832/weather_data/2020-09-16

Pablo-Romero, M. del P., Pozo-Barajas, R., and Molleda-Jimena, G. Residential energy environmental Kuznets curve extended with non-linear temperature effects: a quantile regression for Andalusian (Spain) municipalities, *Environmental Science and Pollution Research*, Vol. 28, No 35, 2021, pp. 48984–48999. <https://doi.org/10.1007/s11356-021-13608-z>

Pettersen, R. C. The chemical composition of wood. In R. Rowell (Ed.), *The chemistry of solid wood*, American Chemical Society, USA, 1984, pp. 57–126. <https://doi.org/10.1021/ba-1984-0207>

Priesmann, J., Nolting, L., Kockel, C., and Praktiknjo, A. Time series of useful energy consumption patterns for energy system modelling, *Scientific Data*, Vol. 8, No 1, 2021, pp. 1–12. <https://doi.org/10.1038/s41597-021-00907-w>

Project Lightness. *Lightness Project Website*, n.d. <https://www.lightness-project.eu/>

Proyecto SECH-SPAHOUSEC. *Análisis del consumo energético del sector residencial en España - Informe final*, IDAE (Instituto de Diversificación y Ahorro de la Energía), Spain, 2011. https://www.idae.es/uploads/documentos/documentos_Informe_SPAHOUSEC_ACC_f68291a3.pdf

Prüggl, N. Economic potential of demand response at household level-Are Central-European market conditions sufficient?, *Energy Policy*, Vol. 60, 2013, pp. 487–498. <https://doi.org/10.1016/j.enpol.2013.04.044>

Qin, B., Coker, E., and O’Neil, M. *EU ETS 2021 Review -- Big Carbon Is Here to Stay: BNEF*, Bloomberg, United States, 2021. <https://www.bloomberg.com/press-releases/2021-12-15/eu-ets-2021-review-big-carbon-is-here-to-stay-brief>

Quiros-Tortos, J., Navarro-Espinosa, A., Ochoa, L. F., and Butler, T. Statistical representation of EV charging: Real data analysis and applications. *20th Power Systems Computation Conference*, Institute of Electrical and Electronics Engineer (IEEE), 2018. <https://doi.org/10.23919/PSCC.2018.8442988>

Rau, G. H., Willauer, H. D., and Ren, Z. J. The global potential for converting renewable electricity to negative-CO₂-emissions hydrogen, *Nature Climate Change*, Vol. 8, No 7, 2018, pp 621–625. <https://doi.org/10.1038/s41558-018-0203-0>

Red Eléctrica de España. *Cómo consumimos electricidad*, Spain, n.d. https://www.ree.es/sites/default/files/interactivos/como_consumimos_electricidad/como-varia-mi-consumo.html

Ref-e, Mercados EMI, Indra, and Report, F. *Study on Tariff Design for Distribution Systems. Prepared for the European Commission DG General for Energy*. European Commission (Directorate-General for Energy), Belgium, 2015. https://energy.ec.europa.eu/study-tariff-design-distribution-systems_en

Robinson, J., and Erickson, L. E. Infrastructure for Charging Electric Vehicles. In Erickson, L.E., Robinson, J. Brase, G. Cutson, J (Ed.). *Solar Powered Charging Infrastructure for Electric Vehicles*, CRC Press, United States of America, 2016, pp. 35–51. <https://www.routledge.com/Solar-Powered-Charging-Infrastructure-for-Electric-Vehicles-A-Sustainable/Erickson-Robinson-Brase-Cutson/p/book/9780815383710>

Roth, A., Brückman, R., Jimeno, M., Đukan, M., Kitzing, L., Breitschopf, B., Alexander-Haw, A., and Amazo Blanco, A. *Renewable energy financing conditions in Europe: survey and impact analysis*, Aures, Germany, 2021. https://backend.orbit.dtu.dk/ws/portalfiles/portal/251879749/AURES_II_D5_2_financing_conditions.pdf

Ruhnau, O., Hirth, L., and Praktiknjo, A. Time series of heat demand and heat pump efficiency for energy system modelling, *Scientific Data*, Vol. 6, No 1, 2019, pp. 1–10. <https://doi.org/10.1038/s41597-019-0199-y>

Schiro, F., Stoppato, A., and Benato, A. Modelling and analyzing the impact of hydrogen enriched natural gas on domestic gas boilers in a decarbonization perspective. *Carbon Resources Conversion*, Vol. 3, 2020, pp. 122–129. <https://doi.org/10.1016/j.crcon.2020.08.001>

Sims, R. E. H., Schock, R. N., Adegbululgbe, A., Fenmann, J., Konstantinaviciute, I., Moomaw, W., Nimir, H. B., Schlamadinger, B., Torres-Martínez, J., Turner, C., Uchiyama, Y., Vuori, S. J. V., Wamukonya, N., and Zhang, X. Energy supply. In B. Metz, O. R. Davidson, P. R. Bosch, R. Dave, and L. A. Meye (Eds.), *Climate Change 2007: Mitigation. Contribution of Working Group III to the Fourth Assessment Report of the Intergovernmental Panel on Climate Change*, Cambridge University Press, United Kingdom, 2007.

CBS (Statistics Netherlands). *CO₂ equivalents*, 2023. <https://www.cbs.nl/en-gb/news/2019/37/greenhouse-gas-emissions-down/co2-equivalents>

Sun, H., Yang, H., and Gao, X. Investigation into spacing restriction and layout optimization of wind farm with multiple types of wind turbines, *Energy*, Vol. 168, No. 2019, 2019, pp. 637–650. <https://doi.org/10.1016/j.energy.2018.11.073>

Tsiropoulos, I., Tarvydas, D., and Lebedeva, N. *Li-ion batteries for mobility and stationary storage applications - Scenarios for costs and market growth*. EUR - Scientific and Technical Research Reports. Publications Office of the European Union, Luxembourg, 2018a, ISBN 978-92-79-97254-6, doi:10.2760/87175, JRC113360. <https://publications.jrc.ec.europa.eu/repository/handle/JRC113360>

Tsiropoulos, I., Tarvydas, D., and Zucker, A. *Cost development of low carbon energy technologies - Scenario-based cost trajectories to 2050*, 2017 edition, Publications Office of the European Union, Luxembourg, 2018b. <https://doi.org/10.2760/23266>

Twidale, S. *Analyst nudge EU carbon price forecasts higher but warn on Ukraine risks*, Reuters, 2022. <https://www.reuters.com/world/europe/analysts-nudge-eu-carbon-price-forecasts-higher-warn-ukraine-risks-2022-04-29/>

U.S. Energy Information Agency. (2020). *Table 8.4. Average Power Plant Operating Expenses for Major U.S. Investor-Owned Electric Utilities, 2010 through 2020 (Mills per Kilowatt-hour)* [Dataset], 2020. https://www.eia.gov/electricity/annual/html/epa_08_04.html

U.S. Pacific Northwest National Laboratory. *Hydrogen Density at different temperatures and pressures (Density (SI).xls)* [Dataset], United States of America, n.d., <https://h2tools.org/hyarc/hydrogen-data/hydrogen-density-different-temperatures-and-pressures>

UK Department for Business, Energy and Industrial Strategy. *Conversion factors 2022: condensed set (for most users)* [Dataset], United Kingdom, 2023. <https://www.gov.uk/government/publications/greenhouse-gas-reporting-conversion-factors-2022>

Urbina, A. Solar electricity in a changing environment: The case of Spain, *Renewable Energy*, Vol. 68, 2014, pp. 264–269. <https://doi.org/10.1016/j.renene.2014.02.005>

Vakkilainen, E. K. (2017). 3 - Boiler Processes. In Vakkilainen, E. K. (Ed.), *Steam Generation from Biomass: Construction and design of large boilers*, 2017 pp. 57–86. <https://doi.org/10.1016/b978-0-12-804389-9.00003-4>

Vanwortswinkel, L., and Wouter, N. (2010). Industrial Combustion Boilers. IEA Energy Technology Systems Analysis Programme, Denmark, 2010. https://iea-etsap.org/E-TechDS/HIGHLIGHTS%20PDF/I01-ind_boilers-GS-AD-qct%201.pdf

Wang, B., Zhao, D., Dehghanian, P., Tian, Y., and Hong, T. Aggregated Electric Vehicle Load Modelling in Large-Scale Electric Power Systems, *IEEE Transactions on Industry Applications*, Vol. 56, No 5, 2020, pp. 5796–5810. <https://doi.org/10.1109/TIA.2020.2988019>

Ward, J. Hierarchical Grouping to Optimize an Objective Function. *Journal of the American Statistical Association*, Vol. 58, No 301, 1963, pp. 236–244. <https://doi.org/10.1080/01621459.1963.10500845>

Yu, Y., Zhang, T., and Guan, Y. Network-Flow-Based Formulations for Convex Hull Pricing with Maximum Start-Ups, *IEEE Transactions on Power Systems*, Vol. 37, No 2, 2022, pp. 1198–1206. <https://doi.org/10.1109/TPWRS.2021.3100560>

Zhou, Y., and Searle, S. *Cost of Renewable Hydrogen Produced Onsite at Hydrogen Refuelling Stations in Europe*. The International Council on Clean Transportation, Washington, 2022. <https://theicct.org/wp-content/uploads/2022/02/fuels-eu-cost-renew-H-produced-onsite-H-refueling-stations-europe-feb22.pdf>

Zimmermann, F., Bublitz, A., Keles, D., Dehler, J., and Fichtner, W. An analysis of long-term impacts of demand response on investments in thermal power plants and generation adequacy. *International Conference on the European Energy Market EEM*, 2016. <https://doi.org/10.1109/EEM.2016.7521216>

Definitions

| | |
|-------|--|
| ACER | Agency for the Cooperation of Energy Regulators |
| ASHP | Air Sourced Heat Pumps |
| BATS | Batteries |
| BDEW | German Association of Energy and Water Industries |
| BGW | German Federation of the Gas and Water Industry |
| BW | Bandwidth |
| CAPEX | Capital Expenses |
| CCGT | Combined Cycle Gas Turbines |
| CDD | Cooling Degree Days |
| CHP | Combined Heat and Power |
| COP | Coefficient of Performance |
| DAI | Distributed Artificial Intelligence |
| DE | Germany |
| DHW | Domestic Heat Water |
| DSR | Demand Side Response |
| DSO | Distributor System Operator |
| EB | Energy based |
| EC | Energy Community |
| ED | Electrical Demand |
| ENS | Energy Not Served |
| ELVIS | Electric Vehicle Charging Infrastructure Simulator |
| ERAA | European Resources Adequacy Assessment |
| ES | Spain |
| ESES | Energy System Evolution Scenario |
| EP | Electrical Power |
| EU | European Union |
| EUA | European Union Allowances |
| EUI | Energy Use Intensity |
| EV | Electric Vehicle |
| FCEL | Fuel cell |
| GAMS | General Algebraic Modelling Language |
| GAST | Gas Turbines |
| GHG | Greenhouse Gas |
| GR | Greece |
| GSHP | Ground Sourced Heat Pumps |
| HDD | Heating Degree Days |
| HDAM | Hydro-reservoirs |
| HP | Heat Pump |

| | |
|--------|---|
| HPHR | Open-loop Hydro Pumped Storage |
| PHPS | Closed-loop Hydro Pumped Storage |
| HRDT | Hard coal-fuelled Generators |
| HRE4 | Heat Roadmap Europe |
| HRQR | Hydro Run-of-River |
| HV | High Voltage |
| ICCT | International Council on Clean Transportation |
| IEA | International Energy Agency |
| IREC | Catalonia Institute for Energy Research |
| IRENA | International Renewable Energy Agency |
| ISLP | Industrial Standard Load Profiles |
| ITC | Information and Communication Technology |
| JRC | Joint Research Centre |
| kWe | Kilowatt Electrical |
| kWh | Kilowatt-hour |
| kWt | Kilowatt Thermal |
| LCOE | Levelized Cost of Electricity |
| LIGT | Lignite-fuelled generator |
| LV | Low Voltage |
| MFB | Multi Family Buildings |
| MILP | Mixed Integer Linear Programming problem |
| MODECO | Modelling of Energy Communities |
| MV | Medium Voltage |
| MWe | Megawatt Electrical |
| MWh | Megawatt-hour |
| MWt | Megawatt Thermal |
| NACE | Nomenclature of Economic Activities |
| NAICS | North American Industrial Classification System |
| NREL | National Renewable Energy Laboratory |
| NPV | Net Present Value |
| OCGT | Open Cycle Gas Turbine |
| OECD | Economic Cooperation and Development |
| OILT | Oil-fuelled generators |
| ORES | Other Renewables |
| OPEX | Operational Expenses |
| OTHT | Other non-renewables |
| PEM | Proton Exchange Membrane |
| PHOT | Solar photovoltaics |
| PPA | Power Purchase Agreement |

| | |
|-------|--|
| PV | Photovoltaic |
| RAC | Regulamento do Autoconsumo |
| R2M | Research to Market solution |
| SC | Space Cooling |
| SFB | Single Family Building |
| SME | Small and Medium Enterprises |
| SOC | State-of-Charge |
| TD | Thermal Demand |
| TOU | Time-of-Use |
| TP | Thermal Power |
| TYNDP | Ten Year National Development Plan |
| UCED | Unit Commitment and Economic Dispatch |
| VOM | Variable Operational and Maintenance costs |
| VOLL | Value of Lost Load |
| V2G | Vehicle-to-Grid |
| WACC | Weighted Average Cost of Capital |
| WD | Working days |
| WK | Weekend |
| WSHP | Water Sourced Heat Pumps |
| WTOF | Wind Offshore |
| WTON | Wind Onshore |

List of boxes

| | |
|---|----|
| Box 1. Defining “close enough” optimal solutions under limited testing times..... | 52 |
| Box 2 Drawing the line between economic benefits and purely financial profit generation..... | 55 |
| Box 3. Key trends from the modelled energy prices under a power system evolution led by distributed energy | 88 |

List of figures

| | |
|--|----|
| Figure 1. Power production and services by energy citizens per member state expected in 2050 | 9 |
| Figure 2. Installed power by technology in Germany in 2025, 2030 and 2030 for selected reference scenario | 13 |
| Figure 3. Installed power by technology in Spain in 2025, 2030 and 2030 for selected reference scenario .. | 13 |
| Figure 4. Monthly mean, maximum and minimum air temperature values registered in each target region... <td>14</td> | 14 |
| Figure 5. Mean air temperature per hour registered each season in the analysed regions..... | 15 |
| Figure 6. Mean solar load factor per hour registered each season in the analysed regions..... | 15 |
| Figure 7. Mean wind load factor per hour registered each season in the analysed regions | 15 |
| Figure 8. Community-energy market interaction considered for all archetypes except the Virtual community | 17 |
| Figure 9. Annual energy consumption in MWh/year per household (Single-family and Multi-Family buildings) and region disaggregated by end usage | 34 |
| Figure 10. Distribution of companies per working day cluster in each economic sector | 36 |
| Figure 11. Hourly curves showing total energy demand (heat and electricity) for selected industrial standard load profiles from the JERICHO-E database [data adjusted to 1000 MWh/day]..... | 38 |
| Figure 12. EV share in total passenger cars fleet per year | 41 |
| Figure 13. Economic assumptions considered for smart and non-smart EV charging stations..... | 43 |
| Figure 14. Schematic diagram of the optimization models used within MODECO project..... | 49 |
| Figure 15. Feasible operational region for a CHP unit given four operational points | 61 |
| Figure 16. Monthly heat demand per sector in the Business park archetype in 2025 | 64 |
| Figure 17. Mean heat consumption reported in 2025 in the Business park archetype in Germany and Spain | 65 |
| Figure 18. Daily electricity demand per sector in the Business park archetype in Spain [2025]..... | 65 |
| Figure 19. Daily electricity demand per sector in the Business park archetype in Germany [2025]..... | 66 |
| Figure 20. Mean electricity consumption reported in 2025 in the Business park archetype in Germany and Spain..... | 66 |
| Figure 21. Mean heat consumption reported in 2025 in the Industrial polygon archetype..... | 68 |
| Figure 23. Monthly heat demand by temperature level in the Industrial polygon in 2025 | 69 |
| Figure 24. Mean electricity consumption reported in 2025 in the Industrial polygon archetype (Others include EV and heat pump electrical consumption)..... | 70 |
| Figure 25. Monthly heat demand per sector in the Rural town archetype in 2025 | 72 |
| Figure 26. Mean heat consumption reported in 2025 in the Rural town communities in Germany and Spain | 72 |
| Figure 27. Daily electricity demand per sector in the Rural town archetype in Germany [2025] | 73 |
| Figure 28. Daily electricity demand per sector in the Rural town archetype in Spain [2025] | 73 |
| Figure 29. Mean electricity consumption reported in 2025 in the Rural town communities in Germany and Spain..... | 74 |
| Figure 30. Monthly heat demand per sector in the Urban district archetype in 2025 | 76 |
| Figure 31. Mean heat consumption reported in 2025 in the Urban district communities in Germany and Spain | 76 |
| Figure 32. Annual heat consumption and associated CO2 emissions for the Urban district archetype | 77 |

| | |
|---|-----|
| Figure 33. Daily electricity demand per sector in the Urban district archetype in Germany [2025] | 77 |
| Figure 34. Daily electricity demand per sector in the Urban district archetype in Spain [2025] | 78 |
| Figure 35. Mean electricity consumption reported in 2025 in the Urban district communities | 78 |
| Figure 36. Annual electricity consumption and associated CO ₂ emissions for the Urban district archetype.... | 79 |
| Figure 37. Monthly heat demand per sector in the Virtual community archetype in 2025 | 81 |
| Figure 38. Mean heat consumption reported in 2025 in the virtual community archetype in Germany and Spain..... | 81 |
| Figure 39. Monthly electricity demand per sector in the Virtual community archetype in 2025 | 82 |
| Figure 40. Mean electricity consumption reported in 2025 in the Virtual community archetype | 82 |
| Figure 41. Annual demand versus energy dispatched per technology and year in Germany and Spain..... | 84 |
| Figure 42. Mean marginal price per season and year registered in Spain and Germany..... | 86 |
| Figure 43. Mean daily marginal price registered in Spain in 2025, 2030 and 2040..... | 87 |
| Figure 44. Mean daily marginal price registered in Germany in 2025, 2030 and 2040..... | 87 |
| Figure 45. Mean marginal price per hour and year registered in Spain and Germany | 88 |
| Figure 46. TOU energy tariffs applicable to Energy communities in Germany | 89 |
| Figure 47. TOU energy tariffs applicable to Energy communities in Spain..... | 90 |
| Figure 48. Investments performed in the Business park archetype under different Use-of-Network structures | 92 |
| Figure 49. Electrical balance for the Business park communities under a Bandwidth tariff in two representative days in January and August 2040 [Maximum Ω] | 93 |
| Figure 50. Annual investments performed in the Business park archetype under the Bandwidth tariff case .. | 93 |
| Figure 51. Solar LCOE in Germany and Spain versus mean marginal price during high solar radiation hours | 94 |
| Figure 52. Electrical balance for the Business park communities under a Peak power tariff in two representative days in February and August 2040 [Minimum Ω]..... | 95 |
| Figure 53. Electrical balance for the Business park communities under a No Charges tariff in two representative days in February and August 2040 [Minimum Ω]..... | 96 |
| Figure 54. Investments performed in the Industrial polygon under different Use-of-Network structures..... | 97 |
| Figure 55. Electrical balance for the Industrial polygon communities under a Bandwidth tariff in selected representative days in January and August 2040 [Maximum Ω]..... | 98 |
| Figure 56. Wind LCOE in Germany and Spain versus mean marginal price | 99 |
| Figure 57. Annual investments performed in the Industrial polygon archetype under the Bandwidth tariff case..... | 99 |
| Figure 58. Electrical balance for the Industrial polygon communities under a Peak power tariff in selected representative days in January and August 2040 [Maximum Ω]..... | 100 |
| Figure 59. Investments performed in the Rural town under different Use-of-Network structures | 101 |
| Figure 60. Electrical balance for the Rural town communities under a Peak power tariff in selected representative days in January and August 2040 [Maximum Ω]..... | 102 |
| Figure 61. Electrical balance for the Rural town communities under a TOU tariff in selected representative days in January and August 2040 [Maximum Ω] | 103 |
| Figure 62. Investments performed in the Urban district under different Use-of-Network structures | 104 |

| | |
|---|-----|
| Figure 63. Electrical balance for the Urban district communities under a Peak power tariff in selected representative days in January and August 2040 | 105 |
| Figure 64. Electrical balance for the Urban district communities under a Bandwidth tariff in selected representative days in January and August 2040 | 106 |
| Figure 65. Electrical balance for the Urban district communities under a TOU tariff in selected representative days in January and August 2040 [Maximum Ω] | 107 |
| Figure 66. Investments performed in the Virtual community under different Use-of-Network structures | 108 |
| Figure 67. Electrical balance for the Virtual communities under a Bandwidth tariff in selected representative days in January and August 2040 [Maximum Ω] | 109 |
| Figure 68. Electrical balance for the Virtual communities under a Peak power tariff in selected representative days in January and August 2040 [Maximum Ω] | 110 |
| Figure 69. Electrical balance for the Virtual communities under a TOU tariff in selected representative days in January and August 2040 [Maximum Ω] | 111 |
| Figure 70. Annual investments performed in the Virtual community archetype under the TOU case..... | 111 |
| Figure 71. Investments performed in German archetypes under a TOU tariff with dynamic, flat and PPA prices..... | 114 |
| Figure 72. Investments performed in German archetypes under the base tariff scenarios considering different discount rates..... | 115 |
| Figure 73. Annual demand, purchased electricity and local generation per type of technology in German cases | 118 |
| Figure 74. Annual demand, purchased electricity and local generation per type of technology in Spanish cases | 119 |
| Figure 75. Annual thermal demand and heat generation per type of technology in German cases. | 120 |
| Figure 76. Annual thermal demand and heat generation per type of technology in Spanish archetypes. | 121 |
| Figure 77. CO2 emissions from the operation of installed assets versus base case in the German archetypes | 123 |
| Figure 78. CO2 emissions from the operation of installed assets versus base case in the Spanish archetypes | 124 |
| Figure 79. Mean annual fuel cost and total fuel consumption in the Industrial polygon | 126 |
| Figure 80. CO2 emissions from the operation of installed assets versus base case in the German archetypes | 126 |
| Figure 81. Annual electrical balance, energy sales income and electrical cost avoided in German scenarios | 129 |
| Figure 82. Annual electrical balance, energy sales income and electrical cost avoided in Spanish scenarios | 130 |
| Figure 83. Avoided energy costs in the Spanish scenarios disaggregated by cost component..... | 131 |
| Figure 84. Avoided energy costs in the German scenarios disaggregated by cost component | 132 |
| Figure 85. Disaggregated energy payments (price, taxes, Use-of-Network chargers) in German scenarios.. | 135 |
| Figure 86. Disaggregated energy payments (price, taxes, Use-of-Network chargers) in Spanish scenarios.. | 136 |
| Figure 87. CHP assumed configuration considered for small natural gas-fuelled units. | 201 |
| Figure 88. CHP assumed configuration for small biomass-fuelled units. | 201 |
| Figure 89. Simplified feasible operational region considered for units (operating points in green) | 202 |
| Figure 90. Reference hydrogen tank dimensions and occupied surface area | 204 |

List of tables

| | |
|--|----|
| Table 1. Definition of Renewable and Citizen energy community in the European legislation | 8 |
| Table 2. Minimum and maximum WACC values considered for each target region | 16 |
| Table 3. Summary of the rules applied to self-consumption under the Portuguese normative | 18 |
| Table 4. Number and type of building in each archetype for year 2025 | 19 |
| Table 5 Biomass prices considered for Germany and Spain in the target years [EUR/MWh]..... | 19 |
| Table 6 Green hydrogen prices for Germany and Spain in the target years [EUR/MWh]..... | 20 |
| Table 7 Technologies considered in each Energy community archetype as potential investment options | 21 |
| Table 8 Comparison of CAPEX and OPEX values proposed by MODECO against ESES' assumptions for available technologies | 22 |
| Table 9 Regional data used to calculate the applicable Unit Distribution Tariff per voltage level | 24 |
| Table 10 Applicable capacity-based charges per country and voltage level | 26 |
| Table 11 Applicable contracted bandwidth cost and penalization fees per country and voltage level | 27 |
| Table 12 <i>Per unit</i> taxes applicable to energy carriers of interest according to OECD data..... | 28 |
| Table 13 Type of customer represented in the electrical standard load profiles developed by BDEW | 30 |
| Table 14 Annual electricity demand from Single-family and Multi-family units without considering space cooling..... | 31 |
| Table 15 Building types considered in the gas standard load profiles methodology..... | 33 |
| Table 16 Sink and source temperature applicable to considered heat pump technologies | 39 |
| Table 17 CAPEX, OPEX and useful life considered for heat pumps and boilers used in residential users | 39 |
| Table 18 Installation and operation costs of equipment for heat pump's participation in DSR programs..... | 40 |
| Table 19 Number of non-smart charging stations considered in each archetype by year and owner category..... | 42 |
| Table 20 Assumptions considered for charging stations for domestic and business use | 42 |
| Table 21 Assumptions for standard EV models considered | 43 |
| Table 22 Number of EV circulating in the energy communities per year disaggregated by owner type..... | 44 |
| Table 23 GHG emission factors for natural gas combustion in the residential sector | 46 |
| Table 24 Indicators associated with solar PV and Energy communities. | 50 |
| Table 25 Definition of the cost terms used in the investment model's objective function | 53 |
| Table 26 CO ₂ emission factors associated to natural gas, hydrogen and biomass combustion..... | 62 |
| Table 27 Business park indicators..... | 63 |
| Table 28 CO ₂ emissions associated with energy usage in the Business park archetype | 64 |
| Table 29 Industrial polygon indicators | 67 |
| Table 30 CO ₂ emissions associated with energy usage in the Industrial polygon archetype | 67 |
| Table 31 Rural town indicators..... | 70 |
| Table 32 CO ₂ emissions associated with energy usage in the Rural town archetype | 71 |
| Table 33 Urban district indicators | 74 |
| Table 34 CO ₂ emissions associated with energy usage in the Urban district archetype | 75 |

| | |
|--|-----|
| Table 35 Virtual community indicators | 79 |
| Table 36 CO ₂ emissions associated with energy usage in the Virtual community archetype | 80 |
| Table 37 Annual volume of CO ₂ emissions associated to power generation in Germany and Spain | 85 |
| Table 38 Mean annual marginal price registered in Germany and Spain for each target year..... | 86 |
| Table 39 Hours classified as peak in each country, year and season | 90 |
| Table 40 Value of the objective function obtained for each case in million euros [M€]..... | 91 |
| Table 41 Use-of-Network charges applied in the Bandwidth scenarios by region and voltage level | 133 |
| Table 42 Use-of-Network charges (€/MWh) applicable in the TOU scenario by year, user and voltage level. | 134 |
| Table 44. Nomenclature for parameters in the Investment model | 161 |
| Table 45. Variables for the Investment model..... | 163 |
| Table 46. Objective function for the Investment model..... | 165 |
| Table 48. Available roof and land equations for the Investment model..... | 169 |
| Table 49. Wind generation parameters for the Investment model..... | 170 |
| Table 50. Wind generation equations for the Investment model..... | 170 |
| Table 51. Solar generation parameters for the Investment model | 171 |
| Table 52. Solar generation equations for the Investment model | 171 |
| Table 53. Electrical Storage parameters for the Investment model | 171 |
| Table 54. Electrical Storage equations for the Investment model | 171 |
| Table 55. Hydrogen Storage parameters for the Investment model | 172 |
| Table 56. Hydrogen Storage equations for the Investment model | 173 |
| Table 57. Electrolyzer parameters for the Investment model..... | 174 |
| Table 58. Electrolyzer equations for the Investment model | 174 |
| Table 59. CHP parameters for the Investment model..... | 174 |
| Table 61. V2G parameters for the Investment model | 176 |
| Table 63. Demand response parameters for the Investment model..... | 178 |
| Table 64. Demand response equations for the Investment model..... | 178 |
| Table 65. Boiler parameters for the Investment model..... | 178 |
| Table 66. Boiler equations for the Investment model..... | 179 |
| Table 67. Sets for the Operational model..... | 180 |
| Table 68. Parameters for the Operational model | 180 |
| Table 69. Variables for the operational Model..... | 185 |
| Table 72. Peak power constraints for the Operational model..... | 189 |
| Table 73. Time of Use constraints for the Operational model..... | 189 |
| Table 78. Demand response constraints for the Operational model | 192 |
| Table 80. Hydrogen Storage constraints for the Operational model | 194 |
| Table 81. Boilers constraints for the Operational model..... | 195 |
| Table 82. Scalar parameters for PV solar technologies | 196 |

| | |
|---|-----|
| Table 83. Scalar parameters for Wind turbine technologies..... | 197 |
| Table 84. Scalar parameters for EV smart chargers..... | 198 |
| Table 85. Scalar parameters for biomass-fuelled CHP | 199 |
| Table 87 Efficiency and fuel characteristics considered for each CHP configuration | 202 |
| Table 88 Scalar parameters for the PEM electrolyzer..... | 203 |
| Table 89 Scalar parameters for the Hydrogen storage tank | 204 |
| Table 90 Scalar parameters for energy and power based batteries (0.35 C-rate)..... | 205 |
| Table 91 Scalar parameters for boilers | 206 |
| Table 92 Scalar parameters for demand response..... | 207 |
| Table 93. Gap values reported by the EC investment model for the base case tariff scenarios..... | 208 |
| Table 94. Gap values reported by the EC investment model for the price rate sensitivity cases | 208 |
| Table 95. Gap values reported by the EC investment model for the discount rate sensitivity cases | 209 |
| Table 96. Gap values reported by the EC operational model for the base case tariff scenarios | 210 |

Annexes

Annex 1. Mathematical Formulation for MODECO's Investment Model

Nomenclature

Table 43. Nomenclature for the Investment model

| Set | Description | Elements |
|------------|--|---|
| F | Set of all considered fuels. | $F = \{\text{Natural gas, biomass, hydrogen}\}$, where $f_1 = \text{Natural Gas}$, $f_2 = \text{Biomass}$, $f_3 = \text{Hydrogen}$. |
| K^{GEN} | Different generator technologies considered. PV accounts for Photovoltaic Panels, WT for Wind Turbine, CHP for Combined Heat & Power, and EL for Electrolyser. $S_{CHP_{f_{1,3}}}$ consumes fuel of type f_1 and f_3 , while $S_{CHP_{f_2}}$ only consume fuels type f_2 . | $K^{GEN} = \{S_{PV1}, S_{PV2}, S_{WT1}, S_{WT2}, S_{CHP_{f_{1,3}}}, S_{CHP_{f_2}}, S_{EL}\}$ |
| K^{H_2} | Set of hydrogen storages considered. | $K^{H_2} = \{S_{H_2}\}$ |
| K^{EL} | Set of all Electrolysers considered. | $K^{EL} = \{S_{EL}\}$ |
| K^{EGEN} | Different electrical generator technologies considered. PV accounts for Photovoltaic Panels, WT for Wind Turbine, CHP for Combined Heat & Power. | $K^{EGEN} = K^{GEN} \setminus K^{EL}$ |
| K^{ES} | Different electrical storage technologies considered. ES accounts for Electrical Storage. | $K^{ES} = \{S_{ES1}, S_{ES2}\}$ |
| K^{ST} | Set of all storage technologies considered. S_{H_2} accounts for hydrogen storage. | $K^{ST} = K^{ES} \cup K^{H_2}$ |
| K^{V2G} | Set of V2G chargers considered. | $K^{V2G} = \{v2g\}$, *only one type of V2G can be considered in our modelisation. |
| K^B | Set of Boilers considered. | $K^B = \{S_{B1}, S_{B2}\}$, *only a second type of boiler is considered in Industrial Polygon Archetype |
| K | Set of all technologies considered: generators, storages, vehicle-to-grid chargers (V2G) and electrolyzer. | $K = K^{EGEN} \cup K^{ST} \cup K^{V2G} \cup K^{EL} \cup K^B$ |
| T | Set of time steps in a day. See that N_T is used as the number of time steps considered. | $T = \{0, 1, 2, \dots, N_T = 23\}$ |
| D | Set of representative days. See that N_D is used as the number of representative days considered. | $D = \{0, 1, 2, \dots, N_D\}$ |

| Set | Description | Elements |
|------------|--|---------------------------------|
| M | Set of indexed months. | $M = \{1, 2, \dots, 12\}$ |
| Y | Set of years considered in investment planning. See that N_y is used as the number of years considered | $Y = \{1, 2, \dots, N_y = 15\}$ |
| W | Set of all coordinates where investment is allowed. | $W = \{(y, 1, 0, 0), y \in Y\}$ |
| W_y | Coordinates where investment is allowed in year y . | $W_y = \{(y, 1, 0, 0)\}$ |

Source: own elaboration.

Table 44. Nomenclature for parameters in the Investment model

| Parameter | Description | Units |
|--------------------------------|--|----------------------|
| Prices | | |
| $\lambda_{y,m,d,t}^{buy}$ | Purchase price of kWh . | $\text{€}/kWh$ |
| $\lambda_{y,m,d,t}^{fuel,f_i}$ | Purchase prices of fuel $f_i \in F$. | $\text{€}/mol_{f_i}$ |
| $\lambda_{y,m,d,t}^{ev}$ | Price for the user of the V2G charge. | $\text{€}/kWh$ |
| $\lambda_{y,m,d,t}^{sell}$ | Sell price of kWh . | $\text{€}/kWh$ |
| $\lambda_{y,m}^{peak}$ | Peak power price in month m and year y . | $\text{€}/kWh$ |
| $\lambda_{y,m}^{fix}$ | Fix power price in month m and year y . | $\text{€}/kWh$ |
| $\lambda_{y,m}^{exceed}$ | Price of exceeded power in month m and year y . | $\text{€}/kWh$ |
| λ^{dr} | Cost of the activation of demand response. | $\text{€}/kWh$ |
| $C_{S_k,y}^{inv,GEN}$ | Investment cost for kW _e of s_k installed in year y , for $s_k \in K^{GEN} \cup K^B$. | $\text{€}/kW$ |
| $C_{S_k,y}^{op,GEN}$ | Operational cost for kW _e of s_k installed in year y , for $s_k \in K^{GEN} \cup K^B$. | $\text{€}/kW$ |
| $C_{S_k,y}^{inv,ES}$ | Investment cost for kWh of s_k installed in year y , for $s_k \in K^{ES}$. | $\text{€}/kWh$ |
| $C_{S_k,y}^{op,ES}$ | Operational cost for kWh of s_k installed in year y , for $s_k \in K^{ES}$. | $\text{€}/kWh$ |
| $C_{S_k,y}^{inv,H_2}$ | Investment cost for m^3 of s_k installed in year y , for $s_k \in K^{H_2}$. | $\text{€}/m^3$ |
| $C_{S_k,y}^{op,H_2}$ | Operational cost for m^3 of s_k installed in year y , for $s_k \in K^{H_2}$. | $\text{€}/m^3$ |

| Parameter | Description | Units |
|-----------------------------|--|-------------------------|
| $C_{S_k,y}^{inv,EL}$ | Investment cost for kW of s_k installed in year y , for $s_k \in K^{EL}$. | €/kW |
| $C_{S_k}^{sv,EL}$ | Salvage value for a kW of s_k installed, for $s_k \in K^{EL}$. | €/kW |
| $C_{S_k,y}^{op,EL}$ | Operational cost for kW of s_k installed in year y , for $s_k \in K^{GEN}$. | €/kW |
| $C_y^{inv,V2G}$ | Investment cost for V2G charger installed in year y . | €/charger |
| $C_y^{sv,v2g}$ | Salvage value for V2G charger installed. | €/charger |
| $C_y^{op,v2g}$ | Operational cost for V2G charger installed in year. | €/charger |
| C^{gen} | Cost for generated kWh , only in Virtual Community. | €/kWh |
| Loads | | |
| $L_{y,m,d,t}^{el}$ | Electrical load curve. | kW |
| $L_{y,m,d,t}^{th}$ | Thermal load curve. | kW |
| $L_{y,m,d,t}^{ev}$ | Private household EV load curve. | kW |
| $L_{y,m,d,t}^{HP}$ | HP electrical load curve. | kW |
| $L_{y,m,d,t}^{th,h}$ | High temperature thermal load curve (only for industrial archetype). | kW |
| EVs | | |
| $EV_{y,m,d,t}^{in}$ | Number of EV that come in at public V2G charging station. | Positive integer vector |
| $EV_{y,m,d,t}^{out}$ | Number of EV that leave in at public V2G charging station. | Positive integer vector |
| Renewable Generation | | |
| $LF_{y,m,d,t}^{WT}$ | Wind power load factor. kW generated per kW installed. | kW/kW installed |
| $LF_{y,m,d,t}^{PV}$ | Solar power load factor. kW generated per kW installed. | kW/kW installed |
| Other | | |
| Δ_t | Time interval between time steps, in hours. | (0,1] |
| $\omega_{y,m,d}$ | Weight of representative day d in month m and year y . | Positive integer |
| $A_{S_k}^{GEN}$ | Surface occupied by kW of generator s_k installed. | m^2/kW |

| Parameter | Description | Units |
|----------------------|--|------------------------|
| $A_{s_k}^{ES}$ | Surface occupied by kWh of storage s_k installed. | m^2/kWh |
| $A_{s_k}^{H_2}$ | Surface occupied by m^3 of hydrogen storage s_k installed. | m^2/m^3 |
| A^{V2G} | Surface occupied by charger installed. | $m^2/charger$ |
| $A_{y,m,d,t}^{roof}$ | Total available surface available for installing technologies in roof. | m^2 |
| $A_{y,m,d,t}^{land}$ | Total available surface available for installing technologies in land. | m^2 |
| LS_{s_k} | Life stamp of sub technology s_k . | Positive integer value |

Source: own elaboration.

Table 45. Variables for the Investment model

| Variables | Description | Domain | Units |
|--|---|--------|---------|
| $p_{s_k,y,m,d,t}^{gen,el}$ | Generated electrical power by technology s_k . | R^+ | kW |
| $p_{s_k,y,m,d,t}^{gen,th}$ | Generated thermal power by CHP type s_k . | R^+ | kW |
| $p_{y,m,d,t}^{sell}$ | Power injected to the grid. | R^+ | kW |
| $p_{y,m,d,t}^{buy}$ | Electrical power bought from the grid. | R^+ | kW |
| $f_i^{buy}_{y,m,d,t}$ | Fuel f_i bought externally. | R^+ | mol/h |
| $p_{s_k,y,m,d,t}^{ch}$ | Charged power to electrical storage $s_k \in K^{ES}$. | R^+ | kW |
| $p_{s_k,y,m,d,t}^{dch}$ | Discharged power from electrical storage $s_k \in K^{ES}$. | R^+ | kW |
| $p_{v2g,y,m,d,t}^{ch}$ | Charged power to electrical storage $s_k \in K^{V2G}$. | R^+ | kW |
| $p_{v2g,y,m,d,t}^{dch}$ | Discharged power from $s_k \in K^{V2G}$. | R^+ | kW |
| $soc_{s_k,y,m,d,t}^{ES}$ | Energy stored in storage $s_k \in K^{ES}$. | R^+ | kWh |
| $soc_{y,m,d,t}^{ev}$ | Energy stored in storage $s_k \in K^{V2G}$. | R^+ | kWh |
| $e_{s_k,\hat{y},\hat{m},\hat{d},\hat{t}}^{inst,a}$ | Installed energy capacity for technology $s_k \in K^{ES}$ in area a={land, roof}. | R^+ | kWh |
| $v_{s_k,\hat{y},\hat{m},\hat{d},\hat{t}}^{inst}$ | Installed volume for technology $s_k \in K^{H_2}$. | R^+ | m^3 |
| $n_{\hat{y},\hat{m},\hat{d},\hat{t}}^{inst}$ | Installed number of V2G chargers. | N | int |
| $p_{s_k,y,m,d,t}^{cons,EL}$ | Power consumed by electrolyser $s_k \in K^{EL}$. | R^+ | kW |

| Variables | Description | Domain | Units |
|--|---|--------|---------------------------|
| $f_{3s_k,y,m,d,t}^{gen,EL}$ | Hydrogen generated by electrolyzer $s_k \in K^{EL}$. | N | mol_{H_2}/h |
| $f_{3S_{CHPf_{1,3}},y,m,d,t}^{cons,CHP}$ | Hydrogen (fuel f_3) consumed by CHP type $S_{CHPf_{1,3}}$ (only for industrial archetype). | R^+ | $\frac{mol_{H_2}}{h}$ |
| $f_{1S_{CHPf_{1,3}},y,m,d,t}^{cons,CHP}$ | Natural gas (fuel f_1) consumed by CHP type $S_{CHPf_{1,3}}$ (gas). | R^+ | $\frac{mol_{gas}}{h}$ |
| $f_{2S_{CHPf_2},y,m,d,t}^{cons,CHP}$ | Biomass f_2 consumed by CHP type S_{CHPf_2} (biomass). | R^+ | $\frac{mol_{biomass}}{h}$ |
| $m_{s_k,y,m,d,t}^{H_2}$ | Quantity of hydrogen inside the hydrogen storage $s_k \in K^{H_2}$. | R^+ | mol_{H_2} |
| $f_{3s_k,y,m,d,t}^{ch}$ | Hydrogen rate inflow to $s_k \in K^{H_2}$. | R^+ | mol_{H_2}/h |
| $f_{3s_k,y,m,d,t}^{dch}$ | Hydrogen rate outflow from $s_k \in K^{H_2}$. | R^+ | mol_{H_2}/h |
| $x_{s_k,y,m,d,t}^{H_2}$ | Binary indicator charge/discharge in $s_k \in K^{H_2}$. | N | [0,1] |
| $ev_{y,m,d,t}^{in}$ | Number of captured number of EV's that come in. | N | Positive integer |
| $ev_{y,m,d,t}^{out}$ | Number of captured number of EV's that go out. | N | Positive integer |
| $ev_{y,m,d,t}^{con}$ | Number of captured number of EV's that are plugged in. | N | Positive integer |
| $x_{y,m,d,t}^{inc}$ | Binary indicator for the increment of demand. | N | [0,1] |
| $x_{y,m,d,t}^{dec}$ | Binary indicator for the decrement of demand. | N | [0,1] |
| $u_{y,m,d,t}^{inc}$ | Increased power demand. | R^+ | kW |
| $u_{y,m,d,t}^{dec}$ | Decreased power demand. | R^+ | kW |
| $x_{s_k,y,m,d,t}^{su}$ | Binary indicator for start-up $\forall s_k \in K^{CHP}$. | N | [0,1] |
| $x_{s_k,y,m,d,t}^{sd}$ | Binary indicator for shut-down $\forall s_k \in K^{CHP}$. | N | [0,1] |
| $u_{s_k,y,m,d,t}^{CHP}$ | Binary indicator for CHP state $\forall s_k \in K^{CHP}$. | N | [0,1] |

Source: own elaboration.

Objective Function

The investment model can be configured with three different objective functions depending on the tariff applied to the cost of electricity, Time of Use (TOU) – applicable to all cases with pure energy-based charges - Peak Power (PP), or Bandwidth (BW) scenarios. And so, the objective function defined for the investment model is the Eq. 18 that was described in Section 4.2.2, which is repeated below.

$$F = -Ben + (Cost_{buy}^{el,tariff} + Cost_{inv} + Cost_{op} + Cost_{dr} + Cost_{fuel} + Cost_{CHP} + Cost_{gen}), \text{tariff} \in \{TOU, PP, BW\}$$

The different terms defining the objective functions are described below,

Table 46. Objective function for the Investment model

| Term | Equation |
|----------------------------|--|
| <i>Ben</i> | The first term accounts for all the benefits obtained from selling energy to the electrical market; $Ben = \sum_{y=1}^{N_y} \left(\sum_{m \in M, d \in D} \frac{\omega_{y,m,d} \cdot \Delta_t}{(1+R)^{y-1}} \cdot \sum_{t \in T} (p_{y,m,d,t}^{\text{sell}} \cdot \lambda_{y,m,d,t}^{\text{sell,el}} + \lambda_{y,m,d,t}^{\text{ev}} \cdot ev_{y,m,d,t}^{\text{in}}) \right)$ |
| <i>Cost_{fuel}</i> | This term adds together all the cost related to the buy of the different fuels considered, $Cost_{\text{fuel}} = \sum_{y=1}^{N_y} \left(\sum_{m \in M, d \in D, t \in T} \frac{\omega_{y,m,d} \cdot \Delta_t}{(1+R)^{y-1}} \cdot \left(\sum_{f_i \in F} f_{i,y,m,d,t}^{\text{buy}} \cdot \lambda_{y,m,d,t}^{\text{fuel,f}_i} \right) \right)$ |
| <i>Cost_{inv}</i> | The third term <i>Cost_{inv}</i> accounts for the investment costs from all years. $Cost_{\text{inv}} = Cost_{\text{inv},A} + Cost_{\text{inv},B}$ <p>For the technologies with life stamp equal or greater than the investment period, then the first sum is the investment cost multiplied by the capacity installed.</p> $Cost_{\text{inv},A} = \sum_{s_k \in K^{\text{GEN}}} \sum_{y=1}^{N_y} \left(\frac{C_{s_k,y}^{\text{inv,GEN}} \cdot (N_y - y + 1)}{(1+R)^{y-1} \cdot LS_{s_k}} \right) \cdot \left(\sum_{\hat{y}, \hat{m}, \hat{d}, \hat{t} \in W_y} p_{s_k, \hat{y}, \hat{m}, \hat{d}, \hat{t}}^{\text{inst}} \right)$ $+ \sum_{s_k \in K^{\text{ES}}} \sum_{y=1}^{N_y} \left(\frac{C_{s_k,y}^{\text{inv,ES}} \cdot (N_y - y + 1)}{(1+R)^{y-1} \cdot LS_{s_k}} \right) \cdot \left(\sum_{\hat{y}, \hat{m}, \hat{d}, \hat{t} \in W_y} e_{s_k, \hat{y}, \hat{m}, \hat{d}, \hat{t}}^{\text{inst}} \right)$ $+ \sum_{s_k \in K^{H_2}} \sum_{y=1}^{N_y} \left(\frac{C_{s_k,y}^{\text{inv,H}_2} \cdot (N_y - y + 1)}{(1+R)^{y-1} \cdot LS_{s_k}} \right) \cdot \left(\sum_{\hat{y}, \hat{m}, \hat{d}, \hat{t} \in W_y} v_{s_k, \hat{y}, \hat{m}, \hat{d}, \hat{t}}^{\text{inst}} \right)$ <p>In the case of the technologies that have a life stamp lower than the investment period, then the computation is a little bit different.</p> |

| Term | Equation |
|-------------|---|
| | $ \begin{aligned} Cost_{inv,B} = & \sum_{y=1}^{LS_{V2G}} \frac{C_y^{inv,V2G}}{(1+R)^{y-1}} \cdot \left(\sum_{\hat{y}, \hat{m}, \hat{d}, \hat{t} \in W_y} n_{\hat{y}, \hat{m}, \hat{d}, \hat{t}}^{inst} \right) \\ & + \sum_{y=LS_{V2G}+1}^{N_y} \left(\frac{N_y - y + 1}{LS_{V2G}} \cdot \frac{C_y^{inv,V2G}}{(1+R)^{y-1}} \right) \cdot \left(\sum_{\hat{y}, \hat{m}, \hat{d}, \hat{t} \in W_y} n_{\hat{y}, \hat{m}, \hat{d}, \hat{t}}^{inst} \right) \\ & - \sum_{y=1}^{LS_{V2G}} \frac{C_y^{inv,V2G} \cdot C_y^{sv,V2G}}{(1+R)^{N_y-1}} \cdot \left(\sum_{\hat{y}, \hat{m}, \hat{d}, \hat{t} \in W_y} n_{\hat{y}, \hat{m}, \hat{d}, \hat{t}}^{inst} \right) \\ & + \sum_{y=LS_{V2G}}^{N_Y} \left(\frac{C_y^{inv,V2G}}{(1+R)^{y-1}} \cdot \frac{N_y - y}{LS_{V2G}} \right) \cdot \left(\sum_{\hat{y}, \hat{m}, \hat{d}, \hat{t} \in W_y} n_{\hat{y}, \hat{m}, \hat{d}, \hat{t}}^{inst} \right) \\ & + \sum_{s_k \in K^{EL}} \left(\sum_{y=1}^{LS_{s_k}} \frac{C_{s_k,y}^{inv,EL}}{(1+R)^{y-1}} \cdot \left(\sum_{\hat{y}, \hat{m}, \hat{d}, \hat{t} \in W_y} p_{s_k, \hat{y}, \hat{m}, \hat{d}, \hat{t}}^{inst,EL} \right) \right. \\ & + \sum_{y=LS_{s_k}+1}^{N_y} \left(\frac{N_y - y + 1}{LS_{s_k}} \cdot \frac{C_{s_k,y}^{inv,EL}}{(1+R)^{y-1}} \right) \cdot \left(\sum_{\hat{y}, \hat{m}, \hat{d}, \hat{t} \in W_y} p_{s_k, \hat{y}, \hat{m}, \hat{d}, \hat{t}}^{inst,EL} \right) \\ & - \sum_{y=1}^{LS_{s_k}} \frac{C_{s_k,y}^{inv,EL} \cdot C_{s_k,y}^{sv,EL}}{(1+R)^{N_y-1}} \cdot \left(\sum_{\hat{y}, \hat{m}, \hat{d}, \hat{t} \in W_y} p_{s_k, \hat{y}, \hat{m}, \hat{d}, \hat{t}}^{inst,EL} \right) \\ & \left. + \sum_{y=LS_{s_k}}^{N_Y} \left(\frac{C_{s_k,y}^{inv,EL}}{(1+R)^{y-1}} \cdot \frac{N_y - y}{LS_{s_k}} \right) \cdot \left(\sum_{\hat{y}, \hat{m}, \hat{d}, \hat{t} \in W_y} p_{s_k, \hat{y}, \hat{m}, \hat{d}, \hat{t}}^{inst,EL} \right) \right) \end{aligned} $ |
| $Cost_{op}$ | <p>The fourth term $Cost_{op}$ accounts for the operational costs from all years. At each year, it is considered the total kWh or capacity installed for each technology and multiply this term by the base operational cost $C_{k,y}^{op}$:</p> $ \begin{aligned} Cost_{op} = & \sum_{s_k \in K^{GEN}} \sum_{y=1}^{N_y} \frac{C_{s_k,y}^{inv,GEN} \cdot C_{s_k}^{op,GEN}}{(1+R)^{y-1}} \cdot \left(\sum_{\hat{y}, \hat{m}, \hat{d}, \hat{t} \in W_y} p_{s_k, \hat{y}, \hat{m}, \hat{d}, \hat{t}}^{inst} \right) \\ & + \sum_{s_k \in K^{ES}} \sum_{y=1}^{N_y} \frac{C_{s_k,y}^{inv,ES} \cdot C_{s_k}^{op,ES}}{(1+R)^{y-1}} \cdot \left(\sum_{\hat{y}, \hat{m}, \hat{d}, \hat{t} \in W_y} e_{s_k, \hat{y}, \hat{m}, \hat{d}, \hat{t}}^{inst} \right) \\ & + \sum_{s_k \in K^{H_2}} \sum_{y=1}^{N_y} \frac{C_{s_k,y}^{inv,H_2} \cdot C_{s_k}^{op,H_2}}{(1+R)^{y-1}} \cdot \left(\sum_{\hat{y}, \hat{m}, \hat{d}, \hat{t} \in W_y} v_{s_k, \hat{y}, \hat{m}, \hat{d}, \hat{t}}^{inst} \right) \\ & + \sum_{s_k \in K^{V2G}} \sum_{y=1}^{N_y} \frac{C_{s_k,y}^{inv,V2G} \cdot C_{s_k}^{op,V2G}}{(1+R)^{y-1}} \cdot \left(\sum_{\hat{y}, \hat{m}, \hat{d}, \hat{t} \in W_y} n_{s_k, \hat{y}, \hat{m}, \hat{d}, \hat{t}}^{inst} \right) \\ & + \sum_{s_k \in K^B} \sum_{y=1}^{N_y} \frac{C_{s_k,y}^{inv,B} \cdot C_{s_k}^{op,B}}{(1+R)^{y-1}} \cdot \left(\sum_{\hat{y}, \hat{m}, \hat{d}, \hat{t} \in W_y} P_{s_k, ini}^B + p_{s_k, \hat{y}, \hat{m}, \hat{d}, \hat{t}}^{inst, B} \right) \end{aligned} $ |
| $Cost_{dr}$ | Cost depending on the power amount increased or decreased for demand respond |

| Term | Equation |
|-----------------------|--|
| | services $\sum_{y=1}^{N_y} \left(\sum_{m \in M, d \in D, t \in T} \frac{\omega_{y,m,d}}{(1+R)^{y-1}} \cdot \lambda^{dr} \cdot (x_{y,m,d,t}^{inc} + x_{y,m,d,t}^{dec}) \right)$ |
| $Cost_{gen}$ | Cost associated to the generation of electrical energy. Only applies in the Virtual Community archetype. $Cost_{gen} = \sum_{y=1}^{N_y} \sum_{m \in M, d \in D} \frac{\omega_{y,m,d} \cdot \Delta_t}{(1+R)^{y-1}} \cdot C^{gen}$ $\cdot \left(\sum_{t \in T} \sum_{s_k \in \{SPV_1, SPV_2, SWT_1, SWT_2\}} p_{s_k,y,m,d,t}^{gen} + \sum_{s_k \in K^{ES}} p_{s_k,y,m,d,t}^{dch} + p_{v2g,y,m,d,t}^{dch} \right)$ |
| $Cost_{buy}^{el,TOU}$ | $Cost_{buy}^{el,TOU} = \sum_{y=1}^{N_y} \left(\sum_{m \in M, d \in D} \frac{\omega_{y,m,d} \cdot \Delta_t}{(1+R)^{y-1}} \cdot \sum_{t \in T} p_{y,m,d,t}^{buy} \cdot \lambda_{y,m,d,t}^{buy,el} \right)$ |
| $Cost_{buy}^{el,PP}$ | $Cost_{buy}^{el,PP} = \sum_{y=1}^{N_y} \left(\sum_{m \in M, d \in D} \frac{\omega_{y,m,d} \cdot \Delta_t}{(1+R)^{y-1}} \cdot (p_{y,m}^{peak} \cdot \lambda_{y,m}^{peak}) \cdot \sum_{t \in T} p_{y,m,d,t}^{buy} \cdot \lambda_{y,m,d,t}^{buy,el} \right)$ |
| $Cost_{buy}^{el,BW}$ | $Cost_{buy}^{el,BW} = \sum_{y=1}^{N_y} \left(\sum_{m \in M} \frac{\lambda_{y,m}^{fix} \cdot P^{BW} \cdot \Delta_t}{(1+R)^{y-1}}$ $\cdot \sum_{d \in D, t \in T} \omega_{y,m,d} \cdot ((p_{y,m,d,t}^{out,inf} + p_{y,m,d,t}^{out,sup}) \cdot \lambda_{y,m}^{exceed} + p_{y,m,d,t}^{buy} \cdot \lambda_{y,m,d,t}^{buy,el}) \right)$ |

Source: own elaboration.

The objective is to minimize F in the domain D given by all the constraints defined in this document. Consider the following:

- $\omega_{y,m,d}$ is the coefficient weighting the selected representative days.
- The objective function is considered from a Net Present Value point of view, and so, we are bringing to the present all the benefits and costs. All monetary quantities q_n from year y are multiplied for the term: $\frac{1}{(1+R)^{y-1}}$.
- In order to simplify the objective function, it is assumed that $p_{s_k,\hat{y},\hat{m},\hat{d},\hat{t}}^{inst} = p_{s_k,\hat{y},\hat{m},\hat{d},\hat{t}}^{inst,land} + p_{s_k,\hat{y},\hat{m},\hat{d},\hat{t}}^{inst,roof}$ and $e_{s_k,\hat{y},\hat{m},\hat{d},\hat{t}}^{inst} = e_{s_k,\hat{y},\hat{m},\hat{d},\hat{t}}^{inst,land} + e_{s_k,\hat{y},\hat{m},\hat{d},\hat{t}}^{inst,roof}$

Balance equations

Table 47. Balance equations for the Investment model

| Term | Equation |
|---|---|
| Eq. 29 Electrical balance | The sum of loads is equal to the total generation $\forall t \in T, d \in D, m \in M, y \in Y$; $L_{y,m,d,t}^{el} + L_{y,m,d,t}^{ev} + L_{y,m,d,t}^{HP} + u_{y,m,d,t}^{inc} + \sum_{s_k \in K^{EL}} p_{s_k,y,m,d,t}^{cons,EL} + \sum_{s_k \in K^{ES}} p_{s_k,y,m,d,t}^{ch} + p_{v2g,y,m,d,t}^{ch}$ $+ p_{y,m,d,t}^{sell} = p_{y,m,d,t}^{buy} + u_{y,m,d,t}^{dec} \sum_{s_k \in K^{gen}} p_{s_k,y,m,d,t}^{gen,el} + \sum_{s_k \in K^{ES}} p_{s_k,y,m,d,t}^{dch}$ $+ p_{v2g,y,m,d,t}^{dch}$ |
| Eq. 30 Thermal balance | Thermal load is equal to the sum of thermal power generated by CHP and boiler type B1 generation $\forall t \in T, d \in D, m \in M$ and $y \in M$, and depending on the archetype, for the corresponding $f_i \in F$ |
| | $L_{y,m,d,t}^{th} = \sum_{s_k \in \{S_{CHP_{f_{1,3}}}, S_{CHP_{f_2}}\}} p_{s_k,y,m,d,t}^{gen,th,CHP} + \sum_{s_k \in \{S_{B1}\}} p_{s_k,y,m,d,t}^{gen,th,B}$ |
| Eq. 31 High thermal balance (only in Industrial Polygon) | High thermal load is equal to thermal power generated by high boiler generation, type B2, $\forall t \in T, d \in D, m \in M, y \in M$, and depending on the archetype, for the corresponding $f_i \in F$ |
| | $L_{y,m,d,t}^{high,th} = \sum_{s_k \in \{S_{B2}\}} p_{s_k,y,m,d,t}^{gen,th,B}$ |
| Eq. 32 Hydrogen balance | The sum of hydrogen (fuel f_3) generated by the electrolyser, the hydrogen discharged from the hydrogen storages and the hydrogen bought, is equal to the sum of the hydrogen consumed by the CHP, the boilers and the hydrogen charged to the hydrogen storage $\forall t \in T, d \in D, m \in M, y \in Y$; |
| | $f_3_{y,m,d,t}^{buy} + \sum_{s_k \in K^{EL}} f_3_{s_k,y,m,d,t}^{gen,EL} + \sum_{s_k \in K^{HS}} f_3_{s_k,y,m,d,t}^{dch}$ $= \sum_{s_k \in K^B} f_3_{s_k,y,m,d,t}^{cons,B} + \sum_{s_k \in \{S_{CHP_{f_{1,3}}}\}} f_3_{s_k,y,m,d,t}^{cons,CHP} + \sum_{s_k \in K^{H_2}} f_3_{s_k,y,m,d,t}^{ch}$ |
| Eq. 33 Natural gas balance | The natural gas (fuel f_1) bought is equal to the gas consumed by boilers and CHP $\forall t \in T, d \in D, m \in M, y \in Y$; |
| | $f_1_{y,m,d,t}^{buy} = f_1_{y,m,d,t}^{cons,B1} + f_1_{y,m,d,t}^{cons,B2} + \sum_{s_k \in \{S_{CHP_{f_{1,3}}}\}} f_1_{s_k,y,m,d,t}^{cons,CHP}$ |
| Eq. 34 Biomass balance | The biomass (fuel f_2) bought is equal to the biomass consumed CHP_{f_2} , $\forall t \in T, d \in D, m \in M, y \in Y$; |
| | $f_2_{y,m,d,t}^{buy} = \sum_{s_k \in \{S_{CHP_{f_2}}\}} f_2_{s_k,y,m,d,t}^{cons,CHP}$ |

| | |
|-----------------------------------|---|
| Eq. 35 Avoid oversizing | The total amount of power generation installed has to be lower or equal total amount of electrical demand $\forall t \in T, d \in D, m \in M, y \in Y$; |
| | $\sum_{Y,M,D,T} \left(\omega_{y,m,d} \cdot \left(\sum_{s_k \in K^{GEN}} p_{s_k,y,m,d,t}^{gen,el} + \sum_{s_k \in K^{ES}} p_{s_k,y,m,d,t}^{dch} \right) \right)$ $\leq \sum_{Y,M,D,T} \omega_{y,m,d} \cdot (L_{y,m,d,t}^{el} + L_{y,m,d,t}^{HP} + L_{y,m,d,t}^{ev})$ |
| Eq. 36 Avoid oversizing | The total capacity of electrical storage installed has to be lower than the available maximum electrical generation at $\forall (y, m, d, t) \in W$; |
| | $\sum_{s_k \in \{S_{ES_1}, S_{ES_2}\}} (e_{y,m,d,t}^{inst,roof} + e_{y,m,d,t}^{inst,roo}) \cdot C_{s_k}^{rate,ES} \leq \sum_{s_k \in K^{GEN}} p_{y,m,d,t}^{inst,s_k}$ |

Source: own elaboration.

Available roof and land

Table 48. Available roof and land equations for the Investment model

| Term | Equation |
|-------------------------------------|---|
| Eq. 38 Roof area | The investment in roof area is limited by A^{roof} ; $\sum_{s_k \in \{S_{ES_1}, S_{ES_2}\}} \sum_{Y,M,D,T} e_{s_k,y,m,d,t}^{inst,roof} \cdot A_{s_k} + \sum_{s_k \in \{S_{PV_2}\}} \sum_{Y,M,D,T} p_{s_k,y,m,d,t}^{inst} \cdot A_{s_k} \leq A^{roof}$ |
| Eq. 39 Land area | The investment in roof area is limited by A^{land} ; $\sum_{Y,M,D,T} n_{v2g,y,m,d,t}^{inst} \cdot A_{v2g} + \sum_{s_k \in K^{H_2}} \sum_{Y,M,D,T} v_{s_k,y,m,d,t}^{inst} \cdot A_{s_k}$ $+ \sum_{s_k \in \{S_{ES_1}, S_{ES_2}\}} \sum_{Y,M,D,T} e_{s_k,y,m,d,t}^{inst,land} \cdot A_{s_k}$ $+ \sum_{s_k \in K^{GEN} \setminus \{S_{PV_2}\}} \sum_{Y,M,D,T} p_{s_k,y,m,d,t}^{inst} \cdot A_{s_k} \leq A^{land}$ |
| Eq. 40 First day per year | The installation of technologies is allowed only the first day of each year, $\forall t \in T, d \in D, m \in M, y \in Y, \forall s_k \in K$, and $\forall a \in \{land, roof\}$; $p_{s_k,y,m,d,t}^{inst,a} \geq 0, \text{ if } (y, m, d, t) \in W, \text{ otherwise } p_{s_k,y,m,d,t}^{inst,a} = 0.$ |
| Eq. 41 Peak power | Purchasing power has to be lower than its monthly peak power, $\forall m \in M, y \in Y$; $p_{y,m}^{peak} \geq p_{y,m,d,t}^{buy}$ |

| | |
|--|---|
| constraints | |
| Eq. 42 Bandwidth constraints | Purchasing power and selling power have to be bounded by the bandwidth power. The power required outside the band is accounted for monthly in the corresponding variables. $\forall m \in M, y \in Y;$ $p_{y,m,d,t}^{buy} - p_{y,m}^{out,inf} \leq P^{BW}$ $p_{y,m,d,t}^{sell} - p_{y,m}^{out,sup} \leq P^{BW}$ |
| Eq. 43 Bounds for bought power | Purchasing power and selling power cannot be happening at the same time. $p_{y,m,d,t}^{buy} \leq M \cdot (1 - x^{el})$ |
| Eq. 44 Bounds for sold power | Purchasing power and selling power cannot be happening at the same time. $p_{y,m,d,t}^{sell} \leq x^{el} \cdot M$ |

Source: own elaboration.

Wind generation

Table 49. Wind generation parameters for the Investment model

| Parameter | Description | Units/Domain |
|---------------------|--|---------------------------------|
| K^{WT} | Set of wind turbine types. | $K^{WT} = \{S_{WT1}, S_{WT2}\}$ |
| $P_{s_k,ini}^{WT}$ | Initial power of s_k installed, $\forall s_k \in K^{WT}$. | kW^+ |
| $\eta_{s_k,y}^{WT}$ | Efficiency of s_{wt} in year y. | [0,1] |

Source: own elaboration.

| Term | Equation |
|----------------------------------|---|
| Eq. 45 Wind generation | Wind generation depending on the power installed $\forall t \in T, d \in D, m \in M, y \in Y$, and $\forall s_k \in \{S_{WT1}, S_{WT2}\}$; $p_{s_k,y,m,d,t}^{gen,el} = \eta_{s_k,y}^{WT} \cdot LF_{y,m,d,t}^{WT} \cdot \left(P_{s_k,ini}^{WT} + \sum_{y=1}^{N_y} \left(\sum_{\hat{y}, \hat{m}, \hat{d}, \hat{t} \in W_y} p_{s_k,\hat{y},\hat{m},\hat{d},\hat{t}}^{inst} \right) \right)$ |

Table 50. Wind generation equations for the Investment model

Source: own elaboration.

Solar Generation

Table 51. Solar generation parameters for the Investment model

| Parameter | Description | Units/Domain |
|---------------------|--|---------------------------------|
| K^{PV} | Set of PV panel types. The first type of PV is installed in land, whereas the second one is installed in roof. | $K^{PV} = \{S_{PV1}, S_{PV2}\}$ |
| $P_{s_k,ini}$ | Initial power of s_{pv} . | kW^+ |
| $\eta_{s_k,y}^{PV}$ | Efficiency of s_k in year y. | [0,1] |

Source: own elaboration.

Table 52. Solar generation equations for the Investment model

| Term | Equation |
|-----------------------------------|---|
| Eq. 46 Solar generation | Total solar power generated $\forall t \in T, d \in D, m \in M$ and $y \in Y$, for $s_k \in \{S_{PV1}, S_{PV2}\}$; $p_{s_k,y,m,d,t}^{gen,el} = \eta_{s_k,y}^{PV} \cdot LF_{y,m,d,t}^{PV} \cdot \left(P_{s_k,ini} + \sum_{y=1}^{N_y} \sum_{\hat{y}, \hat{m}, \hat{d}, \hat{t} \in W_y} p_{s_k,\hat{y},\hat{m},\hat{d},\hat{t}}^{inst} \right)$ |

Source: own elaboration.

Electrical Storage

Table 53. Electrical Storage parameters for the Investment model

| Parameter | Description | Units/Domain |
|-------------------------|--|---------------------------------|
| K^{ES} | Set of storage types. | $K^{ES} = \{S_{ES1}, S_{ES2}\}$ |
| $\eta_{s_k,y}^{dch,ES}$ | Discharging Efficiency of s_k in year y. | [0,1] |
| $\eta_{s_k,y}^{ch,ES}$ | Charging Efficiency of s_k in year y. | [0,1] |
| $SOC_{s_k}^{max}$ | Max. SOC allowed. | [0,1] |
| $SOC_{s_k}^{min}$ | Min. SOC allowed. | [0,1] |
| $SOC_{s_k}^{ini}$ | Initial daily SOC. | [0,1] |
| $SOC_{s_k}^{final}$ | Min. final daily SOC. | [0,1] |
| $C_{s_k}^{rate,ES}$ | Power rate as compared to the capacity of the battery. | R^+, h^{-1} |

Source: own elaboration.

Table 54. Electrical Storage equations for the Investment model

| Term | Equation |
|---------------|--|
| Eq. 47 | Energy balance into the storage $\forall t \in T, d \in D, m \in M$ and $y \in Y$; and $\forall s_k \in K^{ES}$; |

| | |
|---|--|
| Energy balance | $soc_{s_k,y,m,d,t}^{ES} = \begin{cases} SOC_{s_k}^{ini} \cdot \sum_{i=1}^y \sum_{\hat{m}, \hat{d}, \hat{t} \in W_i} (e_{s_k,i,\hat{m},\hat{d},\hat{t}}^{inst,land} + e_{s_k,i,\hat{m},\hat{d},\hat{t}}^{inst,roof}) + \eta_{s_k,y}^{ch,ES} \cdot \Delta_t \cdot p_{s_k,y,m,d,t}^{ch} - \frac{\Delta_t \cdot p_{s_k,y,m,d,t}^{dch}}{\eta_{s_k,y}^{d,ES}} \\ SOC_{s_k,y,m,d,t-1}^{ES} + \eta_{s_k,y}^{ch,ES} \cdot \Delta_t \cdot p_{s_k,y,m,d,t}^{ch} - \frac{\Delta_t \cdot p_{s_k,y,m,d,t}^{dch}}{\eta_{s_k,y}^{d,ES}} \end{cases} \quad \forall t > 1$ |
| Eq. 48 Only charge/discharge mode allowed | The technology $s_k \in K^{ES}$ can only be in charge mode, or discharge mode $\forall t \in T, d \in D, m \in M$ and $y \in Y$; $p_{s_k,y,m,d,t}^{ch} \leq x_{s_k,y,m,d,t}^{ES} \cdot M$ $p_{s_k,y,m,d,t}^{dch} \leq (1 - x_{s_k,y,m,d,t}^{ES}) \cdot M$ |
| Eq. 49 Bound of power through C-rate relation | Power Upper bound $\forall t \in T, d \in D, m \in M$ and $y \in Y$, and $s_k \in K^{ES}$; $p_{s_k,y,m,d,t}^{ch} + p_{s_k,y,m,d,t}^{dch} \leq \sum_{i=1}^y \sum_{\hat{m}, \hat{d}, \hat{t} \in W_i} (e_{s_k,i,\hat{m},\hat{d},\hat{t}}^{inst,land} + e_{s_k,i,\hat{m},\hat{d},\hat{t}}^{inst,roof}) \cdot C_{s_k}^{rate,ES}$ |
| Eq. 50 SOC bounds | Maximum and minimum energy amount of energy allowed into the storage $\forall t \in T, d \in D, m \in M, y \in Y$; and $s_k \in K^{ES}$; $SOC_{s_k}^{min} \cdot e_{s_k,y}^{inst,tot} \leq soc_{y,m,d,t}^{s_k} \leq SOC_{s_k}^{max} \cdot \sum_{i=1}^y \sum_{\hat{m}, \hat{d}, \hat{t} \in W_i} (e_{s_k,i,\hat{m},\hat{d},\hat{t}}^{inst,land} + e_{s_k,i,\hat{m},\hat{d},\hat{t}}^{inst,roof})$ |
| Eq. 51 Final daily SOC bound | Minimum final state of charge of the storage at the end of each day $d \in D, m \in M, y \in Y$; and $s_k \in K^{ES}$; $soc_{y,m,d,t_f}^{s_k} \geq SOC_{s_k}^{final} \cdot \sum_{i=1}^y \sum_{\hat{m}, \hat{d}, \hat{t} \in W_i} (e_{s_k,i,\hat{m},\hat{d},\hat{t}}^{inst,land} + e_{s_k,i,\hat{m},\hat{d},\hat{t}}^{inst,roof})$ |

Source: Modification of the model from Igualada González et al. (2013)

Hydrogen Storage

Table 55. Hydrogen Storage parameters for the Investment model

| Parameter | Description | Units/Domain |
|----------------------|---|---|
| K^{H_2} | Set of types of Hydrogen Storages considered. | $K^{H_2} = \{S_{H_2}\}$ |
| R | Gas constant. | $8.31446 \frac{m^3 \cdot P_a}{K \cdot mol}$ |
| $T_{s_k}^{mean}$ | Mean temperature inside the tank s_k . | K |
| $\eta_{s_k,y}^{dch}$ | Discharging Efficiency of s_k in year y . | [0,1] |
| $\eta_{s_k,y}^{ch}$ | Charging Efficiency of s_k in year y . | [0,1] |
| $CR_{s_k}^{H_2}$ | Maximum mols per hour that can get out/in the tank per m^3 of tank. | $mol/(m^3 \cdot h)$ |

| Parameter | Description | Units/Domain |
|------------------|--|-----------------|
| Q_{sk}^{max} | Maximum pressure allowed. | P_a |
| Q_{sk}^{min} | Minimum pressure allowed. | P_a |
| Q_{sk}^{ini} | Initial daily quantity of hydrogen per m^3 . | mol_{H_2}/m^3 |
| Q_{sk}^{final} | Final daily pressure. | P_a |

Source: own elaboration.

Table 56. Hydrogen Storage equations for the Investment model

| Term | Equation |
|---|--|
| Eq. 52 Hydrogen balance | Mol of H_2 equation in the storage $\forall t \in T, d \in D, m \in M$ and $y \in Y$, and $\forall s_k \in K^{H_2}$; $m_{s_k,y,m,d,t}^{H_2} = \begin{cases} \frac{Q_{sk}^{ini}}{R \cdot T_{sk}^{mean}} \cdot \sum_{i=1}^y \sum_{\hat{m}, \hat{d}, \hat{t} \in W_y} v_{s_k,i,\hat{m},\hat{d},\hat{t}}^{inst} + \eta_{s_k,y}^{ch} \cdot \Delta_t \cdot f_{3,s_k,y,m,d,t}^{ch} - \frac{\Delta_t \cdot f_{3,s_k,y,m,d,t}^d}{\eta_{s_k,y}^d}, & t = 1 \\ m_{s_k,y,m,d,t-1}^{H_2} + \eta_{s_k,y}^{ch} \cdot \Delta_t \cdot f_{3,s_k,y,m,d,t}^{ch} - \frac{\Delta_t \cdot f_{3,y,m,d,t}^d}{\eta_{s_k,y}^d}, & t > 1 \end{cases}$ |
| Eq. 53 Bi-directionality relation | The hydrogen tank cannot charge and discharge hydrogen at the same time step $\forall t \in T, d \in D, m \in M, y \in Y$, and $\forall s_k \in K^{H_2}$; $0 \leq f_{3,s_k,y,m,d,t}^{ch} \leq x_{s_k,y,m,d,t}^{H_2} \cdot M$ $0 \leq f_{3,s_k,y,m,d,t}^d \leq (1 - x_{s_k,y,m,d,t}^{H_2}) \cdot M$ |
| Eq. 54 Charge/discharge bounds | The hydrogen charge and discharge is bound by the volume installed and the C-rate considered $\forall t \in T, d \in D, m \in M, y \in Y$, and $\forall s_k \in K^{H_2}$; $f_{3,s_k,y,m,d,t}^{ch} + f_{3,s_k,y,m,d,t}^d \leq \sum_{i=1}^y \sum_{\hat{m}, \hat{d}, \hat{t} \in W_y} v_{s_k,i,\hat{m},\hat{d},\hat{t}}^{inst} \cdot CR_{s_k}^{H_2}$ |
| Eq. 55 SOC bounds | Limits for the pressure inside the tank step $\forall t \in T, d \in D, m \in M, y \in Y$, and $\forall s_k \in K^{H_2}$; $Q_{sk}^{min} \cdot \sum_{i=1}^y \sum_{\hat{m}, \hat{d}, \hat{t} \in W_y} v_{s_k,i,\hat{m},\hat{d},\hat{t}}^{inst} \leq R \cdot T_{sk}^{mean} \cdot m_{s_k,y,m,d,t}^{H_2} \leq Q_{sk}^{max} \cdot \sum_{i=1}^y \sum_{\hat{m}, \hat{d}, \hat{t} \in W_y} v_{s_k,i,\hat{m},\hat{d},\hat{t}}^{inst}$ |
| Eq. 56 Final daily pressure bound | Minimum quantity of hydrogen stored at the end of each day $d \in D, m \in M, y \in Y$, and $\forall s_k \in K^{H_2}$; $R \cdot T_{sk}^{mean} \cdot m_{s_k,y,m,d,t_f}^{H_2} \geq Q_{sk}^{final} \cdot \sum_{i=1}^y \sum_{\hat{m}, \hat{d}, \hat{t} \in W_y} v_{s_k,i,\hat{m},\hat{d},\hat{t}}^{inst}$ |

Source: own elaboration.

Electrolyzer

Table 57. Electrolyzer parameters for the Investment model

| Parameter | Description | Units/Domain |
|-------------------|--|--|
| K^{EL} | Set of electrolyzers considered. | $K^{EL} = \{S_{EL}\}$ |
| LHV_{H_2} | Lower heating value of hydrogen at 1° C. | $6.9222 \cdot 10^{-5} \frac{kWh}{mol}$ |
| $\eta_{S_k}^{EL}$ | Electrolyser s_k efficiency. | [0,1] |

Source: own elaboration.

Table 58. Electrolyzer equations for the Investment model

| Term | Equation |
|---|--|
| 1. Eq. 57 Power consumed bounds | The power consumed by electrolyser depends on the total power installed $\forall t \in T, d \in D, m \in M, y \in Y$, and $\forall s_k \in K^{EL}$; $0 \leq p_{s_k,y,m,d,t}^{cons,EL} \leq \sum_{i=1}^y \sum_{\hat{m}, \hat{d}, \hat{t} \in W_y} p_{s_k,i,\hat{m},\hat{d},\hat{t}}^{inst,EL}$ |
| 2. Eq. 58 Hydrogen generation | Relation between power consumed and hydrogen generated $\forall t \in T, d \in D, m \in M, y \in Y$, and $\forall s_k \in K^{EL}$; $f_{3s_k,y,m,d,t}^{gen,EL} = \frac{\eta_{s_k}^{EL} \cdot p_{s_k,y,m,d,t}^{cons,EL}}{LHV_{H_2}}$ |

Source: (Nojavan et al., 2017)

Combined Heat and Power

Table 59. CHP parameters for the Investment model

| Parameter | Description | Units/Domain |
|--------------------------------|---|--|
| K^{CHP} | Set of types of CHP depending on fuel type. | $K^{CHP} = \{S_{CHP_{f_1,3}}, S_{CHP_{f_2}}\}$. The first type can consume gas and hydrogen while the second type consumes biomass. |
| $\eta_{S_k}^{CHP}$ | Heat and electricity power ratio of $s_k \in K^{CHP}$. | [0,1] |
| $\eta_{S_{CHP_{f_2}}}^{f_2}$ | Conversion factor from fuel f_2 (biomass) to electricity by $S_{CHP_{f_2}}$. | [0,1] |
| $\eta_{S_{CHP_{f_1,3}}}^{f_1}$ | Conversion factor from fuel f_1 (natural gas) to electricity by $S_{CHP_{f_1,3}}$. | [0,1] |

| Parameter | Description | Units/Domain |
|--------------------------------|--|------------------|
| $\eta_{S_{CHP} f_{1,3}}^{f_3}$ | Conversion factor from fuel f_3 (hydrogen) to electricity by $S_{CHP} f_{1,3}$. | [0,1] |
| $U_{s_k}^{ini}$ | Initial daily state of $s_k \in K^{CHP}$. | {0,1} |
| $T_{s_k}^{su}$ | Minimum uptime of $s_k \in K^{CHP}$. | hours |
| $T_{s_k}^{sd}$ | Minimum shutdown time of $s_k \in K^{CHP}$. | hours |
| $SU_{s_k}^{max}$ | Maximum number of times that a $s_k \in K^{CHP}$ can be opened. | Positive integer |

Source: own elaboration.

Table 60. CHP equations for the Investment model

| Term | Equation |
|---------------------------------------|--|
| Eq. 59 Power consumed bound | Lower bound for power installed in $\forall t \in T, d \in D, m \in M$ and $y \in Y, \forall s_k \in K^{CHP}$; $0 \leq p_{s_k,y,m,d,t}^{gen,el} \leq \sum_{i=1}^y \sum_{\hat{m}, \hat{d}, \hat{t} \in W_y} p_{s_k,i,\hat{m},\hat{d},\hat{t}}^{inst}$ |
| Eq. 60 Power consumed bound | Bound of power generated by state of CHP, $\forall t \in T, d \in D, m \in M$ and $y \in Y, \forall s_k \in K^{CHP}$; $0 \leq p_{s_k,y,m,d,t}^{gen,el} \leq u_{s_k,y,m,d,t}^{CHP} \cdot M$ |
| Eq. 61 Power consumed bound | Generated power equals the fuel consumed by the conversion factor to electrical power, $\forall t \in T, d \in D, m \in M$ and $y \in Y$. For the natural gas CHP, $p_{S_{CHP} f_{1,3},y,m,d,t}^{gen,el} = f_{1S_{CHP} f_{1,3},y,m,d,t}^{cons,CHP} \cdot \eta_{S_{CHP} f_{1,3}}^{f_1} + f_{3S_{CHP} f_{1,3},y,m,d,t}^{cons,CHP} \cdot \eta_{S_{CHP} f_{1,3}}^{f_3}$ For the biomass CHP, $p_{S_{CHP} f_2,y,m,d,t}^{gen,el} = f_{2S_{CHP} f_2,y,m,d,t}^{cons,CHP} \cdot \eta_{S_{CHP} f_2}^{f_2}$ |
| Eq. 62 Heat generation | Relation between thermal power and electrical power $\forall t \in T, d \in D, m \in M$ and $y \in Y, \forall s_k \in K^{CHP}$; $p_{s_k,y,m,d,t}^{gen,th,CHP} = \frac{1}{\eta_{s_k}^{CHP}} \cdot p_{s_k,y,m,d,t}^{gen,el}$ |
| Eq. 63 Initial state | Initial daily state operation $\forall d \in D, m \in M, y \in Y$, and $\forall s_k \in K^{CHP}$; $u_{s_k,y,m,d,t_0}^{CHP} = U_{s_k}^{ini,CHP}$ |

| | |
|---|--|
| Eq. 64 Change of state | A constraint to know if CHP changes the state on to off or off to on $\forall t \in T, d \in D, m \in M, y \in Y$, and $\forall s_k \in K^{CHP}$; $u_{s_k,y,m,d,t}^{CHP} - u_{s_k,y,m,d,t-1}^{CHP} = x_{s_k,y,m,d,t}^{su} - x_{s_k,y,m,d,t}^{sd}$ |
| Eq. 65 Time limit | A minimum uptime for the CHP plant $\forall t \in T, d \in D, m \in M, y \in Y$, and $\forall s_k \in K^{CHP}$; $\sum_{i=t-T_{s_k}^{su}+1}^t x_{s_k,y,m,d,t}^{su} \leq u_{s_k,y,m,d,t}^{CHP}$ |
| Eq. 66 Time limit switch down | A minimum shutdown time for the CHP plant $\forall t \in T, d \in D, m \in M, y \in Y$, and $\forall s_k \in K^{CHP}$; $\sum_{i=t-T_{s_k}^{sd}+1}^t x_{s_k,y,m,d,t}^{sd} \leq u_{y,m,d,t}^{CHP}$ |
| Eq. 67 Maximum number of times that CHP can be opened per day | A minimum shutdown time for the CHP plant $\forall t \in T, d \in D, m \in M, y \in Y$, and $\forall s_k \in K^{CHP}$; $\sum_{t \in T} x_{s_k,y,m,d,t}^{su} \leq SU_{s_k}^{max}$ |

Source: own elaboration.

Vehicle-to-Grid

Table 61. V2G parameters for the Investment model

| Parameter | Description | Units/Domain |
|---------------------|--|------------------------|
| $\eta_{v2g,y}^d$ | Discharging Efficiency in year y . | [0,1] |
| $\eta_{v2g,y}^{ch}$ | Charging Efficiency in year y . | [0,1] |
| SOC_{ev}^{min} | Minimum SOC allowed. | [0,1] |
| SOC_{ev}^{max} | Maximum SOC allowed. | [0,1] |
| SOC_{ev}^{ini} | Initial state of charge per EV. | [0,1] |
| SOC_{ev}^{end} | Final state of charge at the departure time. | [0,1] |
| $E_{ev,y}^b$ | EV battery capacity. | kWh |
| $P_{s_{v2g}}^{max}$ | Maximum charging & discharging power from V2G charger. | kW |
| EV_{ini}^{con} | Number of EV that are connected at first time step of the day. | Positive integer value |

Source: own elaboration.

Table 62. V2G equations for the Investment model

| Term | Equation |
|---|--|
| Eq. 68 Number of EVs that come in | <p>Let EV^{con} be the number of vehicles that would ideally try to be connected at each time step,</p> $EV_{y,m,d,1}^{con} = EV_{ini}^{con} + EV_{y,m,d,1}^{in} - EV_{y,m,d,1}^{out}, \forall y, m, d,$ $EV_{y,m,d,t}^{con} = EV_{y,m,d,t-1}^{con} + EV_{y,m,d,t}^{in} - EV_{y,m,d,t}^{out}, \forall y, m, d, t > 1$ <p>Then, the number of EVs that can go in is;</p> $ev_{y,m,d,t}^{in} \leq EV_{y,m,d,t}^{in} \forall y, m, d,$ |
| Eq.69 EVs connected bounds | <p>Then, the number of connected EVs is bounded as follows;</p> $ev_{y,m,d,t}^{con} \leq EV_{y,m,d,t}^{con} \forall y, m, d, t$ $ev_{y,m,d,1}^{con} \leq \sum_{i=1}^y \sum_{\hat{m}, \hat{d}, \hat{t} \in W_y} n_{v2g,i,\hat{m},\hat{d},\hat{t}}^{inst} \forall y, m, d$ |
| Eq.70 EVs connected balance | <p>The number of connected EVs is;</p> $ev_{y,m,d,1}^{con} = EV_{ini}^{con} + ev_{y,m,d,1}^{in} - ev_{y,m,d,1}^{out} \forall y, m, d$ $ev_{y,m,d,t}^{con} = ev_{y,m,d,t-1}^{con} + ev_{y,m,d,t}^{in} - ev_{y,m,d,t}^{out} \forall y, m, d, \forall t > 1$ |
| Eq.71 SOC upper bound | <p>Maximum energy stored allowed $\forall t \in T, d \in D, m \in M$ and $y \in Y$;</p> $soc_{y,m,d,t}^{ev} \leq SOC_{ev}^{max} \cdot ev_{y,m,d,t}^{con} \cdot E_{ev,y}^b$ |
| Eq.72 SOC lower bound | <p>The minimum SOC allowed $\forall t \in T, d \in D, m \in M$ and $y \in Y$ depends on the number of EVs plugged in, the final expected SOC for the EVS that will go out in the next time step, and the initial SOC of the EVs that come in;</p> $soc_{y,m,d,t}^{ev} \geq \begin{cases} ev_{y,m,d,t}^{con} \cdot SOC_{ev}^{min} \cdot E_{ev,y}^b + ev_{y,m,d,t+1}^{out} \cdot (SOC_{ev}^{end} - SOC_{ev}^{min}) \cdot E_{ev,y}^b; & \forall t > 1, d, m, y \\ ev_{y,m,d,t}^{con} \cdot SOC_{ev}^{ini} \cdot E_{ev,y}^b + ev_{y,m,d,t+1}^{out} \cdot (SOC_{ev}^{end} - SOC_{ev}^{ini}) \cdot E_{ev,y}^b; & t = 1, \forall d, m, y \end{cases}$ |
| Eq.73 SOC balance | $soc_{y,m,d,t}^{ev}$ $= \begin{cases} ev_{y,m,d,ini}^{con} \cdot SOC_{ev}^{ini} \cdot E_{ev,y}^b + \eta_{v2g,y}^{ch} \cdot \Delta_t \cdot p_{v2g,y,m,d,1}^{ch} - \frac{\Delta_t \cdot p_{v2g,y,m,d,1}^{ch}}{\eta_{v2g,y}^d}; & \forall d, m, y \\ soc_{y,m,d,t-1}^{ev} + \eta_{v2g,y}^{ch} \Delta_t \cdot p_{v2g,y,m,d,t}^{ch} - \frac{\Delta_t \cdot p_{v2g,y,m,d,t}^{ch}}{\eta_{v2g,y}^d}; & \forall t > 1, d, m, y \end{cases}$ |
| Eq.74 Charge and discharge bounds | <p>Maximum charge and discharge power given by the chargers, $\forall t \in T, d \in D, m \in M, y \in Y$;</p> $p_{v2g,y,m,d,t}^{ch} + p_{v2g,y,m,d,t}^d \leq ev_{y,m,d,t}^{con} \cdot P_{v2g}^{max}$ |
| Eq.75 Final daily SOC | <p>Minimum final SOC per day $\forall d \in D, m \in M, y \in Y$;</p> $soc_{y,m,d,t_f}^{ev} \geq ev_{y,m,d,t_f}^{con} \cdot SOC_{v2g}^{end} \cdot E_{ev,y}^b$ |

Source: Modification of the model from Meenakumar et al. (2020).

Demand Response

Table 63. Demand response parameters for the Investment model

| Parameter | Description | Units/Domain |
|-----------------|---|--------------|
| S_{dr}^{inc} | Load increase share. | [0,1] |
| S_{dr}^{dec} | Load decrease share. | [0,1] |
| S_{dr}^{flex} | Load increase share. | [0,1] |
| U^{inc} | Initial state of increment at first time step of every day. | [0,1] |
| U^{dec} | Initial state of decrement at first time step of every day. | [0,1] |
| T^{dr} | Maximum time of demand response. | hours |
| N^{dr} | Number of activations per day. | N |

Source: own elaboration.

Table 64. Demand response equations for the Investment model

| Term | Equation |
|---------------------------------|---|
| Eq.76 Initial state | Initial state of demand response, $\forall y \in Y, m \in M, d \in D$; $u_{y,m,d,t_0}^{inc} = U^{inc}$ $u_{y,m,d,t_0}^{dec} = U^{dec}$ |
| Eq.77 Decrease demand | Upper bound of decreased amount of power demand $\forall t \in T, d \in D, m \in M, y \in Y$; $0 \leq x_{y,m,d,t}^{dec} \leq u_{y,m,d,t}^{dec} \cdot D_{hp,t} \cdot S_{dr}^{flex} \cdot S_{dr}^{dec}$ |
| Eq.78 Increase demand | Upper bound of increased amount of power demand $\forall t \in T, d \in D, m \in M, y \in Y$; $0 \leq x_{y,m,d,t}^{inc} \leq u_{y,m,d,t}^{inc} \cdot D_{hp,t} \cdot S_{dr}^{flex} \cdot S_{dr}^{inc}$ |
| Eq.79 Time limit | Consecutive time step of demand response activation $\forall t \in T, d \in D, m \in M, y \in Y$; $\sum_{i=t-T_{dr}+1}^{t+1} (x_{y,m,d,i}^{dec} + x_{y,m,d,i}^{inc}) \leq \overline{T_{dr}}$ |

Source: Modification of the model from Heitkoetter et al. (2021).

Boiler

Table 65. Boiler parameters for the Investment model

| Parameter | Description | Units/Domain |
|-----------|---------------------------|----------------------------|
| K^B | Set of Boilers considered | $K^B = \{S_{B1}, S_{B2}\}$ |

| Parameter | Description | Units/Domain |
|--------------------|--|-------------------------|
| $P_{s_k,y,ini}^B$ | Installed power of boilers in year y , $\forall s_k \in K^B$. | kWt |
| η_{S_k,f_i}^B | Conversion from fuel f_i , $i = 1,3$, to thermal power | $\frac{kWt}{mol_{f_i}}$ |
| S_{dr}^{flex} | Load increase share. | [0,1] |
| U^{inc} | Initial state of increment at first time step of every day. | [0,1] |
| U^{dec} | Initial state of decrement at first time step of every day. | [0,1] |
| T^{dr} | Maximum time of demand response. | hours |
| N^{dr} | Number of activations per day. | N |

Source: own elaboration.

Table 66. Boiler equations for the Investment model

| Term | Equation |
|--|--|
| Eq.80 Relation between power and consumption | $p_{s_k,y,m,d,t}^{gen,th,B} = \sum_{s_k \in K^B} \sum_{f \in \{f_1, f_3\}} \eta_{S_k,f_i}^B \cdot f_{s_k,y,m,d,t}^{cons,B}$ |
| Eq.81 Power generation bound | Upper bound of decreased amount of power demand $\forall t \in T, d \in D, m \in M, y \in Y$; $p_{s_k,y,m,d,t}^{gen,th,B} \leq P_{s_k,y,ini}^B + \sum_{i=1}^y \sum_{\hat{m}, \hat{d}, \hat{t} \in W_y} p_{s_k,i,\hat{m},\hat{d},\hat{t}}^{inst,B}$ |
| Eq.82 Installed power bound boiler | Limit power installed by the initial power installed at first timestep, $\forall y \in Y$; $P_{s_k,y,ini}^B + \sum_{i=1}^y \sum_{\hat{m}, \hat{d}, \hat{t} \in W_y} p_{s_k,i,\hat{m},\hat{d},\hat{t}}^{inst,B} \leq P_{s_k,1,ini}^B$ |
| Eq.83 Decide gas or hydrogen | At each time step only gas or hydrogen consumption is allowed $\forall t \in T, d \in D, m \in M, y \in Y$, and $\forall s_k \in K^B$; $f_{s_k,y,m,d,t}^{cons,B} \leq (1 - u_{s_k,y,m,d,t}^B) \cdot M$ $f_{s_k,y,m,d,t}^{cons,B} \leq u_{s_k,y,m,d,t}^B \cdot M$ |

Source: own elaboration.

Annex 2. Mathematical Formulation for MODECO's Operational Model

Sets and parameters

Table 67. Sets for the Operational model

| Set | Description | Elements |
|---------------------|---------------------------------------|---------------------------------|
| T | Set of time intervals. | $t \in T$ |
| \mathcal{N}_{es} | Set of numbers of Electrical Storage. | $n_{es} \in \mathcal{N}_{es}$ |
| \mathcal{N}_{chp} | Set of numbers of CHP. | $n_{chp} \in \mathcal{N}_{chp}$ |
| D | Set of days. | $d \in D$ |
| M | Set of months. | $m \in M$ |
| J | Discount rate scenarios | $j \in J$ |
| L | Price scenarios | $l \in L$ |

Source: own elaboration.

Table 68. Parameters for the Operational model

| Parameter | Description | Units | Source |
|---------------|---|------------|--------|
| Curves | | | |
| $H_{tbl,t}$ | Thermal base load at time t . | kWh_{th} | |
| $H_{tbl,t}^H$ | High thermal base load at time t | kWh_{th} | |
| $D_{hp,t}$ | Heat pumps demand at time t | kW | |
| $D_{ebt,t}$ | Electrical base load demand at time t | kW | |

| Parameter | Description | Units | Source |
|---------------------------------|---|-------|-----------------------------|
| $P_{pv,t}$ | Power given to the net from PV at time t | kW | Based on Investment outputs |
| $P_{wt,t}$ | Power given to the net from WT at time t | kW | Based on Investment outputs |
| $N_{EV,t}^c$ | Number of EV connecting to a charger station at the beginning of time t. | N | Based on Investment outputs |
| $N_{EV,t}^d$ | Number of EV disconnecting to a charging station at the beginning of time t | N | Based on Investment outputs |
| $N_{EV,t}^{Con}$ | Number of EV plugged in | N | Based on Investment outputs |
| Costs | | | |
| λ_t^{buy} | Cost for energy bought at time t. | €/kWh | UCED output |
| λ_t^{sell} | Price for energy sold at time t. | €/kWh | UCED output |
| $\lambda_t^{net_gen}$ | Network cost for energy generation at time t | €/kW | |
| λ_m^{peak} | Peak power cost. | €/kW | |
| λ^{fix} | Fix cost for using the red. | €/kW | |
| λ^{exceed} | Cost for exceeding the power band. | €/kW | |
| λ_t^{h2} | Cost for hydrogen consumption at time t | €/kWh | |
| λ_t^b | Cost for biomass consumption at time t | €/kWh | |
| λ_t^g | Cost for gas consumption at time t | €/kWh | |
| $\lambda_{EV,t}^{ch}$ | Cost for the EV entering the charging station at time t | € | |
| $\lambda_{n^{chp},t}^{sd}$ | Cost for closing the CHP at time t. | €/kWh | |
| $\lambda_{n^{chp},t}^{su}$ | Cost for opening the CHP at time t. | €/kWh | |
| λ^{dr} | Demand response cost. | €/kW | |
| Parameter per technology | | | |

| Parameter | Description | Units | Source |
|--------------------------|---|------------------------------------|-------------------|
| \overline{P}_{EL} | Maximum power consumed by the electrolyser. | kW | Investment output |
| \overline{P}_{band} | Maximum selling/buying power of the band. | kW | |
| \underline{P}_{EL} | Lower limit of power in electrolyser. | kW | Investment output |
| \overline{N}_{EL}^{H2} | Maximum rate of hydrogen molar in electrolyser. | Nm ³ /h | Investment output |
| LHV_{H_2} | Lower heating value of hydrogen. | $\frac{kWh}{mol}$ | |
| η_{EL} | Electrolyser efficiency. | [0,1] | |
| Q_0^{H2} | Hydrogen tank pressure in the first time. | Pa | |
| \overline{Q}^{H2} | Upper limit of hydrogen tank pressure. | Pa | |
| \underline{Q}^{H2} | Lower limit of hydrogen tank pressure. | Pa | |
| R | Gas constant. | $\frac{m^3 \cdot Pa}{K \cdot mol}$ | |
| $T_{H_2}^{mean}$ | Mean temperature inside the vessel. | K | |
| V^{H2} | Overall tank volume. | m ³ | Investment output |
| N_{dr}^{day} | Number of demand response activations per day. | N | |
| T^{dr} | Maximum consecutive time steps allowed of demand response. | hours | |
| $N_{chargers}^{total}$ | Total number of chargers available. | N | Investment output |
| E_{ev}^b | Energy capacity of an individual EV Battery. | kWh | |
| P_{v2g}^{max} | Maximum charging power of a V2G charging node. | kW | |
| EV_{ini}^{con} | Initial number of EV plugged in the charging station. | N | Investment output |
| $E_{ev,0}$ | Initial state of charge of battery Pool. | [0,1] | |
| η_{ev}^{ch} | Charging efficiency of the EV. | [0,1] | |
| η_{ev}^{dch} | Discharging efficiency of the EV. | [0,1] | |
| $SOC_{EV,0}$ | Initial state of charge of individual EV arriving at the charging station | [0,1] | |

| Parameter | Description | Units | Source |
|---------------------------|---|-------|-------------------|
| $SOC_{EV,f}$ | Final state of charge of individual EV departing at the charging station | [0,1] | |
| SOC_{ev}^{max} | Maximum state of charge for Individual EV Battery. | [0,1] | |
| SOC_{ev}^{min} | Minimum state of charge for Individual EV Battery. | [0,1] | |
| SOC_{ev}^{ini} | Initial State of charge (SOC) of an individual EV Battery. | [0,1] | |
| SOC_{ev}^{fin} | Final expected SOC of an individual EV Battery. | [0,1] | |
| P_{nes} | Minimum power for each type of Electrical Storage | kW | Investment output |
| \overline{P}_{nes} | Maximum power for each type of Electrical Storage | kW | Investment output |
| $SOC_{nes,0}$ | Initial state of charge for each Electrical Storage at time initial | [0,1] | |
| η_{nes}^{dch} | Discharge Efficiency of the Electrical Storage for each type of battery | [0,1] | |
| η_{nes}^{ch} | Charge Efficiency of the Electrical Storage for each type of Battery. | [0,1] | |
| \overline{SOC}_{nes} | Maximum state of charge for Electrical Storage for each Electrical Storage. | [0,1] | |
| SOC_{nes} | Minimum state of charge for Electrical Storage for each Electrical Storage. | [0,1] | |
| E_{nes} | Electrical Storage capacity for each type of Electrical Storage. | kWh | Investment output |
| HR_{CHP}^b | Heat rate of biomass to power in CHP. | | |
| C_{CHP}^{Gel} | Conversion factor from gas to electrical power | | |
| C_{CHP}^{Hel} | Conversion factor from hydrogen to electrical power | | |
| C_{CHP}^{Gth} | Conversion factor from gas to thermal power | | |
| C_{CHP}^{Hth} | Conversion factor from hydrogen to thermal power | | |
| $\overline{P}_{n^{chp}}$ | Maximum Electrical power for each CHP. | kW | Investment output |
| $\underline{P}_{n^{chp}}$ | Minimum Electrical power for each CHP. | kW | Investment output |

| Parameter | Description | Units | Source |
|--------------------------|--|-------------------|-------------------|
| $\overline{H_{n^{chp}}}$ | Maximum Thermal power for each CHP. | kWh _{th} | Investment output |
| $U_{n^{chp},0}$ | Initial state of the CHP for each CHP at initial time. | [0,1] | |
| $T_{n^{chp}}^{sd}$ | Minimum off time for each CHP. | hours | |
| $T_{n^{chp}}^{su}$ | Minimum uptime for each CHP. | hours | |
| $P_{n^{chp}}^B$ | Theoretical Electrical power B for each CHP. | kW | Investment output |
| $P_{n^{chp}}^D$ | Theoretical Electrical power D for each CHP. | kW | Investment output |
| $H_{n^{chp}}^C$ | Theoretical thermal power C for each CHP. | kWh _t | Investment output |
| $\overline{P_{hs}}$ | Maximum power for Electrical Storage. | kW | Investment output |
| S_{dr}^{inc} | Load increase share. | [0,1] | |
| S_{dr}^{dec} | Load decrease share. | [0,1] | |
| S_{dr}^{flex} | Flexible Share. | [0,1] | |
| $U_{dr,0}^{inc}$ | Initial state of increment at time initial. | [0,1] | |
| $U_{dr,0}^{dec}$ | Initial state of descend at time initial. | [0,1] | |
| N_{dr}^{daily} | Number of demand response activations per day | hours | |
| $\overline{N_{dr}}$ | Maximum time of demand response | hours | |
| $H2^{allowed}$ | If hydrogen is allowed in the archetype | [0,1] | |
| P_{inst}^b | Installed power for boilers | kW | Investment output |
| $\overline{PH2}$ | Maximum power for hydrogen tank | kW | Investment output |
| P^{PVR} | Installed power of PV on roof | kW | Investment output |
| P^{PVL} | Installed power of PV on land | kW | Investment output |
| P^{WTL} | Installed power of low wind turbine | kW | Investment output |
| H_b^{H2} | Conversion hydrogen to heat in the boiler | | |
| H_b^G | Conversion gas to heat in the boiler | | |
| η_{PV}^{land} | Efficiency of PV land in year | [0,1] | |
| η_{PV}^{roof} | Efficiency of PV roof in year | [0,1] | |

| Parameter | Description | Units | Source |
|--------------------|-------------------------------|-------|--------|
| η_{WT}^{low} | Efficiency of WT low in year | [0,1] | |
| η_{WT}^{high} | Efficiency of WT high in year | [0,1] | |

Source: own elaboration.

Variables

Table 69. Variables for the operational Model

| Variable | Description | Units/Domain |
|-------------------|--|--------------|
| $v2g_t^{in}$ | V2G vehicles entering the charging station at time t. | N |
| $v2g_t^{out}$ | V2G vehicles departing the charging station at time t | N |
| $e_{ev,t}$ | Energy level of EVs Battery Pool at time t . | kWh |
| $p_{ev,t}^{ch}$ | Charging power of EVs Battery Pool at time t . | kW |
| $p_{ev,t}^{dch}$ | Discharging power of EVs Battery Pool at time t . | kW |
| $u_{nes,t}$ | State of the EVs Battery Pool {1 is charging, 0 otherwise} at time t . | [0,1] |
| $p_{nes,t}^{ch}$ | Charging power for each type of Electrical Storage at time t . | kW |
| $p_{nes,t}^{dch}$ | Discharging power for each type of Electrical Storage at time t . | kW |
| $soc_{nes,t}$ | State of charge for each type of Electrical Storage at time t . | [0,1] |
| $u_{nchp,t}$ | State of the CHP {1 is open, 0 closed} at time t . | [0,1] |
| $x_{nchp,t}^{su}$ | Change off to on for each CHP at time t . | [0,1] |
| $x_{nchp,t}^{sd}$ | Change on to off for each CHP at time t . | [0,1] |
| $p_{nchp,t}$ | Electrical power for each CHP at time t . | kW |
| $h_{nchp,t}$ | Thermal power for each CHP at time t . | kW_{th} |
| $u_{dr,t}^{inc}$ | State of increment {1 is incrementing, 0 otherwise} at time t . | [0,1] |
| $u_{dr,t}^{dec}$ | State of descend {1 is descending, 0 otherwise} at time t . | [0,1] |
| $x_{dr,t}^{inc}$ | Increased power at time t . | kW |

| Variable | Description | Units/Domain |
|---------------------|--|-----------------|
| $x_{dr,t}^{dec}$ | Decreased power at time t . | kW |
| p_t^{buy} | Buying power at time t from the grid. | kW |
| p_t^{sell} | Selling power at time t to the grid. | kW |
| u_t^{buy} | State of direction in the grid tie {1 buy, 0 sell} at time t . | [0,1] |
| p_m^{peak} | Peak power per month. | kW |
| $z_{band,t}^{buy}$ | Buying exceed power of the band at time t . | kW |
| $z_{band,t}^{sell}$ | Selling exceed power of the band at time t . | kW |
| $p_{el,t}$ | Electrical power consumed by electrolyze at time t . | kW |
| u_t^{H2} | Electrolyser and CHP cannot produce or consume hydrogen from the storage at the same time. | [0,1] |
| $n_{el,t}^{H2}$ | Produced hydrogen mol/H by electrolyze at time . | $\frac{mol}{H}$ |
| q_t^{H2} | Pressure level of the tank. | Pa |
| $n_{nCHP,t}^{H2}$ | Consumed hydrogen molar/H by CHP. | $\frac{mol}{H}$ |
| $p_{hs,t}^{ch}$ | Power charged in the hydrogen Storage. | kW |
| $p_{hs,t}^{dch}$ | Power Discharged in the hydrogen Storage. | kW |
| $n_{EV,t}^{total}$ | Total number of EV in the charging Station at time t | N |
| $p_{wt,t}$ | Electrical power for wind turbine at time t | kW |
| $p_{pv,t}$ | Electrical power for photovoltaic at time t | kW |
| $h_{b,t}$ | Thermal power produced by the boilers at time t | kW_{th} |
| $h2_{b,t}$ | Hydrogen consumed by the boilers at time t | |
| $h2_{CHP,t}$ | Hydrogen consumed by the CHP at time t | |
| $g_{b,t}$ | Gas consumed by the boilers at time t | |
| $x_{b,t}$ | The boiler is consuming gas or hydrogen | [0,1] |
| g_t^{bought} | Gas bought for the boiler or the CHP | |
| $h2_t^{bought}$ | Hydrogen bought | |
| b_t^{bought} | Biomass bought | |

| Variable | Description | Units/Domain |
|-------------------|--|--------------|
| $g_{chp,t}$ | Gas consumed by the CHP at time t | |
| $b_{CHP,t}$ | Biomass consumed by the CHP at time t | |
| $h2_{b,t}^{high}$ | Hydrogen consumed by boilers for high temperature at time t | |
| $g_{b,t}^{high}$ | Natural gas consumed by boilers for high temperature at time t | |
| $x_{el,t}$ | Electrolyzer is active or not | [0,1] |

Source: own elaboration.

Objective Function

Table 70. Objective function for the Operational model

| Objective function | Equation |
|--------------------|--|
| Peak Power | <p>Min (Peak power cost) + (buy/sell energy from the grid) + (demand responds activations cost) + (CHP operation costs).</p> $\begin{aligned} \text{Min } & \sum_{m \in M} (C^{peak} \cdot p_m^{peak}) + \Delta_t \sum_{t \in T} (\lambda_t^{buy} \cdot p_t^{buy} - \lambda_t^{sell} \cdot p_t^{sell} + \lambda^{dr} (x_{dr,t}^{inc} + x_{dr,t}^{dec}) \\ & + \lambda_t^{net_{gen}} \cdot (p_{pv,t} + p_{wt,t} + \\ & p_{ev,t}^{dch} + \sum_{n_{es} \in N^{es}} (p_{n_{es},t}^{dch})) + \sum_{(n_{chp} \in N^{chp})} (\lambda_{n_{chp},t}^{sd} \cdot x_{n_{chp},t}^{sd} + \lambda_{n_{chp},t}^{su} \cdot x_{n_{chp},t}^{su}) + \lambda_t^{h2} \cdot \\ & h2_t^{bought} + \lambda_t^b \cdot b_t^{bought} + \\ & \lambda_t^g \cdot g_t^{bought} - \lambda_{EV,t}^{ch} \cdot v2g_t^{in}) \end{aligned}$ |
| Bandwidth | <p>Min (buy/sell energy from the grid) + (fixed and variable band costs) + (demand responds activations cost) + (CHP operation costs)</p> $\begin{aligned} \text{Min } & \Delta_t \sum_{t \in T} (\lambda_t^{buy} \cdot p_t^{buy} - \lambda_t^{sell} \cdot p_t^{sell} + \lambda^{fix} \cdot \overline{P_{band}} + \lambda^{exceed} * (z_{band,t}^{buy} + z_{band,t}^{sell}) \\ & + \lambda^{dr} (x_{dr,t}^{inc} + x_{dr,t}^{dec}) + \end{aligned}$ |

| | |
|-------------|---|
| | $\lambda_t^{netgen} \cdot (p_{pv,t} + p_{wt,t} + p_{ev,t}^{dch} + \sum_{n_{es} \in \mathcal{N}^{es}} (p_{n_{es},t}^{dch})) + \sum_{(n_{chp} \in \mathcal{N}^{chp})} (\lambda_{n_{chp},t}^{sd} \cdot x_{n_{chp},t}^{sd} + \lambda_{n_{chp},t}^{su} \cdot x_{n_{chp},t}^{su}) + \lambda_t^{h2} \cdot h2_t^{bought} + \lambda_t^b \cdot b_t^{bought} + \lambda_t^g \cdot g_t^{bought} - \lambda_{EV,t}^{ch} \cdot v2g_t^{in})$ |
| Time of Use | Min (buy/sell energy from the grid) + (demand responds activations cost) +(CHP operation costs); $Min \Delta_t \sum_{t \in T} (\lambda_t^{buy} \cdot p_t^{buy} - \lambda_t^{sell} \cdot p_t^{sell} + \lambda^{dr} (x_{dr,t}^{inc} + x_{dr,t}^{dec}) + \lambda_t^{netgen} \cdot (p_{pv,t} + p_{wt,t} + p_{ev,t}^{dch} + \sum_{n_{es} \in \mathcal{N}^{es}} (p_{n_{es},t}^{dch})) + \sum_{(n_{chp} \in \mathcal{N}^{chp})} (\lambda_{n_{chp},t}^{sd} \cdot x_{n_{chp},t}^{sd} + \lambda_{n_{chp},t}^{su} \cdot x_{n_{chp},t}^{su}) + \lambda_t^{h2} \cdot h2_t^{bought} + \lambda_t^b \cdot b_t^{bought} + \lambda_t^g \cdot g_t^{bought} - \lambda_{EV,t}^{ch} \cdot v2g_t^{in})$ |

Source: own elaboration.

Balance Equations

Table 71. Balance constraints for the Operational model

| Term | Equation |
|------------------------------------|---|
| Eq.84 Power balance | The electrical power balance must be satisfied $\forall t \in T$; $p_t^{buy} + P_{pv,t} + P_{wt,t} + \sum_{\mathcal{N}^{chp}} (p_{n_{chp},t}) + p_{ev,t}^{dch} + \sum_{\mathcal{N}^{es}} p_{n_{es},t}^{dch} + x_{dr,t}^{dec} = p_t^{sell} + D_{el,t} + x_{dr,t}^{inc} + p_{ev,t}^{ch} + \sum_{\mathcal{N}^{es}} (p_{n_{es},t}^{ch}) + p_{el,t}$ |
| Eq.85 Thermal power balance | The thermal power balance must be satisfied $\forall t \in T$; $\sum_{\mathcal{N}^{chp}} h_{n_{chp},t} + h_{b,t} \geq H_{tbl,t}$ |
| Eq.86 Hydrogen Balance | Hydrogen balance must be satisfied $\forall t \in T$; $n_{el,t}^{H2} + p_{hs,t}^{dch} + h2_t^{bought} = h2_{b,t} + h2_{b,t}^{high} + p_{hs,t}^{ch} + h2_{CHP,t}$ |

Source: own elaboration.

Peak Power

Table 72. Peak power constraints for the Operational model

| Term | Equation |
|------------------------------------|--|
| Eq.87 Monthly peak power | The Peak power is computed monthly and it's the maximum power bought for each month $\forall t \in T_m$; $p_t^{buy} \leq p_m^{peak}$ |

Source: own elaboration.

Time-of-use

Table 73. Time of Use constraints for the Operational model

| Term | Equation |
|------------------------------|---|
| Eq.88 Bought power | With the help of Eq.96 Time of Use tariff is only allowed to sell or buy power at the same time. This equation determines the bought power $\forall t \in T$; $p_t^{buy} \leq u_t^{buy} \cdot M$ |
| Eq.89 Sold power | With the help of Eq.95 Time of Use tariff is only allowed to sell or buy power at the same time. This equation determines the sold power $\forall t \in T$; $p_t^{sell} \leq (1 - u_t^{buy}) \cdot M$ |

Source: own elaboration.

Bandwidth

Table 74. Bandwidth constraints for the Operational model

| Term | Equation |
|---|---|
| Eq.90 Bought power | With the help of eq.92 Bandwidth tariff is only allowed to sell or buy power at the same time. This equation determines the bought power $\forall t \in T$; $p_t^{buy} \leq u_t^{buy} \cdot M$ |
| Eq.91 Sold power | With the help of eq.91 Bandwidth tariff is only allowed to sell or buy power at the same time. This equation determines the sold power $\forall t \in T$; $p_t^{sell} \leq (1 - u_t^{buy}) \cdot M$ |
| Eq.92 Exceeded bought power over the band | A constraint that tells how much we are beyond the buying limit of the band $\forall t \in T$; $p_t^{buy} - z_{band,t}^{buy} \leq \overline{P_{band}}$ |
| Eq.93 | A constraint that tells how much we are beyond the selling limit of the band $\forall t \in T$; |

| | |
|-----------------------------------|---|
| Exceeded sold power over the band | $p_t^{sell} - z_{band,t}^{sell} \leq \overline{P}_{band}$ |
|-----------------------------------|---|

Source: own elaboration.

Vehicle-to-Grid

Table 75. V2G constraints for the Operational model

| Term | Constraints |
|----------------------------------|--|
| Eq.94 EV in | Electrical vehicles entering the charging station $\forall t \in T$. $v2g_t^{in} \leq N_{EV,t}^c$ |
| Eq.95 EV out | Electricals vehicles exiting the charging station $\forall t \in T$. $v2g_t^{out} \leq M$ |
| Eq.96 EV definition | Defining how many EV are available $\forall t \in T$. $n_{ev,t}^{total} = N_{EV,t}^{Con}$ |
| Eq.97 EV upper limit | An upper limit for how many EV available $\forall t \in T$. $n_{ev,t}^{total} \leq N_{chargers}^{total}$ |
| Eq.98 EVs plugged in | The balance of EV available at the charging station. $n_{ev,t}^{total} = \begin{cases} n_{ev,0}^{total} + v2g_t^{in} - v2g_t^{out} ; & t = 1 \\ n_{ev,t-1}^{total} + v2g_t^{in} - v2g_t^{out} ; & \forall t \in [2, T] \end{cases}$ |
| Eq.99 Energy balance | The balance for the energy available having in to account the loss efficiency for charging and discharging $\forall t \in T$; $\begin{aligned} e_{ev,t} &= e_{ev,t-1} + \Delta_t \\ &\cdot \left(p_{ev,t}^{ch} \cdot \eta_{ev}^{ch} - \frac{p_{ev,t}^{dch}}{\eta_{ev}^{dch}} - v2g_t^{out} \cdot SOC_{EV,f} \cdot E_{ev}^b + v2g_t^{in} \cdot SOC_{EV,0} \right. \\ &\quad \left. \cdot E_{ev}^b \right) \end{aligned}$ |
| Eq.100 SOC bounds | A lower limit for the SOC of EV $\forall t \in T$; $e_{ev,t} \geq n_{ev,t}^{total} \cdot SOC_{ev}^{min} \cdot E_{ev}^b + v2g_{ev,t+1}^{out} \cdot (SOC_{EV,f} - SOC_{ev}^{min}) \cdot E_{ev}^b$ |
| Eq.101 SOC upper limit | An upper limit for the SOC of EV $\forall t \in T$; $e_{ev,t} \leq SOC_{ev}^{max} \cdot n_{ev,t}^{total} \cdot E_{ev}^b$ |
| Eq.102 Limit energy | A lower limit for the energy available $\forall t \in T$; $p_{ev,t}^{ch} + p_{ev,t}^{dch} \leq n_{ev,t}^{total} \cdot P_{v2g}^{max}$ |
| Eq.103 Final SOC | A lower bound for the final SOC. |

| | |
|--|--|
| | $e_{ev,f} \geq E_{ev,0} \cdot E_{ev}^b \cdot n_{ev,f}^{total}$ |
|--|--|

Source: Modification of the model from Meenakumar et al. (2020).

Electrical Storage

Table 76. Electrical Storage constraints for the Operational model

| Term | Constraints |
|--------------------------------------|---|
| Eq.104 Charging bounds | An upper and lower limit for charging that cannot be surpassed $\forall t \in T, \forall n^{es} \in N^{ES}$; $u_{n^{es},t} \cdot \underline{P}_{n^{es}} \leq p_{n^{es},t}^c \leq u_{n^{es},t} \cdot \overline{P}_{n^{es}}$ |
| Eq.105 Discharging bounds | An upper and lower limit for discharging that cannot be surpassed $\forall t \in T, \forall n^{es} \in N^{ES}$; $(1 - u_{n^{es},t}) \cdot \underline{P}_{n^{es}} \leq p_{n^{es},t}^d \leq (1 - u_{n^{es},t}) \cdot \overline{P}_{n^{es}}$ |
| Eq.106 Initial SOC balance | An initial balance of the energy available before the loss of energy for charging or discharging the electrical storage $\forall n^{es} \in N^{ES}$; $soc_{n^{es},1} \cdot E_{n^{es}} = SOC_{n^{es},0} \cdot E_{n^{es}} + \eta_{n^{es}}^{ch} \cdot p_{n^{es},1}^c - \frac{p_{n^{es},1}^d}{\eta_{n^{es}}^{dch}}$ |
| Eq.107 SOC bounds | An upper and lower limit for the SOC $\forall t \in T, \forall n^{es} \in N^{ES}$; $SOC_{n^{es}}^{min} \leq soc_{n^{es},t} \leq SOC_{n^{es}}^{max}$ |
| Eq.108 SOC balance | A balance of the energy available before the loss of energy for charging or discharging the electrical storage $\forall t \in T, \forall n^{es} \in N^{ES}$; $E_{n^{es}} \cdot soc_{n^{es},t} = E_{n^{es}} \cdot soc_{n^{es},t-1} + \Delta_t \cdot \left(\eta_{n^{es}}^{ch} \cdot p_{n^{es},t}^c - \frac{p_{n^{es},t}^d}{\eta_{n^{es}}^{dch}} \right)$ |
| Eq.109 SOC Final | A constraint to impose the final state of charge is at least the same as the initial state of charge. $t = card(T)$ $E_{n^{es}} \cdot soc_{n^{es},t} \leq SOC_{n^{es},0} \cdot E_{n^{es}}$ |

Source: Modification of the model from Igualada González et al. (2013).

Combined Heat and Power

Table 77. CHP constraints for the Operational model

| Term | Equation |
|-------------------------------|---|
| Eq.110 Power bounds | An upper and lower limit for power production that cannot be surpassed $\forall t \in T, \forall n^{chp} \in N^{CHP}$; $u_{n^{chp},t} \cdot \underline{P}_{n^{chp}} \leq p_{n^{chp},t} \leq u_{n^{chp},t} \cdot \overline{P}_{n^{chp}}$ |
| Eq.111 | An upper and lower limit for heat production that cannot be surpassed $\forall t \in T, \forall n^{chp} \in$ |

| | |
|--|--|
| Thermal power generation bound | $N^{CHP};$ $0 \leq h_{n^{chp},t} \leq u_{n^{chp},t} \cdot \overline{H}_{n^{chp}}$ |
| Eq.112 Initial state | Defining if the plant is open or closed at time initial $\forall n^{chp} \in N^{CHP};$ $U_{n^{chp},0} = u_{n^{chp},0}$ |
| Eq.113 Change of state | A constraint to know if the plant changes the state on to off or off to on $\forall t \in T,$ $\forall n^{chp} \in N^{CHP};$ $u_{n^{chp},t} - u_{n^{chp},t-1} = x_{n^{chp},t}^{su} - x_{n^{chp},t}^{sd}$ |
| Eq.114 Time limit | A minimum uptime for the CHP plant $\forall t \in [\underline{T}_{n^{chp}}^{su}, T], \forall n^{chp} \in N^{CHP};$ $\sum_{i=t-\underline{T}_{n^{chp}}^{su}+1}^t x_{n^{chp},t}^{su} \leq u_{n^{chp},t}$ |
| Eq.115 Time limits switch down | A minimum shutdown time for the CHP plant $\forall t \in [\underline{T}_{CHP,n^{chp}}^{sd}, T], \forall n^{chp} \in N^{CHP};$ $\sum_{i=t-\underline{T}_{n^{chp}}^{sd}+1}^t x_{n^{chp},t}^{sd} \leq u_{n^{chp},t}$ |
| Eq.116 Polygon model of CHP A | Limits the Feasible Operating Region of the CHP below the line AB of the trapezoid $\forall t \in T, \forall n^{chp} \in N^{CHP};$ $0 \leq (P_{n^{chp}}^B - \overline{P}_{n^{chp}}) \cdot (h_{n^{chp},t}) + (\overline{P}_{n^{chp}} - p_{n^{chp},t}) \cdot \overline{H}_{n^{chp}}$ |
| Eq.117 Polygon model of CHP B | Limits the Feasible Operating Region of the CHP above the line BC of the trapezoid $\forall t \in T, \forall n^{chp} \in N^{CHP};$ $(p_{n^{chp},t} - P_{n^{chp}}^D) \cdot H_{n^{chp}}^C - (P_{n^{chp}} - P_{n^{chp}}^D)h_{n^{chp},t} \geq -(1 - u_{n^{chp},t} \cdot M)$ |
| Eq.118 Polygon mode of CHP C | Limits the Feasible Operating Region of the CHP above the line CD of the trapezoid $\forall t \in T, \forall n^{chp} \in N^{CHP};$ $(p_{n^{chp},t} - \underline{P}_{n^{chp}}) \cdot (\overline{H}_{n^{chp}} - H_{n^{chp}}^C) - (P_{CHP,n^{chp}}^B - \underline{P}_{n^{chp}}) \cdot (h_{n^{chp},t} - H_{n^{chp}}^C) \leq -(1 - u_{n^{chp},t} \cdot M)$ |

Source: (Mansouri et al., 2020).

Demand Response

Table 78. Demand response constraints for the Operational model

| Term | Equations |
|------|-----------|
|------|-----------|

| Term | Equations |
|--------------------------------------|--|
| Eq.119 Initial state | Defining the initial State of increment and decrease for demand response; $U_{dr,0}^{inc} = u_{dr,0}^{inc}$ $U_{dr,0}^{dec} = u_{dr,0}^{dec}$ |
| Eq.120 Decrease demand | An upper and lower limit for decrease demand response $\forall t \in T$; $0 \leq x_{dr,t}^{dec} \leq u_{dr,t}^{dec} \cdot D_{hp,t} \cdot s_{dr}^{flex} \cdot S_{dr}^{dec}$ |
| Eq.121 Increase demand | An upper and lower limit for increase demand response $\forall t \in T$; $0 \leq x_{dr,t}^{inc} \leq u_{dr,t}^{inc} \cdot D_{hp,t} \cdot s_{dr}^{flex} \cdot S_{dr}^{inc}$ |
| Eq.122 Time limit | The demand response is not allowed to be performed consecutive for more than an upper limit $\forall t \in [T^{dr} - 1, T - 1]$; $\sum_{i=t-T^{dr}+1}^{t+1} (u_{dr,t}^{inc} + u_{dr,t}^{dec}) \leq T^{dr}$ |
| Eq.123 Activations per day | The demand response is not allowed to be performed daily for more than an upper limit $\forall d \in D$; $\sum_{t=(d-1)\cdot dh+1}^{d\cdot dh} (u_{dr,t}^{inc} + u_{dr,t}^{dec}) \leq N_{dr}^{day} \cdot T^{dr}$ |

Source: Modification of the model from Heitkoetter et al. (2021).

Electrolyser

Table 79. Electrolyzer constraints for the Operational model

| Term | Constraints |
|------|-------------|
| | |

| Term | Constraints |
|--------------------------------------|---|
| Eq.125 Power bounds | An upper and lower limit for the electrolyze power $\forall t \in T$; $\underline{P}_{EL} \leq p_{el,t} \leq \overline{P}_{EL}$ |
| Eq.126 Hydrogen bound | The produced hydrogen molar is not allowed to surpass an upper limit $\forall t \in T$; $n_{el,t}^{H2} \leq \overline{N}_{EL}^{H2}$ |
| Eq.127 Hydrogen generation | A loss of efficiency for producing hydrogen molar $\forall t \in T$; $n_{el,t}^{H2} = \frac{\eta_{EL} \cdot p_{el,t}}{LHV_{H_2}}$ |

Source: Modification of the model from Nojavan and Zare (2018).

Hydrogen Storage

Table 80. Hydrogen Storage constraints for the Operational model

| Term | Constraints |
|----------------------------------|---|
| Eq.127 Initial state | The initial pressure of the tank is defined $q_0^{H2} = Q_0^{H2}$ |
| Eq.128 Pressure bounds | An upper and lower limit for the pressure of the tank $\forall t \in T$; $\underline{Q}^{H2} \leq q_t^{H2} \leq \overline{Q}^{H2}$ |
| Eq.129 Storage balance | A provision of the dynamic model for the hydrogen storage pressure $\forall t \in T$; $q_t^{H2} = q_{t-1}^{H2} + \frac{R \cdot T_{H2}^{mean}}{V^{H2}} (n_{el,t}^{H2} - (HR^{H2} \cdot p_{chp,n^{chp},t})) \cdot \Delta t$ |
| Eq.130 Charge Bound | An upper and lower limit for the power charged in the hydrogen storage $\forall t \in T$; $0 \leq p_{hs,t}^{ch} \leq u_{el,t}^{H2} \cdot \overline{P}_{hs}$ |
| Eq.131 Discharge Bound | An upper and lower limit for the power discharged in the hydrogen storage $\forall t \in T$; $0 \leq p_{hs,t}^{dch} \leq (1 - u_{el,t}^{H2}) \cdot \overline{P}_{hs}$ |

Source: Modification of the model from Nojavan and Zare (2018).

Boilers

Table 81. Boilers constraints for the Operational model

| Term | Constraints |
|---------------------------------------|---|
| Eq.132 High thermal balance | High thermal balance $\forall t \in T$: $g_{b,t}^{high} \cdot H_b^G + h2_{b,t}^{high} \cdot H_b^{h2} + = H_{tbl,t}^H$ |
| Eq.133 Thermal balance | Thermal balance $\forall t \in T$: $h_{b,t} = h2_{b,t} \cdot H_b^{h2} + g_{b,t} \cdot H_b^G$ |
| Eq.134 Bounds h2 | An upper and lower limit for the hydrogen $\forall t \in T$. $0 \leq h2_{b,t} \leq P_{inst}^b \cdot M \cdot x_{b,t}$ |
| Eq.135 Bounds gas | An upper and lower limit for the ga $\forall t \in T$. $0 \leq g_{b,t} \leq P_{inst}^b \cdot M \cdot (1 - x_{b,t})$ |
| Eq.136 Boiler bound | An upper and lower limit for the thermal power of the boiler $\forall t \in T$; $0 \leq h_{b,t} \leq P_{inst}^b$ |

Source: own elaboration.

Annex 3. Technical parameters for energy assets in the investment and operational models

The parameters used for each energy asset category are presented below, highlighting in yellow those included in the investment model and in green those used in the operational one. The parameters without colour are used in both models.

| | |
|--|-------------------|
| | Only investment. |
| | Only operational. |
| | Both models. |

In addition to the presented parameters, the operational model requires as inputs the installed capacity per technology and year decided by the investment model. This is not always indicated in the presented tables but it must be considered as a required input. Moreover, there are some yearly, daily or hourly vectors that are also inputted to the model and are not discussed in this document as the assumptions behind these data have been already discussed in the main document body and are available at the Annex database.

For the investment model, all technologies have a parameter indicating the area occupied per unit of capacity installed. However, this area is only considered relevant when dealing with ground-mounted solar PV and wind turbines as they compete for the same available surface. Furthermore, rooftop solar PV is restricted by the available rooftop space. In the industrial archetype, the area occupied by the hydrogen storage is also added as a constraint related to the available land space. For all other technologies, a negligible area value is used (1E-20) to make their space usage insignificant to the decision-making process.

Solar Photovoltaics

Solar PV technologies are distinguished by the equipment location, using different parameters whether it is installed on rooftop or on the ground, as the investment model decides the installed capacity considering the available surface for each case. Weather data and other parameters needed to calculate generated power from solar irradiation are not given as the solar production is calculated based on the Load Factor Curves available at the Annex database.

Table 82. Scalar parameters for PV solar technologies

| Parameter | Description | Value | Units |
|--------------------|--|-------|---------------------|
| ETA_PV_ROOF | Efficiency of PV solar systems in rooftop. | 100% | % |
| ETA_PV_LAND | Efficiency of PV solar systems ground mounted. | 100% | % |
| A_PV_ROOF | Area per capacity unit of PV solar rooftop. | 5.10 | m ² /kWe |
| A_PV_LAND | Area per capacity unit of ground-mounted PV solar. | 29.4 | m ² /kWe |

Source: Own elaboration with data from Drücke et al. (2021); Urbina (2014); Müller et al. (2021); and Cagle et al. (2022).

As observed in Table 82, efficiency values are set at 100% as the Load factor curve already incorporates the typical PV solar panels efficiency. Using the provided hourly load factors for solar PV, an annual capacity factor of 10.9% is calculated for the German case and 18.3% for Spain. These values are close to the average capacity factors reported for both countries, which varies between 10% and 14% for Germany (Drücke et al., 2021) and is estimated above 20% for Spain(Urbina, 2014). The values used for MODECO correspond to a specific region within the country and not an average national value, which explains the discrepancies.

Regarding the surface used per type of solar PV installation, a value of 5.052 m²/kWe is established for rooftop systems based on the value defined by Müller et al. (2021) for glass-back sheet modules. For ground

mounted systems, Cagle et al. (2022) proposed a value of 34 We/m² (equivalent to 29.4 m²/kWe). It is assumed that PV systems on the ground require a larger surface considering the needed space between module lines.

Wind turbines

Onshore wind turbine investments are possible in the Industrial polygon, Rural town and Virtual community archetypes, where two types of turbines can be installed based on their specific capacity which in turn is related to the turbine's rotor diameter¹⁷. The LOW specific capacity is considered to have a hub height of 200 m, and the HIGH specific capacity a hub height of 50 m following the criteria used by the authors of the wind investment and operational costs (Ioannis Tsipopoulos, Dalius Tarvydas, and Andreas Zucker 2018). The two models differ in the required investment per technology, but also in their power generation and land use efficiencies.

Table 83. Scalar parameters for Wind turbine technologies

| Parameter | Description | Value | Units |
|--------------------|---|-------|---------------------|
| ETA_WT_LOW | Efficiency of wind turbines with LOW specific capacity. | 100% | % |
| ETA_WT_HIGH | Efficiency of wind turbines with HIGH specific capacity | 100% | % |
| A_WT_LOW | Area per capacity unit of wind turbines LOW. | 160 | m ² /kWe |
| A_WT_HIGH | Area per capacity unit of wind turbines HIGH. | 67.5 | m ² /kWe |

Source: Own elaboration with data from Ioannis Tsipopoulos, Dalius Tarvydas, and Andreas Zucker (2018); Dalla Longa et al. (2018); Sun, Yang, and Gao (2019); Obane, Nagai, and Asano (2020).

As done with solar, a 100% value is used for the wind turbines efficiencies (ETA_WT_LOW and ETA_WT_HIGH) given that the actual efficiency is already incorporated in the load factor values. The area occupied per installed capacity unit is established using a reference rotor diameter (RD) defined for each wind turbine type. The HIGH specific capacity turbine is assumed to have a rotor diameter of 90 meters based on the Vestas V90 model used as a reference for large turbines (base capacity of 3 MW) in a JRC study on wind potential in Europe (Dalla Longa et al., 2018). The LOW specific capacity model is assumed to have a rotor diameter of 40 meters as defined for small-sized turbines (base capacity of 250 kWe) in the aforementioned JRC's study. The land surface needed per each turbine unit is calculated as 25RD² based on the optimal value suggested by Sun, Yang, and Gao (2019) A similar relation (30RD²) is suggested by Obane, Nagai, and Asano (2020). To obtain the area per capacity unit, the obtained surface is divided by the applicable reference capacity, obtaining the values described in Table 83.

Smart V2G Chargers

Most of the scalar parameters required for the V2G chargers modelling are presented in Section 3.3.2, except for the State of Charge (SOC) operational range for the individual EV units (SOC_MAX_EV and SOC_MIN_EV), which is set as 95%-5% a suggested by Wang et al. (2020) and Fan et al. (2019). The SOC level of the EV arriving (SOC_INI_EV) and departing (SOC_FIN_EV) from the charging station is set based on the findings from Corchero García (2015) as explained in this document. The maximum charging/discharging power at individual charger correspond to the charging stations capacity (11 kWe) assumed for V2G chargers. The charging and discharging efficiencies are considered 95%.

Additionally, the models require to establish the initial number of EV at the start of the day (EV_CON_INI) as well as the associated aggregated energy capacity to that number of vehicles. The first is set as zero for the investment model as the definitive number of installed chargers is unknown prior to the optimization process. For the operational model, in which the number of installed chargers is a given input, it is assumed that at the start of the day (00:00), 25% of the installed chargers are occupied.

¹⁷ A wind turbine's specific capacity or specific power is a parameter that relates the swept area of its rotor to the installed power (watts). It is measured in watts per square meter (W/m²) (Bolinger et al., 2021).

Table 84. Scalar parameters for EV smart chargers

| Parameter | Description | Value | Units |
|---------------------|---|---|----------------------|
| ETA_CH_V2G | Charging efficiency of EV batteries. | 95% | % |
| ETA_DCH_V2G | Discharging efficiency of EV batteries. | 95% | % |
| A_V2G | Surface occupied by an individual charger (disregarded in the final scenarios) | 1E-20 | m ² /unit |
| E_B_V2G | Energy capacity of individual EV batteries. | Calculated based on average fleet capacity. | kWe |
| P_MAX_CH_V2G | Maximum charging/discharging at individual charger | 11 | kWe |
| EV_CON_INI | Initial number of EV (previous to optimization) at the start of the day (00:00). | 0 | EV number |
| EV_POOL_INI | Aggregated energy capacity of battery pool at the start of the day (00:00). | EV_CON_INI *E_B_V2G | kWe |
| SOC_MAX_EV | Maximum SOC for individual EV. | 95% | % |
| SOC_MIN_EV | Minimum SOC for individual EV. | 5% | % |
| SOC_INI_EV | SOC level of individual EV arriving at the charging station. | 58% | % |
| SOC_FIN_EV | SOC level of individual EV departing at the charging station. | 84% | % |

Source: Own elaboration with data from Wang et al. (2020); Fan et al. (2019); and Corchero García (2015).

Combined Heat and Power

In all archetypes, two configurations – small and large units – of Combined Heat and Power (CHP) fuelled by gaseous fuels (natural gas or hydrogen) were initially considered as a potential investment option for all archetypes except the Virtual community. However, after modelling the archetype's electrical and heat demand, only the small-sized configuration (< 20 MWe) is kept. The same is done for the biomass-fuelled CHP units, which are considered an investment option only in the Rural town archetype.

Given the complexities of the investment decision model, a simplified mathematical model is used for both CHP types, assuming a linear relationship between heat and electrical production, and varying mainly the thermal and electrical efficiencies depending on the CHP's assumed configuration per type of fuel used. For the operational model, in which the installed capacity is already known, a more complex model is selected, using a trapezoid with four theoretical operating points representing the unit's Feasible Operational Region (FOR). As noted in Table 85, the higher complexity of the approach used in the operational model translates into a higher number of inputs than in the investment model.

Table 85. Scalar parameters for biomass-fuelled CHP

| Type | Parameter | Description | Value | Units |
|------------------|----------------------|---|---------------------------------------|---------|
| SMALL (< 20 MWe) | CHP_R_POWER_B | Installed capacity for biomass-fuelled CHP | Result from investment model | kWe |
| | MIN_EL_B | Minimum operational power output | CHP_R_POWER_B * 0.4 | kWe |
| | MAX_EL_B | Maximum operational power output | CHP_R_POWER_B * 1 | kWe |
| | MAX_TH_B | Maximum useful heat output | CHP_R_POWER_B * 0.85 * [1/CHP_CONV_B] | kWt |
| | B_POINT_B | Theoretical operating point B | MAX_TH_B | kWt |
| | C_POINT_B | Theoretical operating point C | D_POINT_B * [1/CHP_CONV_B] | kWt |
| | D_POINT_B | Theoretical operating point D | MIN_EL_B | kWe |
| | U_INI_B | Initial state of CHP biomass at optimization start (on/off) | 1 | [1,0] |
| | B_CONV_EL | Fuel to electricity ratio (biomass) | 0.1927 | kWe/mol |
| | B_CHP_CONV | Heat to power ratio (CHP -biomass) | 2.2222 | kWt/kWe |
| | ETA_EL_CHP_B | HP electrical efficiency (CHP - biomass) | 0.35 | % |
| | ETA_H_CHP_B | CHP heat efficiency (CHP - biomass) | 0.78 | % |
| | C_OFF_B | CHP shutdown cost (CHP -biomass) | 0 | Euros |
| | C_ON_B | CHP start-up cost (CHP - biomass) | See Eq. 138 | Euros |

Source: Own elaboration with data from Algie and Wong (2002); Alipour, Zare, and Mohammadi-Ivatloo (2014); Nazari-Heris, Mohammadi-ivatloo, and Nazarpour (2019); Eurostat (2017); Sims et al. (2007); Forest Research (2022); Pettersen (1984); Dimoulkas and Amelin (2015); Yu, Zhang, and Guan (2022); Gambarotta et al. (2015); Facci, Andreassi, and Ubertini (2014); U.S. Energy Information Agency (2020); and Ghaffarpour et al. (2018).

Table 86 Scalar parameters for gas-fuelled CHP

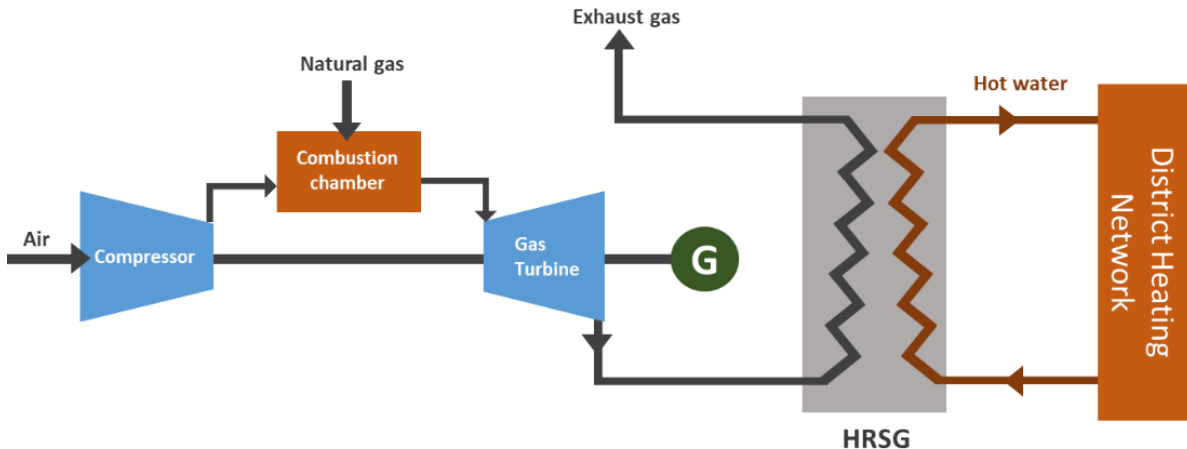
| Type | Parameter | Description | Value | Units |
|------------------|----------------------|---|--|---------|
| SMALL (< 20 MWe) | CHP_R_POWER_G | Installed capacity for gas-fuelled CHP | Result from investment model | kWe |
| | MIN_EL_G | Minimum operational power output | $CHP_R_POWER_G * 0.4$ | kWe |
| | MAX_EL_G | Maximum operational power output | $CHP_R_POWER_G * 1$ | kWe |
| | MAX_TH_G | Maximum useful heat output | $CHP_R_POWER_G * 0.85 * [1/CHP_CONV_B]$ | kWt |
| | B_POINT_G | Theoretical operating point B | MAX_TH_G | kWt |
| | C_POINT_G | Theoretical operating point C | $D_POINT_G * [1/CHP_CONV_G]$ | kWt |
| | D_POINT_G | Theoretical operating point D | MIN_EL_G | kWe |
| | U_INI_G | Initial state of CHP gas at optimization start (on/off) | 1 | [1,0] |
| | G_CONV_EL | Fuel to electricity ratio (natural gas) | 0.09832 | kWe/mol |
| | H_CONV_EL | Fuel to electricity ratio (hydrogen) | 0.03033 | kWe/mol |
| | G_CHP_CONV | Heat to power ratio (CHP -gas) | 1.81818 | kWt/kWe |
| | ETA_EL_CHP_G | HP electrical efficiency (CHP - biomass) | 0.42 | % |
| | ETA_H_CHP_G | CHP heat efficiency (CHP - biomass) | 0.76 | % |
| | C_OFF_G | CHP shutdown cost (CHP -biomass) | 0 | Euros |
| | C_ON_G | CHP start-up cost (CHP - biomass) | See Eq. 138 | Euros |
| | T_SD_G | Minimum off time (CHP gas) | 3 | h |
| | T_SU_G | Minimum on time (CHP – gas) | 4 | h |
| | MAX_ON_G | Maximum amount of times per day that the CHP unit can be turn off and turn on again | 1 | Units |

Source: Own elaboration with data from Algie and Wong (2002); Alipour, Zare, and Mohammadi-Ivatloo (2014); Nazari-Heris, Mohammadi-ivatloo, and Nazarpour (2019); Eurostat (2017); Sims et al. (2007); EUROGAS (2011); Dimoulkas and Amelin (2015); Yu, Zhang, and Guan (2022); Gambarotta et al. (2015); Facci, Andreassi, and Ubertini (2014); U.S. Energy Information Agency (2020); and Ghaffarpour et al. (2018).

The technical parameters applicable per fuel differ as they represent different CHP configurations. In the case of natural gas CHP, the small-sized equipment is assumed to be a gas turbine associated to a Heat Recovery Steam Generator (HRSG) from which heat is transferred to the district heating network (Figure 87). In the case of the biomass units considered for the Rural town archetype, a regular steam turbine cycle coupled with a

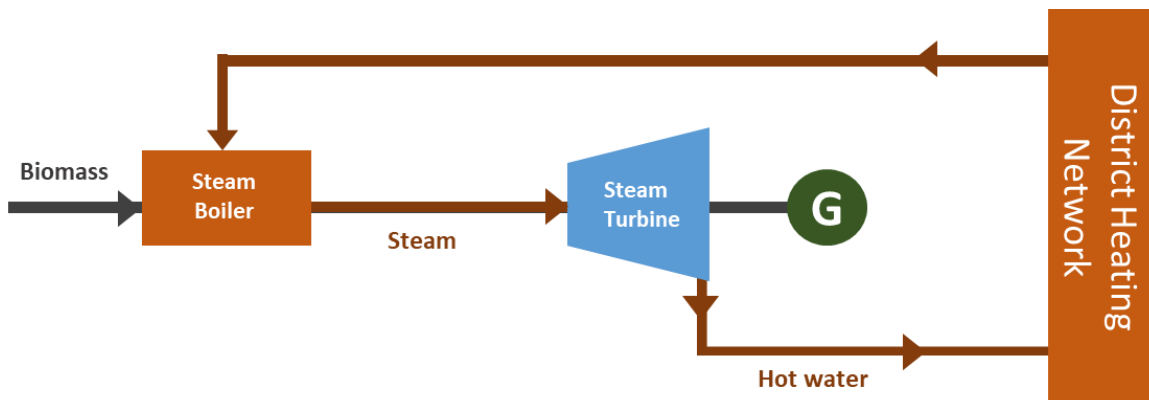
HRSG unit (Figure 88) is considered. As small-sized biomass units are now the only option, pellets are used as the default biomass fuel type.

Figure 87. CHP assumed configuration considered for small natural gas-fuelled units.



Source: Own elaboration.

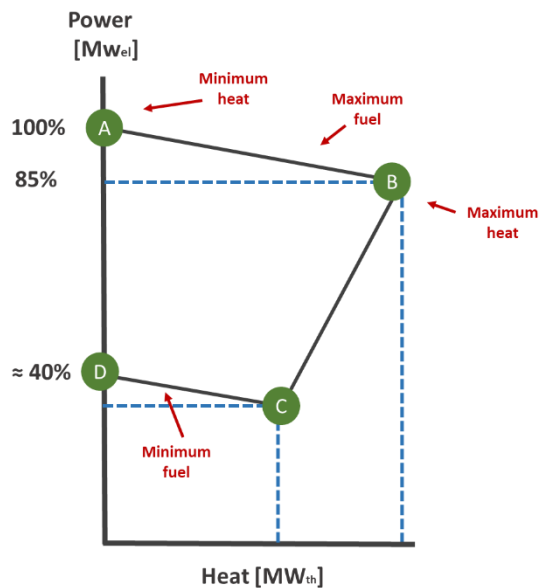
Figure 88. CHP assumed configuration for small biomass-fuelled units.



Source: Own elaboration.

The parameters referring to the theoretical operational points are based on the simplified feasible operational region defined for both CHP. The required operating points (B_POINT, C_POINT, D_POINT) are based on the simplified model proposed by Algie and Wong (2002); Alipour, Zare, and Mohammadi-Ivatloo (2014); and Nazari-Heris, Mohammadi-ivatloo, and Nazarpour (2019). The trapezoid FOR and the required operating points are indicated in Figure 89. As observed, these can be calculated as a percentage of the equipment's rated power under normal conditions; which is the value obtained by the investment model. Point A represents the upper limit of the active power output of the CHP unit, defined as 115% the rated power, based on typical requirements for rotating units as explained by (Algie and Wong, 2002). In the parameters listed in Table 85 and Table 86, Point A can be considered the unit's maximum electrical output (MAX_EL_G and MAX_EL_B) and Point B is the amount of heat produced at the rated power under normal conditions. This is calculated considering the electricity to useful heat ratio (CHP_CONV) defined for each case. Finally, Point D is set as 50% the rated power, and Point C, the corresponding heat production at that point.

Figure 89. Simplified feasible operational region considered for units (operating points in green)



Source: Own elaboration based on the model proposed by Algie and Wong (2002).

The fuel to electricity (B_CONV_EL, G_CONV_EL, H_CONV_EL) and power to heat (CHP_CONV_B, CHP_CONV_G) ratios are calculated for each CHP configuration considered in MODECO, based on the applicable efficiency values. For the fuel to electricity ratio, the system's electrical efficiency (η) is considered as well as the fuel's Low Heating Value (LHV), density (ρ) and molar mass (M) as indicated in Eq. 137. The fuel to heat ratio is defined based on the default power-to-heat values established in the reporting template for heat and power generation aligned with Directive 2012/27/EU of the European Parliament and the Council of 25 October 2012 on energy efficiency (Eurostat, 2017). The considered efficiency values and fuel characteristics used to calculate the fuel-to-electricity ratio are listed in Table 87.

E1. 137 Fuel to electricity ratio for fuel X (biomass, natural gas or hydrogen)

$$X_CONV_EL = LHV \left[\frac{kWh}{m^3} \right] * \frac{1}{\rho} \left[\frac{m^3}{kg} \right] * M \left[\frac{kg}{mol} \right] * \eta_{el}$$

Table 87 Efficiency and fuel characteristics considered for each CHP configuration

| CHP size | Fuel | Configuration | $\eta_{el} [\%]$ | LHV [kWh/m ³] | ρ [kg/m ³] | M [kg/mol] |
|----------|-------------|---------------|------------------|---------------------------|-----------------------------|------------|
| Small | Natural gas | Fig. 1 | 42% | 9.749 | 0.668 | 0.01604 |
| Large | Natural gas | Fig. 2 | 55% | 9.749 | 0.668 | 0.01604 |
| Small | Hydrogen | Fig. 1 | 42% | 2.997 | 0.084 | 0.00202 |
| Large | Hydrogen | Fig. 2 | 55% | 2.997 | 0.084 | 0.00202 |
| Small | Pellets | Fig. 3 | 35% | 875 | 250 | 0.15731 |
| Large | Woodchips | Fig. 3 | 35% | 3,120 | 650 | 0.15731 |

Source: efficiency values correspond to the upper limits per technology stated by Sims et al. (2007); LHV for natural gas is taken from EUROPASS (2011), and density at Normal Temperature and Pressure (NTP) and molar mass correspond to the values applicable to methane (CH₄); LHV and density for biomass is taken from Forest Research (2022) and the molar mass from biomass is roughly approximated by considering the molar mass of cellulose (C₆H₁₀O₅, 162,139 g/mol), hemicellulose (C₅H₈O₄, 132,114 g/mol) and lignin (C₉H₇O₂·C₆H₁₀O₅, 183,03 g/mol) – the latter defined based on the composition found in spruce (*Picea abies*) samples reported by Pettersen (1984) -considering a distribution of 50%, 30%, and 20%, respectively, based on the typical shares for dry wood presented by Pettersen (1984).

The equipment minimum up and down times are set as 4 and 3 hours, respectively, as done in Dimoulkas and Amelin (2015). U_INI_G and U_INI_B are binary variables indicated the state of the CHP unit prior to the optimization [1 = on, 0 = off]. Shutdown costs are assumed as zero for all cases, whereas start-up costs are considered as a value dependent on the system's installed capacity, which is why different approaches are taken for the investment and operational models. In the first case, no costs are considered and instead a restriction is imposed over the number of times per day that the unit can be turn off and turn on. This is assumed as one per day given that generators do not usually start up more than twice per day (Yu et al., 2022), and this is a common assumption made in similar optimization problems.

Finally, the start-up costs considered for the operational model are calculated considering the extra fuel required to warm-up the engines –assumed as the required fuel to operate the machine for 10 minutes at nominal power as done by Gambarotta et al. (2015) – plus the additional equipment wear costs. In the work done by Facci, Andreassi, and Ubertini (2014), the latter costs are hypothesized as equivalent to the value of one hour of maintenance. A similar approach is done in MODECO assuming that maintenance costs for this type of technology represent around 50% of the total operational expenses (U.S. Energy Information Agency, 2020)– without considering fuel costs – and a maintenance period of 48 hours per year as done by Ghaffarpour et al. (2018). As the operational expenses (OPEX) are defined as a percentage of the investment cost (CAPEX), and the CAPEX depends on the final rated power installed (MAX_EL_B), the Eq. 138 is applied to calculate the start-up cost for each case using the applicable parameters to each CHP type (gas or biomass).

Eq. 138 CHP start-up cost calculation

$$\text{Startup cost} = \frac{1 [h]}{6} * \text{CHP_R_POWER}[kW_{el}] * \frac{1}{\text{CONV_EL} \left[\frac{kWh_{el}}{mol} \right]} * \text{FUEL_COST} \left[\frac{EUR}{mol} \right] + \\ \text{CAPEX} \left[\frac{EUR}{kW_{el}} \right] * \text{CHP_R_POWER}[kW_{el}] * \% \text{OPEX} * \frac{0.5}{48}$$

Electrolyzer

The electrolyzer efficiency is set as 67.5% considering that the power-to-hydrogen efficiency for PEM electrolyzer ranges between 65% and 70% for PEM technologies (Hu et al., 2022). The same authors report that the minimum operating load for PEM electrolyzers can be defined between 0-10%, so the upper limit is used as an assumption for the P_MIN_PCTG_EL parameter. For the Low Heating Value (LHV) of hydrogen gas, the value reported by Rau, Willauer, and Ren (2018) is used. For the operational model, the upper power limit considered is the installed rated power defined by the investment model, and the lower limit is based on the defined minimum operating load.

Table 88 Scalar parameters for the PEM electrolyzer

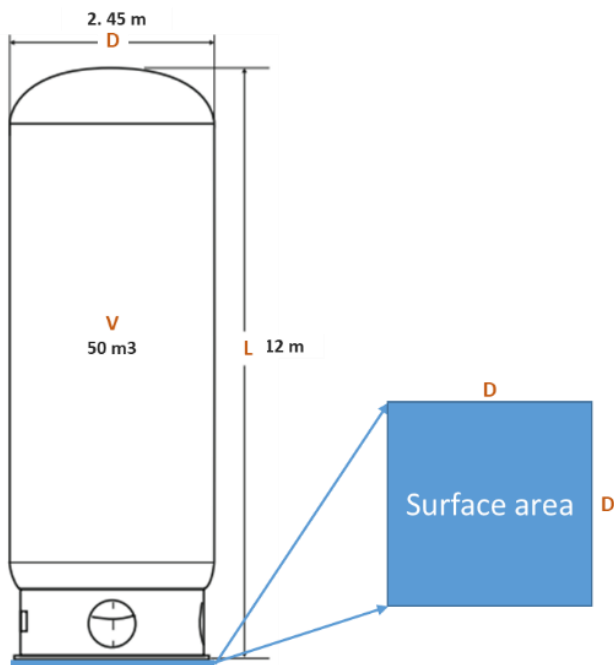
| Parameter | Description | Value | Units |
|----------------------|---|----------------------------|---------------------|
| EL_R_POWER | Rated power | Result from investment | kWe |
| ETA_EL | Power-to-hydrogen efficiency. | 67.5% | % |
| A_EL | Area per unit capacity installed. | 1E-20 | m ² /kWe |
| MAX_P_EL | Maximum power. | EL_R_POWER | kWe |
| MIN_P_EL | Minimum power. | EL_R_POWER * P_MIN_PCTG_EL | kWe |
| P_MIN_PCTG_EL | Minimum operating load. | 0.1 | % |
| LHV_H2 | Lower heating value of hydrogen (H ₂) | 0.067 | kWh/mol |

Source: Own elaboration with data from Hu et al. (2022); and Rau, Willauer, and Ren (2018).

Hydrogen tank

The tank's technical characteristics are defined based on the information presented by (Nojavan et al., 2017). The maximum and minimum pressure inside the vessel are defined as 1,380,000 Pa and 200,000 Pa, and the mean temperature is set at 313 K. The initial daily pressure and minimum daily pressure are both stated as 1,000,000 Pa. The area occupied per unit of volume storage is (A_{HS}) is defined considering a vertical orientation and the diameter and nominal volume of a commercial hydrogen storage tank for industrial applications (Figure 90). It is assumed that the tank requires a square surface whose sides' lengths are equal to the tank diameter.

Figure 90. Reference hydrogen tank dimensions and occupied surface area



Source: Own elaboration based on the technical sheet from Lapesa Grupo Empresarial (n.d.)

Finally, the ratio between tank volume and the maximum hydrogen hourly flow (C_{RATE_HS}) is calculated considering the density of hydrogen at 13.8 bar and 313 K (1.16600 kg/m³) and the gas molar mass (0.00202 kg/mol). The density value is calculated using the data reported in the Hydrogen Tools published by the U.S. Pacific Northwest National Laboratory (n.d.). A discharge duration of 24 hours is considered. No losses from the storage unit are considered so efficiencies are set as 100% (ETA_CH_HS , ETA_DCH_HS).

Table 89 Scalar parameters for the Hydrogen storage tank

| Parameter | Description | Value | Units |
|-------------------|---|---------|-------|
| ETA_CH_HS | Charging efficiency | 1 | % |
| ETA_DCH_HS | Discharging efficiency | 1 | % |
| A_HS | Area per volumetric unit (m³) of hydrogen storage installed | 0.09 | m²/m³ |
| Q_MAX_HS | Maximum pressure inside the tank | 1380000 | Pa |

| Parameter | Description | Value | Units |
|-----------------------|---|------------------------|-------------------------|
| Q_MIN_HS | Minimum pressure inside the tank | 200000 | Pa |
| R_GAS_CONSTANT | R gas constant. | 8.3145 | m ³ Pa/K mol |
| TA_MEAN | Mean temperature inside the vessel | 313 | K |
| P_MAX_CH_HS | Maximum hydrogen rate inflow | Result from investment | mol/h |
| P_MAX_DCH_HS | Maximum hydrogen rate outflow | Result from investment | mol/h |
| Q_INI_HS | Initial daily pressure | 1000000 | Pa |
| Q_FIN_HS | Minimum final daily pressure | 1000000 | Pa |
| C_RATE_HS | Ratio between tank volume and maximum hydrogen hourly flow (in/out) | 24.07499 | mol/ m ³ .h |

Source: Own elaboration with data from Nojavan, Zare, and Mohammadi-Ivatloo (2017); Lapesa Grupo Empresarial (n.d.); and U.S. Pacific Northwest National Laboratory (n.d.).

Batteries

The technical parameters for Li.-ion batteries are listed in Table 90, as observed, all parameters are equal for energy and power-based equipment except for the C-rate, which is based considering the applications described by Tsiropoulos, Tarvydas, and Lebedeva (2018). The charging and discharging efficiencies (ETA_DCH_ES, ETA_CH_ES), and the maximum and minimum State of Charge (SOC) are based on the values projected for 2030 by (Nastasi et al., 2021). The initial (SOC_INI_ES) and final (SOC_FIN_ES) are defined as 50% within MODECO.

Table 90 Scalar parameters for energy and power based batteries (0.35 C-rate)

| Parameter | Description | Value | Units |
|--------------------------|---|-------|-------|
| ETA_DCH_ES_ENERGY | Discharging efficiency for energy-based batteries. | 97.5% | % |
| ETA_CH_ES_ENERGY | Charging efficiency for energy-based batteries. | 97.5% | % |
| MIN_CH_ENERGY | Minimum charging power for energy-based batteries. | 0 | kWh |
| MAX_CH_ENERGY | Maximum charging power for energy-based batteries. | | kWh |
| MIN_DCH_ENERGY | Minimum discharging power for energy-based batteries. | 0 | kWh |
| MAX_DCH_ENERGY | Maximum discharging power for energy-based batteries. | | kWh |
| SOC_INI_ES_ENERGY | Initial State of Charge (SOC) at the start of the day. | 50% | % |
| SOC_FIN_ES_ENERGY | Final State of Charge (SOC) at the end of the day. | 50% | % |
| C_RATE_ES_ENERGY | C-rate for energy-based batteries | 0.35 | - |
| SOC_MAX_ES_ENERGY | Maximum State of Charge (SOC) for energy-based batteries. | 95% | % |

| Parameter | Description | Value | Units |
|--------------------------|---|-------|-------|
| SOC_MIN_ES_ENERGY | Minimum State of Charge (SOC) for energy-based batteries. | 5% | % |
| ETA_DCH_ES_POWER | Discharging efficiency for power-based batteries. | 97.5% | % |
| ETA_CH_ES_POWER | Charging efficiency for power-based batteries. | 97.5% | % |
| MIN_CH_POWER | Minimum charging power for power-based batteries. | 0 | kWh |
| MAX_CH_POWER | Maximum charging power for power-based batteries. | | kWh |
| MIN_DCH_POWER | Minimum discharging power for power-based batteries. | 0 | kWh |
| MAX_DCH_POWER | Maximum discharging power for power-based batteries. | | kWh |
| SOC_INI_ES_POWER | Initial State of Charge (SOC) at the start of the day. | 50% | % |
| SOC_FIN_ES_POWER | Final State of Charge (SOC) at the end of the day. | 50% | % |
| C_RATE_ES_POWER | C-rate for power-based batteries. | 0.35 | - |
| SOC_MAX_ES_POWER | Maximum State of Charge (SOC) for power-based batteries. | 95% | % |
| SOC_MIN_ES_POWER | Minimum State of Charge (SOC) for power-based batteries. | 5% | % |

Source: Own elaboration with data from Nastasi et al. (2021); Tsiropoulos, Tarvydas, and Lebedeva (2018)

Boilers

The fuel-to-heat ratios shown in Table 91 are calculated for natural gas and hydrogen considering the physical properties of both fuels at NTP conditions, as well as the combustion efficiency (η_{comb}) – assumed as 85% for residential (Vakkilainen, 2017) and industrial (Vanwortswinkel and Wouter, 2010) boilers – as shown in Eq. 139. The data for natural gas can be consulted in Table 87. In the case of Hydrogen, a LHV of 2.997 kWh/m³, density (ρ) of 0.090 and molar mass (M) of 0.00202 kg/mol are considered. Finally, the model also requires a limit on the maximum thermal capacity from boilers installed in the community. This is set equal to the capacity available in the starting year (2025), as afterwards the heat generated from boilers decreases due to the assumed growth in other technologies (heat pumps and solar thermal), which is defined exogenously.

Table 91 Scalar parameters for boilers

| Parameter | Description | Value | Units |
|------------------|---|----------|---------|
| G_CONV_B | Fuel (natural gas) mol to heat ratio in residential and commercial boilers. | 0.22388 | kWt/mol |
| H_CONV_B | Fuel (hydrogen) mol to heat ratio in residential and commercial boilers. | 0.068604 | kWt/mol |
| G_CONV_IB | Fuel (natural gas) mol to heat ratio in industrial boilers. | 0.201320 | kWt/mol |
| H_CONV_IB | Fuel (hydrogen) mol to heat ratio in industrial boilers. | 0.062104 | kWt/mol |

| | | | |
|---------------------|---|------------------------------------|-----|
| P_INST_B_INI | Boilers thermal capacity installed each year. | Defined each year based on demand. | kWt |
| P_MAX_B | Maximum boiler capacity installed. | Equal to installed in 2025. | kWt |

Source: Own elaboration with data from Vakkilainen (2017); Vanwortswinkel and Wouter (2010).

Eq. 139 Fuel to electricity ratio per fuel (biomass, natural gas or hydrogen)

$$FUEL_CONV_B = \frac{LHV_{fuel} \left[\frac{kWh}{m^3} \right] * M_{fuel} \left[\frac{kg}{mol} \right]}{\rho_{fuel} \left[\frac{kg}{m^3} \right]} * \eta_{comb}$$

As the considered residential boiler costs are given per unit basis in the used database, these are converted to euros per kilowatt thermal to be used in the investment model. To do so, it is assumed a thermal load of 25 kWt per single-family household (Schiro et al., 2020). For flats, a smaller number is assumed (20 kWt) given their smaller surface. In the case of the boilers in multifamily buildings, the boiler unit in which costs were based are scaled to serve all dwellings in the building. Thus, an average number of 12 dwellings per building unit is assumed considering the available data reported in the Entranz database for European countries (Entranz Project, 2008). Furthermore, it must be considered that in the original database costs are differentiated per multifamily and single-family units, but in MODECO's investment model only one type of boiler is considered so the average cost between these two boiler types is assumed. For industrial boilers, the costs are already given per kilowatt thermal basis, so no conversion is needed.

Demand response

Finally, the parameters used to model the demand response program are listed below. The only value, which was not mentioned in that document is the maximum number of activations per day that is set as 3 activations per day. This value is in line with the range (1-12 activations per day) analysed by Prüggler (2013) and is aligned with the upper value proposed by Zimmermann et al. (2016) for the maximum number of activations expected for shiftable loads (1,100 per year or 3.014 per day).

Table 92 Scalar parameters for demand response

| Parameter | Description | Value | Units |
|------------------|---|-------|-------|
| C_DR | Variable cost for demand response. | .010 | €/kWh |
| S_INC | Available load increase share. | 75% | % |
| S_DEC | Available load decrease share. | 0% | % |
| S_FLEX | Share from demand that participates in demand response. | 40% | % |
| U_INC_INI | Initial state of increment at start of the day. | 0 | [1,0] |
| U_DEC_INI | Initial state of decrement at first time of the day. | 0 | [1,0] |
| T_DR | Maximum time of demand response activation. | 3 | h |
| D_DR | Maximum number of demand response activations per day. | 3 | --- |

Source: Own elaboration with data from Prüggler (2013); and Zimmermann et al. (2016).

Annex 4. Gap values obtained for the scenarios executed in the EC investment model

Table 93. Gap values reported by the EC investment model for the base case tariff scenarios

| Country | Discount rate | Archetype | No Charges | TOU | Bandwidth | Peak Power |
|---------|---------------|--------------------|--------------|-----------|--------------|------------|
| Germany | 1.3% | Business park | < 0,01% | < 0,01% | 0.17% | < 0,01% |
| | | Industrial polygon | < 0,01% | < 0,01% | < 0,01% | < 0,01% |
| | | Urban district | < 0,01% | < 0,01% | < 0,01% | < 0,01% |
| | | Rural town | 0.65% | 4% | < 0,01% | < 0,01% |
| | | Virtual community | < 0,01% | < 0,01% | < 0,01% | < 0,01% |
| Spain | 3.0% | Business park | < 0,01% | < 0,01% | < 0,01% | < 0,01% |
| | | Industrial polygon | < 0,01% | < 0,01% | < 0,01% | < 0,01% |
| | | Urban district | < 0,01% | < 0,01% | < 0,01% | < 0,01% |
| | | Rural town | < 0,01% | < 0,01% | < 0,01% | < 0,01% |
| | | Virtual community | 0.58% | < 0,01% | < 0,01% | < 0,01% |

Source: own elaboration with data from MODECO investment model

Table 94. Gap values reported by the EC investment model for the price rate sensitivity cases

| Country | Discount rate | Archetype | TOU_Flat | TOU_PPA |
|---------|---------------|--------------------|--------------|-----------|
| Germany | 1.3% | Business park | < 0,01% | |
| | | Industrial polygon | 1.25% | 5% |
| | | Urban district | 1.94% | |
| | | Rural town | 5.70% | |
| | | Virtual community | 0.54% | |

Source: own elaboration with data from MODECO investment model

Table 95. Gap values reported by the EC investment model for the discount rate sensitivity cases

| Country | Discount rate | Archetype | TOU | Bandwidth | Peak power |
|---------|---------------|--------------------|-------------|--------------|--------------|
| Germany | 2.5% | Business park | < 0,01% | 0.13% | < 0,01% |
| | | Industrial polygon | < 0,01% | 0.04% | 0.04% |
| | | Urban district | < 0,01% | < 0,01% | < 0,01% |
| | | Rural town | 2.2% | < 0,01% | 0.11% |
| | | Virtual community | < 0,01% | < 0,01% | 0.02% |

Source: own elaboration with data from MODECO investment model

Annex 5. Gap values obtained for the scenarios executed in the EC operational model

Table 96. Gap values reported by the EC operational model for the base case tariff scenarios

| Country | Discount rate | Archetype | Year | TOU | Bandwidth | Peak Power |
|---------|---------------|--------------------|------|--------------|-----------|--------------|
| Germany | 1.3% | Business park | 2025 | < 0,01% | < 0,01% | 0.03% |
| | | Industrial polygon | | < 0,01% | < 0,01% | < 0,01% |
| | | Urban district | | < 0,01% | < 0,01% | < 0,01% |
| | | Rural town | | 1.99% | < 0,01% | < 0,01% |
| | | Virtual community | | < 0,01% | < 0,01% | < 0,01% |
| | | Business park | 2030 | 0.29% | < 0,01% | 0.08% |
| | | Industrial polygon | | < 0,01% | < 0,01% | < 0,01% |
| | | Urban district | | 0.03% | < 0,01% | < 0,01% |
| | | Rural town | | 1.72% | < 0,01% | 0.11% |
| | | Virtual community | | < 0,01% | < 0,01% | < 0,01% |
| | | Business park | 2040 | 1.05% | < 0,01% | 0.23% |
| | | Industrial polygon | | < 0,01% | < 0,01% | < 0,01% |
| | | Urban district | | 0.37% | < 0,01% | 0.46% |
| | | Rural town | | 0.49% | < 0,01% | 0.45% |
| | | Virtual community | | < 0,01% | < 0,01% | < 0,01% |
| Spain | 3.0% | Business park | 2025 | < 0,01% | < 0,01% | 0.58% |
| | | Industrial polygon | | < 0,01% | < 0,01% | < 0,01% |
| | | Urban district | | < 0,01% | < 0,01% | 0.61% |
| | | Rural town | | 0.08% | < 0,01% | 0.87% |
| | | Virtual community | | < 0,01% | < 0,01% | < 0,01% |

| | | | | | |
|--|--------------------|------|--------------|---------|--------------|
| | Business park | 2030 | 0.29% | < 0,01% | 2.42% |
| | Industrial polygon | | < 0,01% | < 0,01% | < 0,01% |
| | Urban district | | 1.46% | < 0,01% | 1.99% |
| | Rural town | | 0.15% | < 0,01% | 4.04% |
| | Virtual community | | < 0,01% | < 0,01% | < 0,01% |
| | Business park | 2040 | 0.05% | < 0,01% | 0.44% |
| | Industrial polygon | | < 0,01% | < 0,01% | < 0,01% |
| | Urban district | | 0.87% | < 0,01% | 2.26% |
| | Rural town | | 0.44% | < 0,01% | 4.78% |
| | Virtual community | | < 0,01% | < 0,01% | < 0,01% |

Source: own elaboration with data from MODECO operational model

GETTING IN TOUCH WITH THE EU

In person

All over the European Union there are hundreds of Europe Direct centres. You can find the address of the centre nearest you online (european-union.europa.eu/contact-eu/meet-us_en).

On the phone or in writing

Europe Direct is a service that answers your questions about the European Union. You can contact this service:

- by freephone: 00 800 6 7 8 9 10 11 (certain operators may charge for these calls),
- at the following standard number: +32 22999696,
- via the following form: european-union.europa.eu/contact-eu/write-us_en.

FINDING INFORMATION ABOUT THE EU

Online

Information about the European Union in all the official languages of the EU is available on the Europa website (european-union.europa.eu).

EU publications

You can view or order EU publications at op.europa.eu/en/publications. Multiple copies of free publications can be obtained by contacting Europe Direct or your local documentation centre (european-union.europa.eu/contact-eu/meet-us_en).

EU law and related documents

For access to legal information from the EU, including all EU law since 1951 in all the official language versions, go to EUR-Lex (eur-lex.europa.eu).

Open data from the EU

The portal data.europa.eu provides access to open datasets from the EU institutions, bodies and agencies. These can be downloaded and reused for free, for both commercial and non-commercial purposes. The portal also provides access to a wealth of datasets from European countries.



The European Commission's science and knowledge service

Joint Research Centre

JRC Mission

As the science and knowledge service of the European Commission, the Joint Research Centre's mission is to support EU policies with independent evidence throughout the whole policy cycle.



EU Science Hub
joint-research-centre.ec.europa.eu



@EU_ScienceHub



EU Science Hub - Joint Research Centre



EU Science, Research and Innovation



EU Science Hub



EU Science



Publications Office
of the European Union